235

ISSN 1343-2230

CNS-REP-30
April, 2001

CNS-REP-30

CNS Report

Proceedings of the CNS International Workshop

Physics of QCD many-body systems

What we learn from the RHIC Year-1 –

CNS, University of Tokyo

February 14-15, 2001

Fermilab Library
0 1160 0089683 7

FERMILAB
JUN 1 1 2001
LIBRARY

Edited by

H. Hamagaki and K. Ozawa

CNS-REP-30

Center for Nuclear Study(CNS)

Graduate School of Science, the University of Tokyo
7-3-1 Hongo, Bunkyo-ku, Tokyo,113-0033, Japan
Correspondence: cnsoffice@cns.s.u-tokyo.ac.jp

Proceedings of the CNS International Workshop

Physics of QCD many-body systems

-- What we learn from the RHIC Year-1 --

Contents

RHIC: the year in review ..... D. Morrison .. 1
Measurements of Global Variables at PHENIX ..... K. Homma .. 18
First results from the STAR experiment at RHIC ..... A. Ogawa .. 37
First results from the STAR experiment at RHIC
- soft hadron physics - ..... M. Kaneta .. 53
π^0 Production in Au+Au Collisions at $s^{1/2}$ = 130 GeV ..... K. Oyama .. 66
Charged Hadron pt Spectra ..... T. Chujo .. 77
Particle ratios in PHENIX at RHIC ..... H. Ohnishi .. 85
CERN SPS hadron measurement
- Flow measurement with a puzzle, and interpretation
of low mt enhancement of pion spectrum - ..... S. Sato .. 95
Hydrodynamical analysis of elliptic flow at SPS and RHIC .... T. Hirano .. 109
Three particles Bose-Einstein correlation
in terms of Coulomb wave function ..... M. Biyajima .. 120
Electron Measurement in PHENIX ..... Y. Akiba .. 128
Observation of ρ/ω meson modification in nuclear matter ... M. Naruki .. 135
Hadronic constraints for vector mesons in medium .....Su Houng Lee .. 147
J/Ψ in pA and AA ..... H. Fujii .. 156
Quark matter in neutron stars ..... T. Tatsumi .. 165
Direct Photons in Pb+Pb Collisions ..... T. Awes .. 176
Photon and Dilepton Emission Rates
from Ultra-Relativistic Heavy Ion Collisions ..... Jan-e Alam .. 194
Re-Hardening of Hadron Transverse Mass Spectra
in Relativistic Heavy-Ion ollisions ..... A. Ohnishi .. 209
Quark-gluon Plasma and Lattice QCD
at Finite Temperature and Density ..... C. Nonaka .. 218
First circular 230
Program 231
Participant list 233

RHIC: the year in review

David Morrison, Brookhaven National Laboratory

overview caveats

- an awful lot has happened in last 6 months
- summary talks at QM'01 concentrated heavily on RHIC results - still not enough time
  - I've "borrowed" liberally from those talks
- I've tried to concentrate on what we now think we know that we certainly didn't know before
  - of course, <u>everything</u> is new

BROOKHAVEN NATIONAL LABORATORY

chronology of events

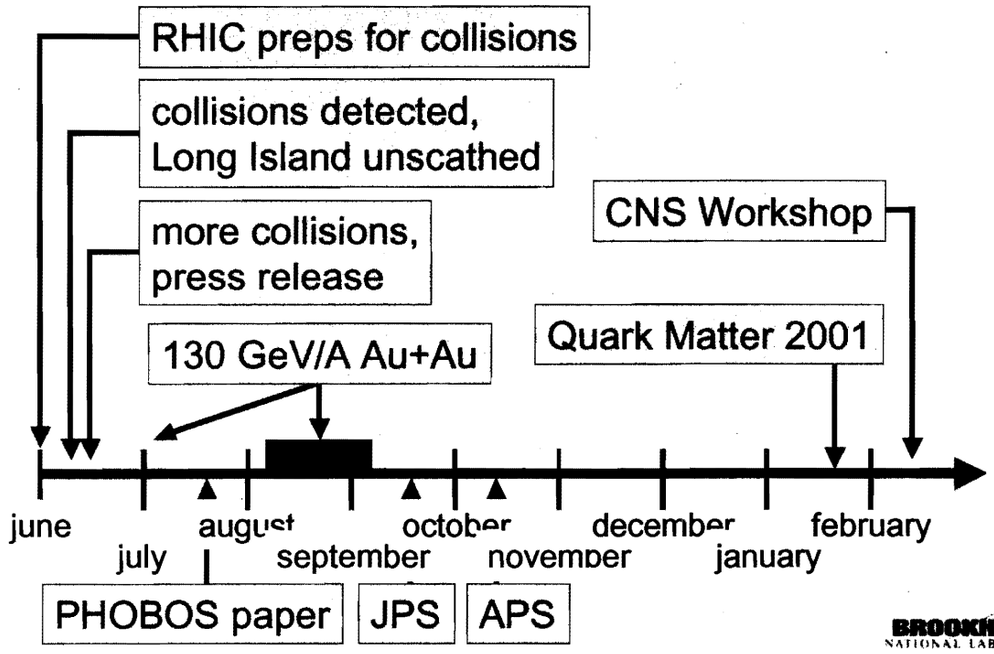

BROOKHAVEN NATIONAL LABORATORY

collisions!

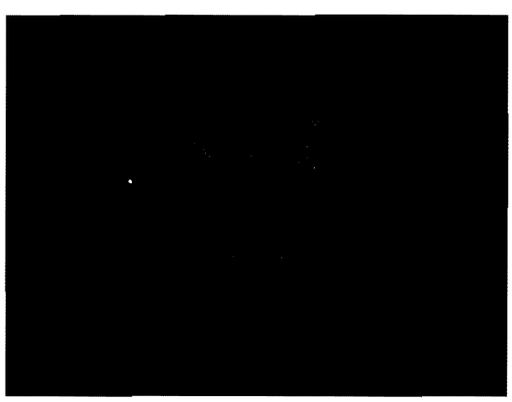

STAR TPC

PHENIX Central Arms

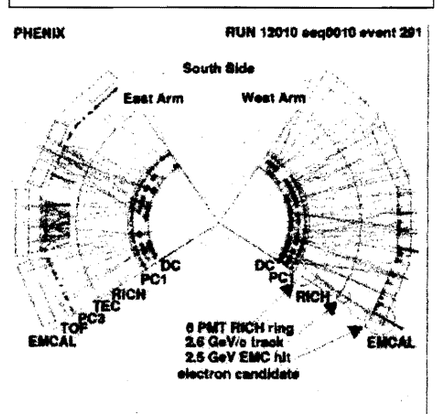

BROOKHAVEN NATIONAL LABORATORY

the lay of the land

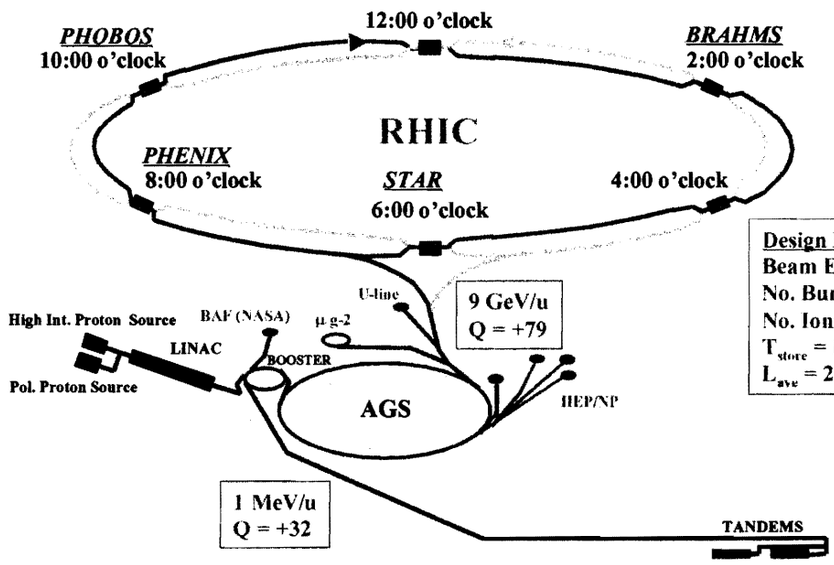

Design Parameters:
Beam Energy = 100 GeV/u
No. Bunches = 57
No. Ions /Bunch = 1×10^9
T_{store} = 10 hours
$L_{ave} = 2 \times 10^{26}$ cm^{-2} sec^{-1}

BROOKHAVEN NATIONAL LABORATORY

the accelerator

- two separate rings sharing one tunnel
- power supplies for some magnets not installed yet
- no storage RF
- accelerated to 130 GeV/A
  - below quench current for final steering dipoles
- few μb^{-1} integrated L

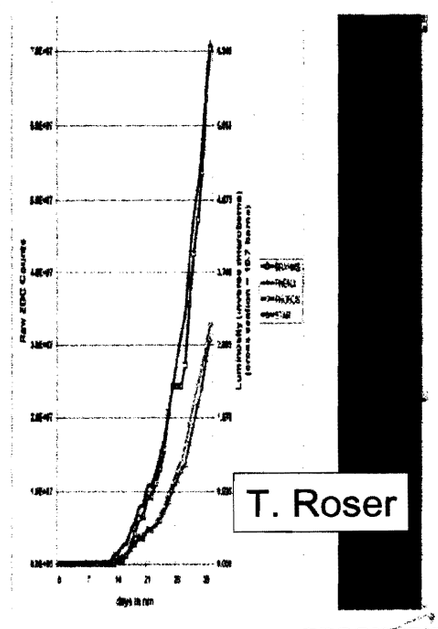

T. Roser

BROOKHAVEN NATIONAL LABORATORY

"phase transition" in the accelerator

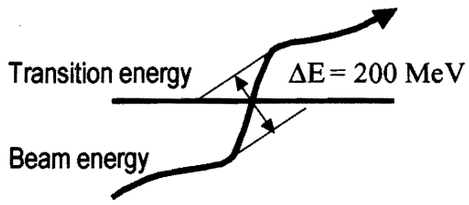

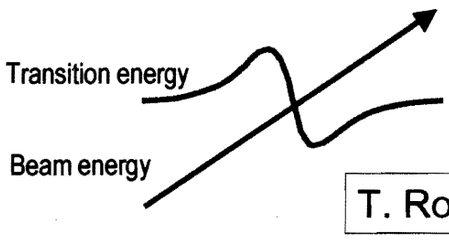

T. Roser

- RHIC is first superconducting accelerator to have to deal with this
  - low, high energy particles in bunch have same orbital frequency
  - intrabeam scattering
- full complement of magnet power supplies will help next year

BROOKHAVEN NATIONAL LABORATORY

global features of Au+Au collisions

- $dN_{ch}/d\eta$ at mid-rapidity
  - models predictions vary by over a factor of two
- $dN_{ch}/d\eta$ vs centrality, η
  - does wounded nucleon model still hold at these energies?
- $dE_T/d\eta$ at mid-rapidity
- net baryon density at mid-rapidity
  - how close are we to a (net) baryon-free central region?

$dN_{ch}/dy|_{y=0}$ 200 GeV/A

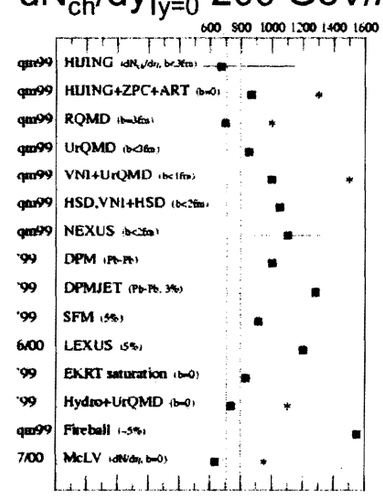

P. Steinberg

BROOKHAVEN NATIONAL LABORATORY

charged particle multiplicity

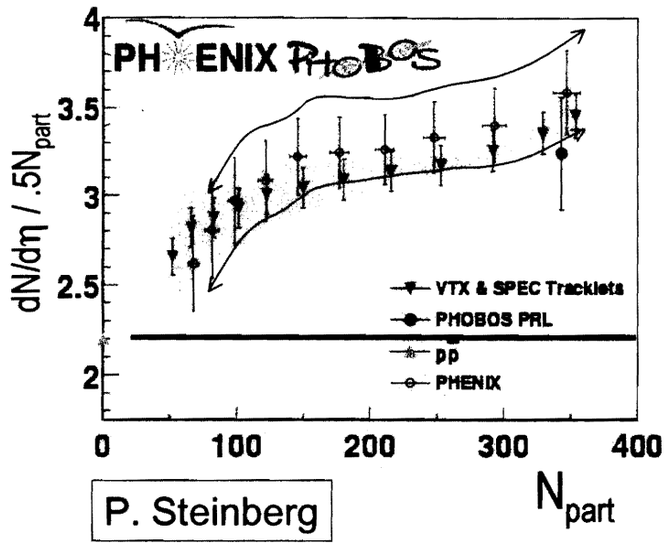

P. Steinberg

- good agreement between different experiments
- wounded nucleon models fails
- evidence for rise with number of collisions
- not at all trivial to determine N_{part}!
- not even easy to determine σ_{tot}!

BROOKHAVEN NATIONAL LABORATORY

pseudo-rapidity distributions

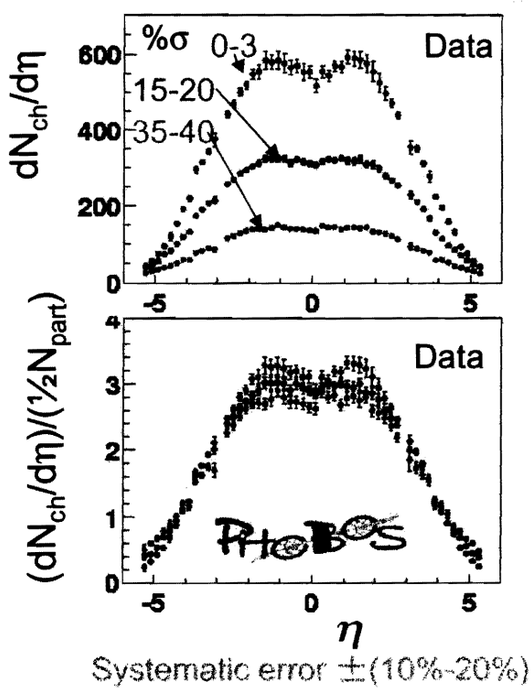

- PHOBOS has really fantastic η coverage
- when wounded nucleon model is divided out, there is still an increase at mid-rapidity
- evidence for some relative <u>decrease</u> in $dN_{ch}/d\eta$ at high η

P. Steinberg

BROOKHAVEN NATIONAL LABORATORY

transverse energy

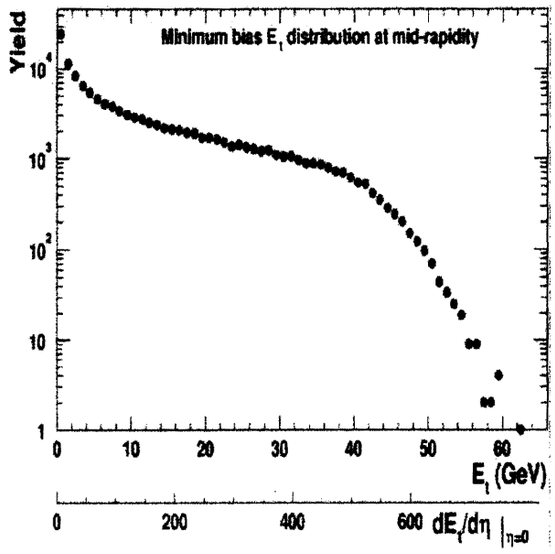

B. Zajc

- acceptance
  - $|\eta| < 0.35$, $\Delta\phi = 45^o$
- studied vs charged multiplicity and N_{part}
- $dN_{ch}/d\eta$ and $dE_T/d\eta$ seem to indicate an energy density of at least 50% greater than in Pb+Pb at SPS
  - modulo parameters in usual Bjorken approach
  - formation time smaller?

BROOKHAVEN NATIONAL LABORATORY

net baryon density (via $\bar{p}/p$)

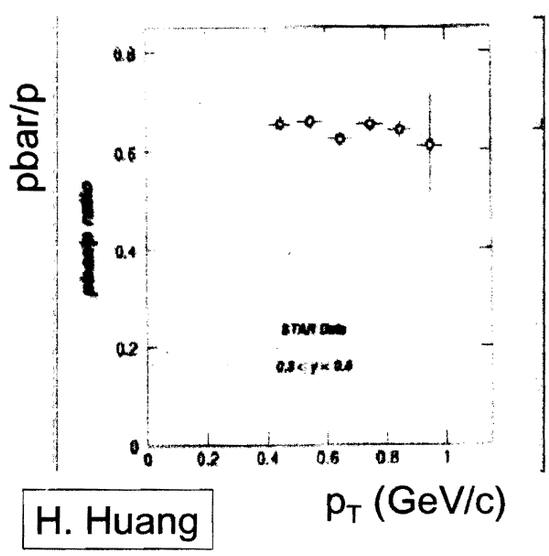

H. Huang

- value of $\bar{p}/p \sim 65\%$
  - implies that 2/3 of protons at y=0 come from pair production
  - $\bar{p}/p < 1$ is not "bad"
- much closer to baryon-free central region compared to SPS
- gluon dominated central region

BROOKHAVEN NATIONAL LABORATORY

global features

- large particle production, rising faster than wounded nucleon model, suggesting significant particle production due to hard processes
- very high energy density; more than 50% higher than SPS is likely
- almost net baryon-free central region
- RHIC collisions look (at first glance) like we had hoped they would look

BROOKHAVEN NATIONAL LABORATORY

measuring elliptic flow: two methods

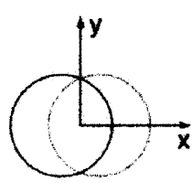

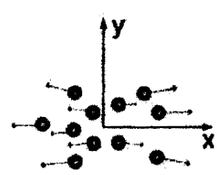

$$\varepsilon = \frac{\langle y^2 - x^2 \rangle}{\langle y^2 + x^2 \rangle}$$

$$v_2 = \langle \cos 2\phi \rangle$$

$$\phi = \operatorname{atan} \frac{p_y}{p_x}$$

particle production relative to an identified reaction plane

$$C(\Delta\phi) = \frac{R(\Delta\phi)}{B(\Delta\phi)}$$

angular correlations

P. Steinberg

BROOKHAVEN NATIONAL LABORATORY

centrality dependence of elliptic flow

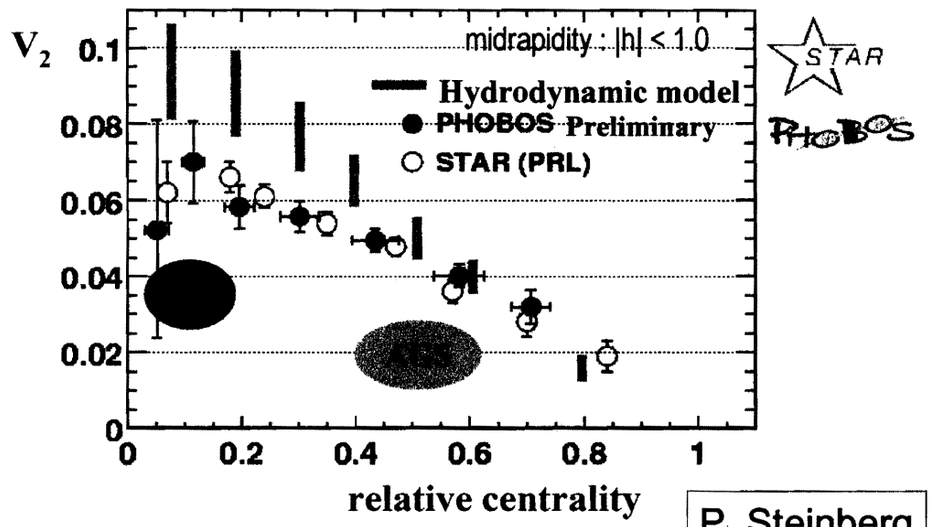

P. Steinberg

surprise: very strong elliptic flow

BROOKHAVEN NATIONAL LABORATORY

p_T dependence of flow

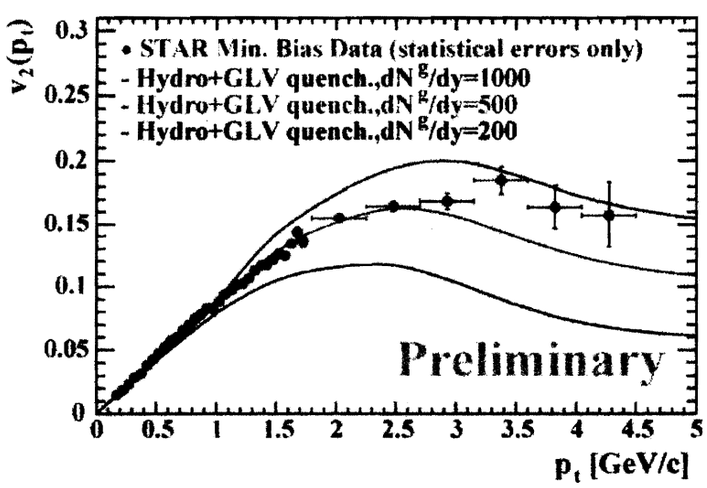

Hydro+GLV: M. Gyulassy, I. Vitev and X.N. Wang, nucl-th/00012092

- flow starts to bend over at ~2 GeV/c
- matches well with models that incorporate jet quenching

R. Snelling

BROOKHAVEN NATIONAL LABORATORY

spacetime extent of source (HBT)

- surprisingly little change in source parameters from SPS
  - people had been prepared for huge sources!
- possible that extraction of HBT values is influenced by very strong flow at RHIC

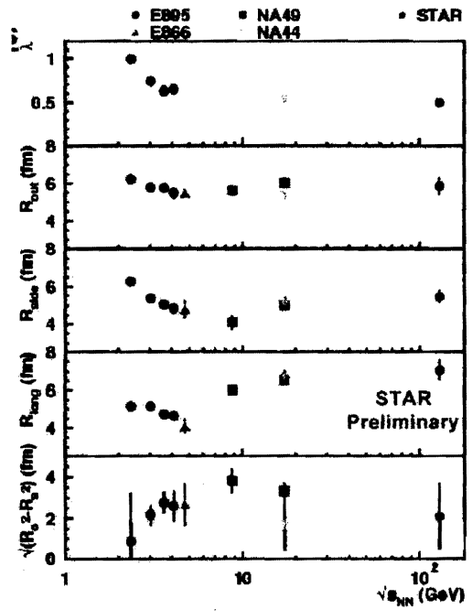

J. Harris

BROOKHAVEN NATIONAL LABORATORY

particle ID by dE/dx in STAR's TPC

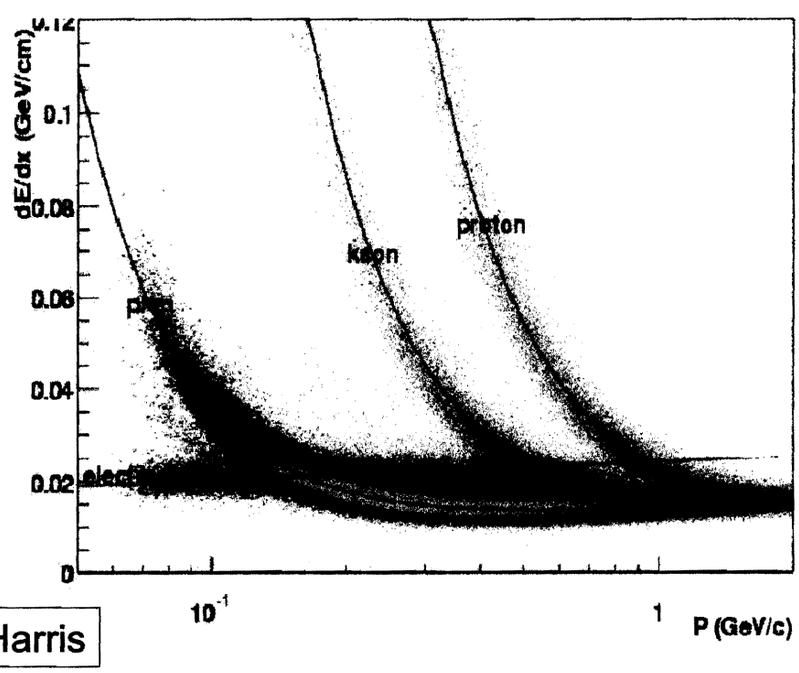

J. Harris

BROOKHAVEN NATIONAL LABORATORY

particle ID by TOF in PHENIX

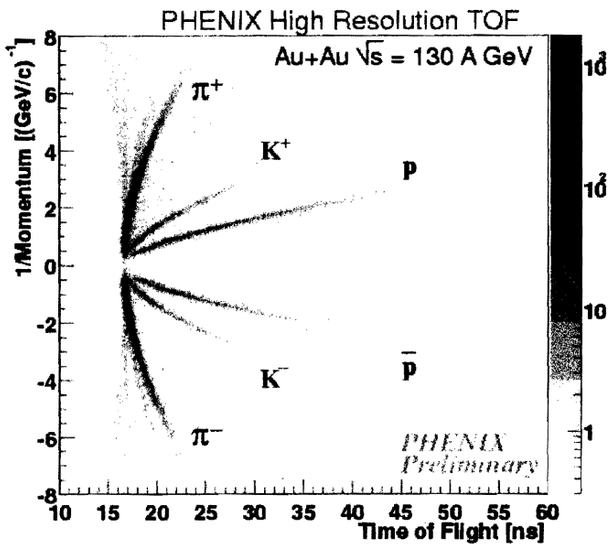

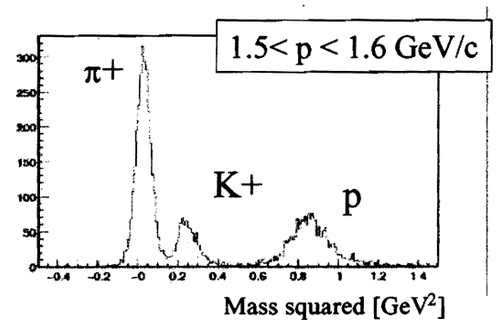

π/K separation < 1.6 GeV/c
Proton separation < 3.5 GeV/c

H. Ohnishi

BROOKHAVEN NATIONAL LABORATORY

topology and invariant mass

(Preliminary)

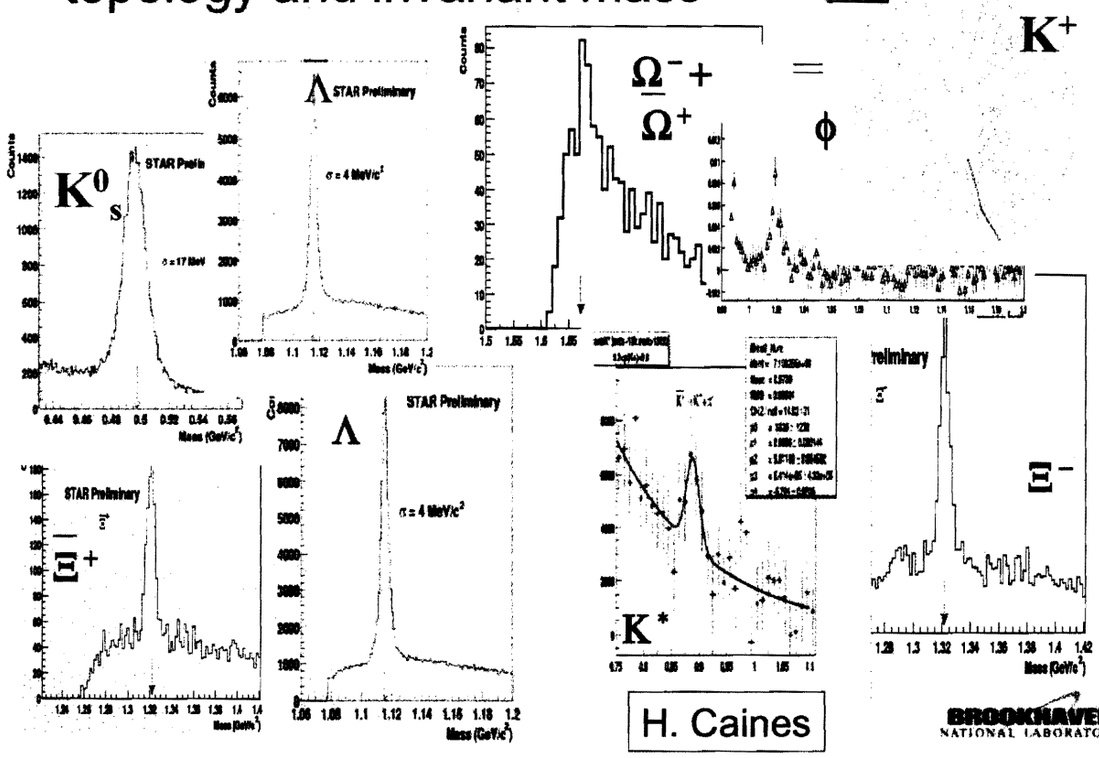

H. Caines

BROOKHAVEN NATIONAL LABORATORY

p+p p_T spectra

- power law p_T fall off
- interpolated to RHIC energies
- provides basis for comparison with high pT single particle specta in Au+Au

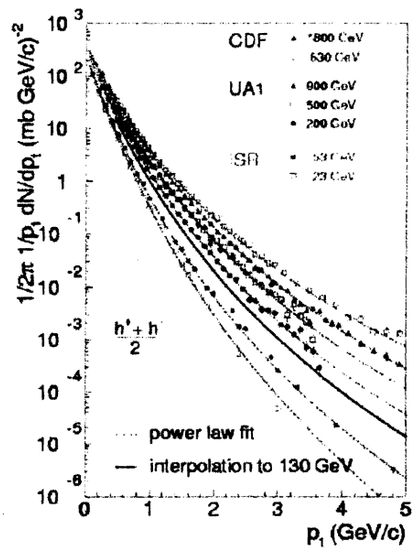

A. Drees

BROOKHAVEN NATIONAL LABORATORY

it's all $\bar{p}$'s out there!

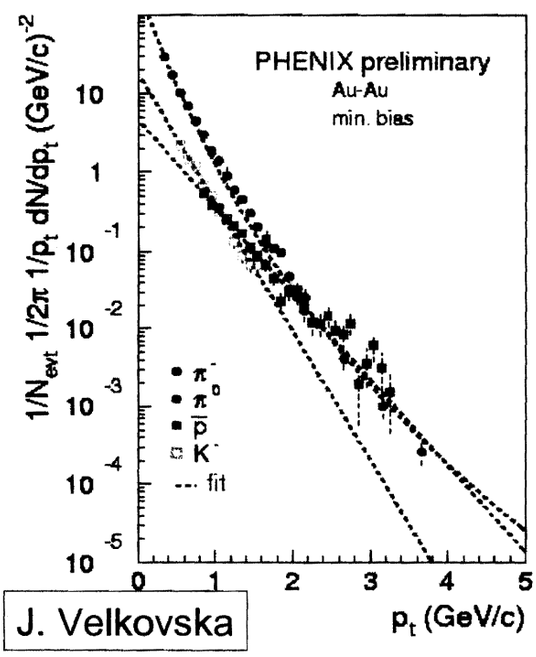

- pbars = π^-'s at about 2.0 - 2.5 GeV/c
- same is true for p's and π^+'s
- odd in picture of high p_T jet fragmentation - you'd expect π's

J. Velkovska

BROOKHAVEN NATIONAL LABORATORY

what is the expected p_T behavior?

Cronin effect: increase in yield vs pT, relative to p+p

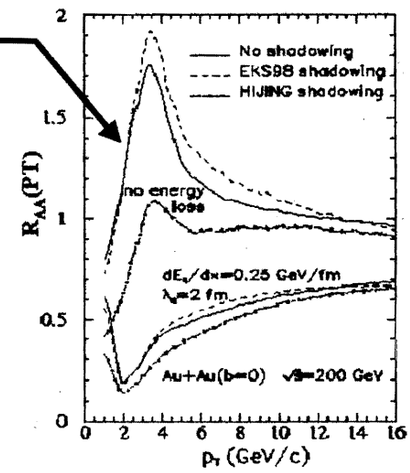

A. Drees

BROOKHAVEN NATIONAL LABORATORY

normalizing yields to p+p

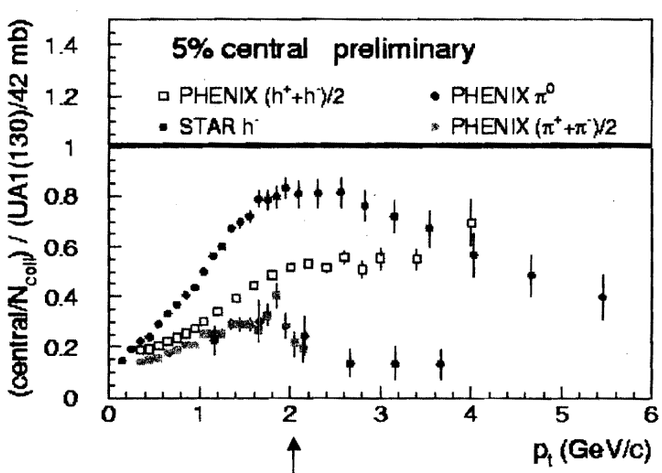

2 GeV/c

no Cronin effect seen - instead particle yields (relative to p+p) turn over and fall at about: p_T = 2 GeV/c

A. Drees

BROOKHAVEN NATIONAL LABORATORY

peripheral Au+Au

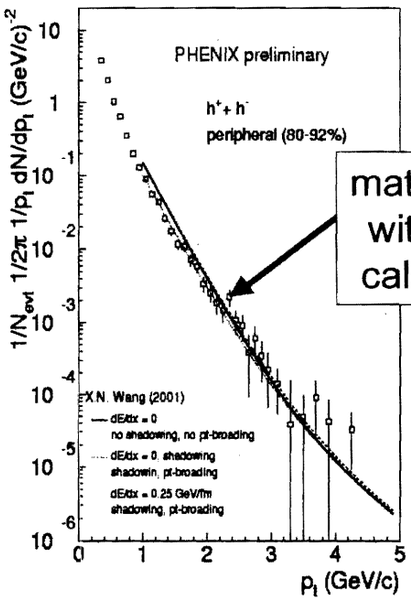

matches well with pQCD calculations

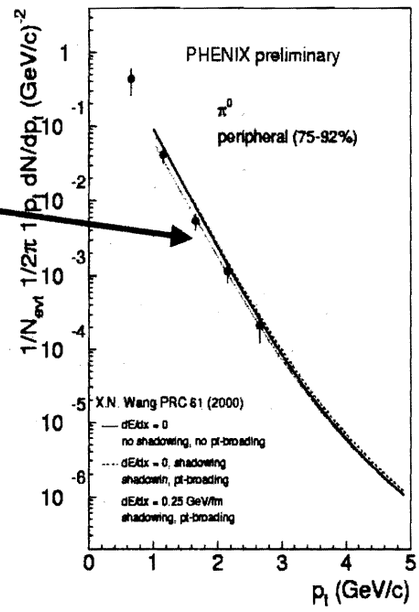

A. Drees, X-N. Wang

BROOKHAVEN NATIONAL LABORATORY

central Au+Au

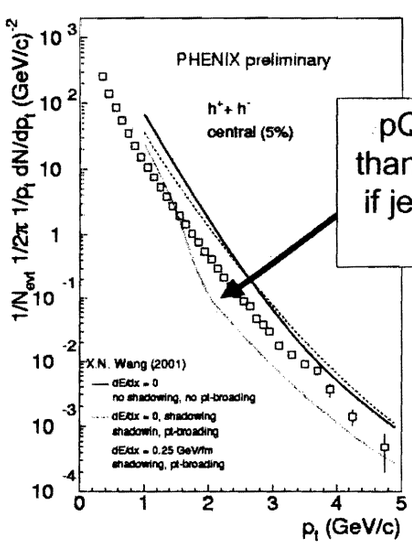

pQCD higher than data; better if jet quenching included

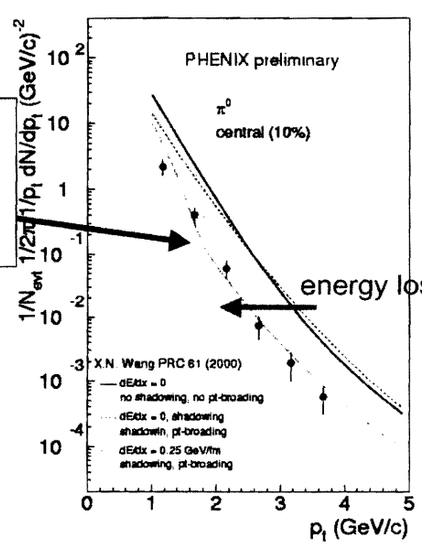

A. Drees, X-N. Wang

BROOKHAVEN NATIONAL LABORATORY

spin physics

- collaborators across STAR and PHENIX
- measuring spin asymmetries in p+p collisions
  - unique RHIC capability (for now)
- will measure gluon spin structure functions
- commissioned production, acceleration, manipulation of spin polarized proton
  - achieved 50% polarization

BROOKHAVEN NATIONAL LABORATORY

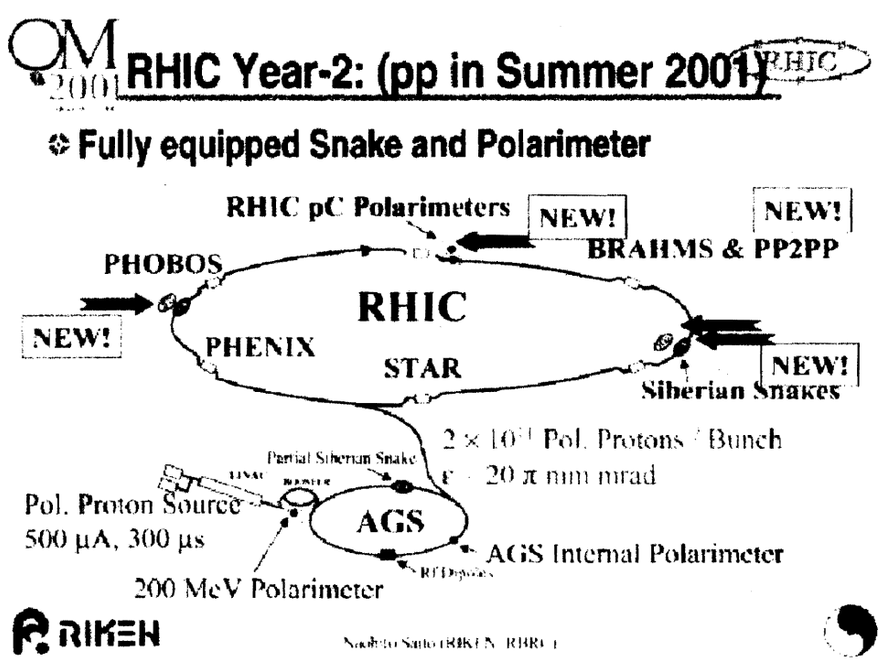

experimental improvements

- RHIC gets more Siberian snakes
- STAR gets a vertex tracker
  - look for displaced vertexes (B mesons)
- PHOBOS gets a true second arm
  - pairs at very low p_T, sensitive to large scales
- PHENIX gets an entire muon arm
  - not the only addition to PHENIX, but it is a big one

BROOKHAVEN NATIONAL LABORATORY

with luminosity we will see ...

- pair physics (e.g., vector mesons: ϕ, J/Ψ)
- very high p_T physics (15-20 GeV π^0's)
- direct photons
- scans in energy and species
- p+A or d+A to establish baseline physics
- systematic studies
  - energy scans
  - species scans

BROOKHAVEN NATIONAL LABORATORY

single electrons

- with more luminosity, look for heavy flavor decay to $e^{\pm}$
- also combine with μ to look for open charm via $D \rightarrow e\mu$

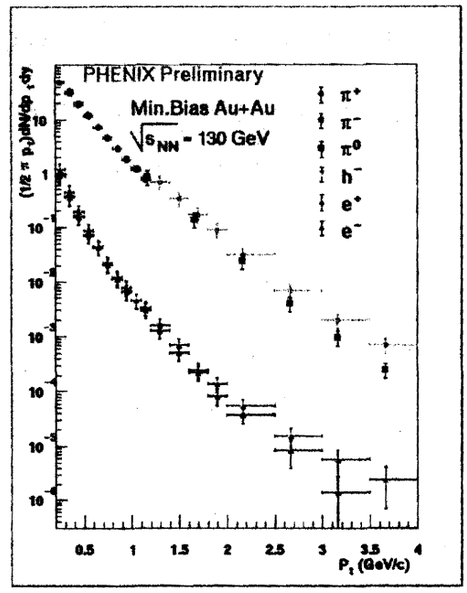

BROOKHAVEN NATIONAL LABORATORY

di-electrons

- not enough integrated luminosity from RHIC to do J/Ψ this last year
- will be possible in this coming run

the true believer sees J/Ψ's here!

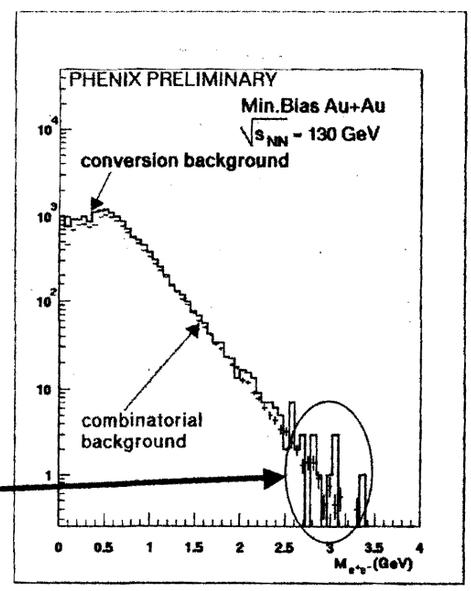

BROOKHAVEN NATIONAL LABORATORY

what didn't I talk about?

- event-by-event fluctuations
- strangeness production
  - soon to be charm production
- slope parameters from p_T, m_T spectra
- equilibration questions
  - baryochemical potential, freeze-out parameters
- direct photons
- literally, dozens of other things!

BROOKHAVEN NATIONAL LABORATORY

summary

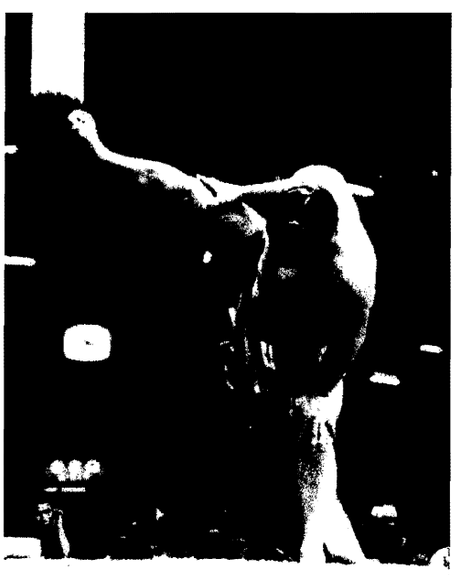

- huge quantity of experimental results - RHIC works!
- collision environment has high energy density, low baryon density, very strong dynamics
- particle composition, flow, π^0 p_T spectra all point promisingly in direction of jet quenching
- spin commissioned
- vector mesons coming with luminosity
- experiments getting new detectors
- next run A+A at full energy, high statistics, polarized p+p too!
- RHIC has stomped onto the physics scene - *ozeki* last year, *yokozuna* this year!

BROOKHAVEN NATIONAL LABORATORY

Measurements of Global Variables at PHENIX

Kensuke Homma for the PHENIX collaboration

Hiroshima University

Measurements of global variables are the first key step to understand a full picuture of dynamical evolution of nucleus-nucleus collisions. I will present the results of measurements on the multiplicity of charged particles and the distribution of transverse energy as seen in the PHENIX during the first year's run. In addition to those rather established measurements as the first year's results, I will also discuss a prospect to measure event-by-event fluctuations as one of important global variables in the PHENIX.

Measurements of Global Variables at PHENIX

Kensuke Homma
Hiroshima Univ., Japan

On behalf of the PHENIX Collaboration

Contents

- **Charged Particle Multiplicity and Transverse Energy in Au+Au Collisions at $\sqrt{s_{NN}}$ = 130 GeV**
  (Nucl-exp/0012008 submitted to PRL)

- **Prospects to search for anomalous event-by-event fluctuations**

Charged Particle Multiplicity and Transverse Energy

- **Introduction:**

  Importance of N_{ch} and E_t measurements
- **The PHENIX detector.**
- **Experimental results:**

  $dN_{ch}/d\eta$ distribution at mid-rapidity

  $dE_t/d\eta$ distribution at mid-rapidity

  Centrality determination
- **Results and discussion:**

  Comparison to model predictions

  Comparison to CERN and AGS data
- **Conclusions.**

Global variables: E_t and N_{ch}

- **Initial conditions, energy density of the system.**

x **Scaling with $\sqrt{s}$.**

x **Mechanism of particle production, soft vs hard?**

Soft: $N_{ch} \propto N_{part}$

Hard: $N_{ch} \propto N_{coll}$

x **Constrain theoretical predictions.**

Theoretical Predictions

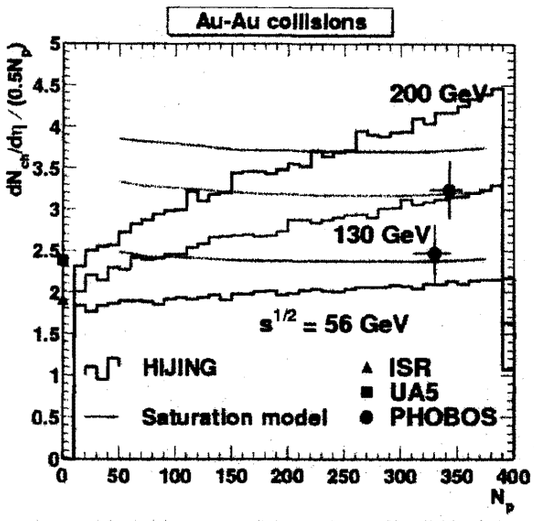

- **Various models predict different trends for $(dN_{ch}/d\eta)/N_{part}$ vs N_{part}:**

  HIJING: (Wang, Gyulassy, nucl-th/0008014)
  $(dN_{ch}/d\eta)/N_{part}$ increases with N_{part}

  Saturation model: (Eskola, Kajantie, and Tuominen hep-ph/0009246)
  $(dN_{ch}/d\eta)/N_{part}$ constant vs N_{part}

PHENIX-Setup: Beam View

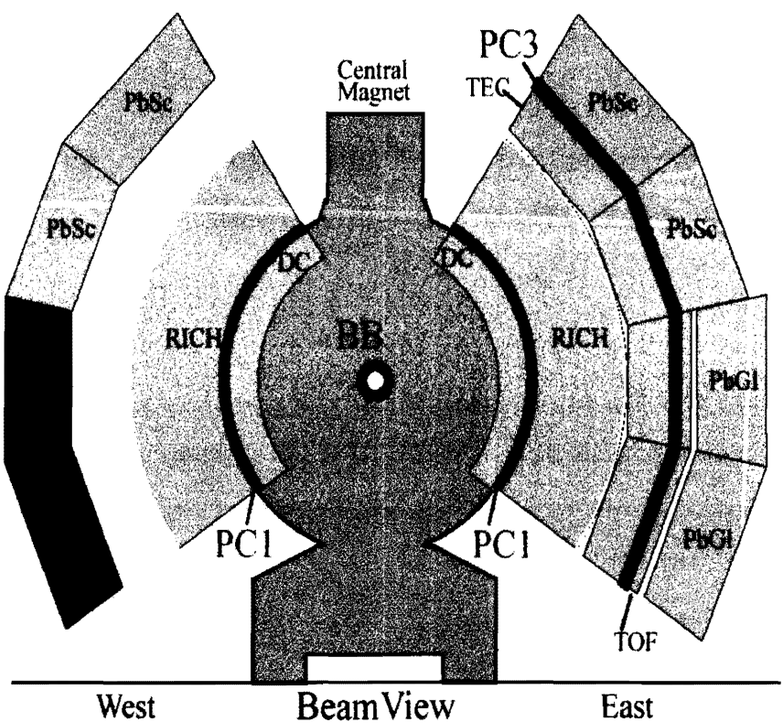

- **Pad Chambers:**

  $R_{PC1} = 2.5$ m
  $R_{PC3} = 5.0$ m

  $|\eta| < 0.35$, $\Delta\phi = 90^o$

  8 x 4320 pads.

  $\varepsilon > 99\%$, $\sigma \sim 2$ mm

- **Lead Scintillator EMCal.**

  $R_{EMCal} = 5.1$ m.

  $|\eta| < 0.38$, $\Delta\phi = 45^o$

  2 x 2592 PMT

  $18X_0$, $\sigma \sim 8\%$ for 1GeV γ-quanta

PHENIX-Setup: Side View

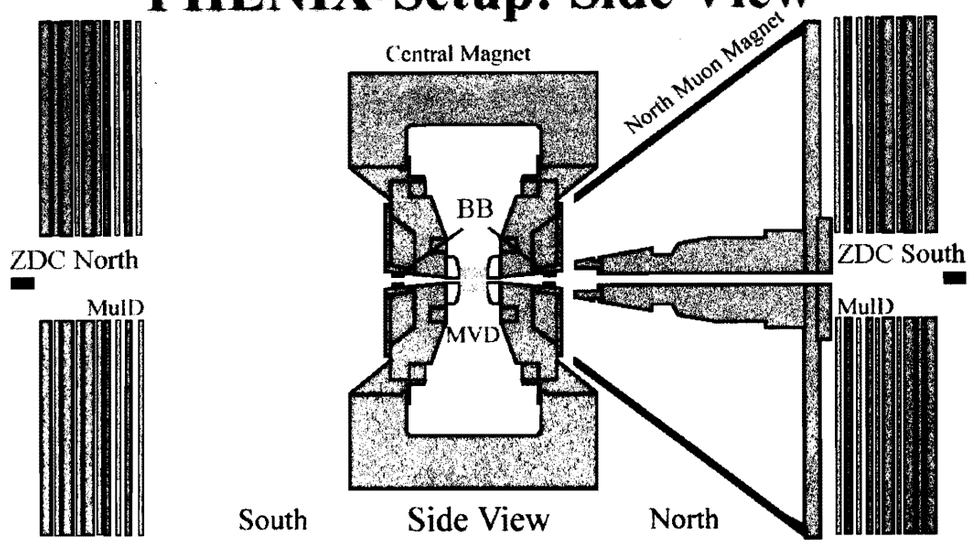

- **Zero Degree Calorimeters**

  Spectator neutrons with $|\eta| > 6$

  $|Z|=18.25$ m

- **Beam Beam Counters**

  64 Cherenkov quartz counters with PMT readout

  $3.0 < |\eta| < 3.9$ $\Delta\phi = 360°$

Trigger and event selection

- **BBC trigger:**

  Coincidence of both BBC
  (at least two photomultipliers fired in each BBC).

  Corresponds to (92 ± 2)% of the geometrical Au-Au cross section ($\sigma_{geo.}$ = 7.2 b).

- **ZDC trigger:**

  Coincidence of both ZDC (E > 10 GeV)

  Includes mutual Coulomb dissociation processes

  97.8% of the BBC trigger events also satisfy ZDC trigger condition.

- **Event vertex restriction:**

  $|Z| < 20$ cm around centre of interaction region.

Charged Multiplicity Determination

- **Procedure: count tracks on a statistical basis, no explicit track reconstruction :**

  Combine all hits in PC3 with all hits in PC1.

  Project resulting lines onto a plane through the beam line.

  Count tracks within a given radius.

  Determine combinatorial background by event mixing

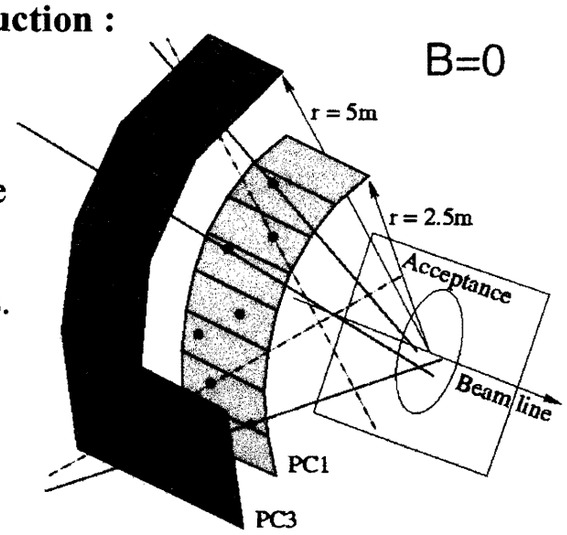

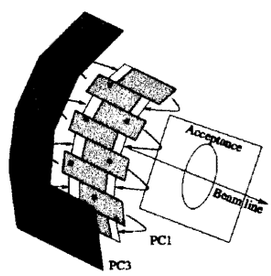

Track Vertex Distribution

- **3 contributions:**

  Peak at low R: primary particles coming from the event vertex

  Combinatorial background: $dN_B/dR \propto R$

  Exponential tail: in-flight decays

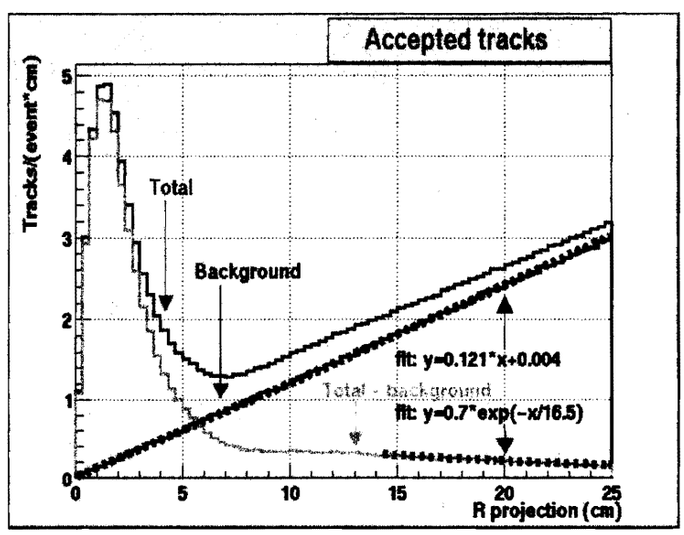

- **Number of tracks per event:**

  Subtract average background on an event-by-event basis

  Count all tracks within R=25 cm
  ($\overset{10}{\Rightarrow}$ 95.9% of all tracks)

Minimum-bias multiplicity distribution at $\sqrt{s_{NN}}$ = 130 GeV

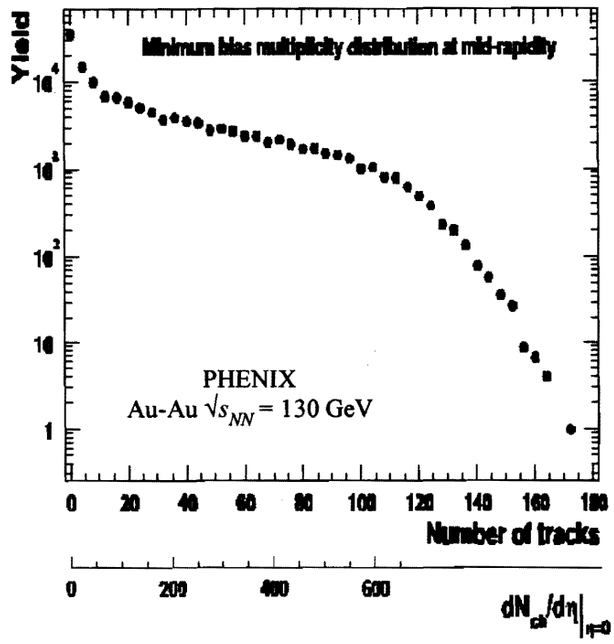

- **92% of σ_{geo} (Missing events are all in the lowest bins)**
- **Shape at high multiplicities determined by fluctuations due to limited acceptance.**
- **Scaling factor (geometry) to one unit of rapidity 5.82 (lower axis).**

Feb 14, 2001

EMCal energy response

- **Energy scale:**

  EMCal measures full energy of γ and $e^{\pm}$

  Slow hadrons are absorbed in EMCal

  Relativistic hadrons produce MIP peak

- **EMCal energy response proportional to E_t:**

  $E_t = 1.17 \pm 0.05\ E_t^{EMCal}$

  EMCal energy resolution not important for the E_t measurement

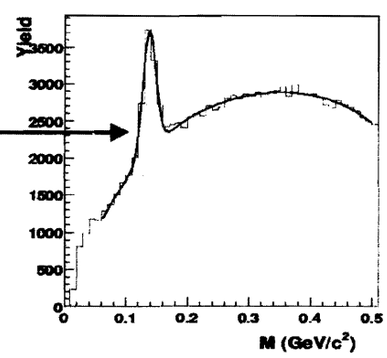

π^0 peak at 136.7 MeV/c^2

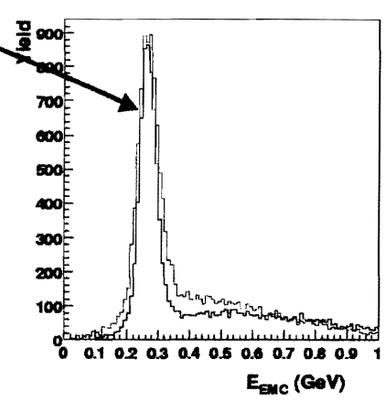

Red curve: Au-Au data. MIP peak at 270 MeV

Blue curve is AGS test beam data with π^+

12

Feb 14, 2001

Minimum-bias transverse energy distribution at $\sqrt{s_{NN}}$ = 130 GeV

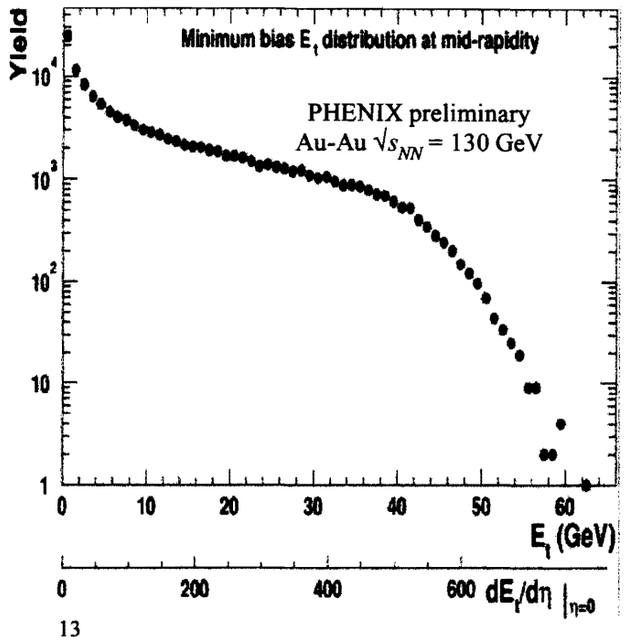

- **92% of σ_{geo} (Missing events are all in the lowest bins)**
- **Shape at high multiplicities determined by fluctuations due to limited acceptance.**
- **Scaling factors:**
  - Transformation 1.17
  - Dead areas 1.03
  - Geometry 10.6

13 Feb 14, 2001

Centrality dependence

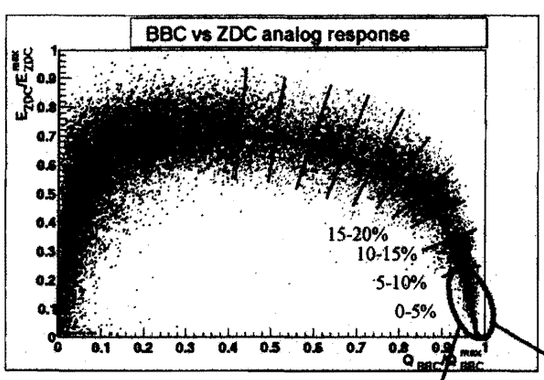

- **Use BBC – ZDC response to define centrality cuts (in 5% bins of σ_{geo})**
- **Determine $\langle dN_{ch}/d\eta \rangle$ and $\langle dE_t/d\eta \rangle$ vs centrality**

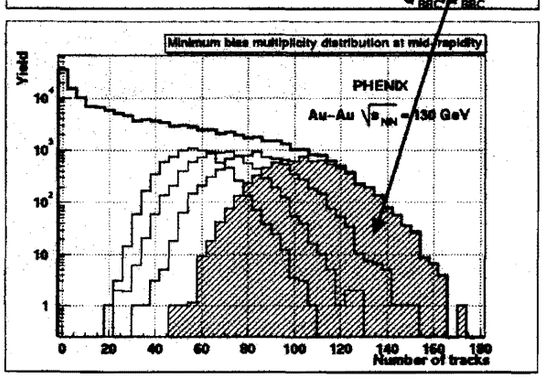

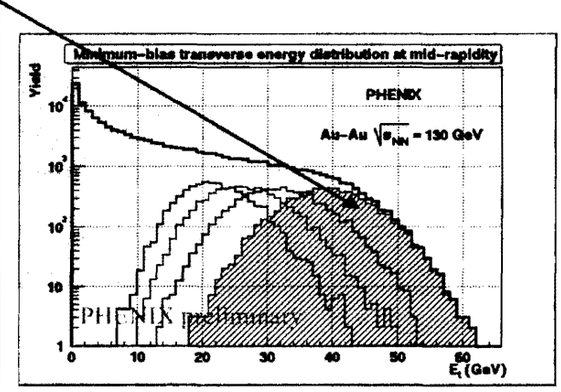

Calculation of N_{part} and N_{coll}

- **Use simulated BBC – ZDC response to define centrality cuts.**
- **Relate them to N_{part} and N_{coll} using Glauber model.**

Straight-line nucleon trajectories

Constant $\sigma_{NN}=(40 \pm 5)mb$.

Woods-Saxon nuclear density:

$$\rho(r)=\rho_o \cdot \frac{1}{1+\exp\left(\frac{r-R}{d}\right)}$$

$$R=1.19A^{1/3}-1.61A^{-1/3}=(6.65\pm0.03)fm$$

$$d=(0.54\pm0.01)fm$$

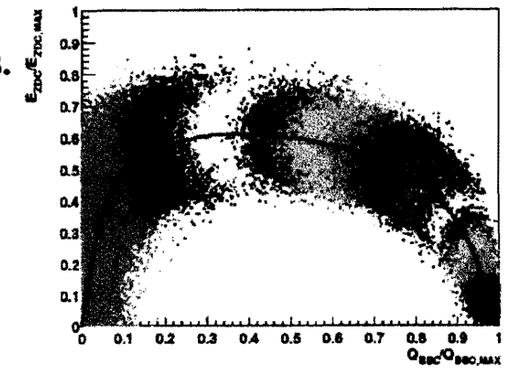

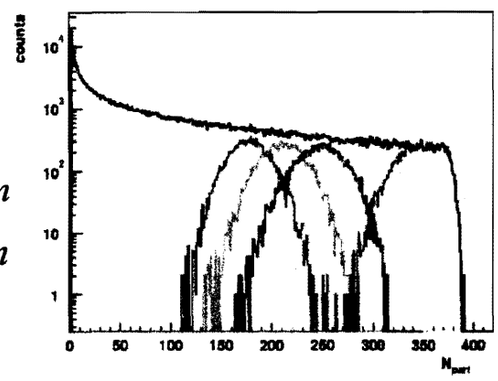

15

Centrality dependence

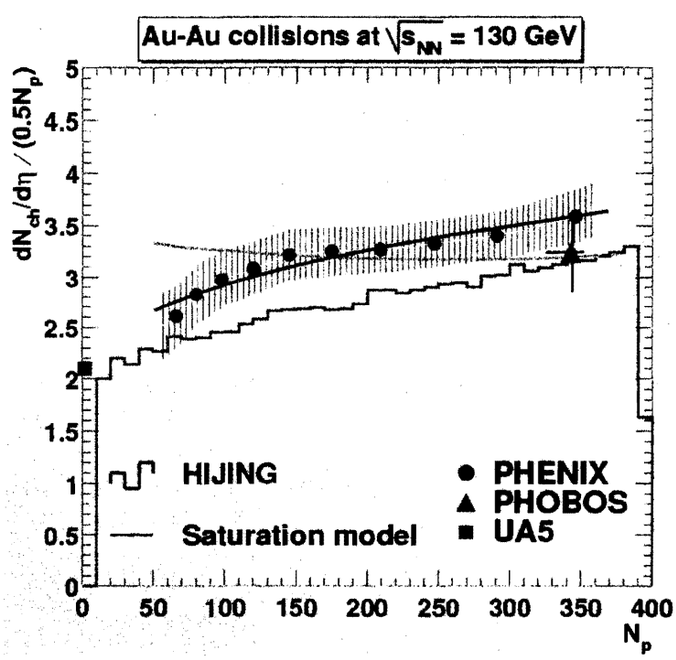

- **Data shows clear increase of $dN_{ch}/d\eta$ per participant vs N_{part}**

In contrast with EKRT saturation model

Similar to HIJING (although data ~15% higher)

16

Feb 14, 2001

Particle production mechanism

$$dX/d\eta\big|_{\eta=0} = A\times N_{part} + B\times N_{coll}$$

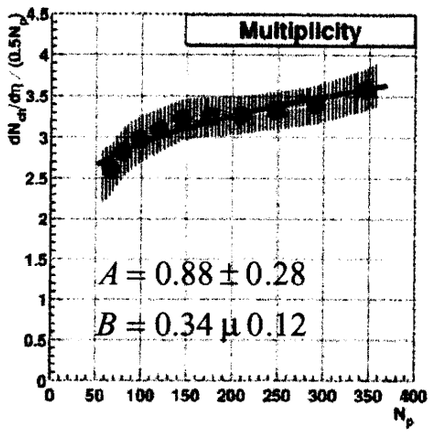

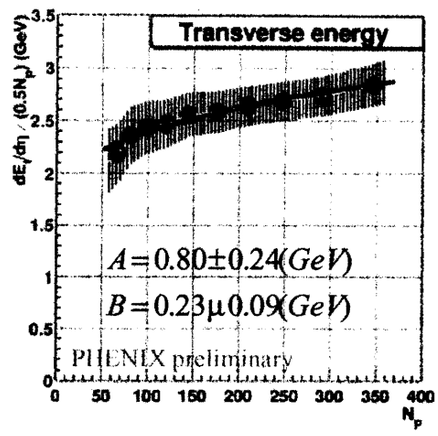

- **Consistent results:**
  $B/A = 0.38 \pm 0.19$ $\qquad$ $B/A = 0.29 \pm 0.18$
- **Hard processes contribution increases with centrality: from ~30% mid-central to ~50% most central**

Comparison to CERN results

$$dX/d\eta\big|_{\eta=0} \propto N_{part}^{\alpha}$$

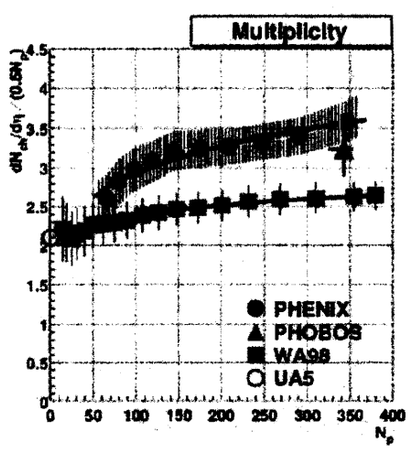

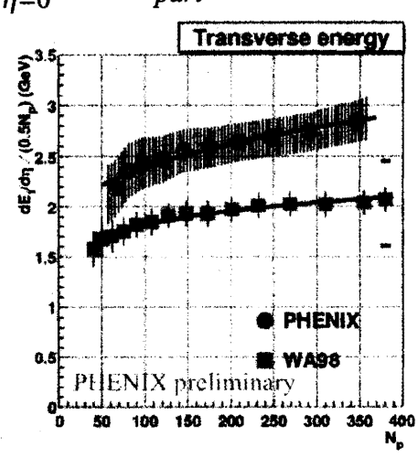

α-value	Multiplicity	Transverse energy
PHENIX	1.16 ± 0.04	1.13 ± 0.05
WA98	1.07 ± 0.04	1.08 ± 0.06
WA97	1.05 ± 0.05	

Transverse energy per charged particle

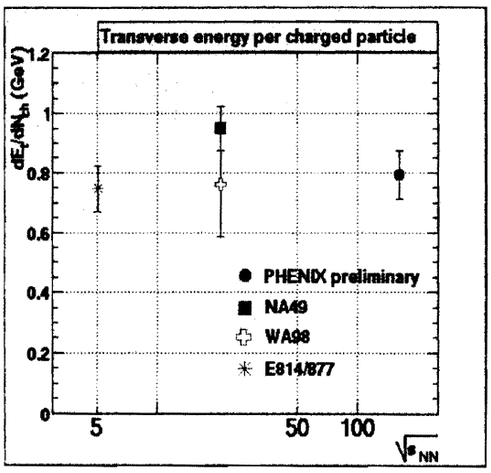

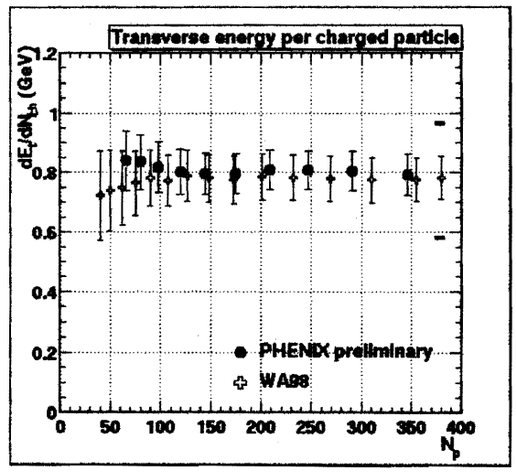

dE_t/dN_{ch} **independent of** $\sqrt{s_{NN}}$ dE_t/dN_{ch} **independent of** N_{part}

$\sqrt{s_{NN}}$ dependence

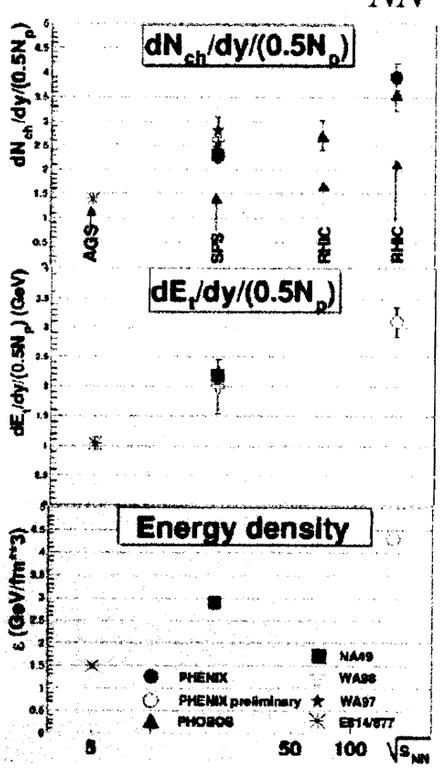

- **Assumptions:**

  in Lab $\frac{dX}{dy} \approx \frac{dX}{d\eta}$ in C.M. $\frac{dX}{dy} \approx 1.1\frac{dX}{d\eta}$

- **Energy density (Bjorken):**

  $$\varepsilon = \frac{1}{\pi R^2 \tau}\frac{dE_t}{dy} \qquad R = 1.12A^{1/3} \qquad \tau = 1 fm/c$$

- **From SPS to RHIC**

  ~50% increase in dN_{ch}/dy

  ~50% increase in dE_t/dy

  at least 50% increase in ε

Conclusions on Nch and Et

- **Centrality dependence of particle $dN_{ch}/d\eta$ and $dE_t/d\eta$ have been measured in $\sqrt{s_{NN}}$ = 130 GeV Au+Au collisions.**
- **Both $dN_{ch}/d\eta$ and $dE_t/d\eta$ per participant increase with centrality:**
  - in qualitative agreement with HIJING
  - in contrast to EKRT saturation model prediction
  - the increase is stronger than at SPS
- **dE_t/dN_{ch} is independent of centrality and of $\sqrt{s_{NN}}$.**

Prospect to Search for Anomalous Event-by-Event Fluctuations

Focus of this talk

- ☐ Construct an analysis framework to search for anomalous fluctuations.
- ☐ Check if the frame work is applicable to a measurement of isospin fluctuations.

Motivation

Introduction

Search for anomalous event-by-event fluctuations on the conserved quantum numbers;

$$A_q \equiv \frac{N_q - N_{\bar{q}}}{N_q + N_{\bar{q}}}$$

where q can be any conserved quantum numbers like *charge*, *baryon number* and *isospin*.

Fluctuation scenarios

a) Most probable Aq is same as standard values, but the size of fluctuation is different from the statistical fluctuation
=> Net charge fluctuations

b) Most probable Aq deviates from standard values => DCC

Assuming anomalous fluctuations could occur at any location and at any size of phase space=> Need multi-resolution analysis

Discrete Wavelet Analysis

2^j bins, j=8
Input Signal

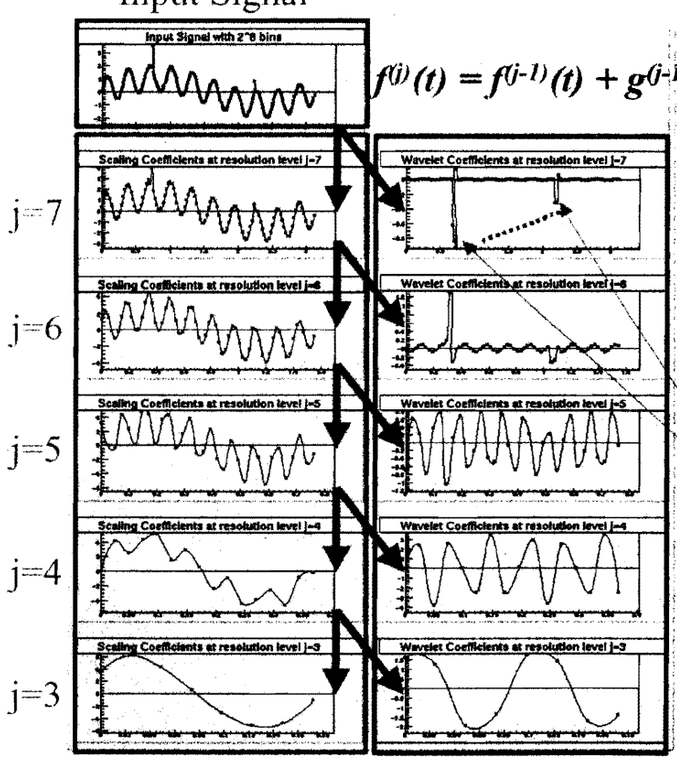

$$f^{(j)}(t) = f^{(j-1)}(t) + g^{(j-1)}(t)$$

Scaling Coefficient $c^{(j)}{}_k$

$$f^{(j)}(t) = \sum_{k=0}^{2^j-1} c^{(j)}{}_k \phi(2^j t - k)$$

Wavelet Coefficient $d^{(j)}{}_k$

$$g^{(j)}(t) = \sum_{k=0}^{2^j-1} d^{(j)}{}_k \psi(2^j t - k)$$

Power Function $P^{(j)}$

$$P^{(j)} = \frac{1}{2^j} \sum_{k=0}^{2^j-1} | d^{(j)}{}_k |^2$$

Observable !

Analyzed by Daubechies3 wavelet

Fluctuation Scenario a)

Introduce artificial rapidity correlation between neutral and charged pions to realize smaller fluctuation size.

$$A_{I_z}(\eta_k) = \frac{N_{\pi^\pm}(\eta_k)/2 - N_{\pi^0}(\eta_k)}{N_{\pi^\pm}/2 + N_{\pi^0}}$$

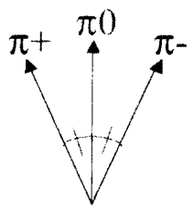

$\Delta\eta = 0.7/2^N$

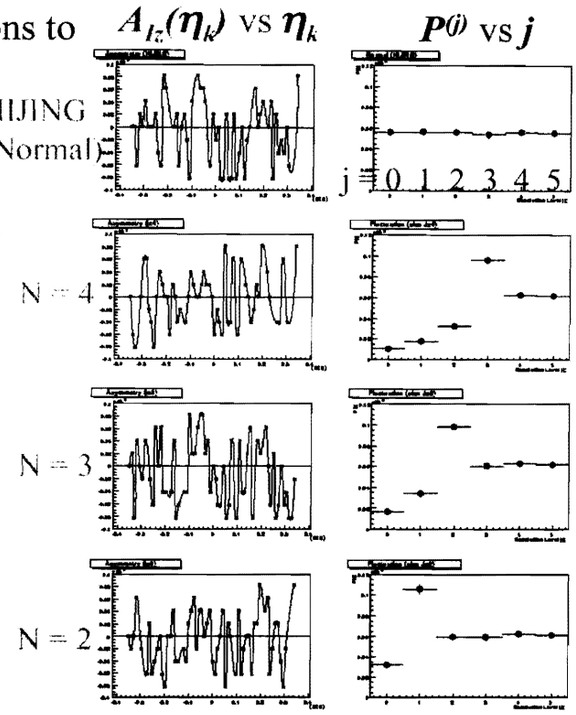

25

Fluctuation Scenario b)

Enhance neutral pions in a rapidity bin by taking 30% neutral pions out of total generated neutral pions.

$$A_{I_z}(\eta_k) = \frac{N_{\pi^\pm}(\eta_k)/2 - N_{\pi^0}(\eta_k)}{N_{\pi^\pm}/2 + N_{\pi^0}}$$

Enhance π^0 in $\Delta\eta = 0.7/2^N$

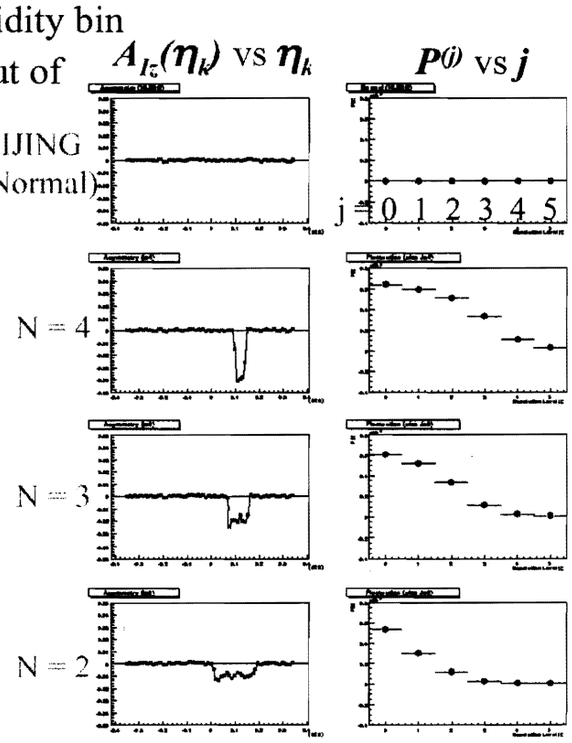

26

Data Analysis

$$A_{I_Z} = \frac{N_{\pi^\pm}/2 - N_{\pi^0}}{N_{\pi^\pm}/2 + N_{\pi^0}} \approx \frac{N_{\pi^\pm} - N_\gamma}{N_{\pi^\pm} + N_\gamma}$$

$$A_{I_Z}(\eta_k) \equiv \frac{N_{PC1}(\eta_k) - N_{\gamma-likeEMCal}(\eta_k)}{N_{PC1} + N_{\gamma-likeEMCal}} \quad \text{in W0+W1}$$

Run selection

one of B-field off runs, run 12426 was used in which obvious detector anomalies could not be seen.

DST version

V03 (available in /phenix/data13/dst_data_v03)

Event selection

1. Trigger selection: ZDC&&BBC (0x4000)
2. PC1 Z-vertex: |Zpc1|< 20 cm
3. Photon selection:
   corrected EMCal energy, ecore > 0.1 GeV
   corrected EMCal ToF, -1.5<tcorr<2.5 ns
4. Rejection of PC1 associated EMCal cluters:
   only for EMCal cluster with ecore < 0.7 GeV,
   EMCal clusters with $d_{EMCal\text{-}PC1}$ < 10 cm were rejected as hadron like clusters, where $d_{EMCal\text{-}PC1}$ is a closest approach distance between a PC1 extrapolated line and a EMCal cluster.
5. Centrality selection: divide into five 20% percentile bins.

After trigger and Z-vertex selection

Data: Red
HIJING: Blue

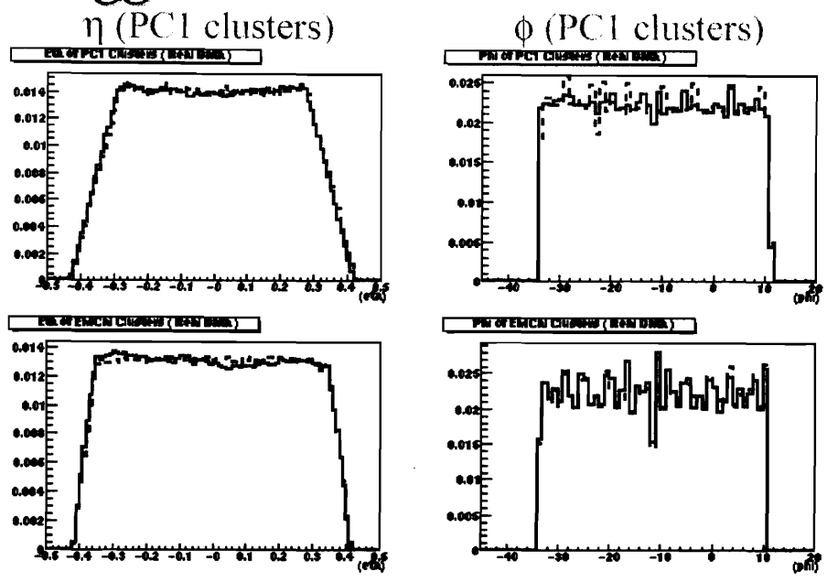

No obvious detector anomaly is seen !

29

Feb 14, 2001

Photon selection

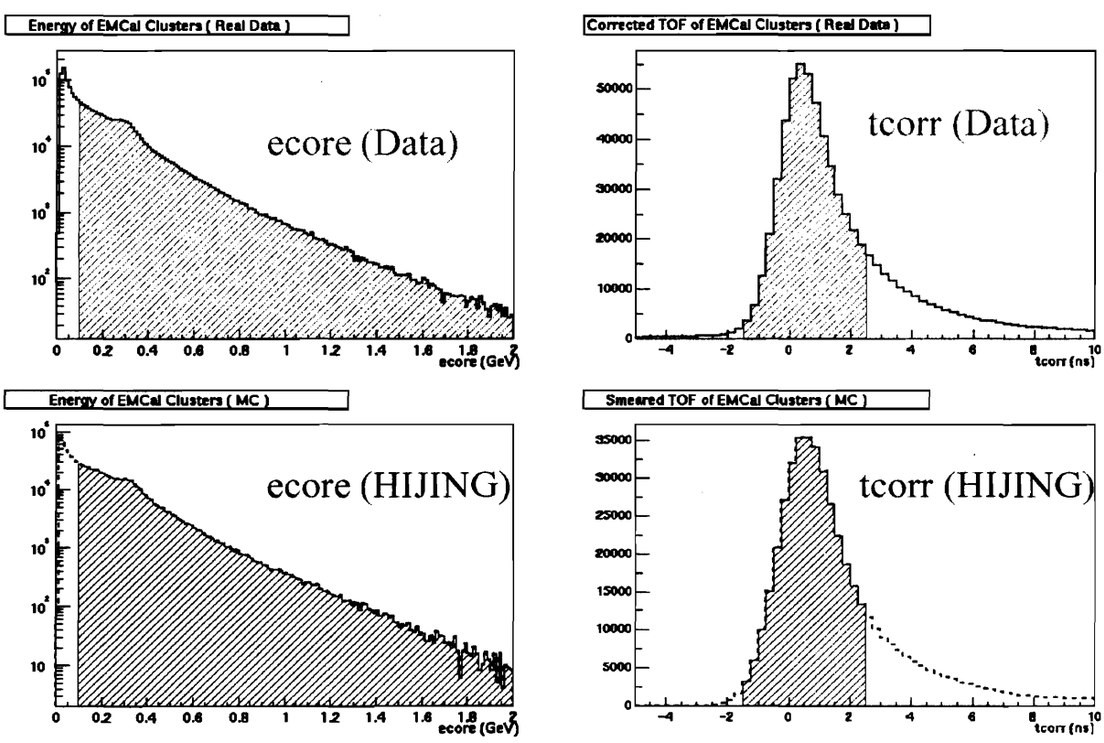

Rejection of PC1 associated EMCal cluters

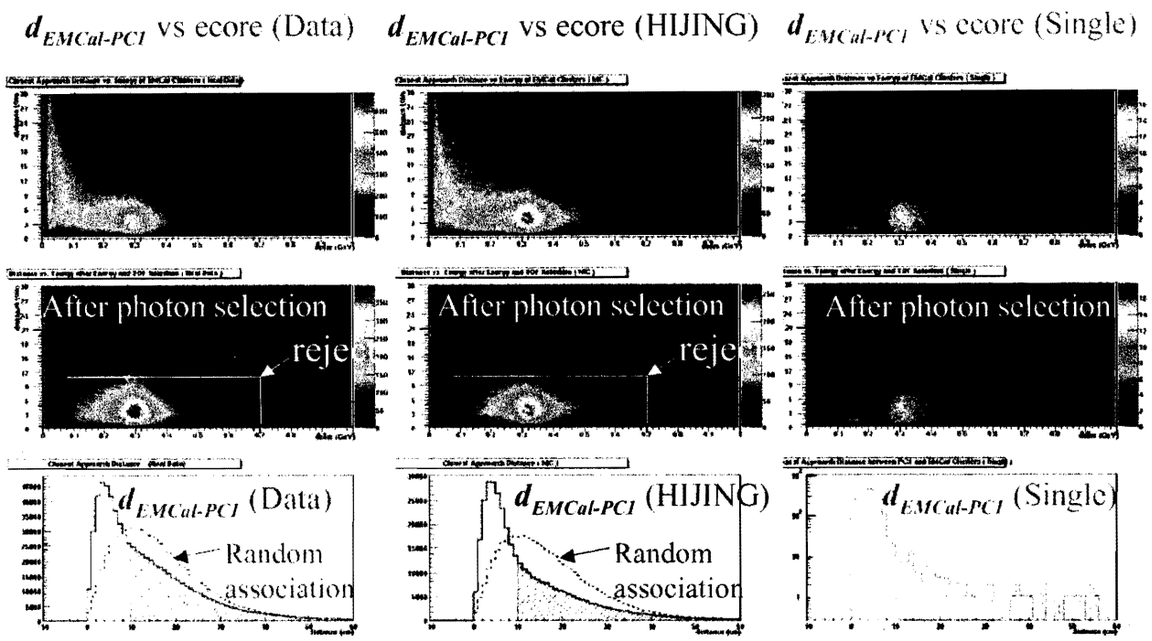

Multiplicity Correlation

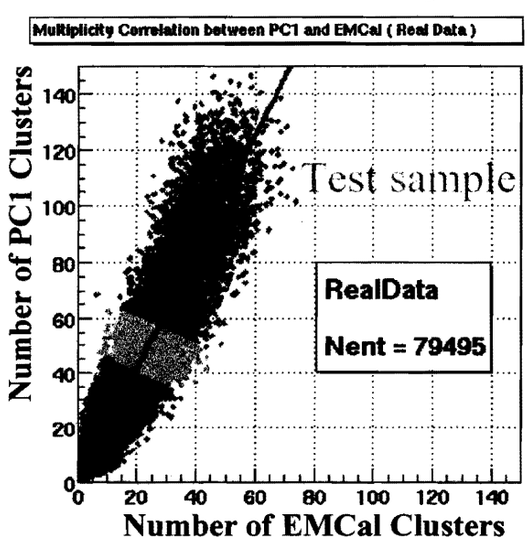

Multiplicity correlation between PC1 and EMCal (Data)

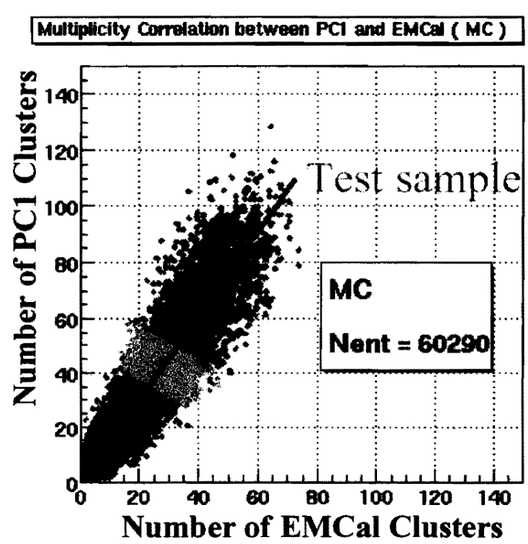

Multiplicity correlation between PC1 and EMCal (HIJING)

$d^{(j)}{}_k$ and $P^{(j)}$ by Haar Wavelet Analysis

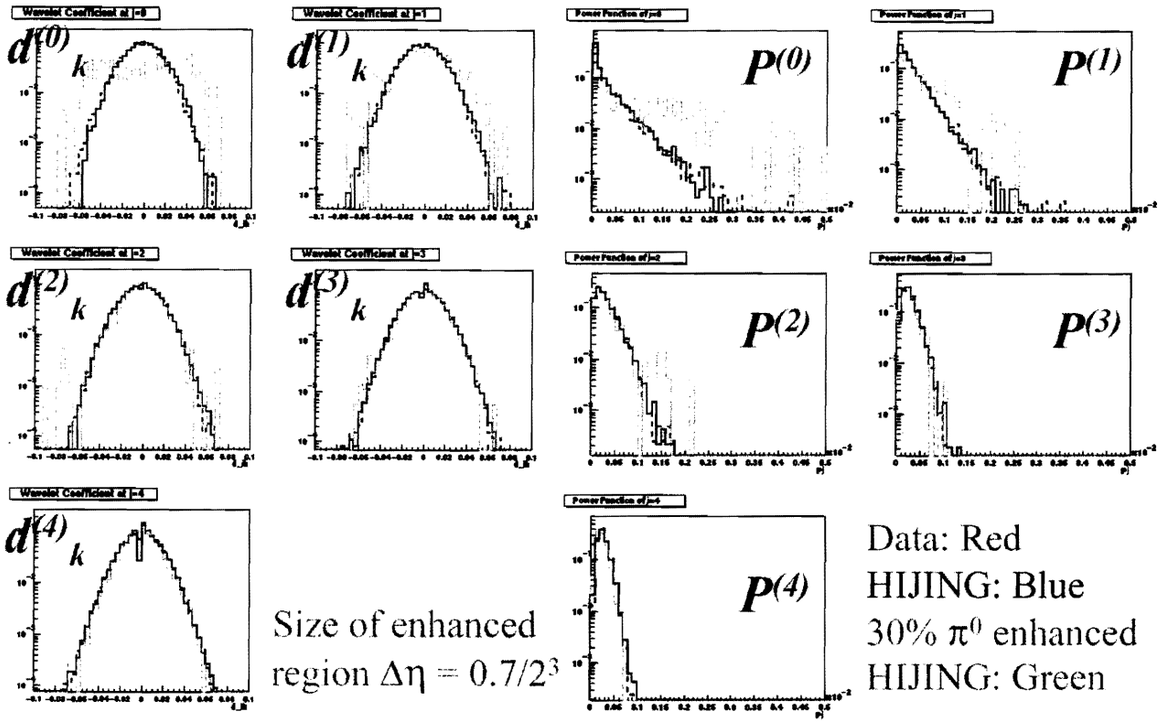

Size of enhanced region $\Delta\eta = 0.7/2^3$

Data: Red
HIJING: Blue
30% π^0 enhanced
HIJING: Green

Resolution Level Dependence

Data: Red

HIJING: Blue

30% π^0 enhanced
HIJING: Green

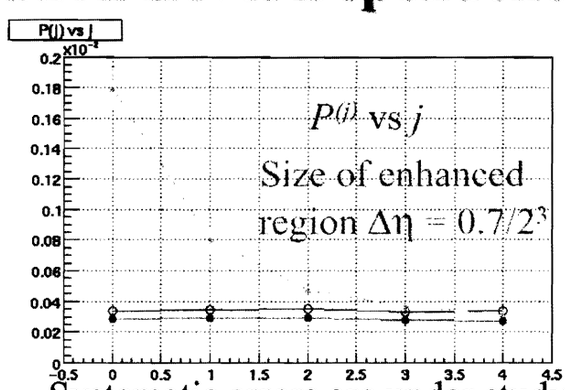

Systematic errors are under study

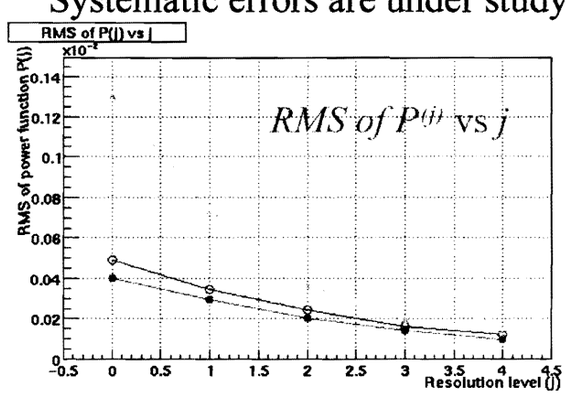

Summary of Fluctuation Study

- We found that the wavelet analysis is an effective way to search for anomalous fluctuations under the PHENIX environment.
- We still need careful study to discuss any physics at this stage.

PHENIX

First results from the STAR experiment at RHIC
Part1
and
Part2 (soft hadron physics)

Akio Ogawa (Penn. State Univ.) for part1
and
Masashi Kaneta (LBL) for part2
for the STAR Collaboration

The Solenoidal Tracker At RHIC (STAR) is a large acceptance detector capable of tracking charged particles and measuring their momenta in the expected high multiplicity environment at RHIC. STAR also has an excellent capability of particle identification. Therefore, our focus of physics is not only identified hadron distribution but event-by-event base analysis. In summer 2000, Relativistic Heavy Ion Collider (RHIC) at Brookhaven National Laboratory had the first operation. We will report the first results from STAR obtained in Au+Au collisions at $\sqrt{s} = 130$ AGeV. In this workshop, we will address single particle spectra, particle correlation, event anisotropy, and event-by-event fluctuations. Additionally, our characteristic physics program, ultra peripheral collisions, will be mentioned.

First Results from STAR Experiment at RHIC -Overview & high pT -

Ogawa Akio
Penn State Univ. / BNL
For the STAR collaboration

2001 Feb 14
CNS workshop at Tokyo Univ.

1

The STAR Collaboration

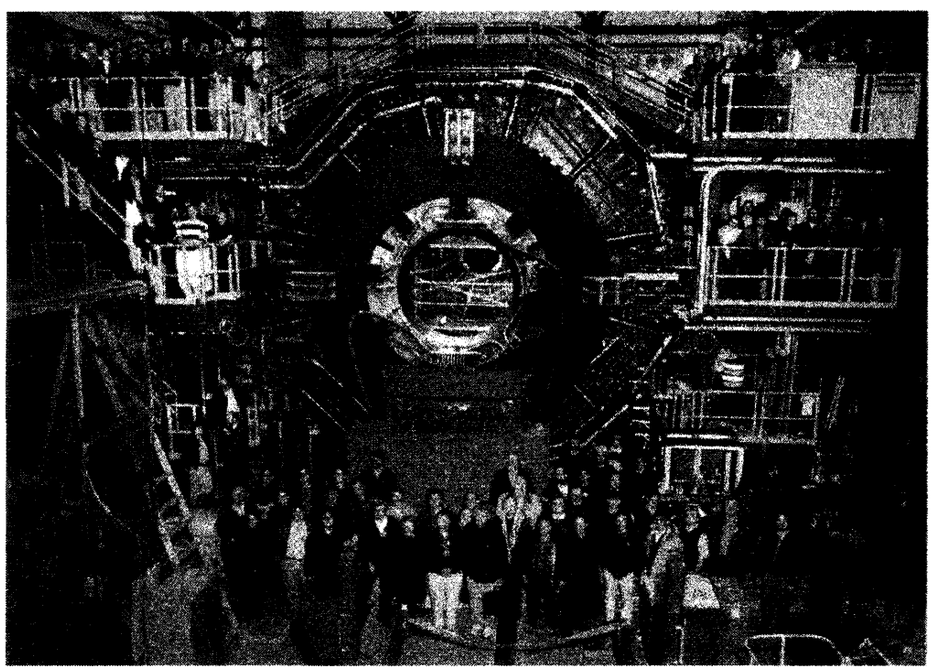

~ 400 collaborators 34 institutions 8 countries

2

STAR Institutions

U.S. Labs:

Argonne, Berkeley, and Brookhaven National Labs

U.S. Universities:

Arkansas, UC Berkeley, UC Davis, UCLA, Carnegie Mellon, Creighton, Indiana, Johns Hopkins, Kent State, MIT, MSU, CCNY, Ohio State, Penn State, Purdue, Rice, UT Austin, Washington, Wayne State, Yale

China:

IHEP - Beijing
IPP - Wuhan

Brazil:

Universidade de Sao Puolo

England:

University of Birmingham

France:

Institut de Recherches Subatomiques Strasbourg, SUBATECH - Nantes

Germany:

Max Planck Institute – Munich
University of Frankfurt

Poland:

Warsaw University
Warsaw University of Technology

Russia:

MEPHI – Moscow, LPP/LHE JINR – Dubna, IHEP - Protvino

3

STAR Detector

Year1 detectors

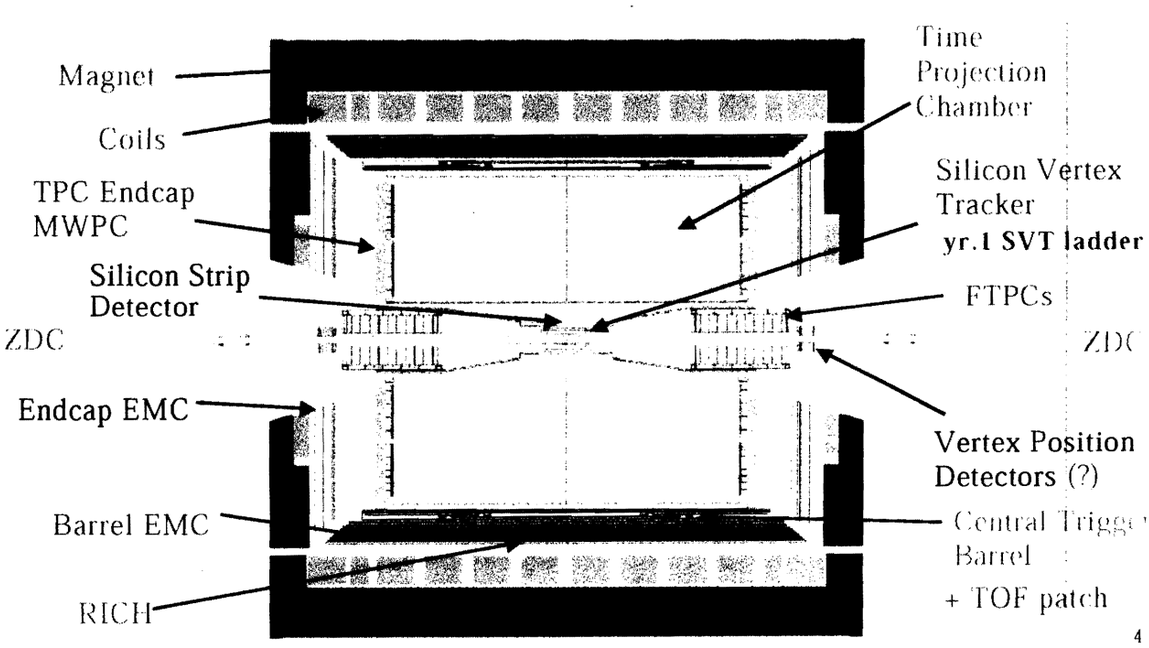

4

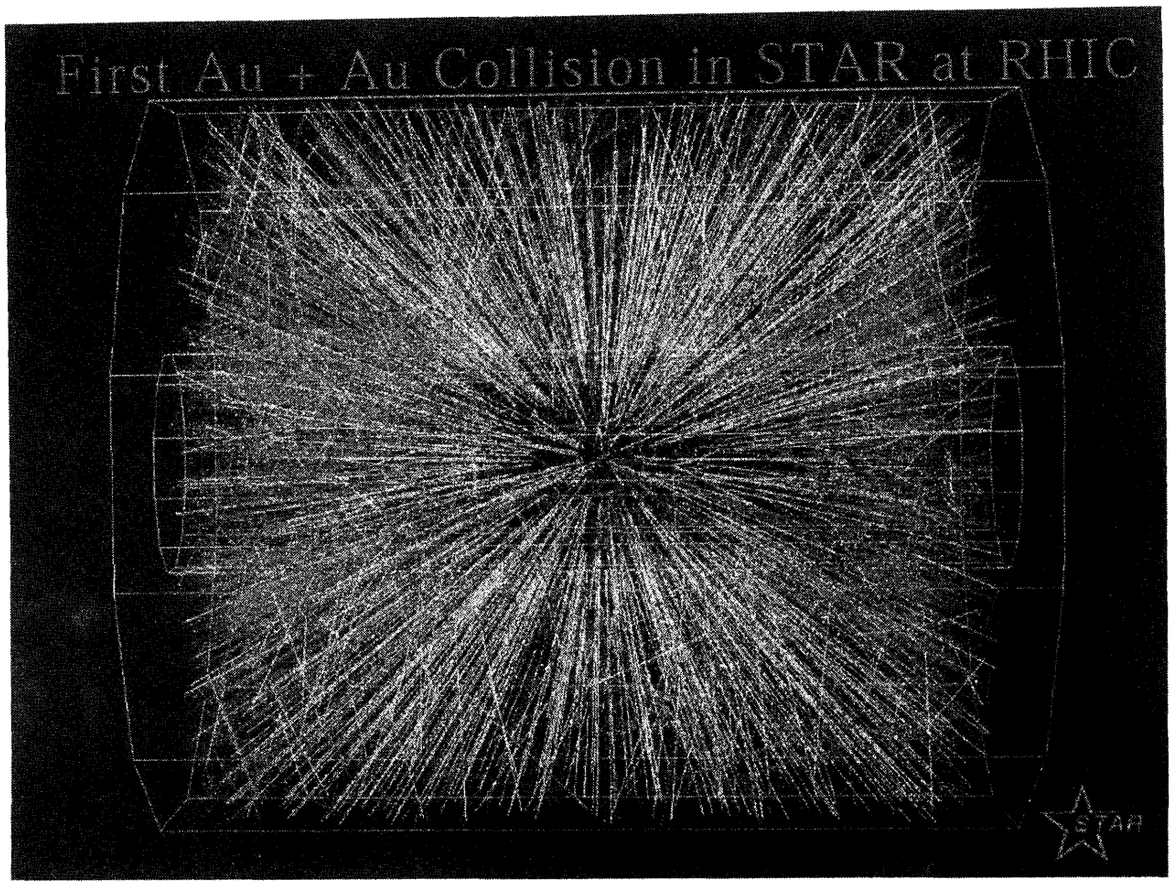
First Au + Au Collision in STAR at RHIC
STAR

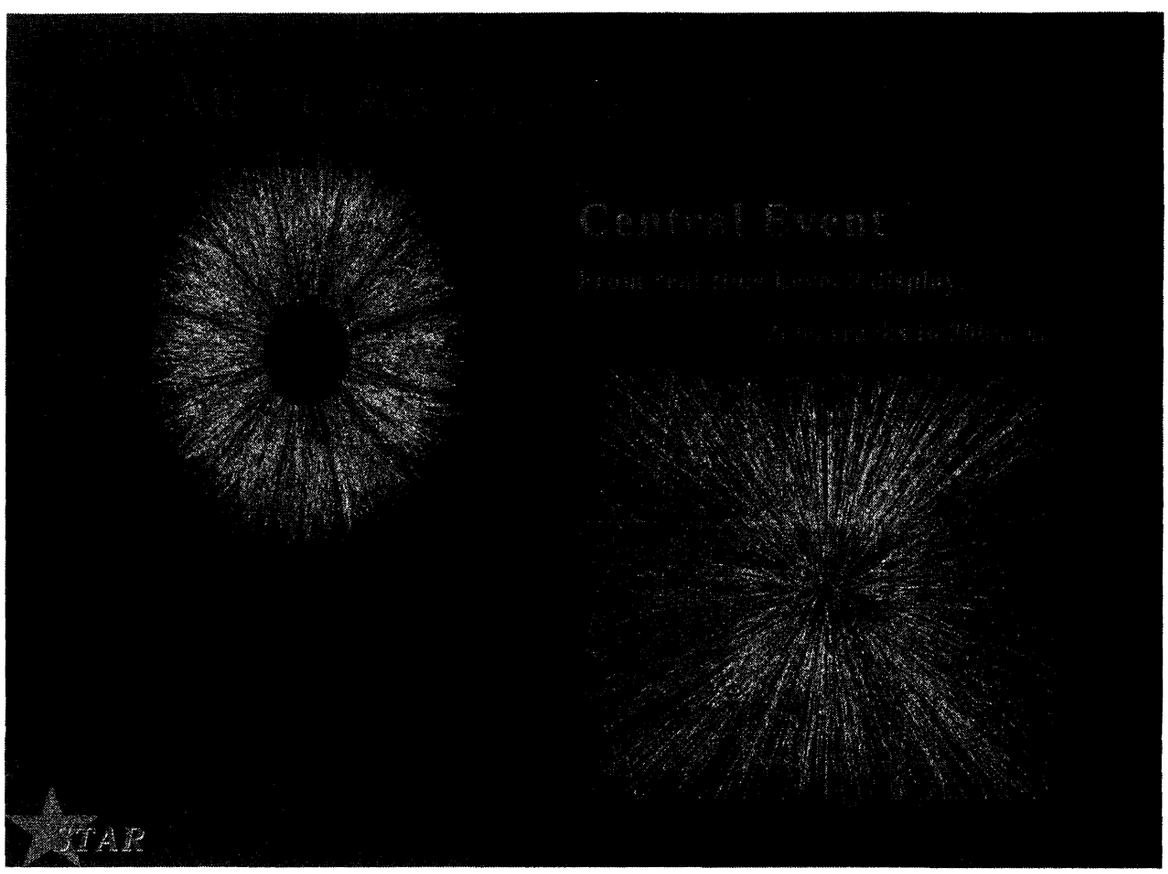
Central Event
STAR

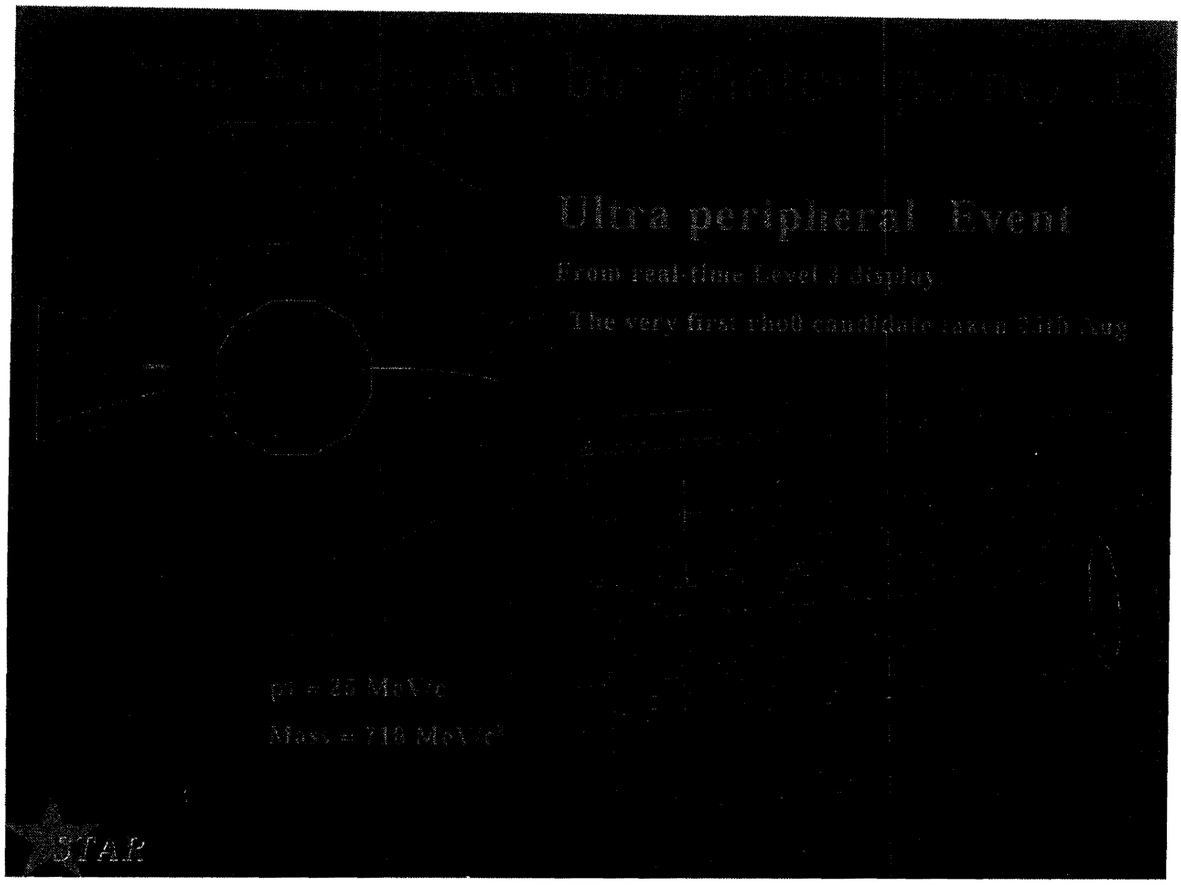

Particle ID Techniques

STAR

dE/dx

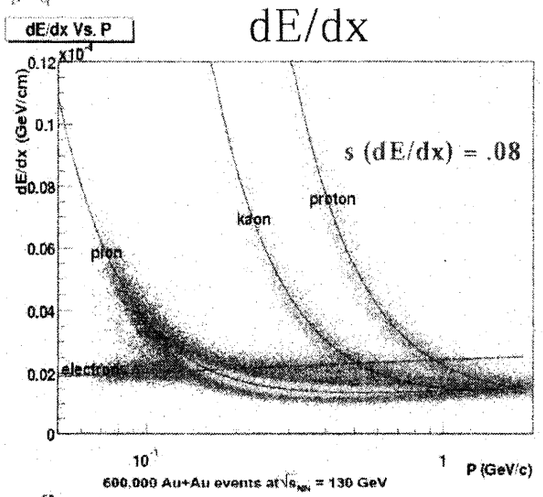

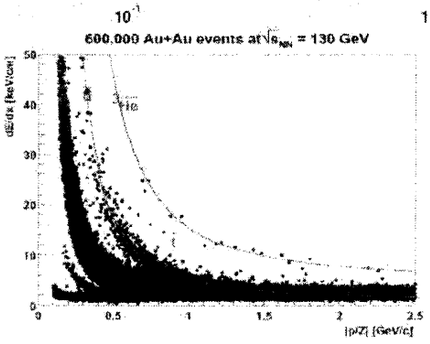

RICH

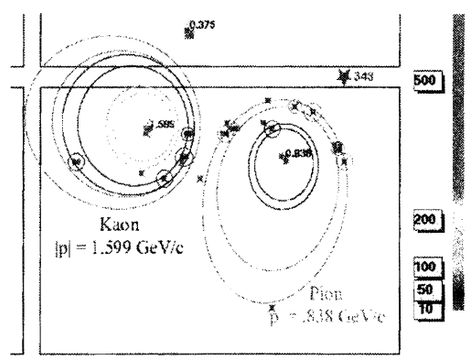

RICH PID range

1 - 3 GeV/c for K/π

1.5 - 5 GeV/c for K/p

dE/dx PID range:

~ 0.7 GeV/c for K/π

~ 1.0 GeV/c for K/p

8

Particle ID

Topology

Secondary vertex:
$K_s \rightarrow \pi + \pi$, $\Lambda \rightarrow p + \pi$,
$\Xi \rightarrow \Lambda + \pi$, $\Omega \rightarrow \Lambda + K$
$\gamma \rightarrow e^+ + e^-$

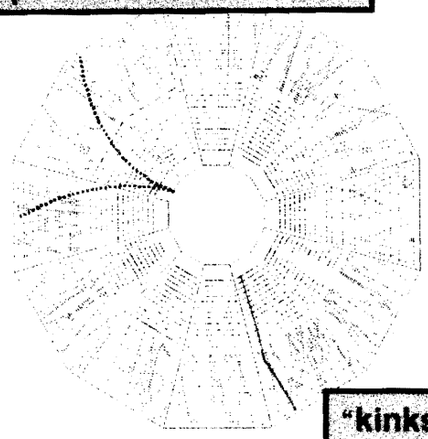

"kinks"
$K^{\pm} \rightarrow \mu^{\pm} +$

Combinatorics

$K_s \rightarrow \pi^+ + \pi^-$ $\phi \rightarrow K^+ + K^-$
$\Lambda \rightarrow p + \pi$ $\rho \rightarrow \pi^+ + \pi^-$

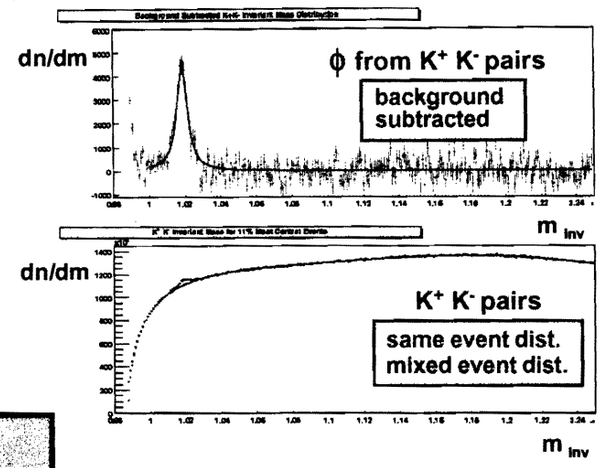

9

STRANGENESS!

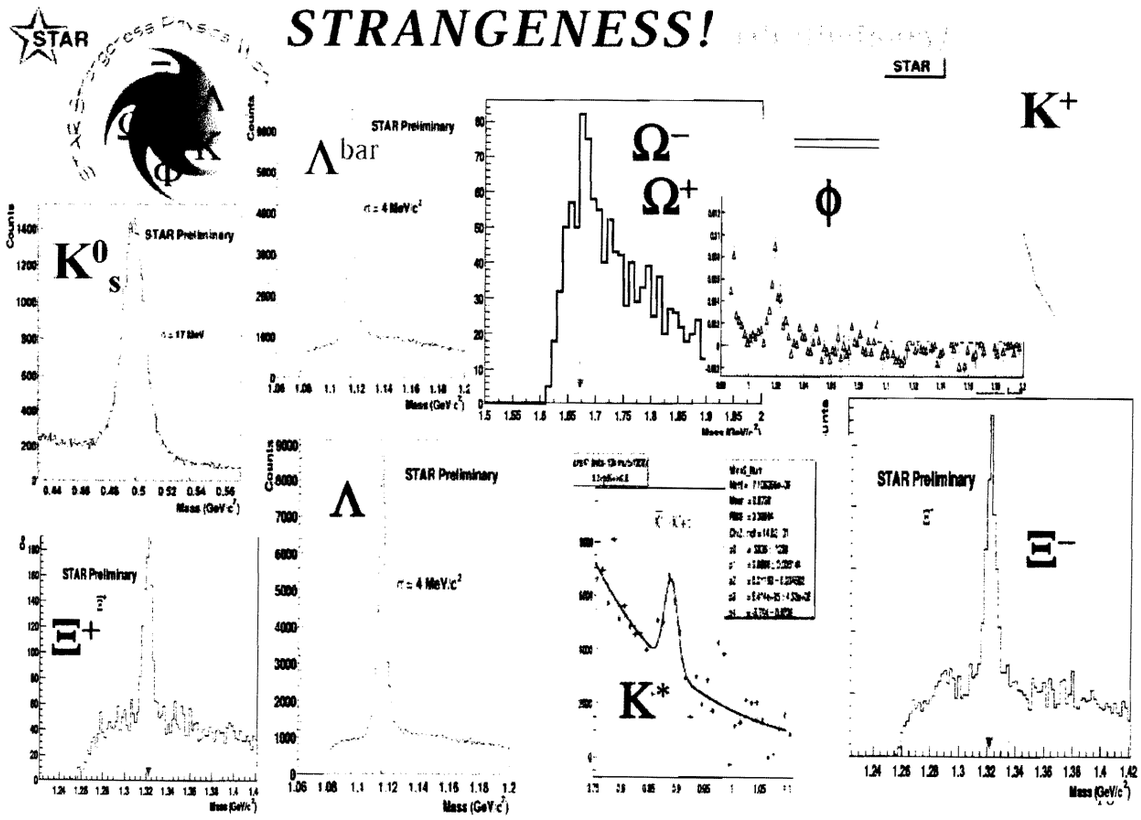

Photon and π^0

- The e^+e^- pair from γ conversion
- Large p_T coverage of γ measurement
  - from 50 MeV/c to 4 GeV/c

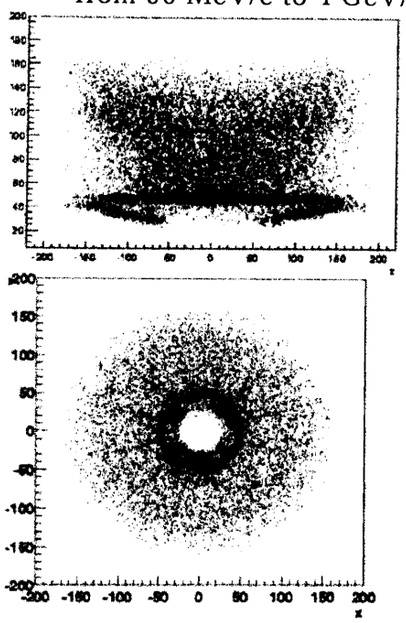

Typical tracks from γ conversion

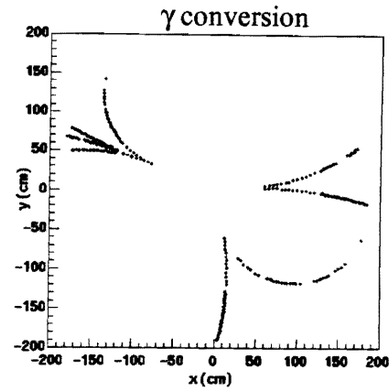

π^0

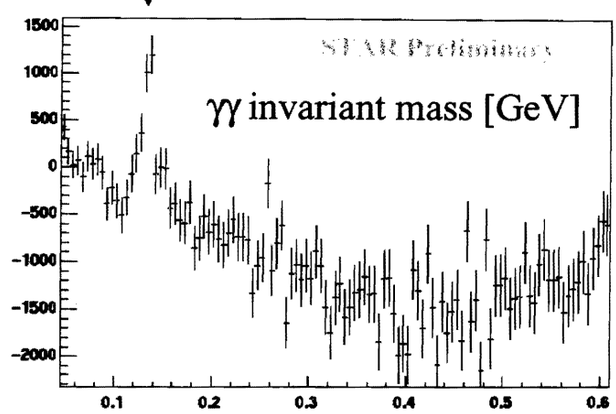

Data from Summer 2000

~1.6 M total triggered events

800K "central" ZDC CTB trigger
+ (L3 for collision vertex)

830K "min bias" ZDC trigger

80K "UPC" CTB (+ L3 trigger)
~7hours of dedicated run

→ Central (top 5%) events
331 K

→ Min bias events
458 K

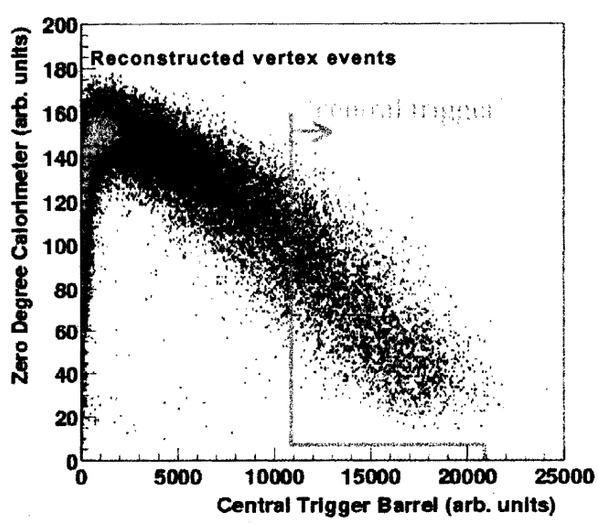

12

Physics results from summer 2000 run

will be covered by this talk & **next talk**

1. **Heavy ion physics**

Spectra	h spectra
	pi, K, P, photon, anti-nucleus spectra
	particle ratios
High p_T	spectra, event anisotropy
Strangeness	**spectra, ratios, HBT**
HBT	**pions**, proton, non-identical, EbyE
Event by Event	**event anisotropy**
	p_t fluctuations, CP violation

2. **Photon & pomeron physics**

   First observation of " Ultra Peripheral Collision "

3. **Spin physics**

   (Polarized proton was in RHIC Sep 2000)

   (Archived ~20% polarization @ 30GeV in 1 week commissioning)

13

"Centrality bin"

n_{ch} - #of primary tracks in $|\eta| < 0.75$

~ 90% of all hadronic Au+Au interactions

Top 5% central

For h⁻ spectra

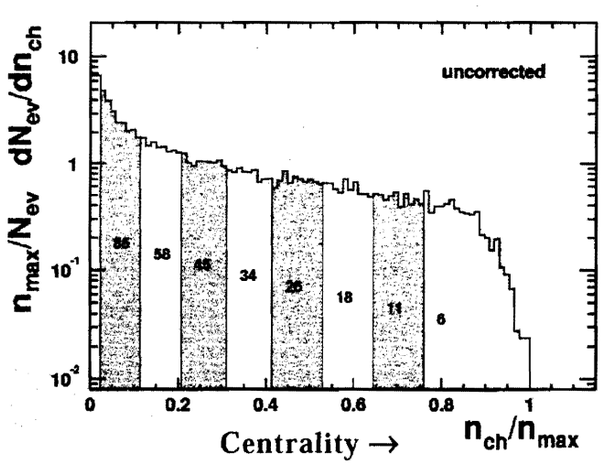

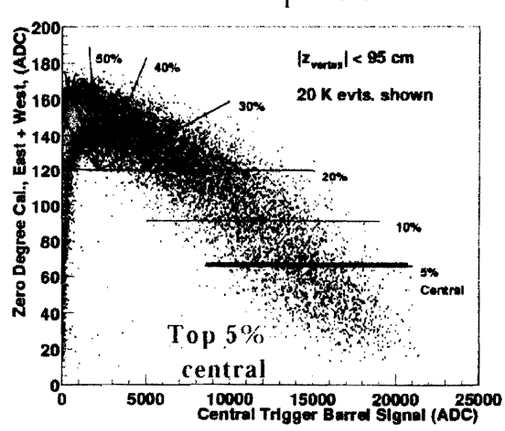

14

Negative Hadrons: η - distribution vs Centrality

dN(h-)/dη = 244 ± 1 ± 16 (p_t > 100 MeV/c)
dN(h-)/dη = 264 ± 1 ± 18 (extrap. to all p_t)

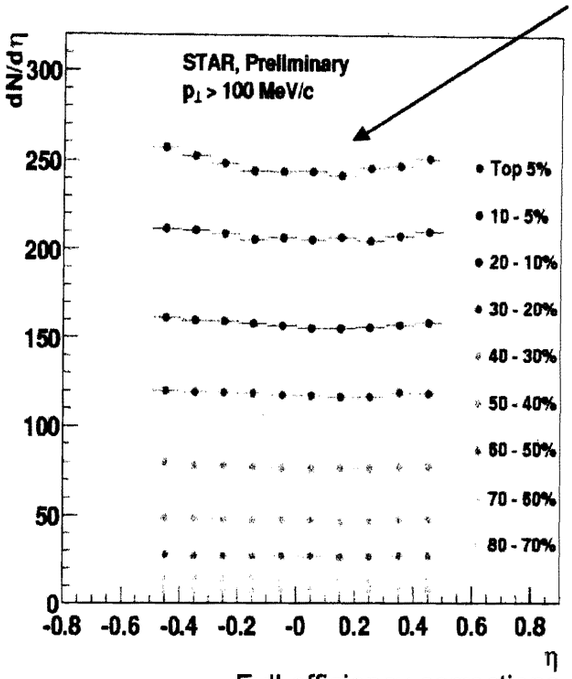

Full efficiency corrections

Increased particle production:
43% compared to Pb+Pb @ 17.2 GeV

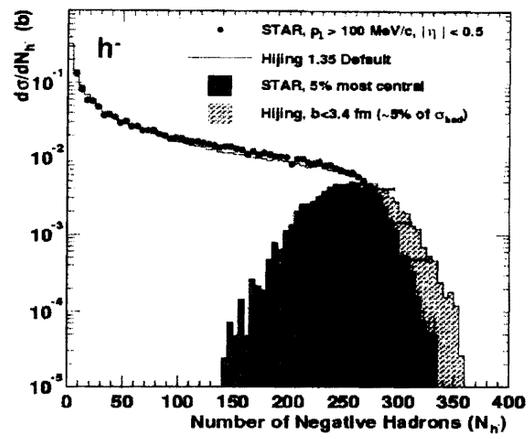

15

h^- : p_t distributions and ⟨ p_t ⟩ vs centrality

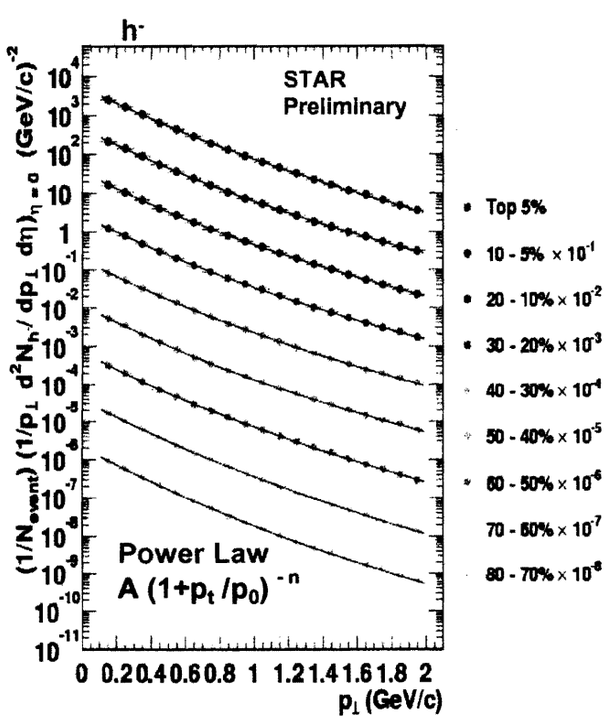

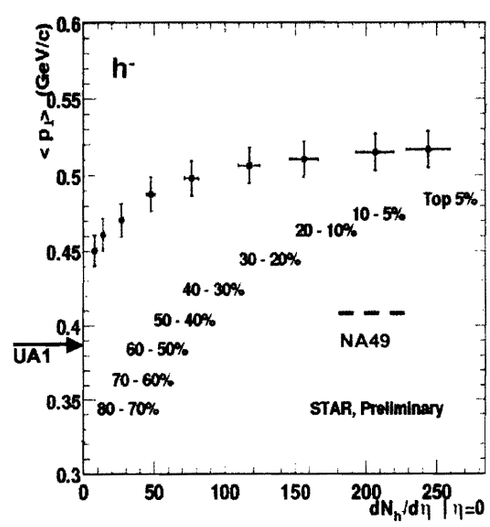

~15% increase in <p_T>
from peripheral to central

16

Negative Hadrons: p_T distributions

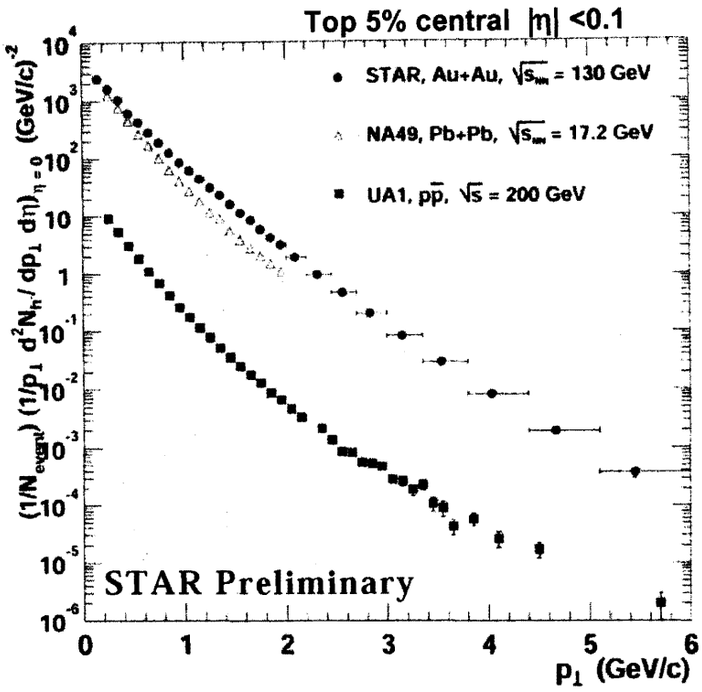

Power Law fit

$A\,(1 + p_T/p_0)^{-n}$

$p_0 = 2.74 \pm 0.11$ GeV/c

$n = 13.65 \pm 0.42$

STAR

$\langle p_t \rangle = 0.514 \pm 0.012$ GeV/c

NA49

$\langle p_t \rangle = 0.414 \pm 0.004$ GeV/c

UA1

$\langle p_t \rangle = 0.392 \pm 0.003$ GeV/c

17

Partonic Energy Loss Predictions: Hadron Spectrum

M. Gyulassy, I. Vitev, X.N. Wang nucl-th/0012092

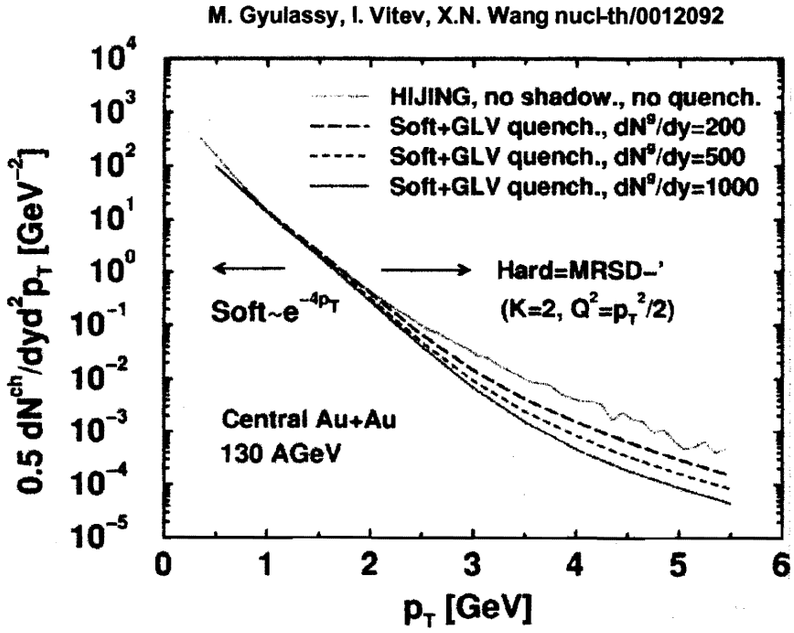

18

h^- Spectrum: Comparison to UA1

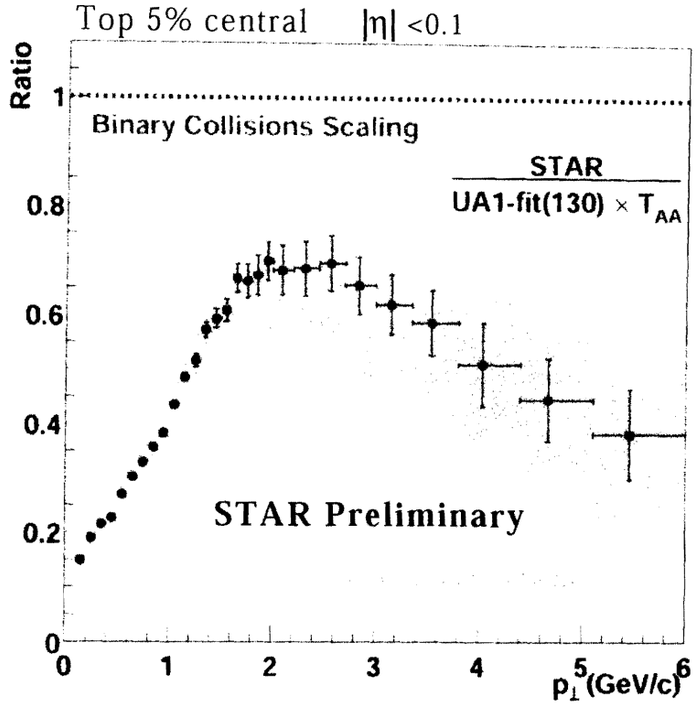

Errors on points: systematic error on STAR data

Gray bars: cumulative error including UA1 scaling

Hard: Binary collisions
$T_{AA} = 26 \pm 2$ mb^{-1}
$N_{AA} / N_{pp} = N_{bin\ coll} = 1050 / 1$
~ 6 collisions / nucleon

Soft: Wounded nucleon
$N_{AA} / N_{pp} = 344 / 2$

19

Partonic Energy Loss Predictions: Azimuthal Anisotropy

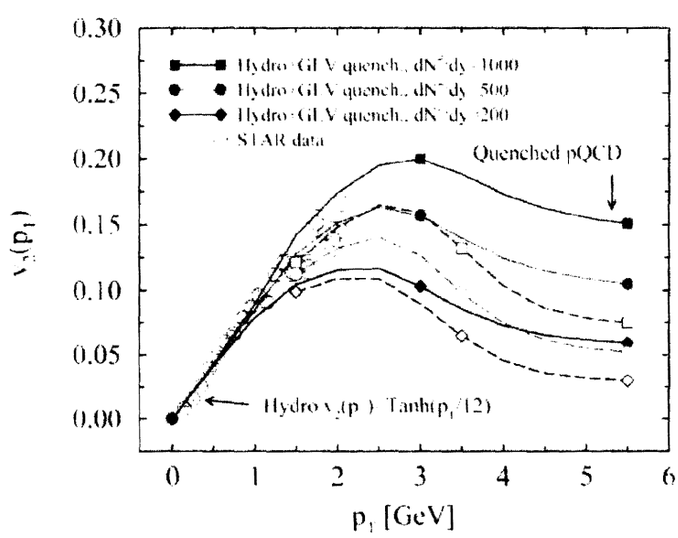

M. Gyulassy, I. Vitev, X.N. Wang nucl-th/0012092

- Azimuthal anisotropy at low p_T provides control of geometry
- Different pathlength as function of f leads to f anisotropy from partonic energy loss

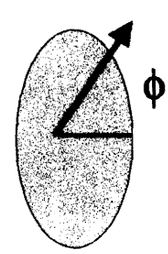

20

Charged particle anisotropy at high p_T

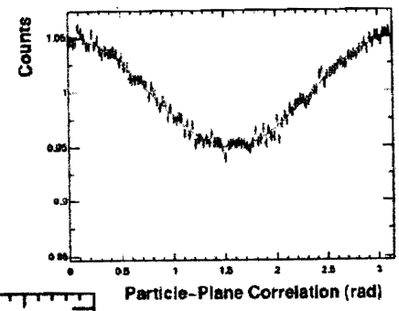

Top 5% central

$$v_2 = \langle \cos(2[\phi - \Psi_2]) \rangle$$

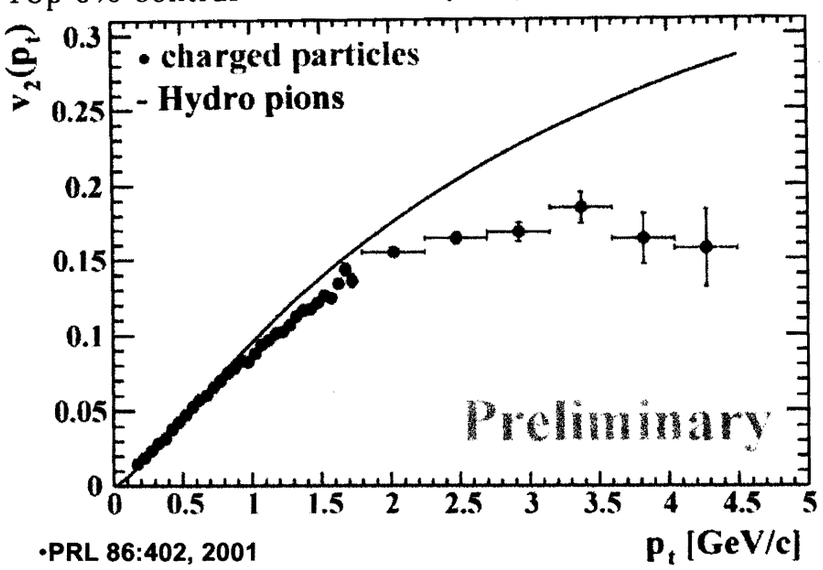

•PRL 86:402, 2001

Only statistical errors shown

Systematic error 10% - 20% for p_t = 2 - 4.5 GeV/c

21

Beyond flow - mini jets?

Anisotropic Flow at p_T=2-5GeV/c

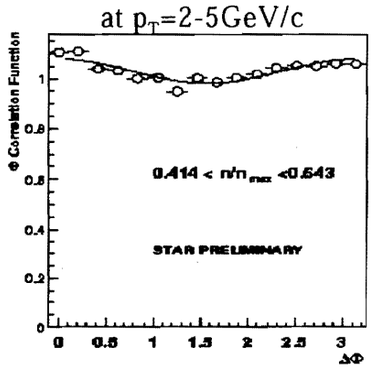

$$\frac{\Delta\phi \text{ distribution}}{\Delta\phi \text{ (mixed pair) dist.}}$$

Measure event plane event by event

Rotate mixing event to eliminate flow effect

$$\frac{\Delta\phi \text{ distribution}}{\Delta\phi \text{ (rotated mixed pair) dist.}}$$

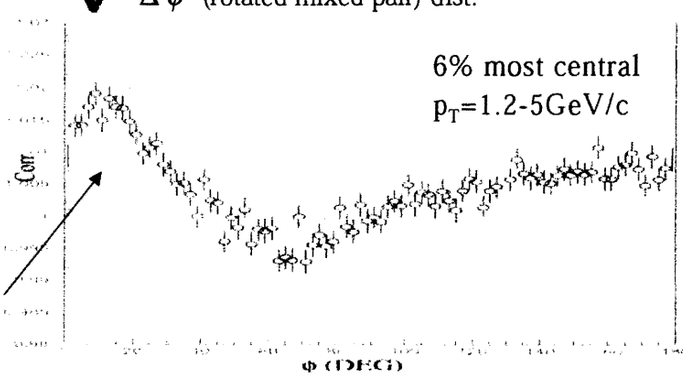

Consistent with Mini-jet expectation

narrow peak at Δφ=0

22

STAR ⟨ p_t ⟩ Fluctuations

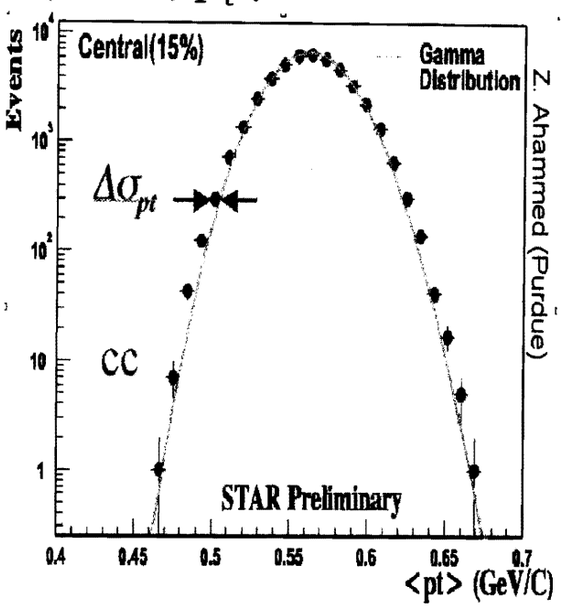

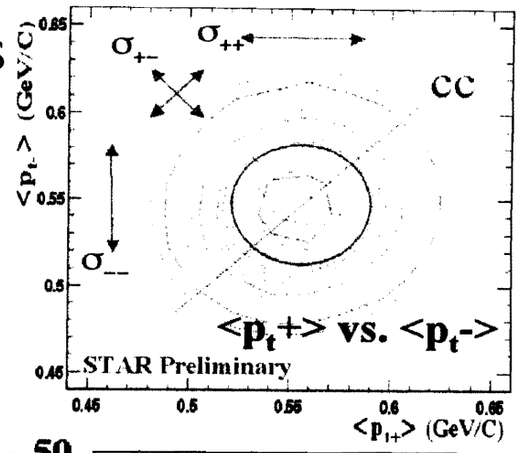

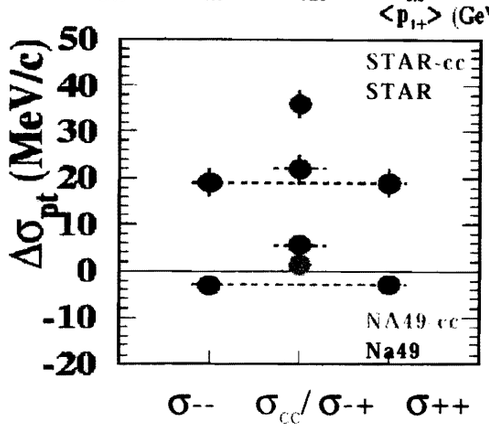

<p_t> fluctuation excess is observed

23

CP violation

QCD conserve CP

During QGP phase transition P&CP may be spontaneously broken

And color E and B field aligns

Lift*Twist -CP odd observable- can be non-zero

Charge positive

Charge negative

$x = Lift = \langle \hat{p}^+ \rangle - \langle \hat{p}^- \rangle$

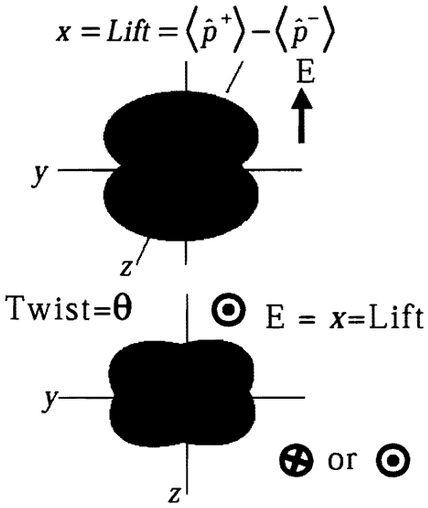

$(Lift*Twist)_1 (Lift*Twist)_2$

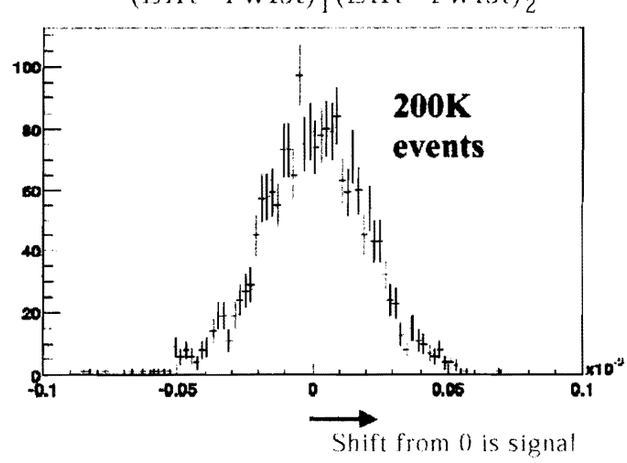

Mean = (4.1+-4.5) 10^{-6}

24

Ultra Peripheral Collisions

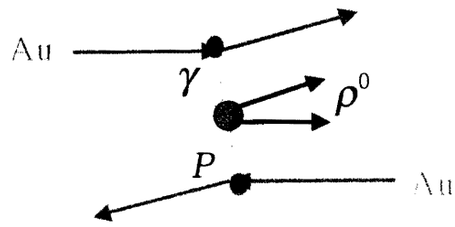

$Au + Au \rightarrow Au + Au + \rho^0$

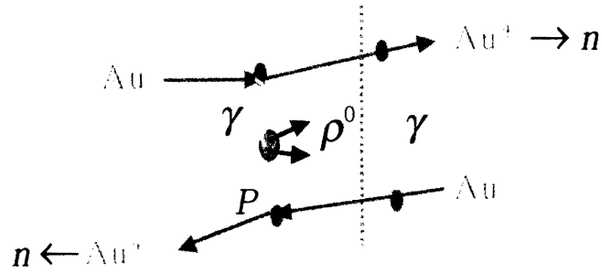

$Au + Au \rightarrow Au^* + Au^* + \rho^0$

to both nuclei (not photo-nucleon):

- Coupling : photon~z^2, Pomeron~$a^{4/3}$
  - Large cross section: 380 mb for Au @130GeV ~ " 5% central "

p_t : Limited by size of Au $p_t \sim 2\hbar\gamma/R_A \sim 60$ MeV/c

- Back-to-back particles in CTB. **and *nothing else***
- Nuclei may be mutually excited: **neutron signal in ZDC**

25

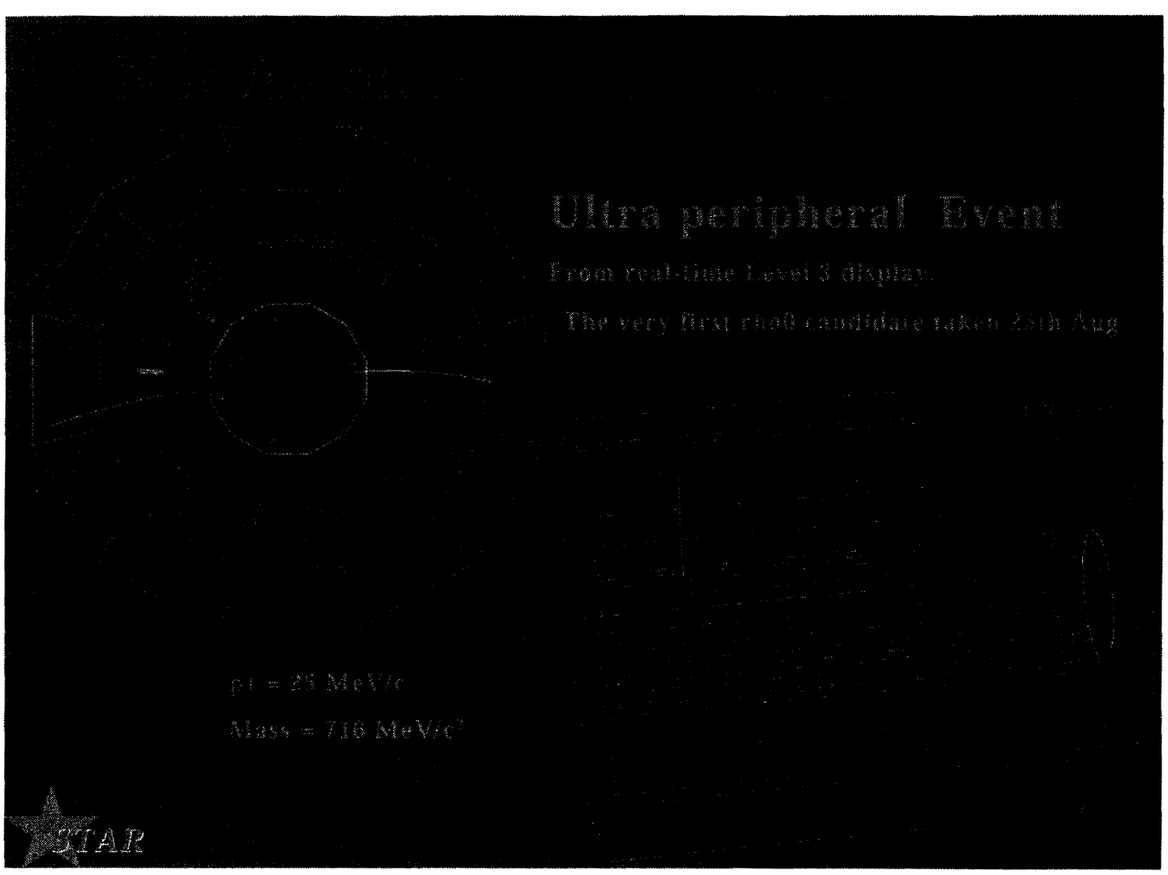

p_T and Mass

UPC trigger (CTB)
Min bias trigger (ZDC)
Combined

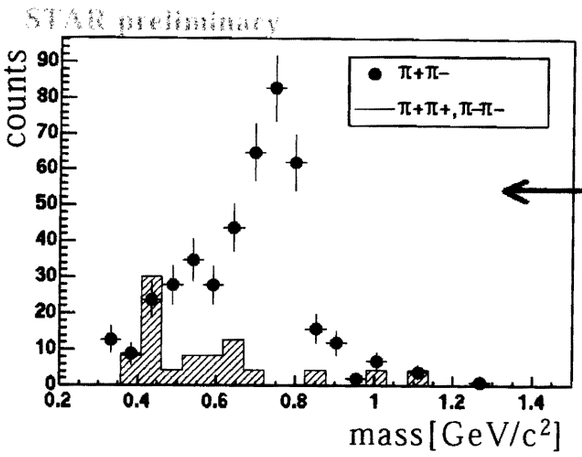

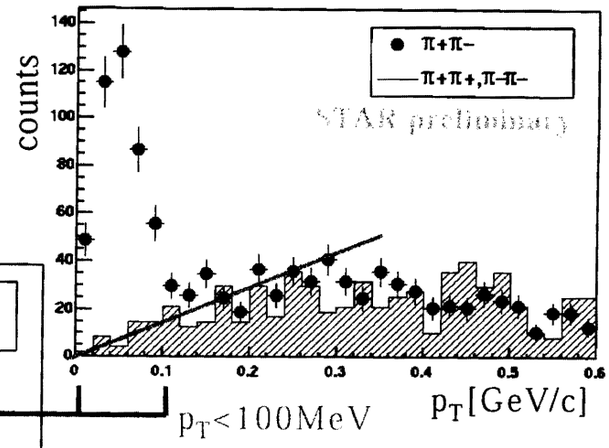

Clear enhancement at low p_T ~60MeV/c
over "background" which drops as you expect from phase space (mostly incoherent photo-nucleon)

First measurement of Coherent EM Production in heavy ion interactions

27

Ultra Peripheral Collisions

Physics topics:

γA ->VA coherent vector meson production

Non-local interference of unstable particles
Production cross sections, ...

$\gamma\gamma$,PP->mesons, leptons

Strong Field QED Z*a ~ 0.6 glue ball search, ...

An example : Interference

Can't differentiate between

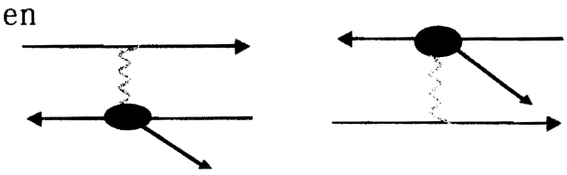

2 slit interferometer!!!

ρ, ω, ϕ J/ψ negative parity: destructive Interference

28

Conclusions

- STAR Detectors worked very well, and collected beautiful data
- h^- spectra never reach hard-scattering limit
  - Turn over at $2 < p_t < 6$ GeV/c
- Strong elliptic flow is measured to high p_T
  - Diverge from thermal models at $2 < p_t < 6$ GeV/c
- Azimuthal correlation is observed beyond elliptic flow
- Excess in mean p_t fluctuations
- No CP violation observed, yet
- First measurement of Coherent EM Production in heavy ion interactions

To be continued to the next talk

29

First results from STAR experiment at RHIC

- Soft hadron physics -

Masashi Kaneta

for the STAR collaboration

Lawrence Berkeley National Lab.

Focus on

- Hadrons
  - Measured : h^-, $\pi^\pm$, $K^\pm$, K^0_s, K^{*0}, $\bar{K}^{*0}$, p, $\bar{p}$, $\bar{d}$, ^3He, $^3\overline{He}$, t, Λ, $\bar{\Lambda}$, Ξ^-, $\bar{\Xi}^+$,
  - In future : π^0, ϕ, $\Omega^- + \bar{\Omega}^-$, ρ, ω, η, η', Δ, $\Lambda(1520)$, $\Sigma(1385)$, J/ψ and more
- Freeze-out conditions of low momentum hadrons by
  - Spectra/Ratios
    - Thermal/Chemical Freeze-out
  - Particle correlations
    - Size parameters, Phase space density
  - Event anisotropy
    - v_2

Spectra

Spectra

- Momentum distributions
  - Information of thermal (kinetic) freeze-out
  - The inverse slope parameter of m_T distribution reflects temperature and radial flow

Identified particle spectra

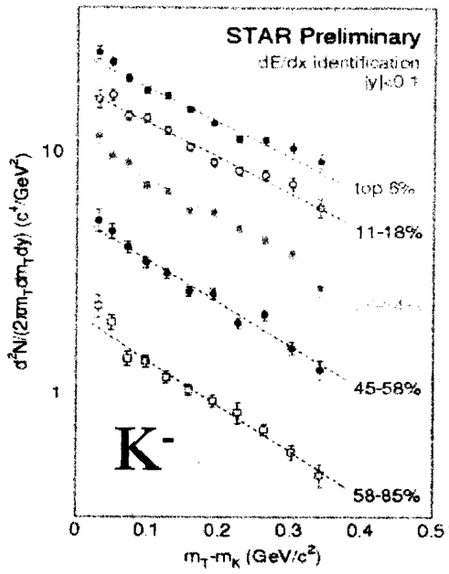

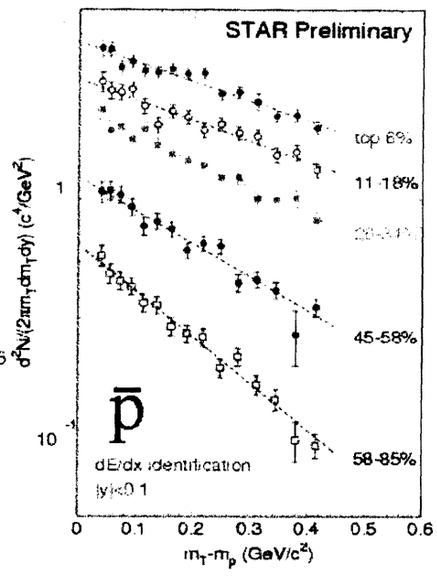

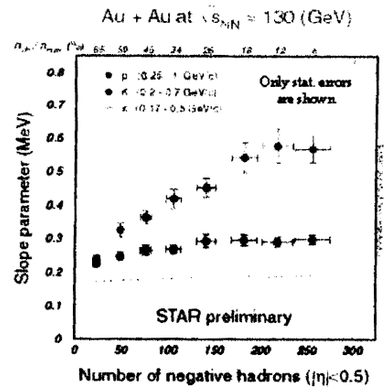

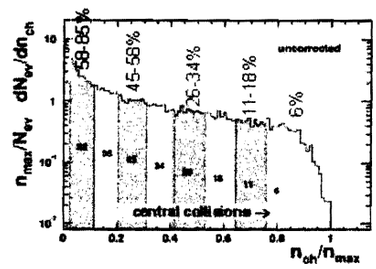

Masashi Kaneta, LBNL

Thermal(Kinetic) freeze-out

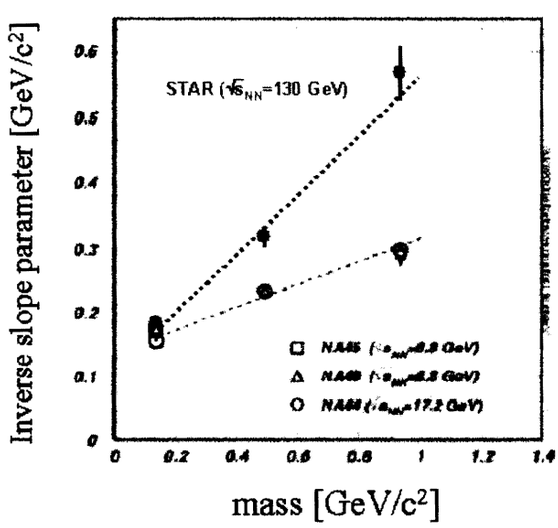

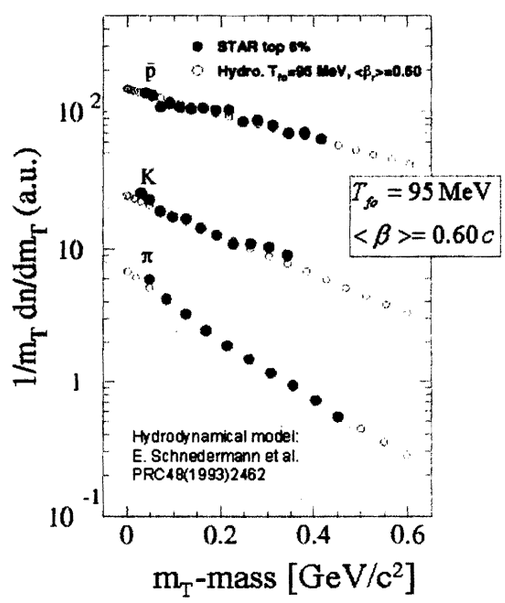

- Thermal freeze-out at RHIC
  - Temperature is similar at SPS
  - Larger radial flow than at SPS

Masashi Kaneta, LBNL

Ratios

Ratios

- p_T dependence anti-particle/particle
  - Test slope for particle and anti-particle
- Anti-baryon/baryon ratio
  - Stopping or transparent?
- Particle ratios from hadrons
  - Chemical freeze-out parameters

$\bar{p}/p$ ratio

- Minimum bias data
- No or weak p_T dependence

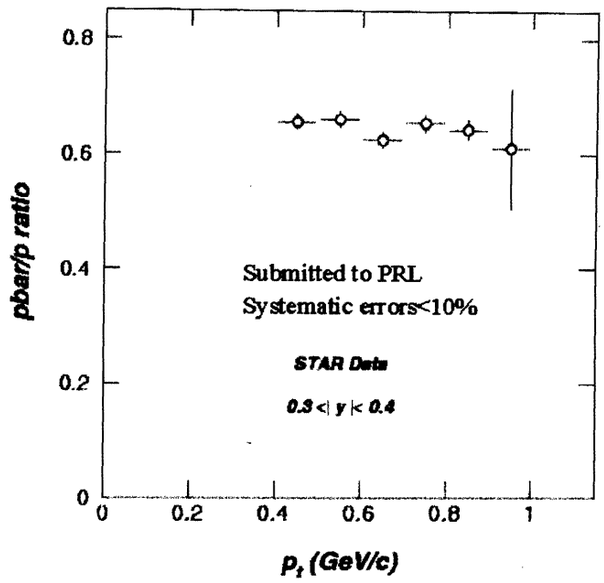

Masashi Kaneta, LBNL

$\bar{\Lambda}/\Lambda$ ratio

- **No significant p_T dependence in the ratio**
- **The mean ratio = 0.72±0.04**

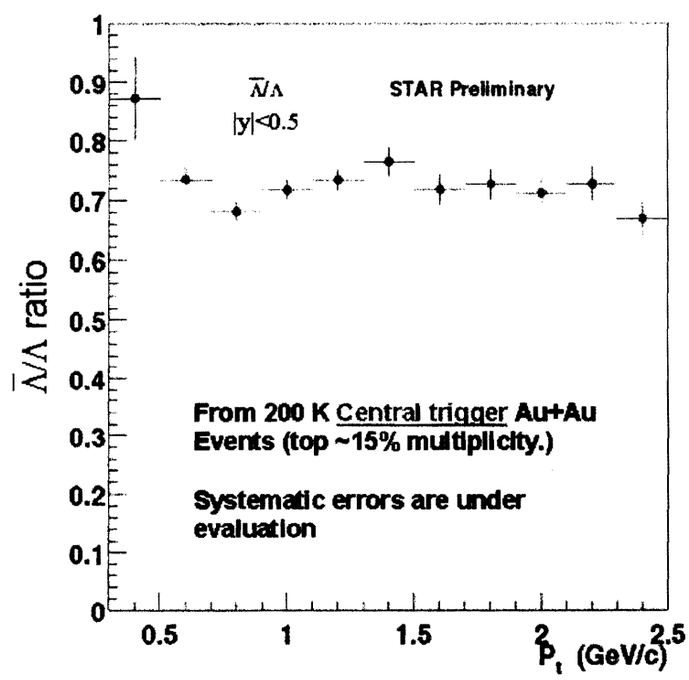

Masashi Kaneta, LBNL

K^+/K^- ratio

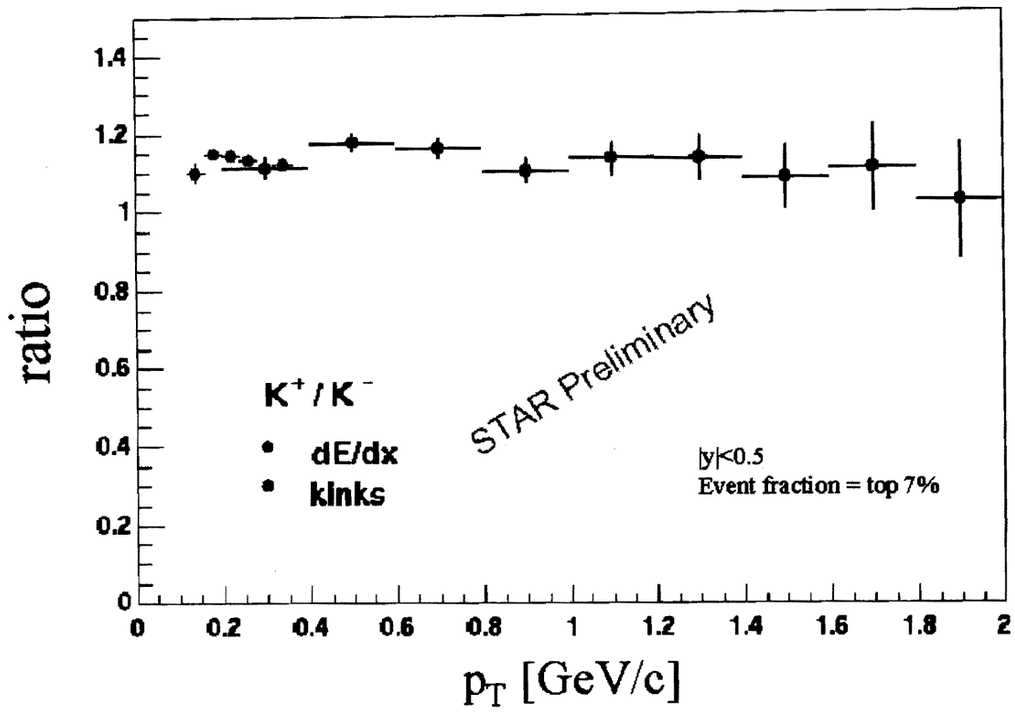

Masashi Kaneta, LBNL

Multiplicity dependence of ratios

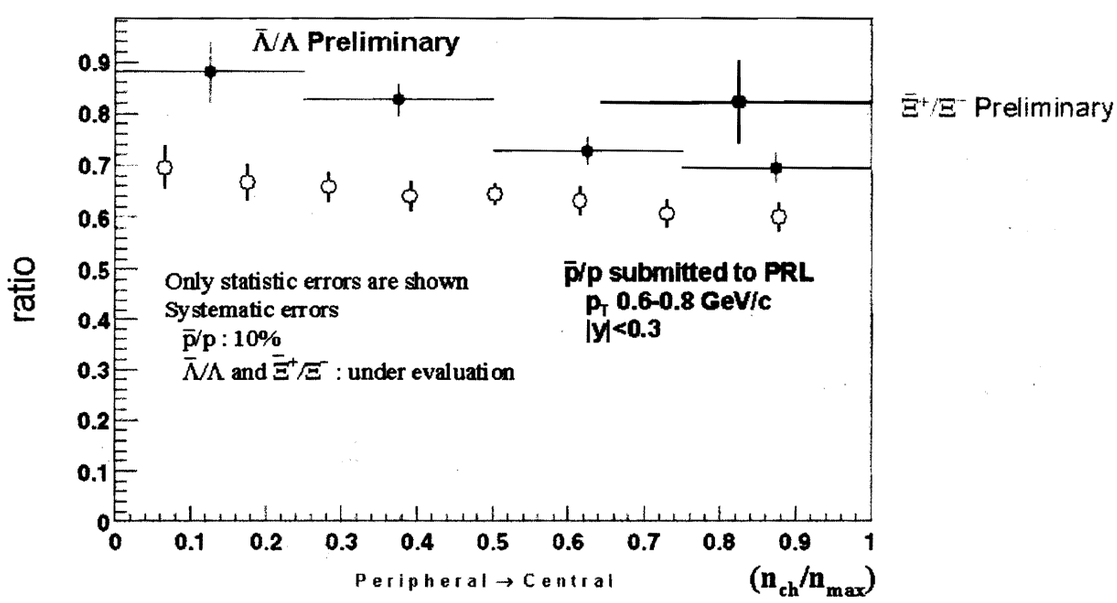

- Not baryon free at mid-rapidity
- An effect of anti-baryon absorption in central collisions?

Masashi Kaneta, LBNL

Chemical freeze-out

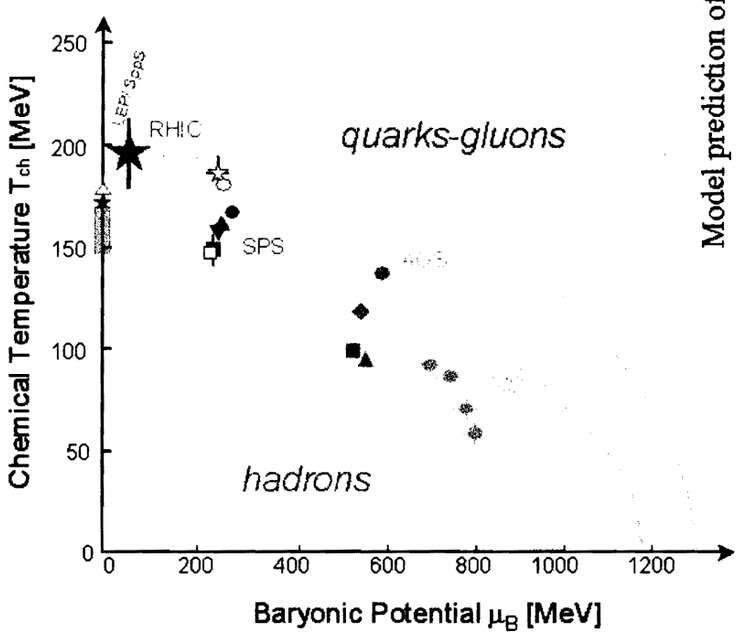

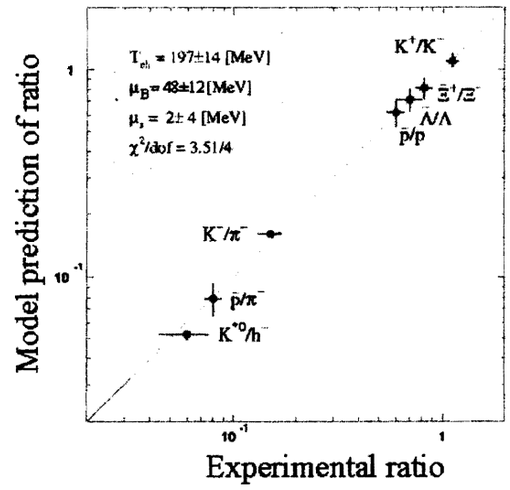

Masashi Kaneta, LBNL

HBT

Masashi Kaneta, LBNL

HBT

Many topics in STAR measurement

- Pion HBT
  - Centrality
  - Transverse momentum
  - The HBT excitation function

Focus in this talk

- Phase space density
- Event-by-Event HBT
- $K^0_s K^0_s$, $\Lambda\Lambda$
- pp, $\bar{p}\bar{p}$
- $\pi\pi\pi$ correlations
- Non-identical particles

Masashi Kaneta, LBNL

The HBT excitation function

- Compilation 3D $\pi\pi$-HBT parameters as a function of $\sqrt{s}$
  - ~10% Central Au+Au(Pb+Pb) events
  - $y \sim 0$
  - $k_T \approx 0.17$ GeV/c

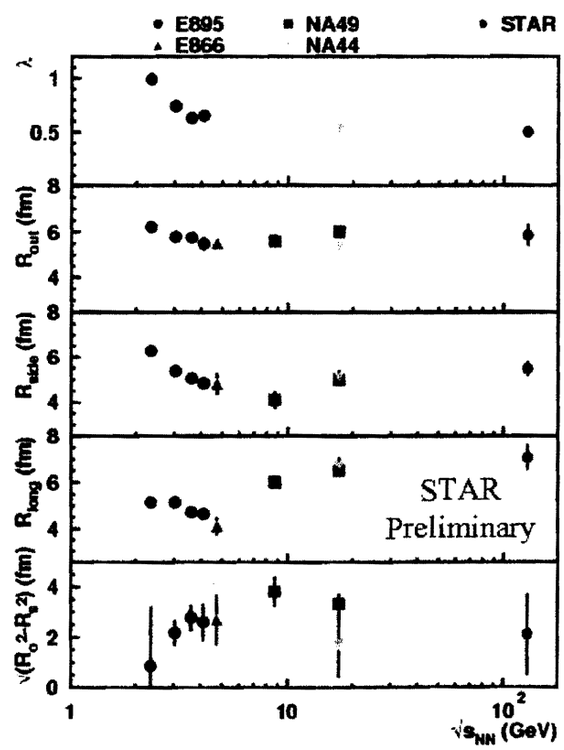

- No significant jump from SPS to RHIC
- We need energy scan between both energy

Masashi Kaneta, LBNL

Event Anisotropy

Masashi Kaneta, LBNL

Event anisotropy

- In momentum space
  - Anisotropy measured as second harmonic parameter v_2

$$v_2 = \langle \cos 2\phi \rangle \qquad \phi = \mathrm{atan}\frac{p_y}{p_x}$$

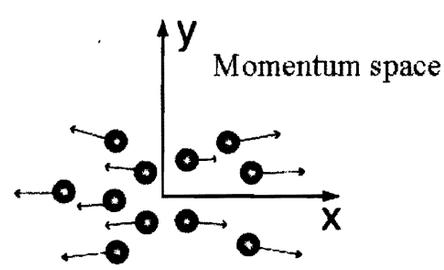

- v_2 will be scale to initial shape parameter ε,
  if the source has a hydrodynamical expansion

Almond shape overlap region in coordinate space

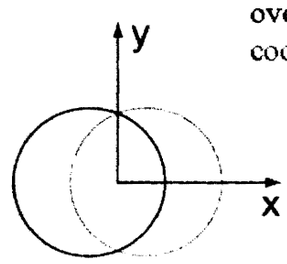

$$\varepsilon = \frac{\langle y^2 - x^2 \rangle}{\langle y^2 + x^2 \rangle}$$

Masashi Kaneta, LBNL

Charged particle v_2 versus Multiplicity

- Boxes show "initial spatial anisotropy" ε scaled by 0.19-0.25

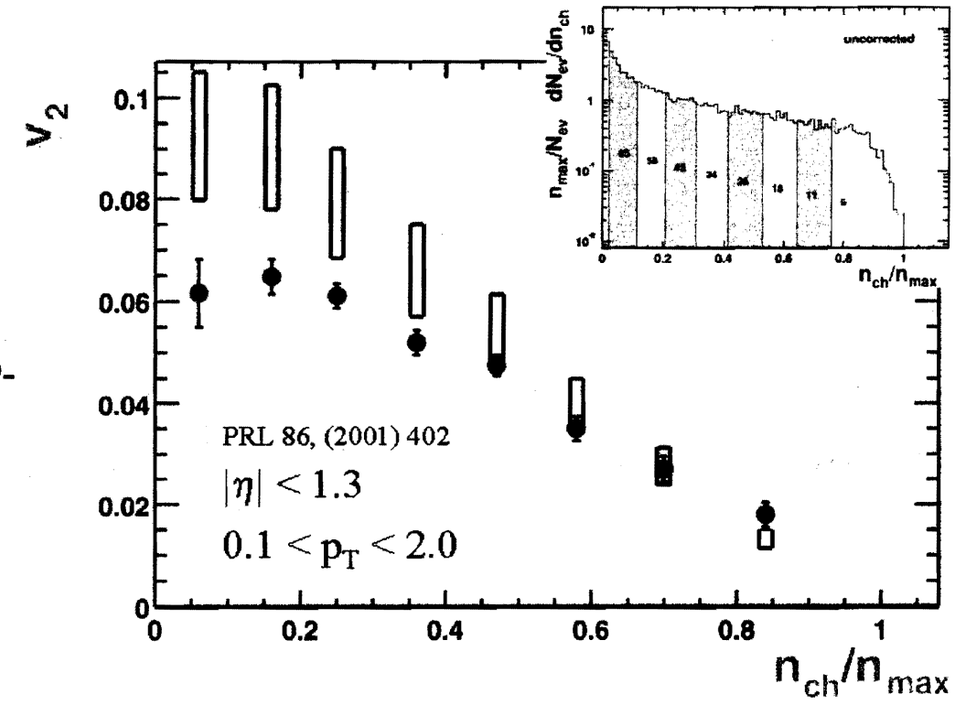

n_{ch} = primary tracks in $|\eta| < 0.75$

Masashi Kaneta, LBNL

Charged π and $\bar{p}$+p, $v_2(p_T)$ (M.B.)

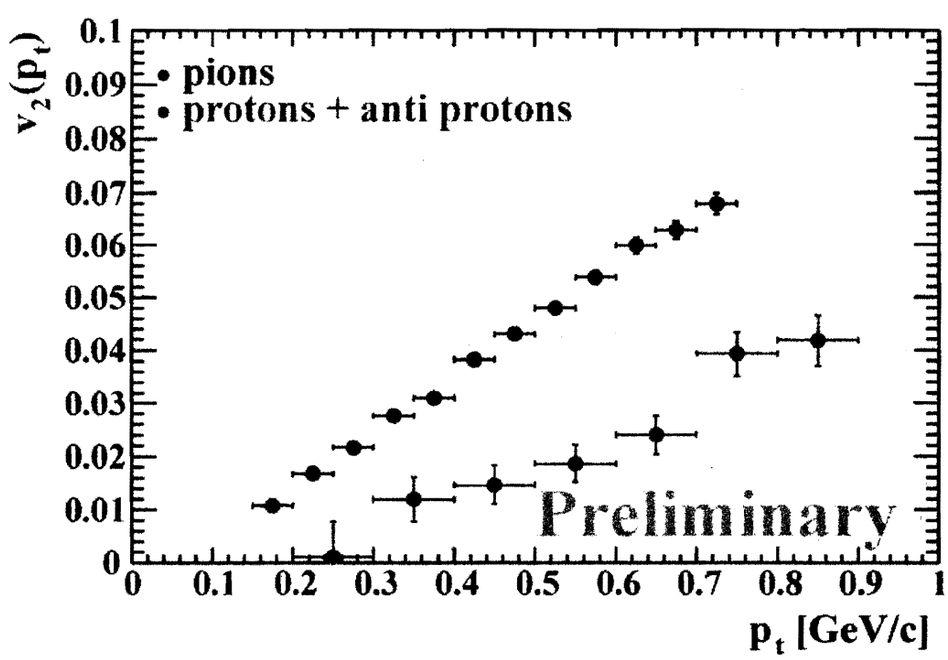

Masashi Kaneta, LBNL

Comparison with a hydrodynamical model

- Hydrodynamical calculations: Huovinen, Kolb and Heinz

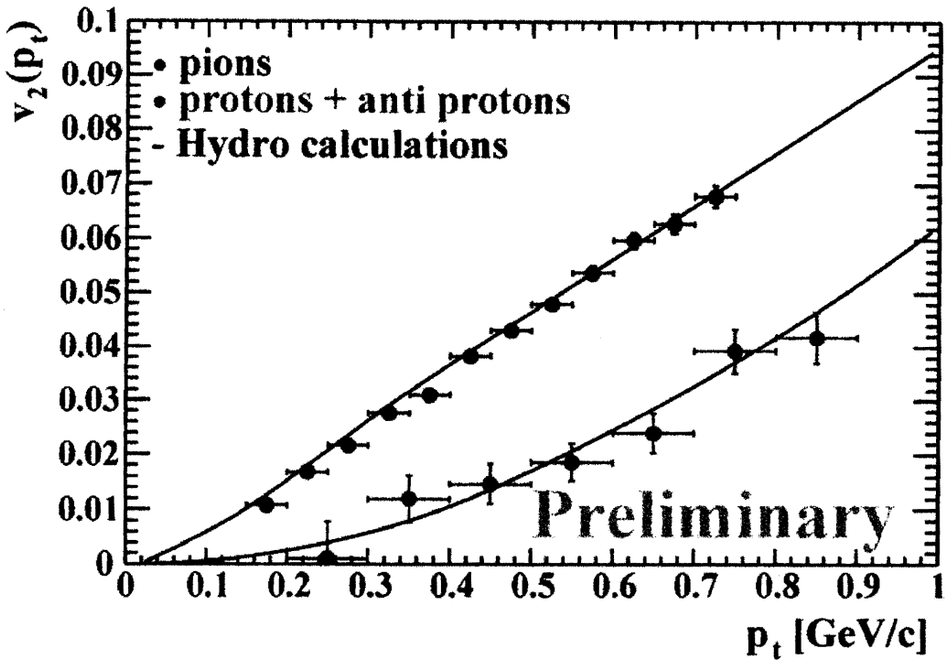

Masashi Kaneta, LBNL

Charged particle anisotropy $0<p_T<4.5$ GeV/c

- Minimum bias data
- Only statistical errors
- Systematic error 10% - 20% for p_t = 2 – 4.5 GeV/c

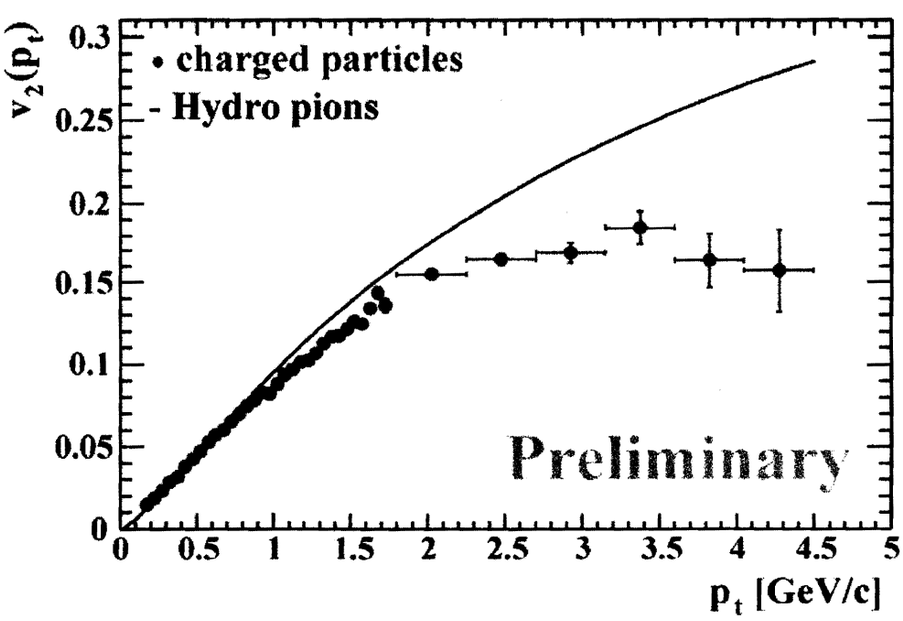

Masashi Kaneta, LBNL

Summary

- Net-baryon ≠ 0 at mid-rapidity
  - Anti-baryon/baryon ratios are toward 1, but still <1
- Chemical Freeze-out
  - T_{ch} : same or higher than at SPS
  - μ_B : smaller than at SPS
- HBT parameters
  - Similar to SPS
- Large anisotropic flow
  - From mid-central to central data, Hydrodynamical model can describe v_2 at low p_T (<2GeV/c)
- Thermal Freeze-out
  - T_{fo} : similar to SPS/AGS
  - Large radial flow
- We need energy scan between SPS and RHIC!

Masashi Kaneta, LBNL

Future plans

- TOF
  - PID up to 2GeV/c of p_T
- SVT
  - Increasing momentum resolution
  - More strangeness baryons
- EMC
  - Electron measurement
- Full fields
  - Higher p_T measurement
  - Increasing momentum resolution
- With high statistics
  - Physics of γ, π^0, and resonances

Masashi Kaneta, LBNL

γ and π^0

- The e^+e^- pair from γ conversion is measured
- Large γ acceptance
  - p_T = 50 MeV/c to ~4 GeV/c, $|\eta|<1.8$

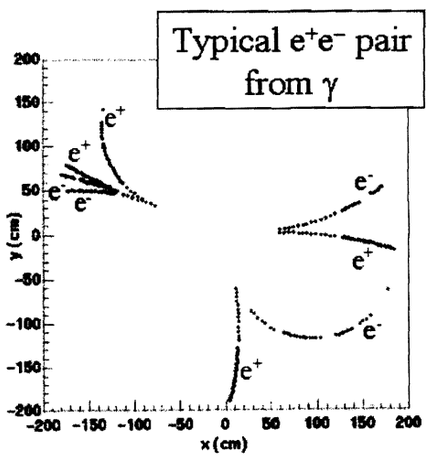

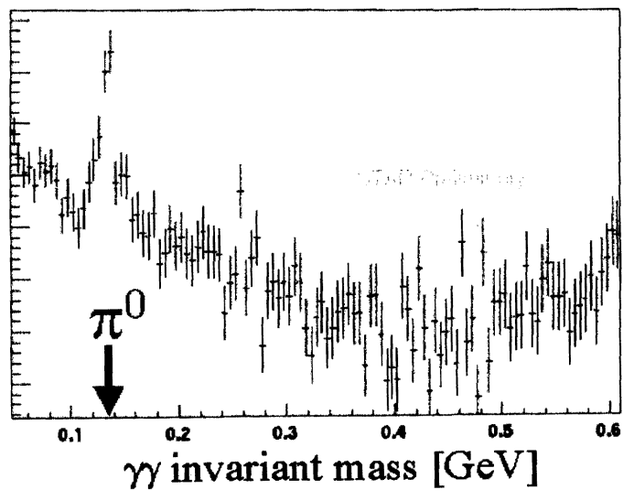

Masashi Kaneta, LBNL

STAR

π^0 Production in Au+Au Collisions at $\sqrt{s_{NN}} = 130$ GeV

Ken Oyama
for the PHENIX Collaboration

Center for Nuclear Study, Graduate School of Science, University of Tokyo
7-3-1 Hongo, Bunkyo-ku, Tokyo 113-0033, JAPAN

The measurement of π^0 production from Au+Au collisions at $\sqrt{s_{NN}}$=130 GeV has been carried out at the PHENIX detector system of RHIC at Brookhaven National Laboratory. The results presented here are based on the data taken during the first physics run between middle of July to end of August 2000. π^0 was reconstructed from two photons measured with a highly segmented electromagnetic calorimeter of PHENIX. The kinematic region of measured π^0s were approximately from 1.0 GeV/c to 4.0 GeV/c in the transverse momentum, and from -0.35 to 0.35 in rapidity.

Motivation of this analysis is to investigate the jet quenching effect in the deconfined quark matter that is produced in the extremely high energy density achieved by RHIC as predicted by the QCD calculations. High transverse momentum π^0s mainly come from jet fragmentations. Jets are produced by initial hard scattering of partons in the colliding nucleus. While the parton traverse the quark matter medium, it is expected that the scattered parton loses its energy by multiple scattering and gluon bremsstrahlung, and jet will be quenched. There are also other effects that modify the production rate of π^0 such as Cronin initial multiple scattering effect, initial k_T broadening, LPM effect, and shadowing, and unknown theoretical ambiguities are still remaining. Such effects could be directly observed through a deficit in the invariant yield of π^0. Since π^0s from the soft interactions are dominant at low momentum (p_T <1.0 GeV/c) and those are not sensitive to the energy loss in the medium, it is important to measure the high momentum π^0.

In this presentation, the centrality dependence of yield and shape of transverse momentum distribution of π^0 are shown, and compared with theoretical calculations by X.-N. Wang *et al.* which include different jet energy loss scenarios. The conclusion of this presentation is that the deficit has been observed in the transverse momentum distribution of π^0 for central Au+Au collisions. It is not explained by straightforward scaling with binary collisions, and it is not inconsistent with the scenario of jet energy loss in the quark matter.

π^0 Production in Au+Au Collisions at $\sqrt{s_{NN}} = 130$ GeV

Ken Oyama
for the PHENIX Collaboration

Center for Nuclear Study, Graduate School of Science, University of Tokyo
7-3-1 Hongo, Bunkyo-ku, Tokyo 113-0033, JAPAN

Outline . . .

- Result of PHENIX first year RUN.
- Central Au+Au collisions
  sqrt(s_{NN}) = 130 GeV.
- High p_T π^0 was reconstructed from two photons.
  -- Explanations of devices.
  -- Analysis method.
  -- Results.
- Is the result explained by composition of
  number of binary collisions?
- Compared to the theoretical models
  assuming jet energy loss in the quark matter.

Physics Motivation

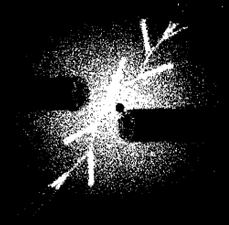

- De-confined quark matter (Q.G.P.) through … Jet quenching.
- Jets ← from initial parton-parton hard collisions.
- Loss its energy in the Q.G.P. gas by
  -- multiple scattering
  (gluon Blemsstrahlung)
  → quenching
- π^0 is one of the final products of jet fragmentation.

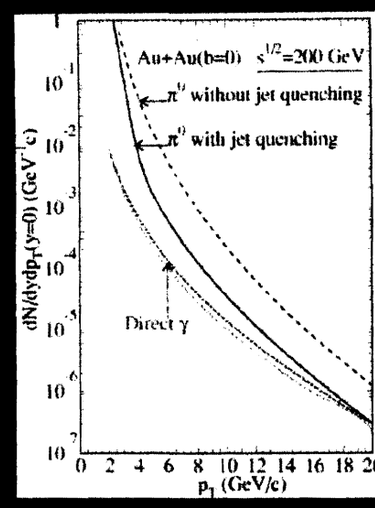

X.-N. Wang, PRC58 2321, Oct. 1998

Configuration

- Measure π^0 by detecting, two photons ($\pi^0 \rightarrow 2\gamma$).
- Photon measurement: Electromagnetic Calorimeters
- Trigger & Global variables:
  ZDC (Zero-degree Calorimeter)
  Centrality measurement.
  BBC (Beam-Beam Counter)
  M.B. trigger.
  Collision time & position.
- Cross check: Tracking system

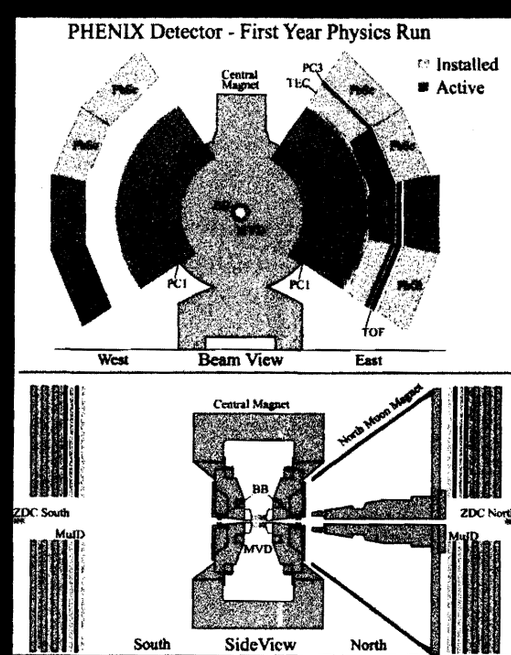

PHENIX PbSc Calorimeter

- Sampling calorimeter
- Pb-Scintillator sandwich
- W.L.S. Optical Fiber → PMT
- Segment Size:

  5.52 x 5.52 x 37.5 [cm^3]
- 5184 channels (2000 RUN)
- Approx. 5 m distant from vertex
- Geometrical Acceptance:

  $-0.35 < \eta < 0.35$, $\Delta\varphi = 22.5°$
- Energy Res. ~ 10 % at 1 GeV.

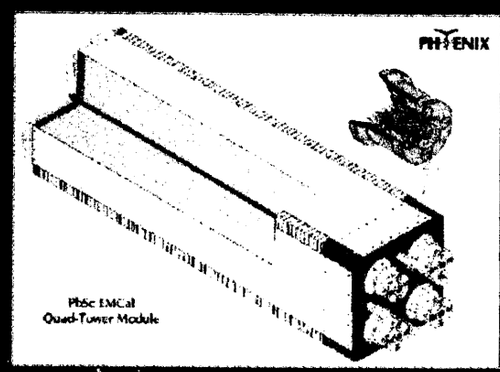

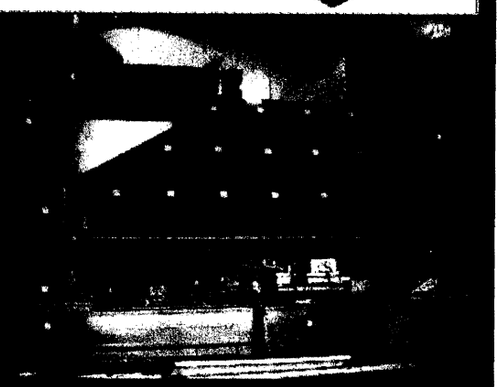

Calorimeter Performance

- Minimum ionization peak in low multiplicity events

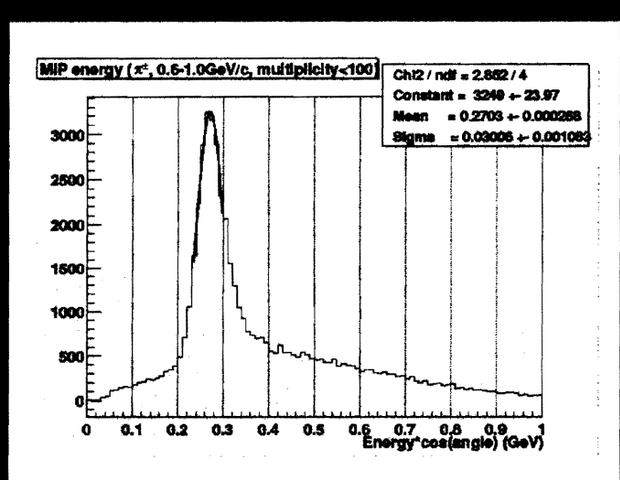

- E/p matching with electrons

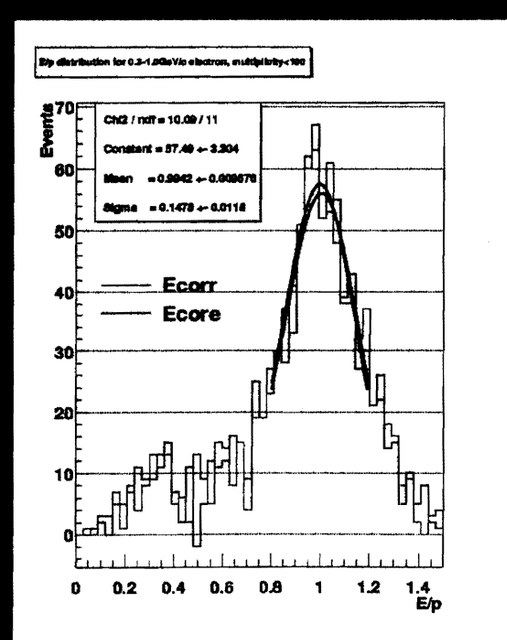

Photon Measurement

- Used EMCal cluster.
- Required two cuts :
  - -- Time-of-Flight of Calorimeter.
    $|tof| < 2.5$ ns. (loose enough)
  - -- Cluster shape (χ^2).
    (deviation from the ideal EM shower shape)
    $\chi^2 < 3.0$
- Cut Efficiency
  - Central = 68 %.
  - Peripheral > 80 %.

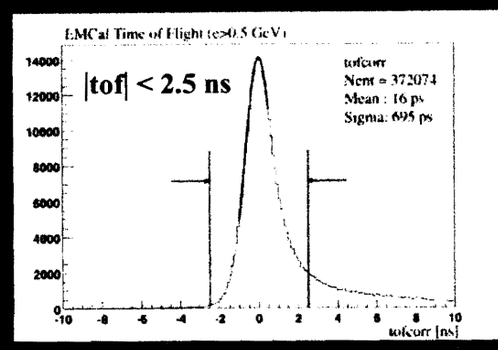

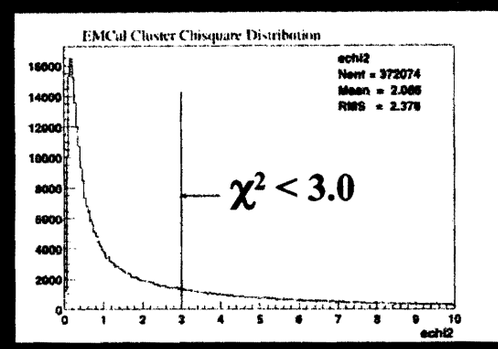

Extracting π^0

- Calculate invariant mass of two γs combination by :

$$m^2_{inv} = 2\, E_a\, E_b\, (1 - \cos\theta_{ab}).$$

E_a , E_b : measured energy of two γs.
θ : opening angle calculated from positions & event vertex.

- Huge combinatorial background
  → Better S/N required.
- Cuts for pair :
  - --- Asymmetry cut :
    $\alpha \equiv |(E_a - E_b) / (E_a + E_b)| < 0.8$
    Avoid very asymmetric decay.
  - --- Opening angle cut
    Avoid broken shower make sharp peak at $m_{inv} = 0$.

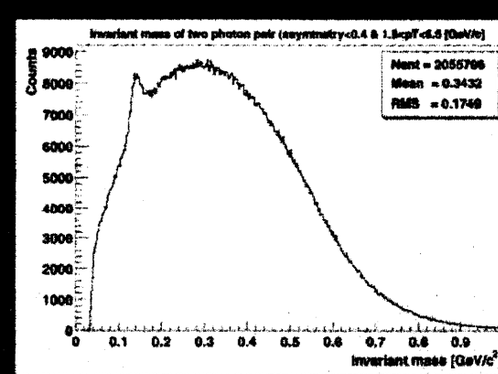

And ... event mixing subtraction

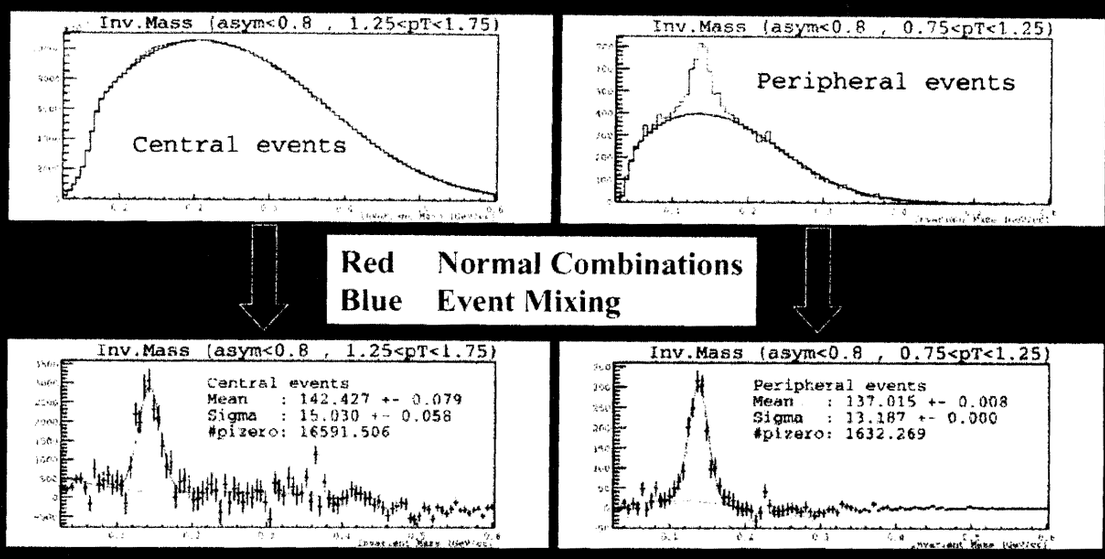

- Background shape was well described by event mixing method.
- Basically the peak has no contamination.
  Ambiguity was estimated among various cuts, fitting methods.

Check Energy Scale

- Energy self-calibrated by π^0 mass peak.
- Still large overlap effect.

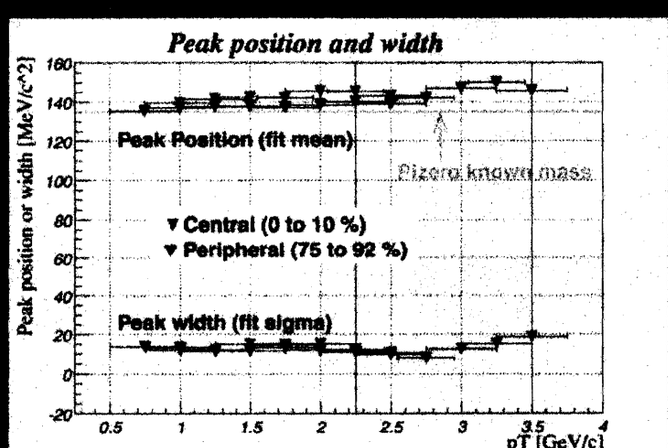

Then, we counted π^0 ....

π^0 p_T Spectra

- Compare:
  - -- Minimum Bias (Blue).
  - -- 10 % Central (Black).
  - -- 75 – 92 % Peripheral (Red).
- Systematic errors & corrections.
  - -- Peak extraction (err. ~ 8 %).
  - -- Acceptance & Efficiency (err 6 to 40 % depends on p_T, centrality)
  - -- Non-vertex pions (err. ~ 5%). (6 to 8 % from non-vtx.)

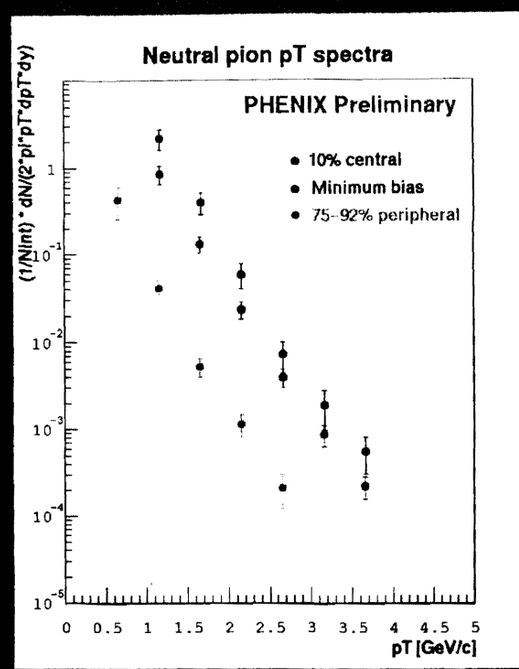

Compare to the WA98 Result

- Compare:

  PHENIX 10% Central
  v.s.
  WA98

- Reached upper p_T limit of WA98 already in Year-1.
- Significant difference in the slope.

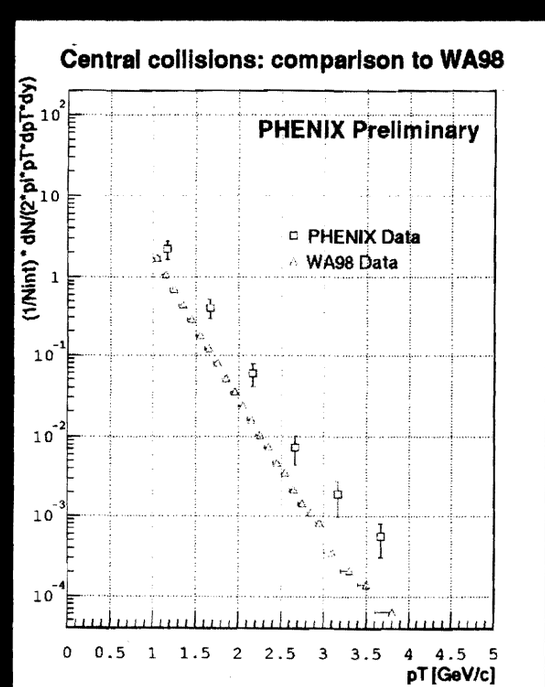

Compare to the UA1 Fit

- Compare:
  75 – 92% peripheral
  v.s.
  UA1 fit : $(h^+ + h^-) / 2$

- Normalized by estimated mean number of binary collisions = 5.5

- Clear deficit at higher p_T.

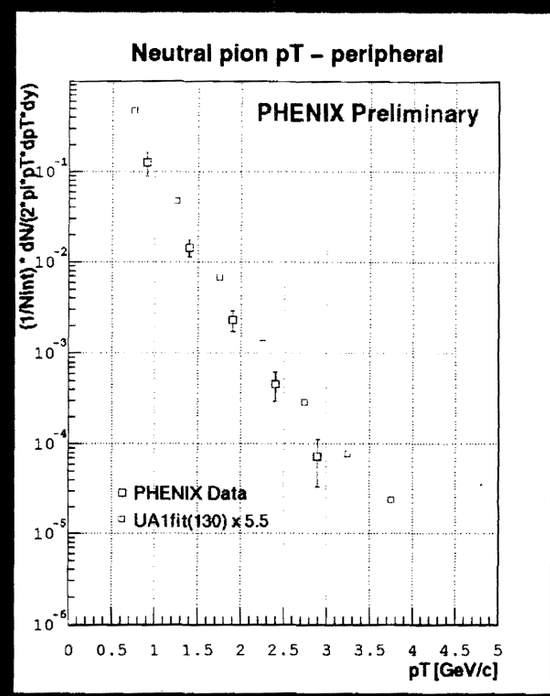

Compare to the Theory (Peripheral)

- Compare:
  75 – 92 % peripheral
  v.s.
  X.-N. Wang prediction

- PHENIX: 5.5 collisions/event
  Theory : 2.7 collisions/event
  Different but close.

- Data not inconsistent with any of the scenarios.
  -- No shadowing, broadening.
  -- With shadowing, broadening.
  -- Jet quenching
  (dE/dx = 0.25 GeV/fm)

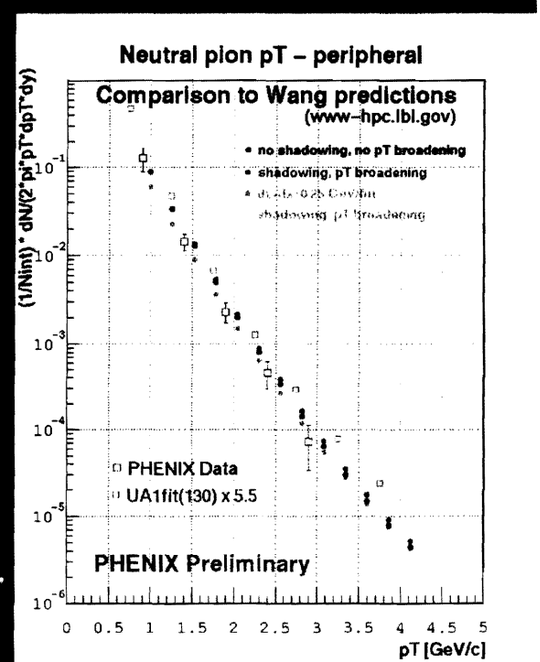

Compare to the Theory Prediction (M.B.)

- Compare:
  PHENIX minimum bias
  v.s.
  X.-N. Wang prediction

- <Ncoll> ~ 220.
- Inconsistent with scenarios without energy loss
- Not inconsistent with dE/dx=0.25 GeV/fm
- Shapes are also little different.

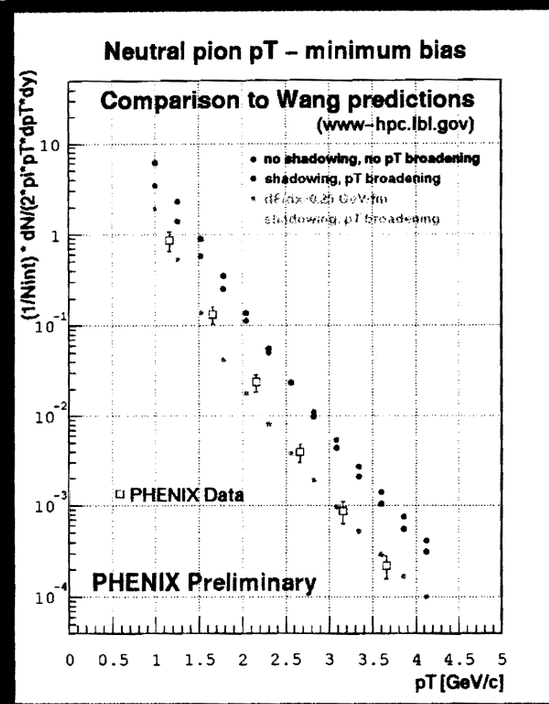

Compare to the Theory (Central)

- Compare:
  PHENIX central
  v.s.
  X.-N. Wang prediction

- <Ncoll> ~ 857 (±120).

- Inconsistent with scenarios without energy loss
- Not inconsistent with dE/dx = 0.25 GeV/fm
- Data are closer to exponential than theory.

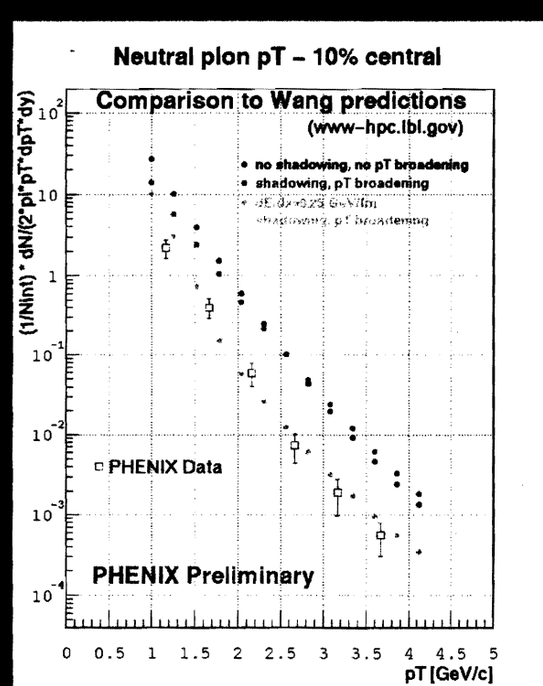

Central / Peripheral

- Central / peripheral ratios of per-collision yields.
- Main systematic error: <Ncoll> in peripheral.
- There is a clear deficit, particularly at higher pT.
- p_T limited by peripheral data.

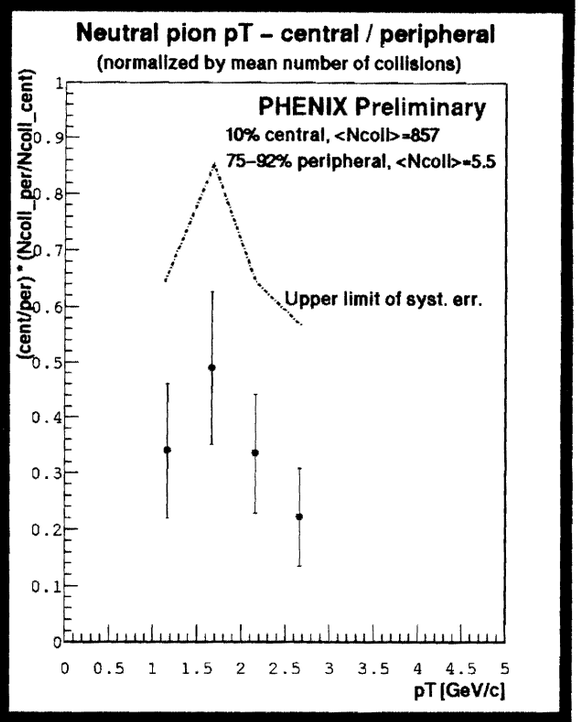

Central / UA1 Fit

- Central / UA1 fit ratios of per-collision yields.
- Systematic error is smaller.
- The deficit observed in central/peripheral is significant.
- Can not explained by scaling of binary collisions.

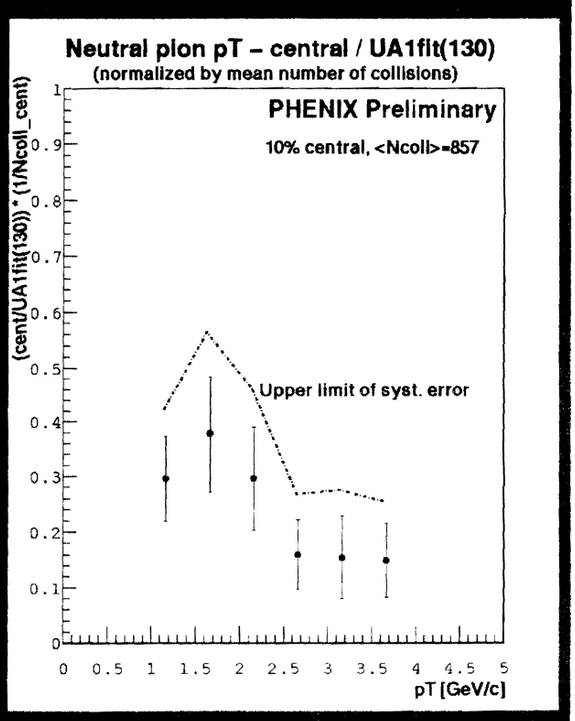

Summary

- We measured π^0 p_T distribution between 1 - 4 GeV/c in Au+Au collisions at $s^{1/2}$ = 130 GeV by electromagnetic calorimeter of PHENIX.
- This is the first result of PHENIX and is unique at RHIC.
- Results inconsistent with straightforward scaling with binary collisions. → We observe a clear deficit.
- Results are not inconsistent with the theory assuming strong jet energy loss effect in the dense medium.

Identified Charged Single Particle Spectra at RHIC-PHENIX

Tatsuya Chujo (BNL)
for the PHENIX Collaboration

PHENIX

BROOKHAVEN NATIONAL LABORATORY

managed by Brookhaven Science Associates for the U.S. Department of Energy

PHENIX

Physics of Identified Hadron Spectrum

From identified single particle spectra,

- **Hydro-dynamical collective expansion velocity (β).**
- **Thermal freeze-out temperature (T_{th}).**

→ **Inverse slope**

- **Chemical freeze-out temperature and chemical potential (T_{ch}, μ_B, μ_s)** → **dN/dy**
- **Jet quenching effect at high p_T by parton energy loss in medium (dE/dx).** → **High p_T spectra**

⬇

Shed light on QGP formation at RHIC

In this talk, we present identified (charged) single particle spectra as a function of centrality, measured at RHIC-PHENIX.

PHENIX Detector Setup

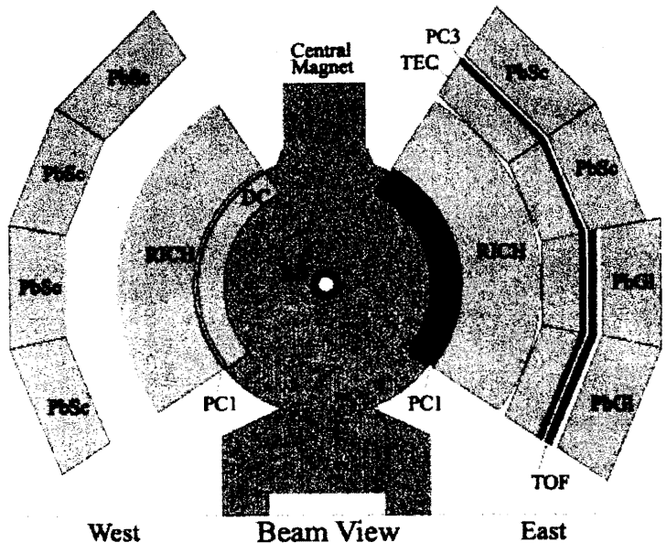

In this analysis, we use

- **Beam-Beam Counter (BBC)**
  z-vertex, start timing for TOF
- **Time-of-Flight (TOF)**
  stop timing measurement
- **Drift Chamber (Dch)**
  momentum, flight path length
- **Pad Chamber 1 (PC1)**
  additional track z-information to Dch

Particle Identification by TOF

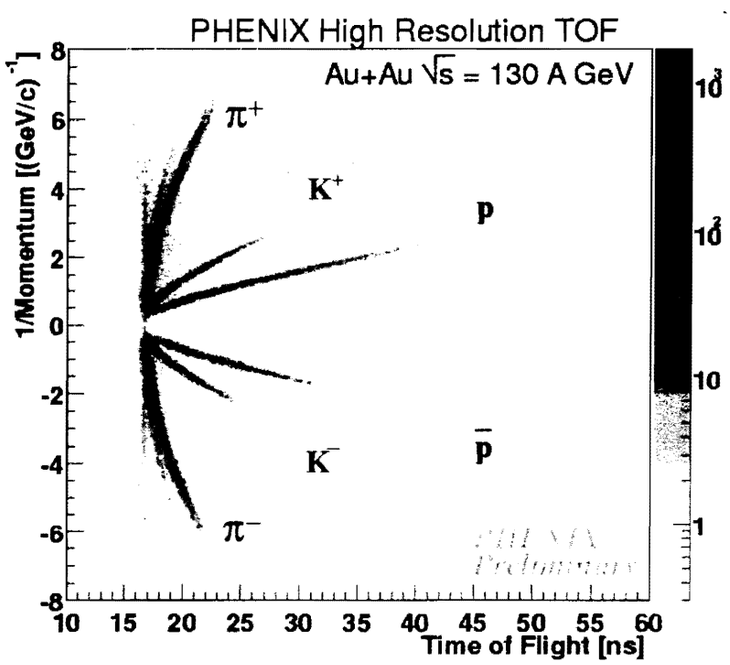

- **Demonstrated Clear PID by TOF**
- **Time-of-Flight resolution**
  σ_{TOF} ~ 110-120 ps

TOF - TOF$_{expected}$

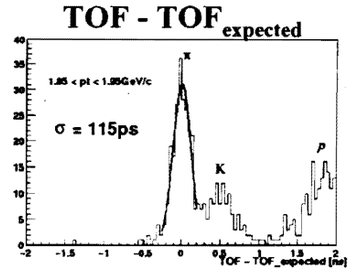

* Fitted π^+ region

PID Cut Criteria

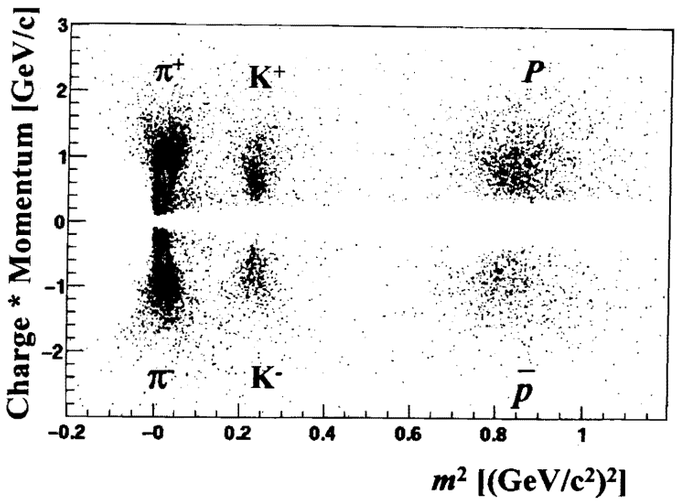

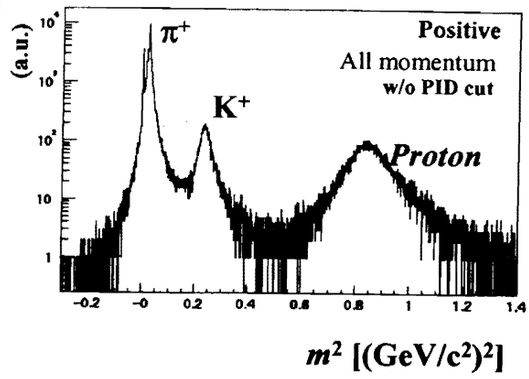

- PID by m^2 vs. momentum space
- $|m^2_{measured} - m^2_0| < 2.5\sigma_m^2$
- Momentum cutoff →

• π :	0.1 < p < 2.0 GeV/c
• K :	0.2 < p < 2.0 GeV/c
• p/pbar :	0.2 < p < 4.0 GeV/c

Correction factor for raw spectra

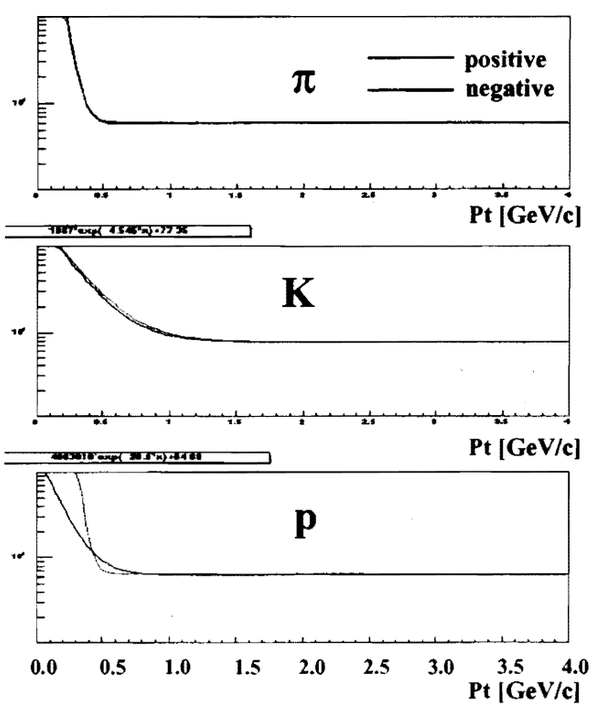

- **Based on single particle Monte Carlo simulation.**
- **Included overall effects**
  1. Tracking efficiency
  2. Geometrical acceptance
  3. Multiple scattering
  4. Decay in flight
  5. Hadronic int.
  6. Dead area of detectors
- **Confirmed that the multiplicity dep. is small by track embedding method in real data.**

Centrality Classes

Dch raw multiplicity distributions

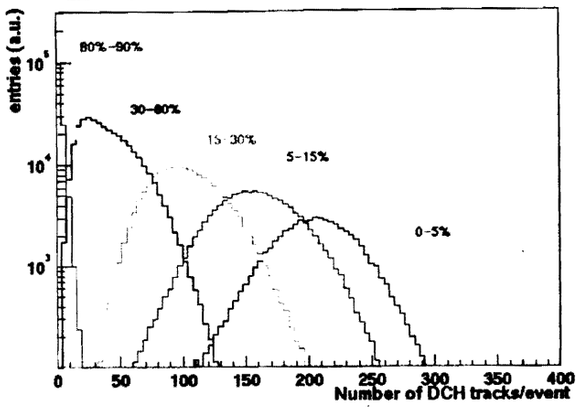

- **Used correlation between BBC charge and ZDC energy to define centrality.**
- **Extracted N_{part} based on Glauber model**

Centrality	Participants
0-5%	347 ± 15%
5-15%	271 ± 15%
15-30%	178 ± 15%
30-60%	76 ± 15%
60-80%	19 ± 60%
80-92%	5 ± 60%

Results : Minimum bias p_T spectra

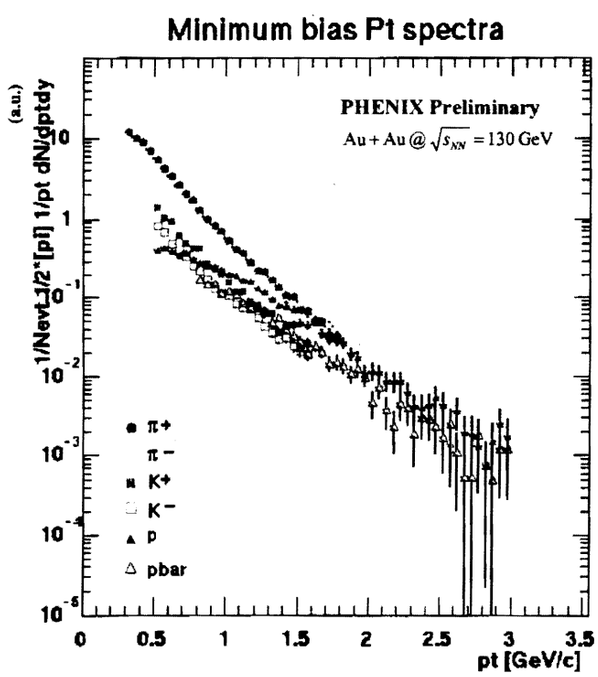

particle	p_T range
π	0.3 - 1.8 GeV/c
K	0.5 - 1.6 GeV/c
proton	0.5 - 3.0 GeV/c
pbar	0.8 - 3.0 GeV/c

- **pions yield ~ proton and pbar yield @ p_T~ 2 GeV/c**

→ Large proton and anti-proton contributions at high p_T.

Minimum bias M_T spectra

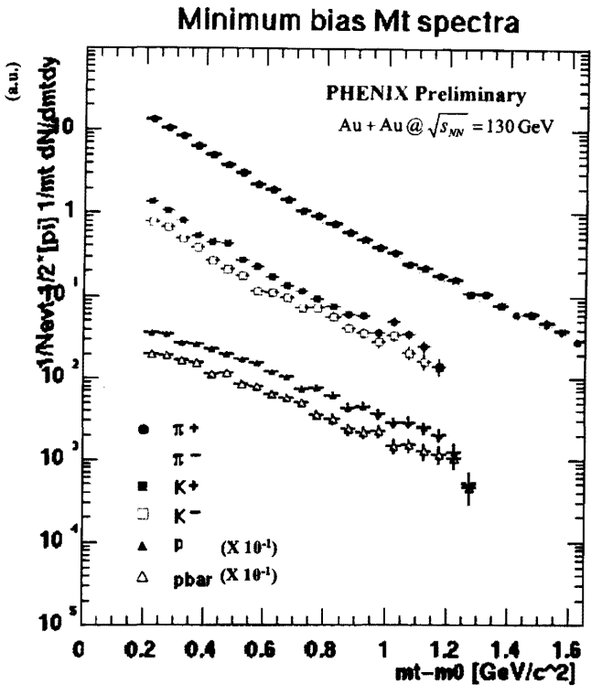

- In $0.2 < m_t - m_0 < 1.2$ [GeV/c^2], spectra for all species scale by single exp. function.
- Similar inverse slope for π and K.
- $T_{proton} > T_\pi$

☆Fitting results by single exp. function

$$\frac{1}{m_T}\frac{dN}{dm_T} \propto A\exp\left(-\frac{m_T - m_0}{T}\right)$$

$\pi^\pm$	~ 205±5 (stat.) ±15 (sys.)	MeV
K ±	~ 215±5 (stat.) ±20 (sys.)	MeV
p, $\overline{p}$	~ 320±10 (stat.) ±20 (sys.)	MeV

Centrality Dependence of M_T Spectra for pions

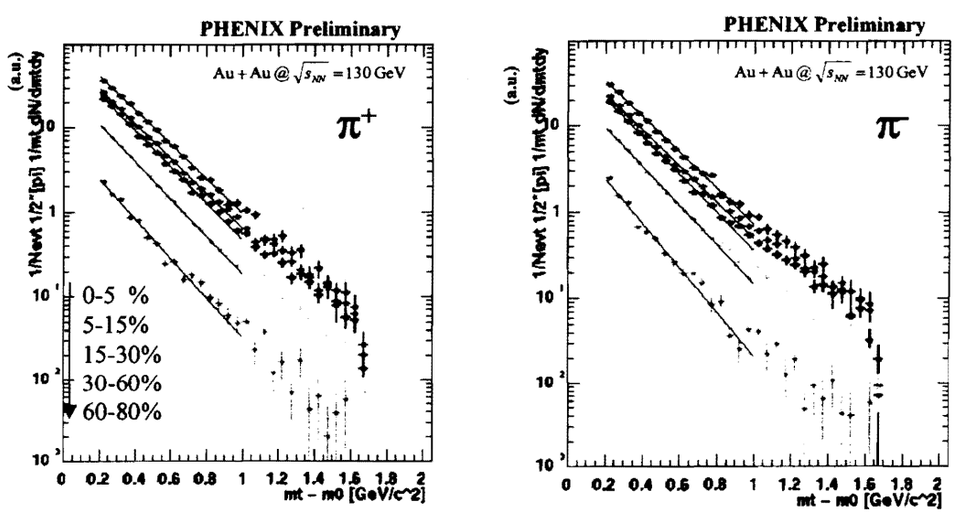

- Single exponential scaling at 0.2 -1.0 GeV in m_t-m_0.
- Almost parallel among all centrality classes.
- T_π (central 0-5%) ~ 210 MeV ±5 (stat.) ±15 (sys.) MeV

Centrality Dependence of M_T Spectra for kaons

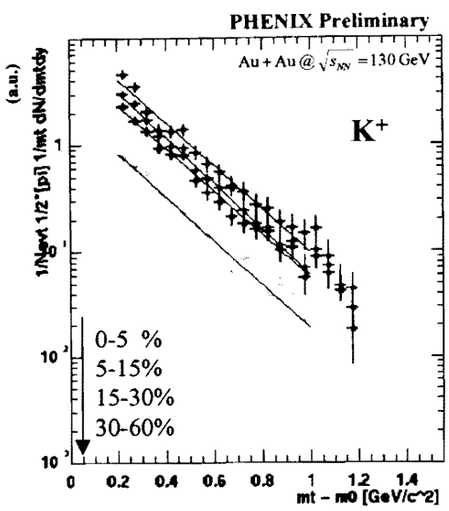

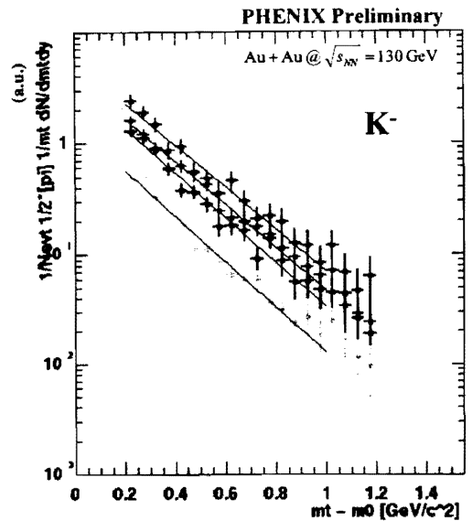

- Single exponential scaling at 0.2 -1.0 GeV in m_t-m_0.
- Parallel slope among all centrality classes.
- T_K (central 0-5%) ~ 217 MeV ±5 (stat.) ±20 (sys.) MeV.
  $\cong T_\pi$

BNL/ Tatsuya CHUJO 02/14/2001 @ CNS workshop, Tokyo Univ.

Centrality Dependence of M_T Spectra for p/pbar

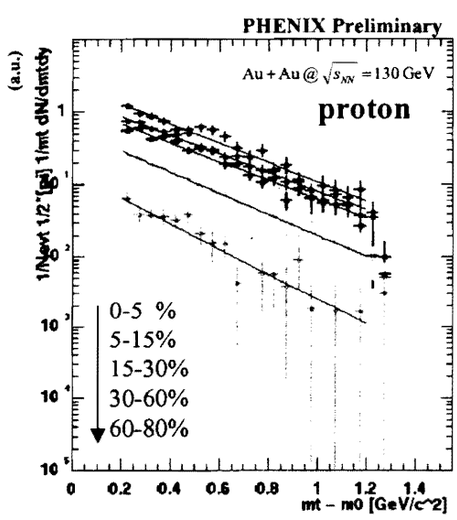

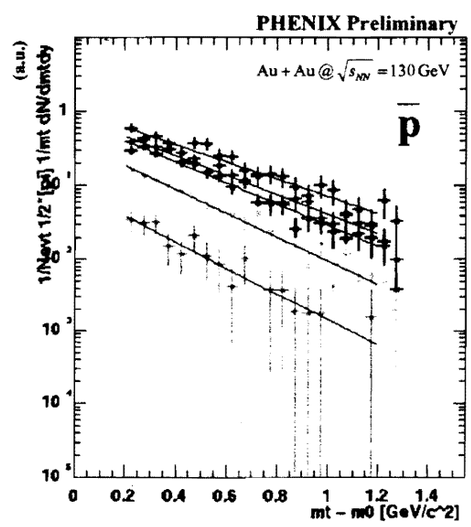

- Single exponential scaling at 0.2 -1.2 GeV in m_t-m_0.
- Gradual increase from centrality 60-80% to 30-60%.
- T_{proton} (central 0-5%) ~ 325 MeV ±17 (stat.) ±20 (sys.) MeV > T_π.

BNL/ Tatsuya CHUJO 02/14/2001 @ CNS workshop, Tokyo Univ.

Centrality dependence of T

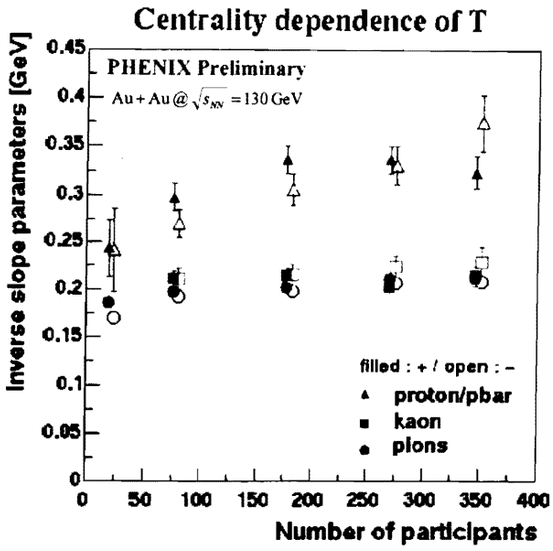

- Weak centrality dependence for T_π and T_K.
- Gradual rise of T_{proton} and T_{pbar} from peripheral to mid-central collisions.
- $T_\pi \cong T_K < T_{proton}$

Mass Dependence of T

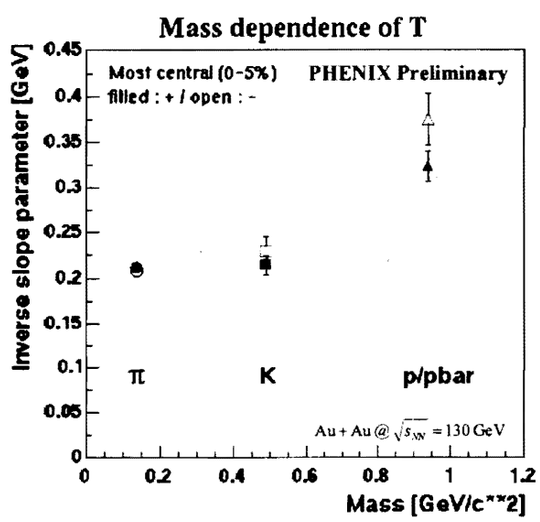

☆Intuitive explanation of mass dependence of T

$$T \propto T_{\text{theremal}} + m \cdot < \beta_t >^2$$

β_t : Transverse expansion velocity

Comparison with CERN Energy

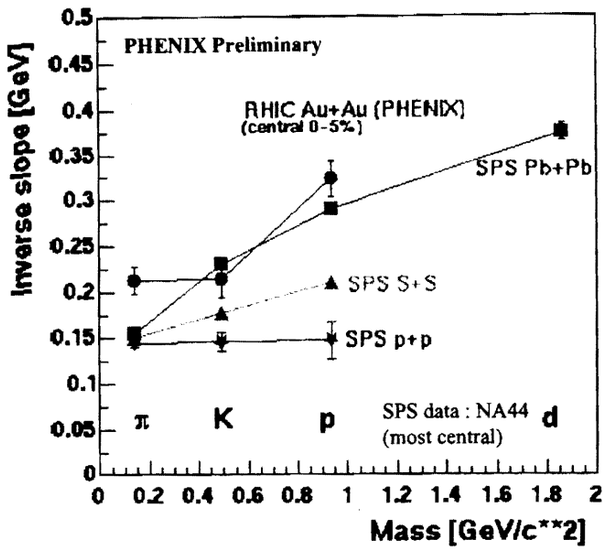

- The slopes of pions and protons at RHIC are higher than that of Pb+Pb collisions at SPS.
- Kaon's slope is almost same at SPS Pb+Pb.

Conclusions

- Single particle spectra for $\pi^{\pm}$, $K^{\pm}$, protons and anti-protons in each centrality class are studied.
- In p_T spectra, a large proton and anti-proton contributions at high p_T.
- Weak centrality dependence of slopes for T_π and T_K.
- Gradual rise of T_{proton} and T_{pbar} from peripheral to mid-central collisions.
- $T_\pi \cong T_K < T_{proton}$ at all centrality classes.
- The slope of pions and protons at RHIC are higher than that of Pb+Pb collisions at SPS.
- Kaon's slope at RHIC is almost same at SPS Pb+Pb.

Particle ratios in PHENIX at RHIC

February 7, 2001

Presented by: Hiroaki Ohnishi

Abstract

The PHENIX experiment at Relativistic Heavy Ion Collider (RHIC) collected more than three million of Au+Au collisions at $\sqrt{s} = 130$ GeV per nucleon during year 2000. The PHENIX Time-of-Flight (ToF) measurement opens an opportunity to investigate identified hadrons with transverse momentum up to 2.0GeV/c. The systematic study of particle yields relates to baryon stopping via proton/anti-proton ratios, to the existence and mechanism of enhanced production of light strange mesons via K/π and K/p ratios, and to comparisons with predictions of chemical and thermal equilibration in these collisions. In this presentation, particle ratios, i.e. K^+/K^- and proton/anti-proton will be presented as a function of centrality and transverse momentum.

Particle ratios in PHENIX at RHIC

Hiroaki Ohnishi

Brookhaven National Laboratory
for the PHENIX Collaboration.

PHENIX Motivation

Investigation of particle production mechanism in heavy ion collisions.

What can we learn from Particle ratios?

≫ Ratios contain basic information about collision dynamics.

- Chemical potential of quarks. ➡ μ_S and μ_B
- Chemical freeze out temperature.
- Degree of baryon stopping power. ➡ pbar/p, μ_B

≫ This information will define boundary conditions of collision dynamics.

➡ Conditions at Freeze-out.

This will be a first step to investigate whether Quark-Gluon-Plasma is formed or not.

Hiroaki Ohnishi [BNL]
CNS workshop 02/14/01

PHENIX Identified Hadron spectra

- Single particle spectra of pion, kaon, proton and their anti particles.
  Au+Au collisions at $\sqrt{s_{NN}}$=130 GeV, Minimum bias data.

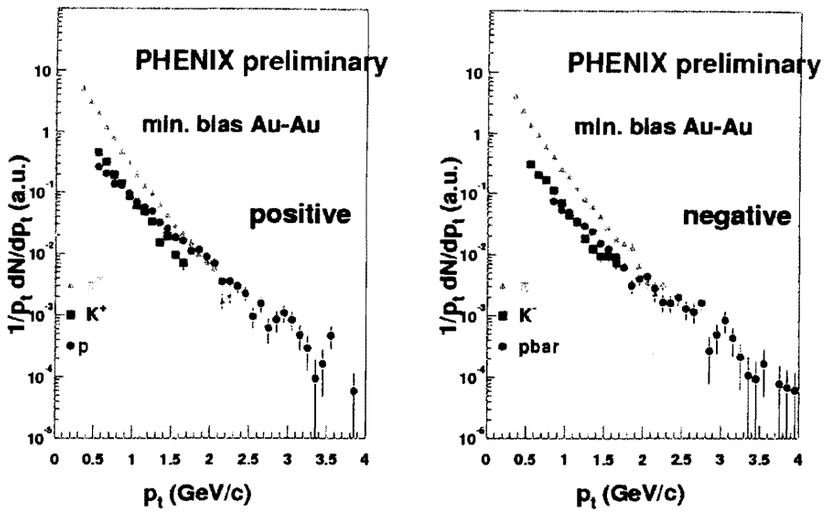

Hiroaki Ohnishi [BNL]
CNS workshop 02/14/01

PHENIX K+/K- ratio

- Expectation from previous experiments
  - K+/K- ratio decreases with increasing $\sqrt{s}$
  - K+/K- ratio in p+p collisions
    - $\sqrt{s}$ = 23 GeV => 1.6
    - $\sqrt{s}$ = 53 GeV => 1.4

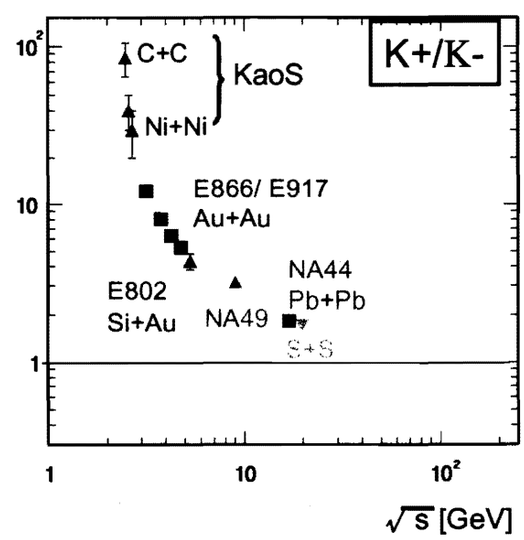

PHENIX K+/K- ratio as a function of P_T

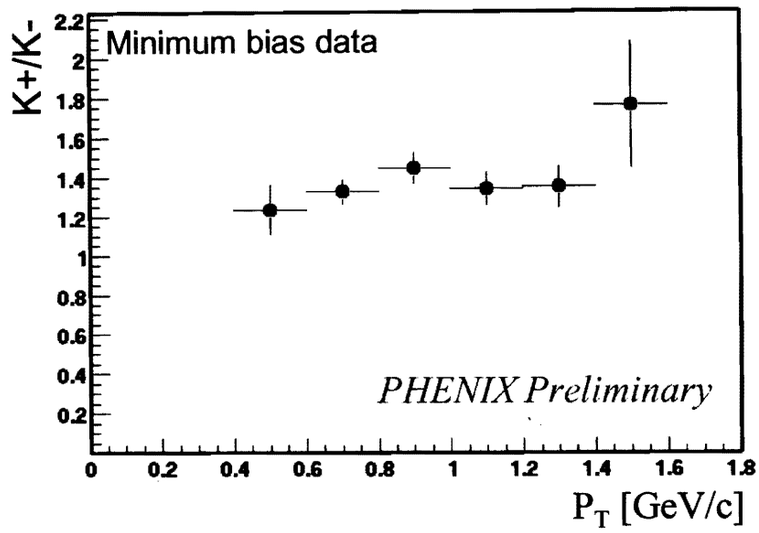

- Within the statistical errors, K+/K- does not depend on P_T over the measured range

PHENIX K+/K- ratio as a function of centrality

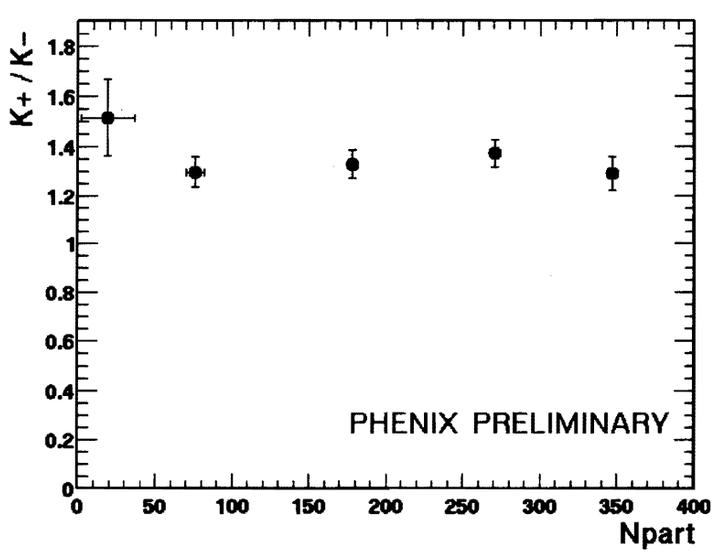

- No dependence as a function of centrality.
- Same trend are measured in SPS and AGS

PHENIX Summary of K+/K- ratio

- K+/K- ratio decreases as a function of $\sqrt{s}$ (0.5GeV/c <PT<1.8GeV/s)

  K+/K- @5% central = 1.29±0.07(stat) ±0.19(sys

- K+/K- production at RHIC follows the trend observed in the experiments at SIS, AGS and SPS.

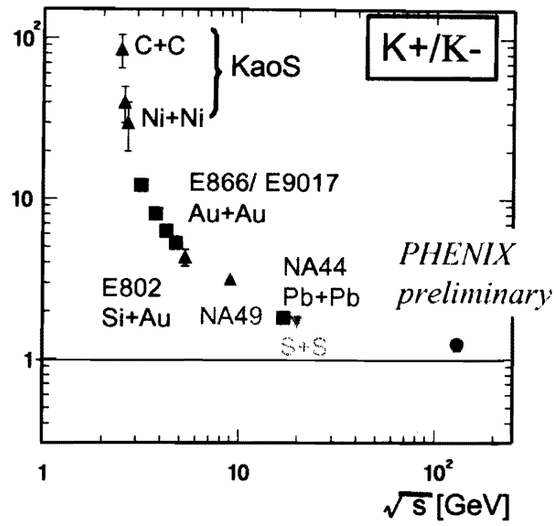

PHENIX pbar/p ratio

- pbar/p ratio is increasing from AGS to SPS.

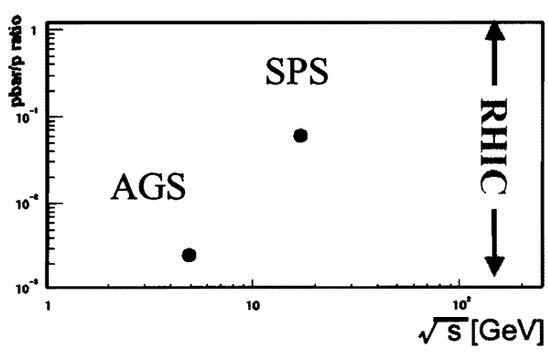

PHENIX pbar/p ratio as a function of centrality

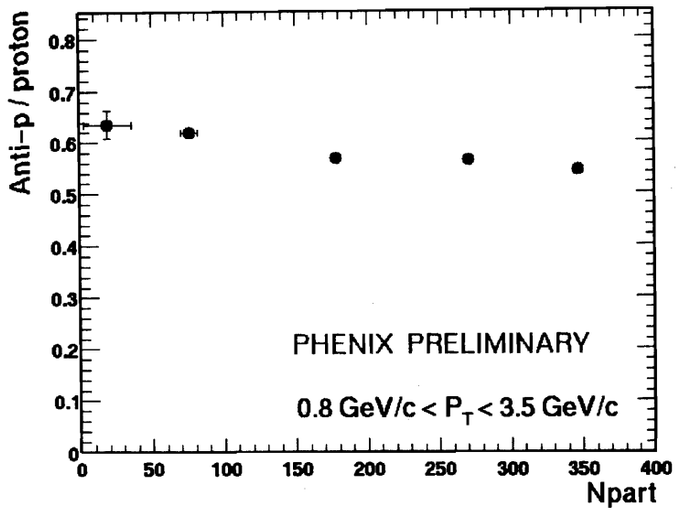

Systematic errors ~15%
Systematic error is not depends on Npart.

pbar/p ratio shows slightly decreasing as a function of centrality.

PHENIX pbar/p ratio as a function of P_T

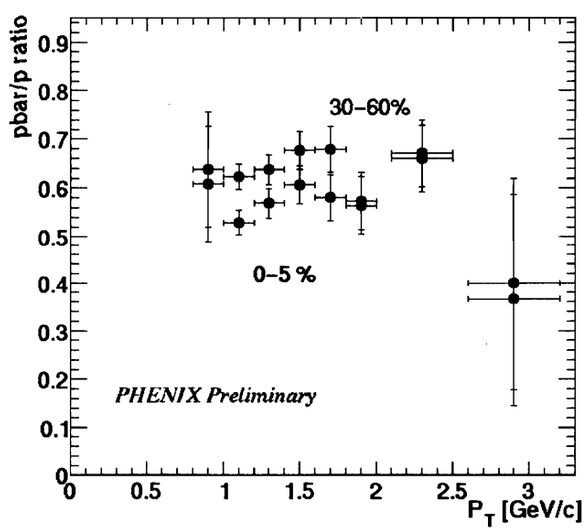

- pbar/p ratio shows constant as a function of P_T up to 3 GeV/c.
- It is vary hard to extract pbar/p ratio at P_T above 3 GeV/c due to small statistics.

Hiroaki Ohnishi [BNL]
CNS workshop 02/14/01

PHENIX pbar/p ratio as a function of P_T

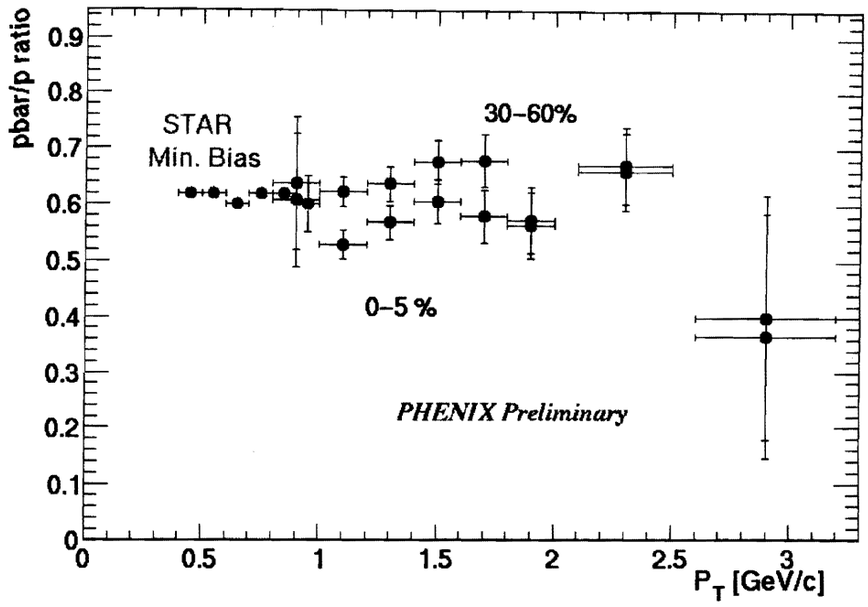

Hiroaki Ohnishi [BNL]
CNS workshop 02/14/01

PHENIX pbar/p ratio as a function of P_T

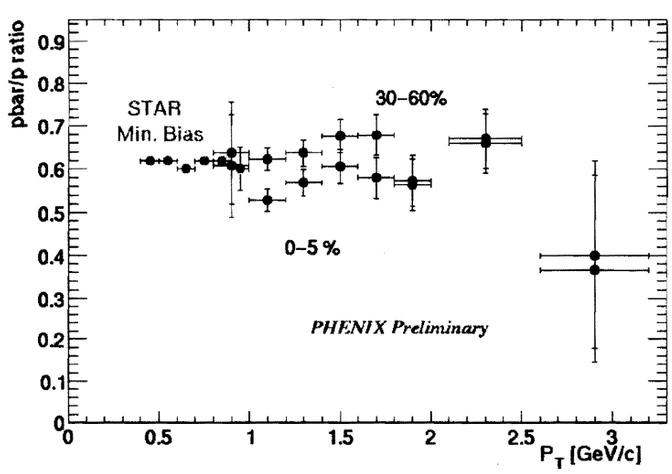

X.N.Wang, PRC58(1998)2321

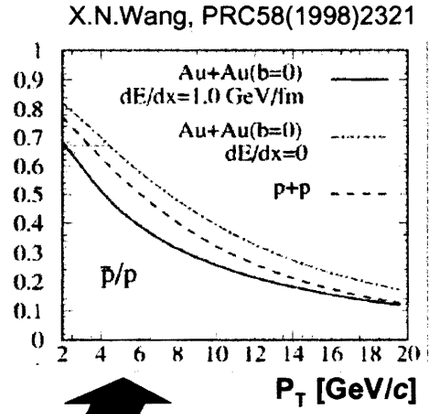

Interesting physics will contain in pbar／p ratio at high P_T.

PHENIX Summary of pbar/p ratio

- pbar/p ratio at RHIC shows dramatically increasing from AGS and SPS energy.
- No clear Centrality and P_T dependence are seen within errors.

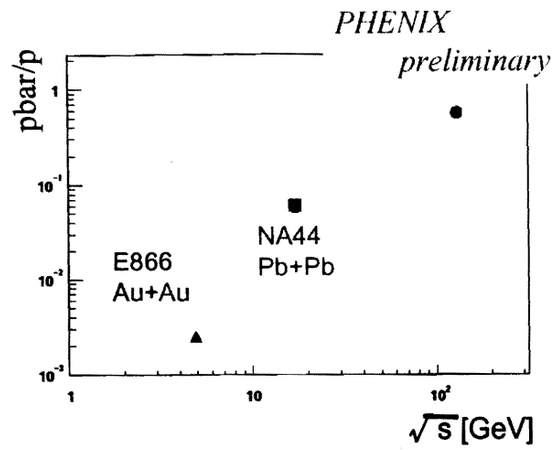

PHENIX K+/K- and pbar/p

- Both K+/K- and pbar/p are closing to 1.0 from AGS to RHIC

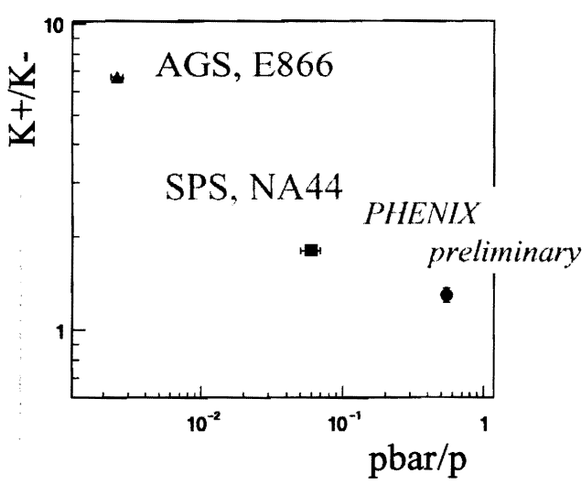

Thermal model tells us…

Baryon chemical potential ~ 50MeV

Not baryon free(μ_B=0).

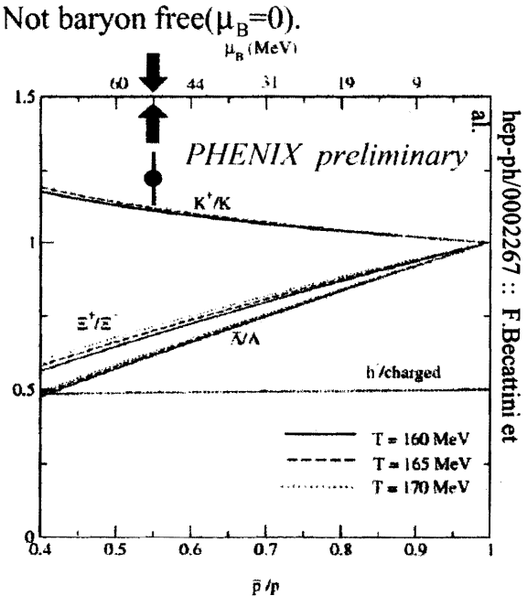

PHENIX Conclusion

- Particle ratios in Au+Au collisions at $\sqrt{s}$=130 GeV are presented.
- No clear centrality dependence are seen in K+/K- ratio. pbar/p shows slightly decreasing as a function of centrality.
- K+/K- and pbar/p ratios show no dependence with P_T. (Kaon; P_T<2.0 GeV/c, Proton; P_T<3.0 GeV/c)
- Particle ratios@ 5% most central event, @mid rapidity
  - K+/K- = 1.29±0.07(stat.)±0.19(sys.)
  - pbar/p = 0.54±0.01(stat.)±0.08(sys.)
- K+/K- and pbar/p ratios are dramatically decreasing / increasing from SPS and AGS energies.
- Baryon density at RHIC is much less than AGS and SPS, but not baryon free at mid rapidity.

PHENIX The PHENIX Experiment

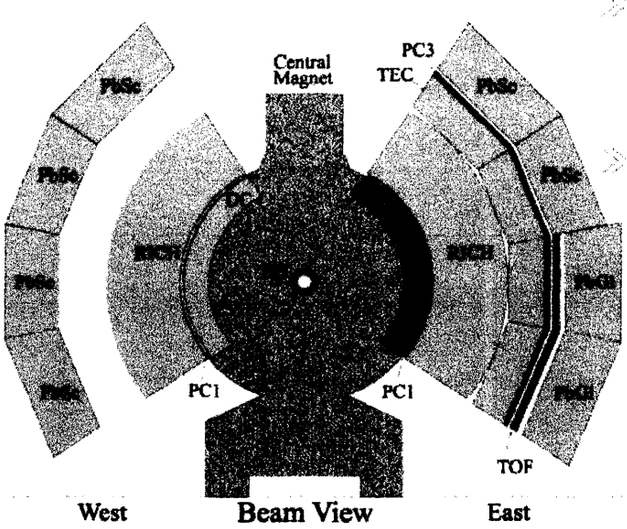

- Tracking system.
  - DC + PC1 + PC3.
- Hadron Identification.
  Time-of Flight measurement
  (Beam/Beam Counter -ToF)
  Time of Flight resolution
  ~120 ps.

PHENIX Particle identification

» Particle identification via Time-of-Flight.

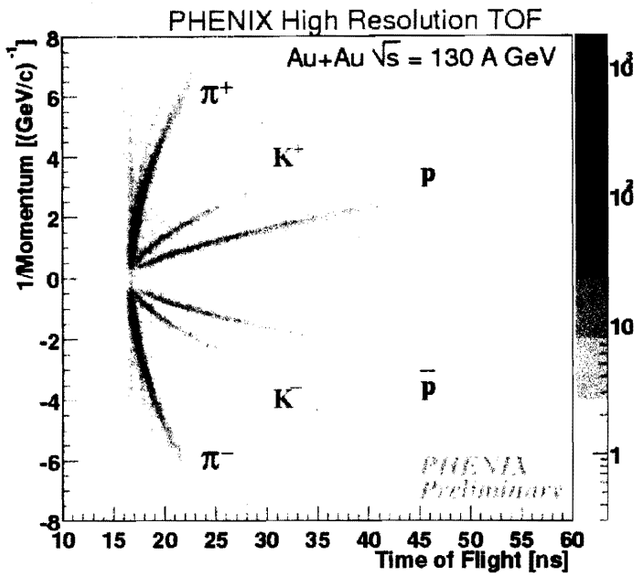

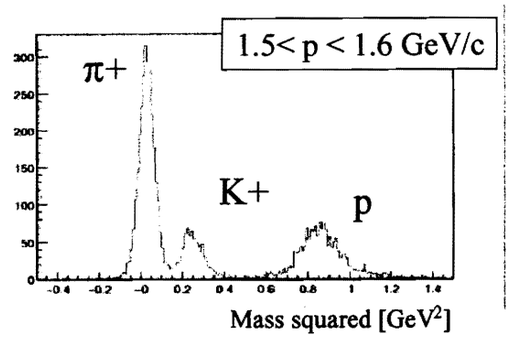

π/K separation < 1.6 GeV/c
Proton separation < 3.5 GeV/c

PHENIX The PHENIX Experiment (II)

» Centrality definition

» Centrality selection based on the correlation between Beam-Beam Counters(BBC) and Zero Degree Calorimeter(ZDC).

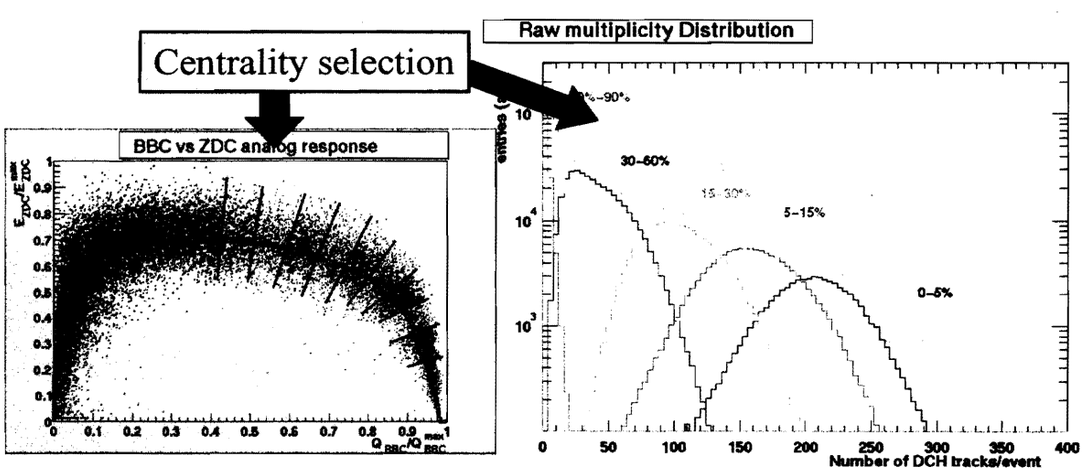

CERN SPS hadron measurement

Flow measurement with a puzzle, and interpretation of low mt enhancement of pion spectrum.

Susumu SATO

University of Tsukuba

For the flow measurement at the SPS energy, several hadron species are analyzed in different rapidity region. Hadron identification in higher momentum at mid-rapidity, the time of flight method take an important role. The reaction plane is measured in target rapidity and the ellipticity of the flow is intensively studied in mid rapidity. The mid rapidity at the SPS energy has less disturbance by the spectator than in lower energy. An interesting feature is reported for the positively charged kaons. The ellipticity of the kaon shows out-of-plane emission pattern, which is the opposite direction of pion. Interpretation of the pattern is still in puzzle, and the comparison with higher energy at RHIC is of current interest. Other puzzle is seen at SPS energy, in pion single spectrum. Large enhancement in low mt region is observed. Interpretation by the contribution of the lowest resonance of nucleons is of large interest. And direct measurement of yield of the positively charged delta resonance enables studies of contribution from the resonance decay in comparison with other effects, like collectivity or the Coulomb effect. Such view is also of large importance at RHIC energy.

CERN SPS hadron measurement

Flow measurement with a puzzle, and interpretation of low m_t enhancement of pion spectrum

Susumu SATO
Univ. of Tsukuba

Contents

1) Ellipticity at mid-rapidity
→ Difference in Kaon
2) Low m_t enhancement
→ Resonance role at mid-rapidity

Flow measurement at SPS

by Plastic Ball + magnetic spectrometer with PID

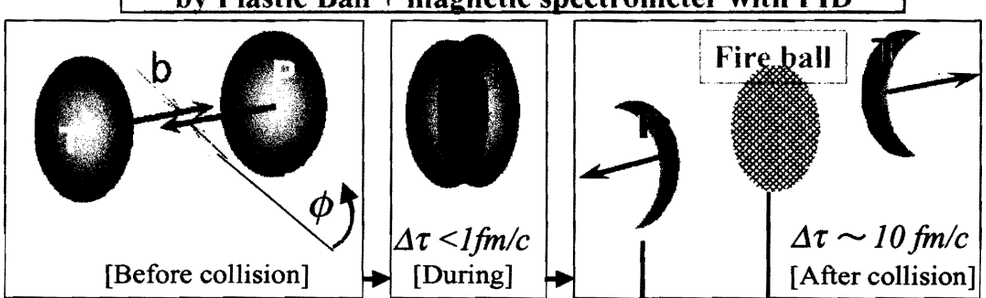

Fourier Expansion of Azimuthal Distributions

$$F(\phi) = F_0\{1 + 2v_1\cos(\phi) + 2v_2\cos(2\phi) + \ldots\}$$

n=0 "Radial Flow", Isotropic transverse flow

n=1 "Directed Flow" Non-isotropic flow

n=2 "Elliptic Flow"

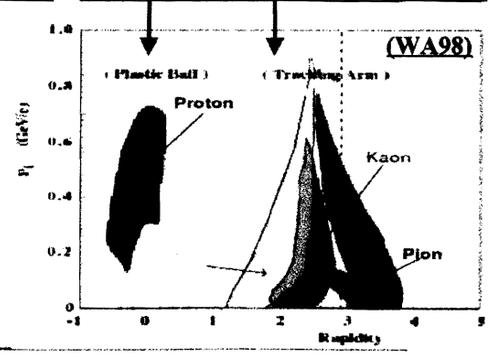

WA98 experimental setup

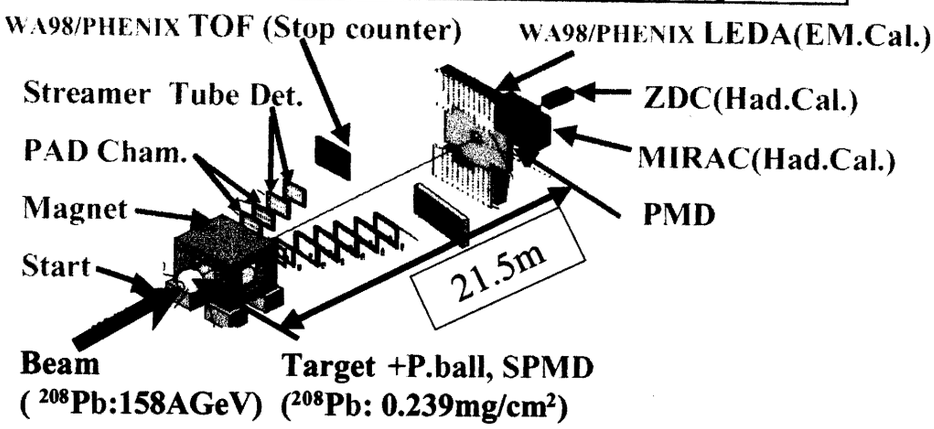

Characterize Fireball from various aspects

- [Hadron] momentum + PID; w/Mag. Spectr.
- [Photon] Eγ; w/EM.Cal.
- [Hadron] global E_T, E_0; w/Had.Cal.
- [Photon] mult. distr.; w/PMD
- [Charged particle] mult. distr.; w/SPMD, P.ball

Reaction Plane determination

By Plastic Ball (dE -E & delayed signal for π^+)

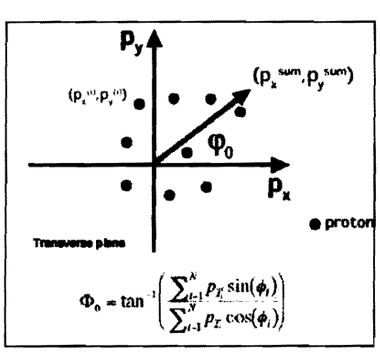

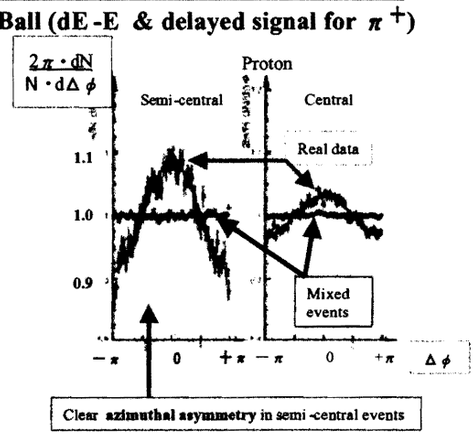

Method proposed by A.M. Poskanzer & S.A. Voloshin, (PRC58,1671(1998))

$\langle\cos(\Phi_0 - \Phi_p)\rangle = 0.360 \pm 0.018$

$\langle\cos(2(\Phi_0 - \Phi_p))\rangle = 0.084 \pm 0.005$

at semi-central col.

Elliptic flow of π^+ and K^+

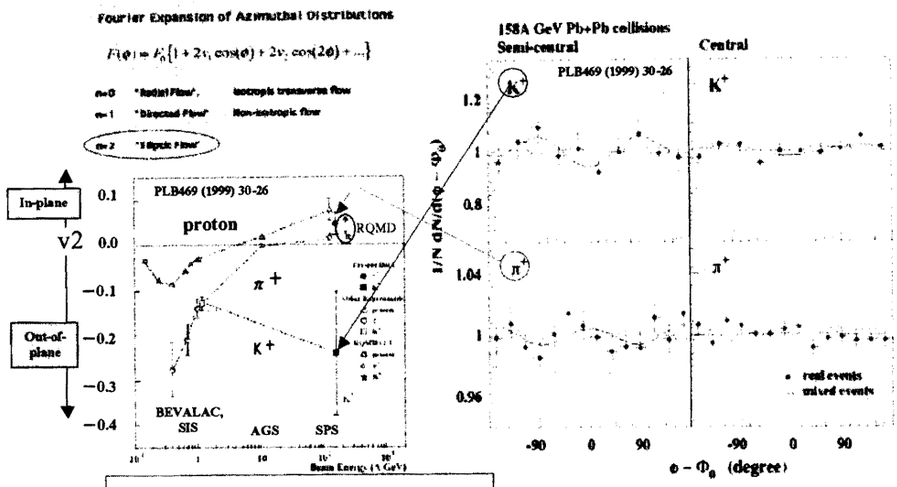

out-of-plane for K^+ with C.L. 95.7%

At SPS energy, Kaon has different ellipticity compared to protons or pions

P_t dependence *at mid-rapidity*

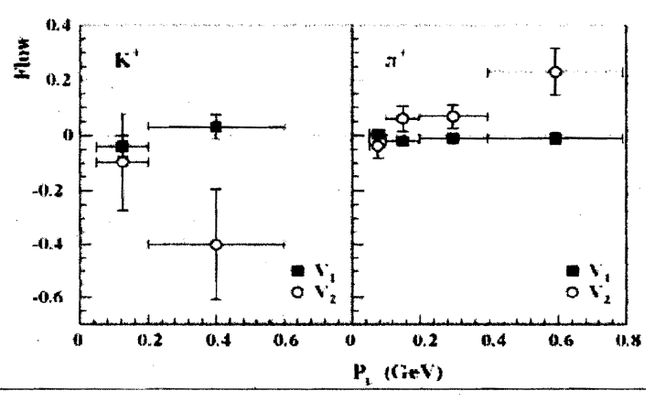

- v2 increase with p_t.
- v1 remains close to zero.

→our acceptance is at mid rapidity

Single Particle Spectra (*pp* collisions)

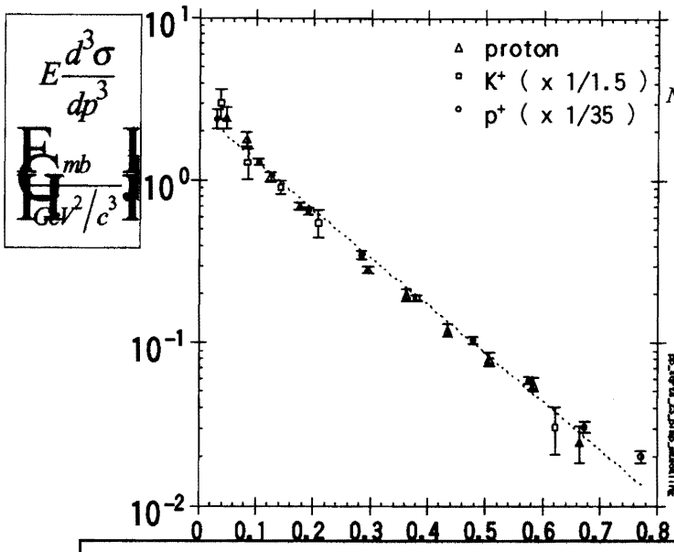

$\sqrt{s} = 23GeV$

Nucl.Phys.B100(75)237

(1)Similar shape, and
(2)Similar slope
for different
particle species
(called m_t-scaling)

mt – m (GeV)

mt-scaling in proton – proton collisions

Single Particle Spectra (*nucleus - nucleus* collisions)

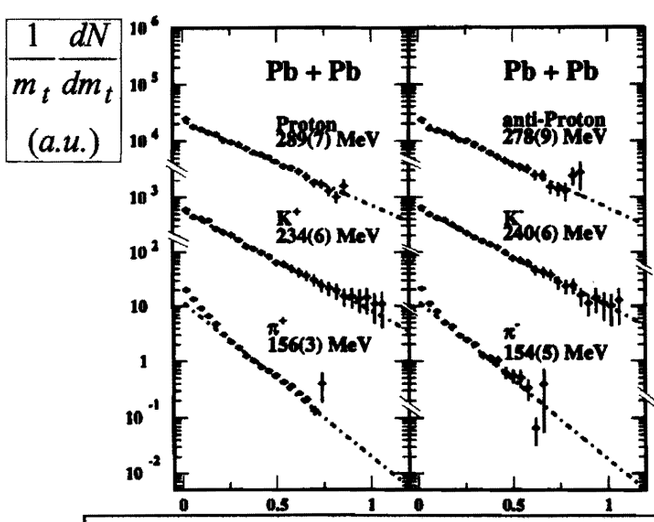

158 *AGeV Pb+Pb*

Nucl.Phys.A610(96)175c

(1)Different shape, and
(2)Different slope
for different
particle species

mt – m (GeV)

Different shape and slope are observed.

Expanding Fireball Model ~ example of good parameterization ~

(1) Single spectra:
transverse kinetic energy (m_t) spectra
PRL80(98)3467

→parameterization for different particle species
T_f~139MeV, $\langle\beta_f\rangle$ ~0.42c

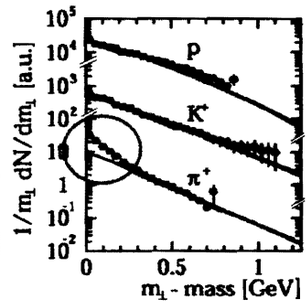

(2) Two particle HBT correlation
Habilitation('97/T.Peitzmann)

→Boost invariance for expansion
$\langle\beta_f\rangle = \Delta R/\tau_f$ ~ 0.43±0.16c

Good explanation
both for singles and two particle correlation,
but not using lower m_t-region

Δ^{++} resonance

- Lowest resonance of nucleon
- M ~ 1232MeV (in Breit-Wigner function)
- $c\tau$ ~ 1.8 fm; (Γ~111MeV)
- Isospin3/2, Spin 3/2
- Decay into pion and proton with >99% branching ratio

$\Delta^{++} \xrightarrow{>99\%} \pi^+ + p$

cf.
$\Delta^+ \xrightarrow{\sim 50\%} \pi^+ + (n)$
$\xrightarrow{\sim 50\%} \pi^0 + p$
$\Delta^- \xrightarrow{>99\%} \pi^- + (n)$
$\Delta^0 \xrightarrow{\sim 50\%} \pi^- + p$
$\xrightarrow{\sim 50\%} \pi^0 + (n)$

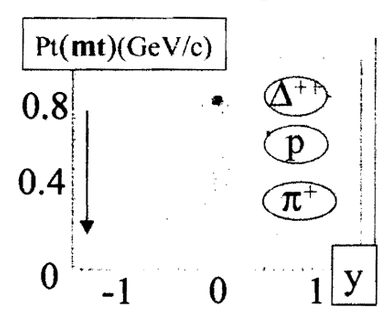

- Decayed pion gives lower transverse kinetic energy

Particle Identification

(with WA98/PHENIX TOF)

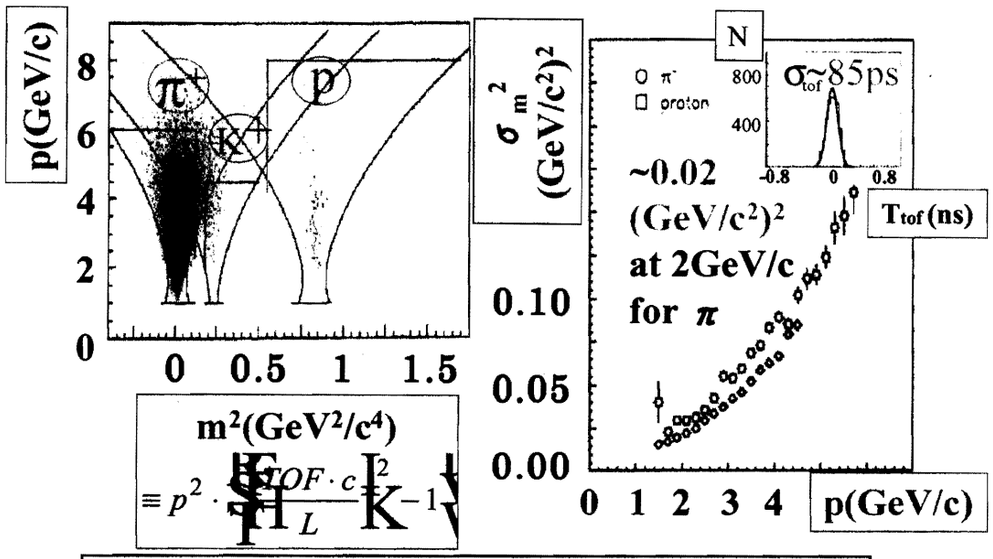

Clear Particle Identification by ToF method

Geometrical Acceptance

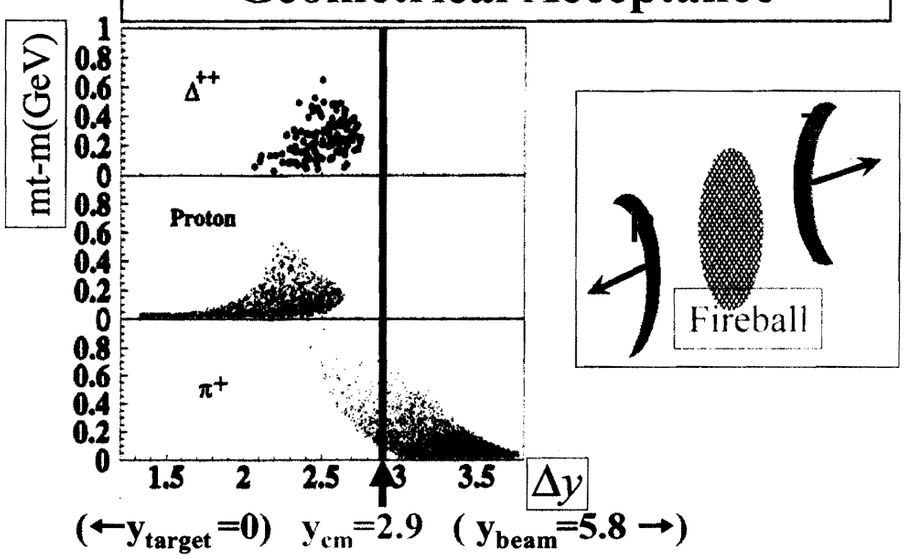

Measure around mid-rapidity,
where hot fireball is expected the most.

Single spectra

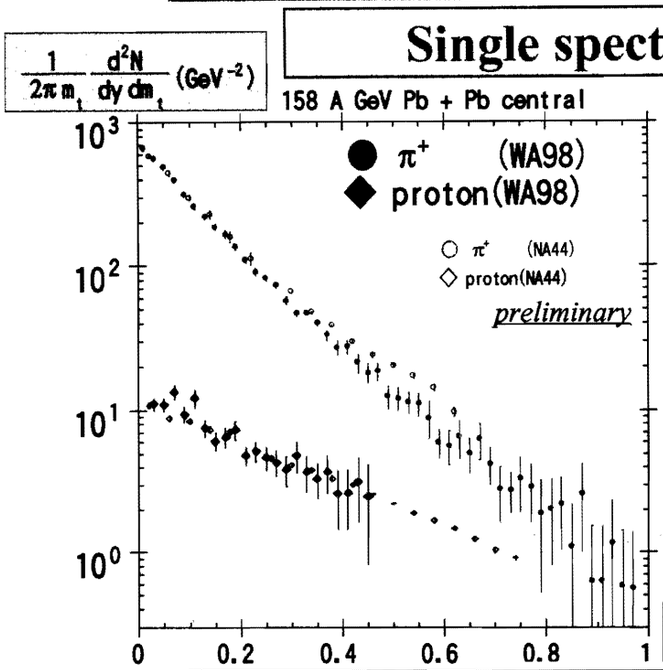

Slope (MeV)	WA 98	NA 44(*)
π^+	142 ±3	156 ±3
p	251 ±25	289 ±7

(*) Nucl.Phys.610(96)175

dN/dy	WA 98	NA 44(**)
π^+	138 ±16	155 ±10
p	25 ±6	27 ±5

(**) M.Kaneta, PhDThesis (1999)

Consistent shapes in different experiments

Parameterization for Δ yield by invariant mass method

Invariant mass

$$m_{inv} \equiv \sqrt{(E_{\pi^+} + E_p)^2 - (\vec{p}_{\pi^+} + \vec{p}_p)^2}$$

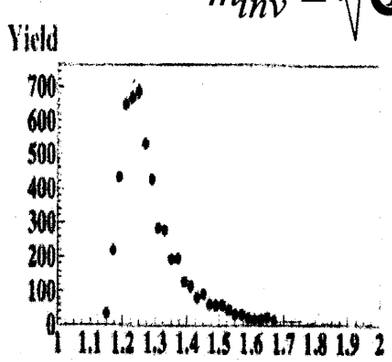

Invariant mass distribution

$$Yield_{raw}(m_{inv}) \propto Yield_{\Delta^{++}}(m_{inv}) + Yield_{comb.B.G.}(m_{inv})$$

$Yield_{comb.B.G.}(m_{inv})$ should be evaluated

Two normalization methods

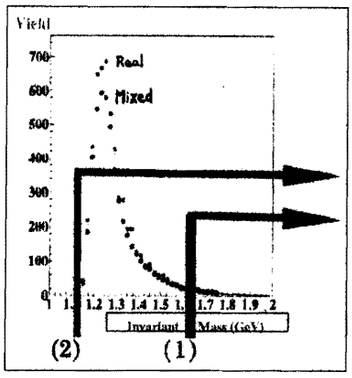

(1) Tail method

normalize only in higher m_{inv} region

(2) Breit-Wigner + Background method

normalize in any m_{inv} region, assuming $Yield_{\Delta^{++}}$ follows Relativistic Breit-Wigner (PRL79('97)4354)

$$Yiled_{\Delta^{++}}(m_{inv}) \overset{assume}{=} \frac{q^3}{q^3+\mu^3} \cdot \frac{1}{4\left(\frac{m_{inv}-m_{\Delta^{++}}}{\Gamma_{\Delta^{++}}}\right)^2+1}$$

q:relative momentum of the pair in its C.M. frame,μ:180MeV/c

Two methods should be consistent

Tail method

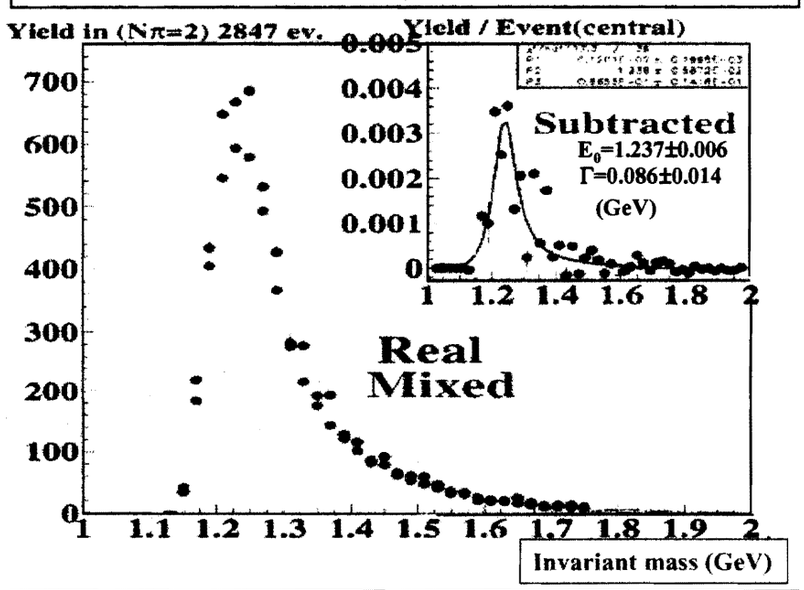

Clear yield can be extracted by tail method

Yield summary table

Value and Statistical Error		
Δ^{++} / spectrometer /ev. (raw)	0.022	±0.010
proton / spectrometer/ev. (raw)	1.080	±0.010
Δ^{++}/proton (raw)	0.021	±0.009
ε_{trk} (3or4cham.)	0.79	±0.02
ε_{PID}	0.60	±0.02
ε_{geo}	0.145	±0.005
Δ^{++}/proton (ε_{trk}, ε_{PID}, ε_{geo} corrected)	0.31	±0.14
Δ/nucleon (isospin corrected)	0.62	±0.28 (stat.) (45%)

Systematic Error	
Uncertainty of Tracking efficiency	±0.06 (sys.) (10%)
Difference in normalization method	±0.02 (sys.) (4%)
Difference for different local multiplicity	±0.08 (sys.) (13%)

At SPS, delta yield is, for the first time, directly measured

Population ratio: Δ/ nucleon

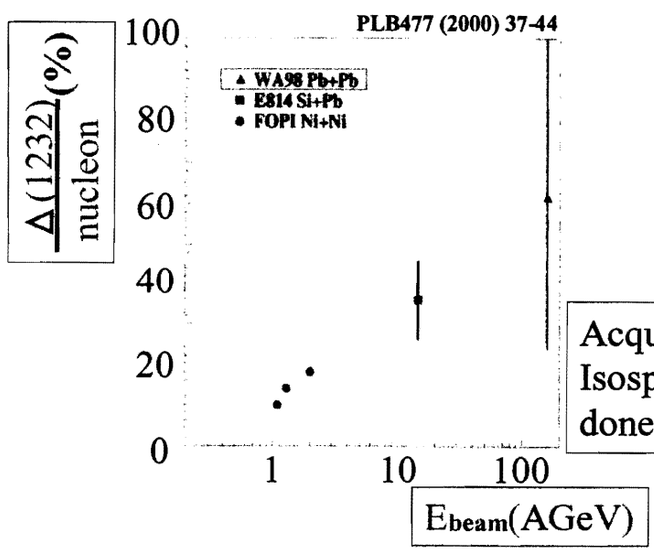

Acquired from Δ / p, Isospin correction done for $^{208}_{82}Pb$

Higher population is seen at SPS

Low mt enhancement in Pb + Pb (1)

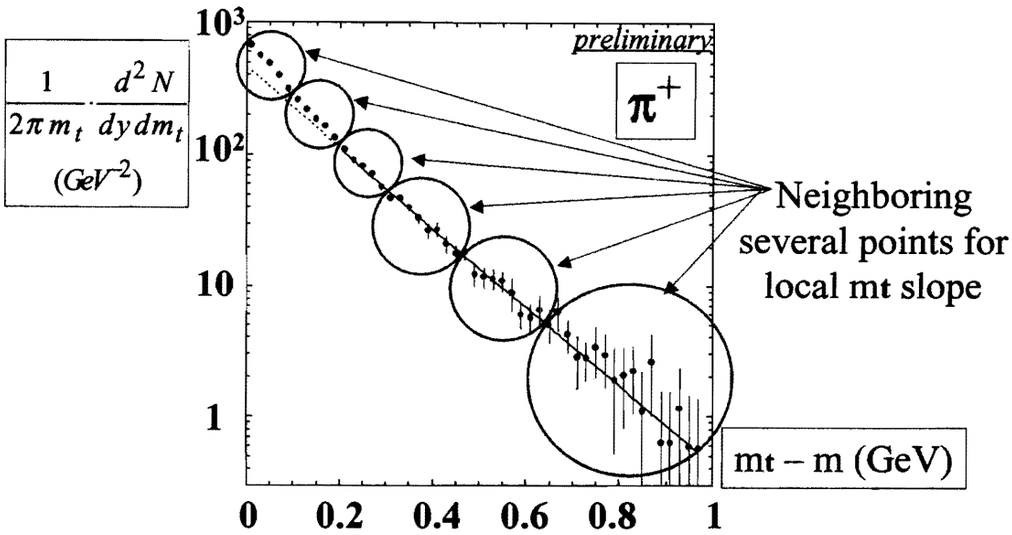

Low m_t enhancement is seen in local m_t slope (Next)

Low mt enhancement in Pb + Pb (2)

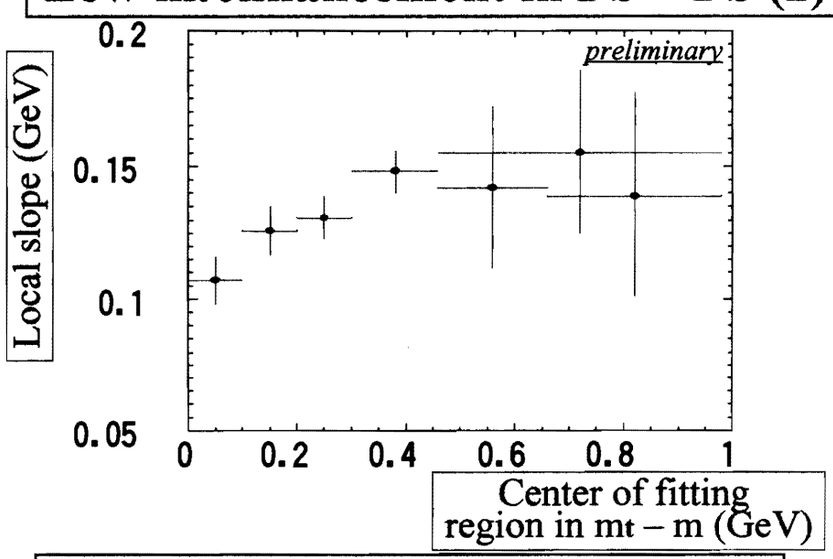

The m_t enhancement is seen in π^+ spectrum in Pb + Pb collisions

Candidates of low mt enhancement

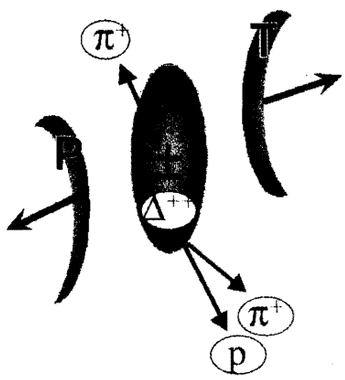

(1) Collective motion

e.g. Collective radial expansion

(2) Coulomb effect

Repulsion/Attraction from Charges

(3) Resonance decay

Δ decay gives lower mt π by kinematics

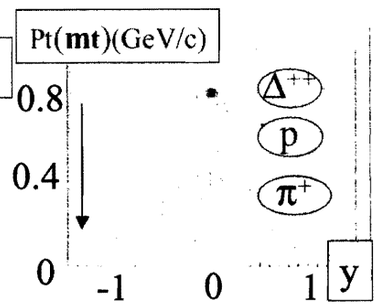

There are more than one candidates

Collective motion (Thermal+expansion)

$$\frac{1}{m_t}\frac{dN}{dm_t} \quad (a.u.)$$

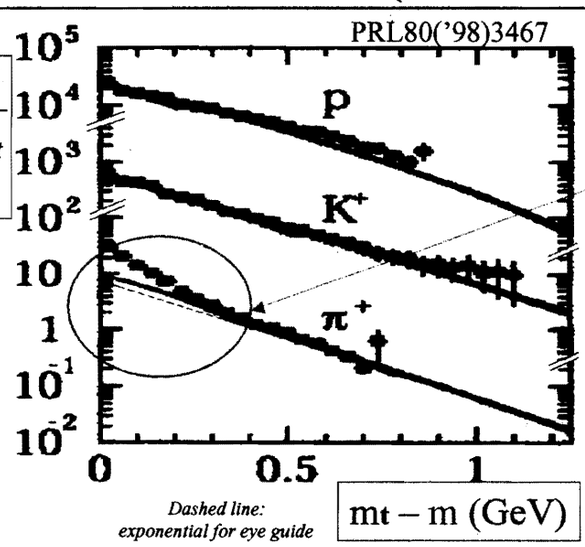

Describing well for different particle species except low m_t π, and shape of π is little affected by collective motion

T=139MeV

β =0.42c

consistent also with two particle HBT correlation

π spectra shape is little affected by Collective motion

Coulomb effect

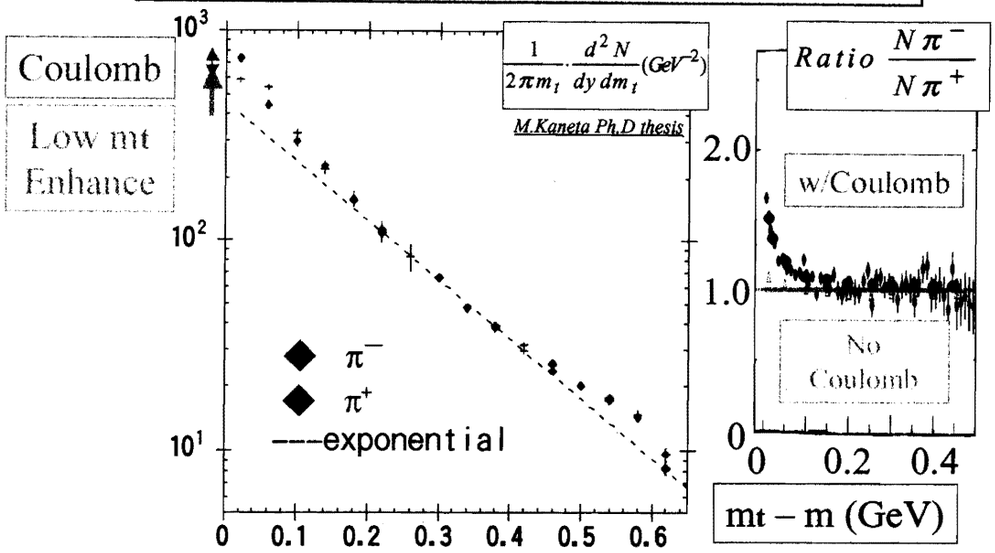

Low m_t enhancement is seen in both charge, and Coulomb effect appears as difference between π^+ and π^-.

Contribution of Δ Resonance

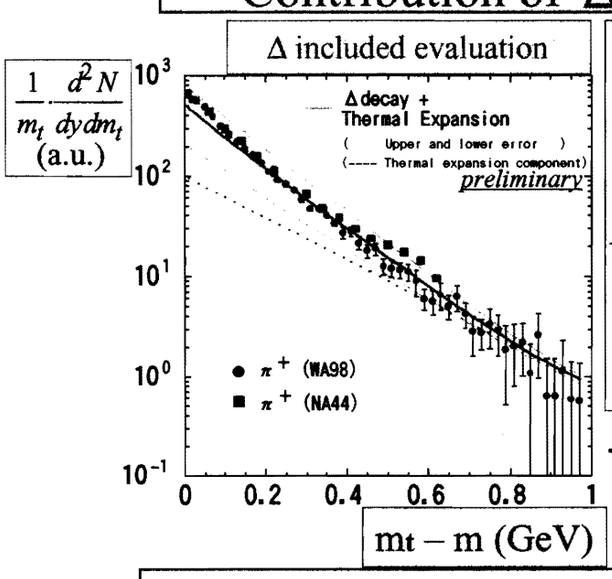

Δ (invariant mass)
with a factor $(1+\alpha)$
$\alpha \equiv$

$$\frac{N_{\Delta\to p(Sc.)+\pi(Not.Sc.)}}{N_{\Delta\to\pi(NotSc.)+p(NotSc.)}}$$

→consistent with simulation (~1.5)

+

thermal model
T=139 MeV,
$\langle\beta\rangle$ =0.42c

"thermal source" + "Δ resonance decay" is consistent with the low-m_t enhancement of π^+.

Summary

At the SPS energy,

- Using fragment at target rapidity, reaction plane determination is performed. An interesting feature in the ellipticity at mid rapidity is seen for the kaons.
  - →(still) out of plane emission
  - →Comparison with RHIC energy is wanted. (PIDed analysis is needed !)
- Large fraction (~ 2/3) of nucleons are in Δ(1232) resonance states.
  - →Additional 1.5 times of Δ are possible to be interpreted to contributed to the pion low m_t enhancement.
  - → Penetration of pion matter is wanted to be studied at RHIC.

Well,.. other resonances

- *Chemical equilibrium tells, heavier baryonic resonance is still minor.*
- *Mesonic resonances*

  for example,
  - *f(400-1200)* → *major contribution in JAM, while no presence at all in RQMD, chemical calc. et al*
  - *ρ/ω* → *no systematic understanding with leptonic decays*

That's still vague...

Hydrodynamical analysis of elliptic flow at SPS and RHIC

Tetsufumi Hirano
Department of Physics, Waseda University

Hydrodynamics has widely been used to describe the space-time evolution of nuclear matter produced in relativistic heavy-ion collisions. First I briefly comment on why hydrodynamics is necessary for studying the physics of heavy-ion collisions. There are a large number of analyses based on the fundamental theory such as an equation of state from lattice QCD, spectral changes of hadrons in medium from low energy effective theories of QCD and so on. Equilibrium at a fixed temperature or density is assumed in these calculations. On the other hand, real nuclear matter produced in heavy-ion collisions is by no means static; It dynamically expands and cools down owing to the pressure gradient. One possible way to connect static models with the dynamical phenomena is the application of the relativistic hydrodynamical model.

Since hydrodynamics is directly connected with the equation of state of nuclear matter, the hydrodynamical analysis of flow is indispensable in understanding the thermodynamical aspects of nuclear matter. Elliptic flow is believed to be a powerful tool to study the nuclear equation of state and the thermalization of the system. On the lines of the above discussion, we investigate non-central collisions at the SPS and RHIC energy by using a (3+1)-dimensional relativistic hydrodynamical model. Initial parameters in the hydrodynamical model are chosen so that we reproduce the single particle spectra of hadrons [1]. Observed pion spectra always contain the contribution from not only pions directly emitted from freeze-out hyper-surface but also decays of resonance particles after freeze-out. The decay of resonance particles after freeze-out dilutes the elliptic flow of nuclear matter. I found that the reduction of elliptic flow is due to the decay kinematics [2]. Taking this effect into account, we analyze the experimental data of elliptic flow at the SPS and RHIC energy and show how large the effect is for the final azimuthal distribution of pions.

References

[1] T. Hirano, K. Tsuda and K. Kajimoto, nucl-th/0011087.

[2] T. Hirano, nucl-th/0004029 (to be published in Phys. Rev. Lett.).

Hydrodynamical analysis of elliptic flow at SPS and RHIC

Tetsufumi Hirano

Department of Physics, Waseda University, Tokyo 169-8555, Japan

In collaboration with
Keiichi Tsuda & Kohei Kajimoto

[1] T.Hirano,K.Tsuda and K.Kajimoto, nucl-th/0011087
[2] T.Hirano, nucl-th/0004029 (to appear in PRL)

Contents

- Why hydrodynamics ?
- v_2 ⟺ `elliptic flow' ??
- v_2 at SPS
- v_2 at RHIC
- Summary

Why Hydrodynamics ?

Theories

- **Lattice QCD**
  Equation of state
- **Effective theories**
  Spectral change of hadrons in medium
- **Etc.**

At fixed T or n_B

STATIC!

HYDRODYNAMICS

Phenomena

Motivation & strategy

Eq. of State (EoS)

- Phase transition between QGP phase and hadron phase
- Softening of EoS

Collective Flow in Relativistic HIC

- Radial flow
- Directed flow
- Elliptic flow

Relativistic Hydrodynamic Model

Relation between 'in-plane' and 'positive v_2' breaks down!

Owing to resonance decays

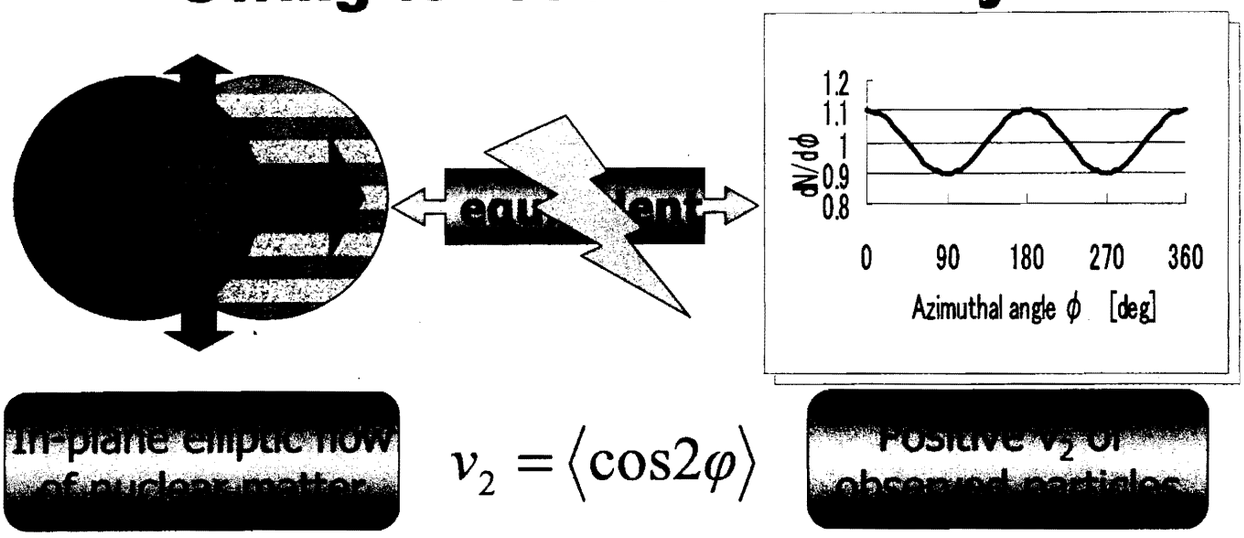

$$v_2 = \langle \cos 2\varphi \rangle$$

Particle emission from hot matter

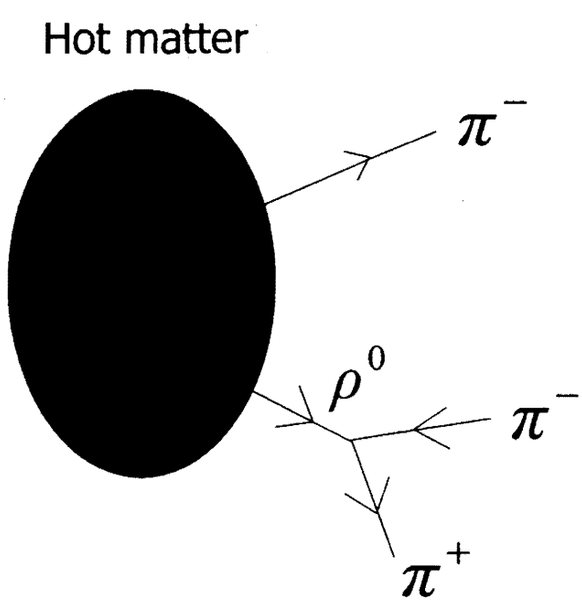

- Direct emission from freeze-out hyper-surface
- Feeding down from resonance decay

Decay Kinematics

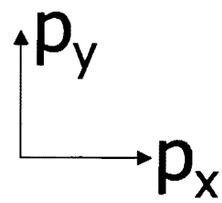

Rest frame

Isotropic emission

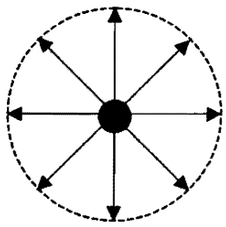

v<v$_c$

$$v_c = \sqrt{1 - \frac{4m^2}{m_R^2}}$$

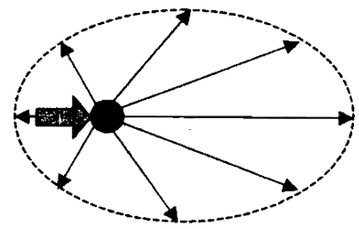

$\rho \rightarrow \pi\pi$

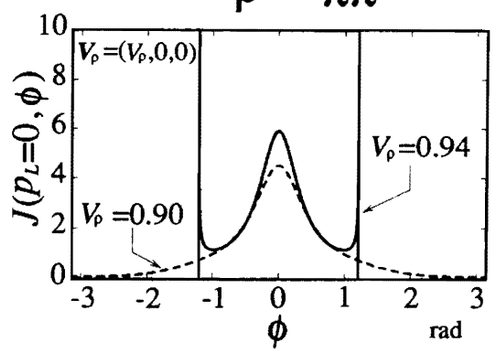

v>v$_c$

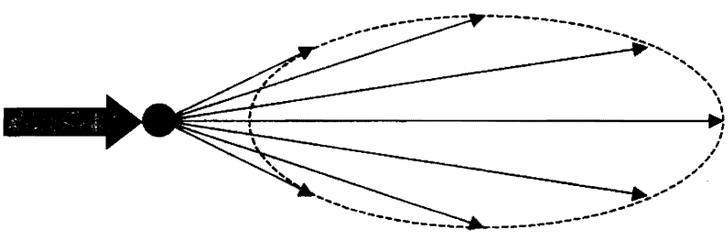

Emission angle is limited.

Effect of decay kinematics on $v_2(p_t)$

-0.5<Y<0.5

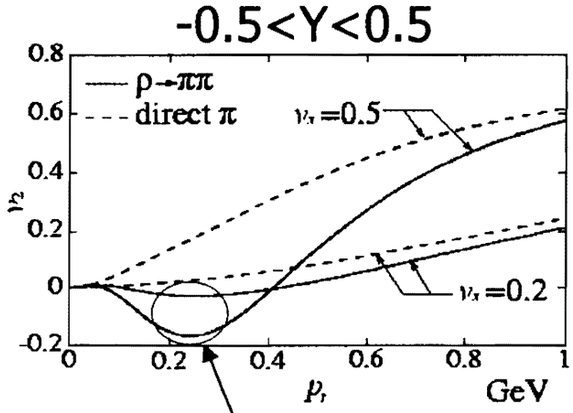

Negative v_2!

See also, T.Hirano, nucl-th/004029, (To appear in Phys.Rev.Lett.).

- Toy model of in-plane elliptic flow

T_f=120 MeV

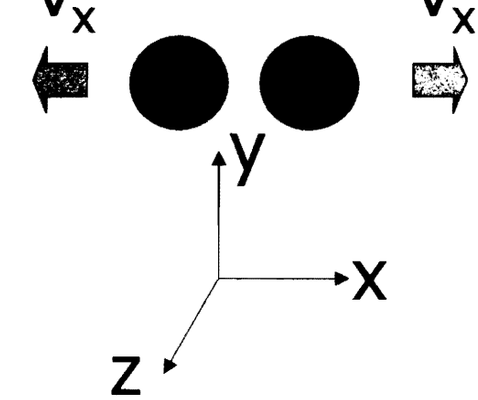

Relativistic hydrodynamic model

Hydrodynamical eq.

$$\partial_\mu T^{\mu\nu} = 0, \partial_\mu n_B^\mu = 0$$

•Energy & momentum tensor

$$T^{\mu\nu} = (E+P)u^\mu u^\nu - Pg^{\mu\nu}$$

E: energy density,
P: pressure, u^μ : 4-velocity

•Baryon flow

$$n_B^\mu = n_B u^\mu$$

n_B:baryon density

EoS*

•Hadron phase
Baryons &mesons
+ exclude volume correction

•Mixed phase

$$T_C(n_B = 0) = 160 \text{ MeV}$$

$$P(n_B = 0) = 59.0 \text{ MeV/fm}^3$$

•QGP phase
u,d,s-quarks and gluon

$$P = \frac{1}{3}E - \frac{4}{3}B, B^{\frac{1}{4}} = 233\text{MeV}$$

*C.Nonaka et al.,Eur.Phys.J.**C17**.663(2000).

Initial geometry (Pb+Pb 158 A GeV at SPS)

Initial time: $t_0 = \frac{2r}{\gamma v} \cong 1.4\,\text{fm}$

Impact parameters:
$b = 2.4, 4.4, 6.4, 8.2, 9.5, 10.6\,\text{fm}$
or $7.2\,\text{fm}$

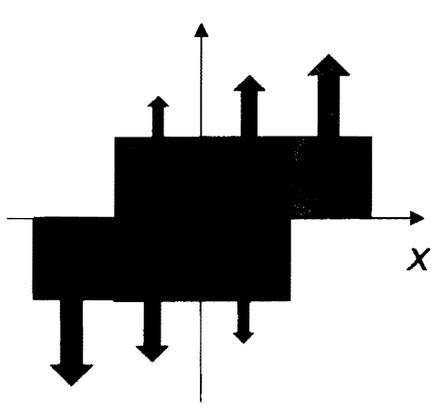

Reaction Plane

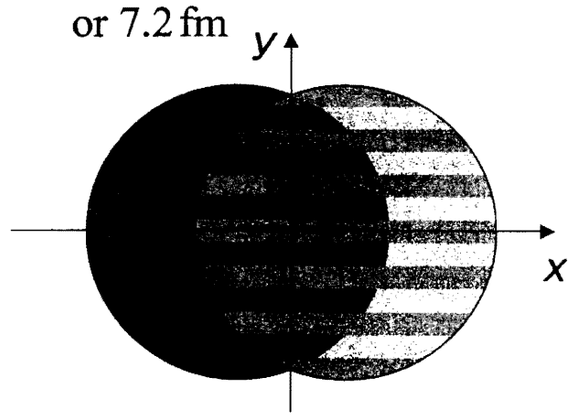

Transverse Plane

Initial parameters at SPS energy (Pb+Pb 158 A GeV)

INPUT

- Initial time: t_i = 1.4 fm
- Initial energy density: E_0 = 3.9 GeV/fm^3
- Initial baryon density: n_{B0} = 0.46 fm^{-3}
- Freeze-out energy density: E_f = 60 MeV/fm^3

$E(x,y,z)=E(z)W(x,y;b)$, $n_B(x,y,z)=n_B(z)W(x,y;b)$

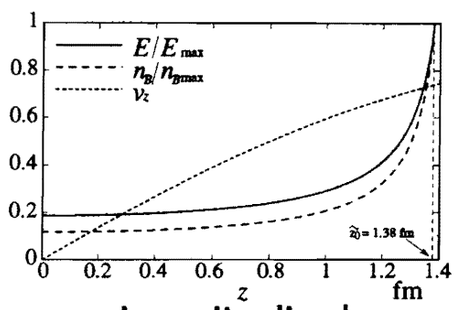

Longitudinal

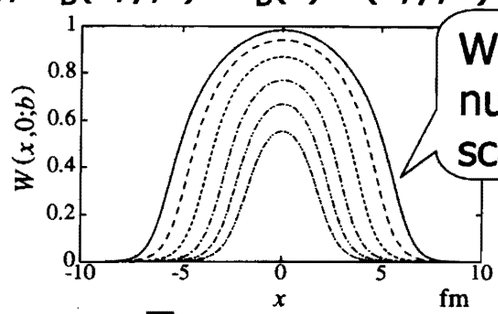

Transverse

Wounded nucleon scaling

Single particle spectra in central collisions at SPS

rapidity distribution

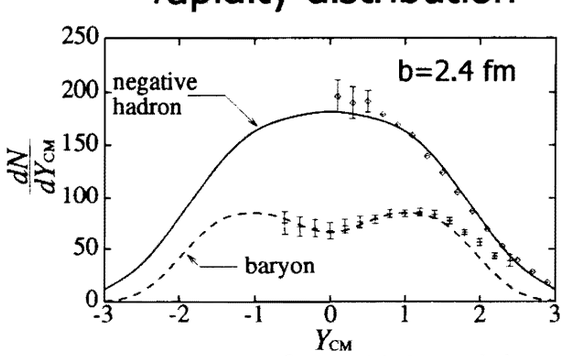

transverse mass distribution

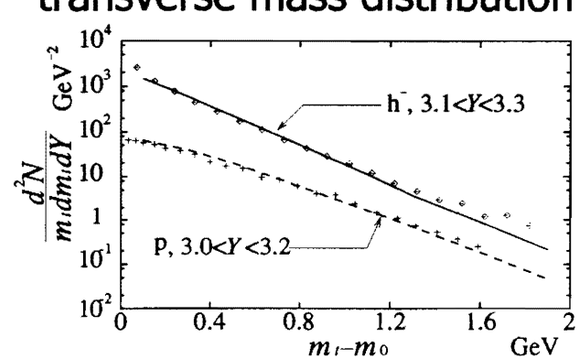

Data from H.Appelshauser et al., PRL**82**,2471(1999).

Parameter tuning in Pb+Pb central collisions

Freeze-out parameter $\begin{cases} \langle T_f \rangle = 117 \text{ MeV} \\ \langle \mu_f \rangle = 323 \text{ MeV} \end{cases}$

Single particle spectra in non-central collisions at SPS

rapidity distribution

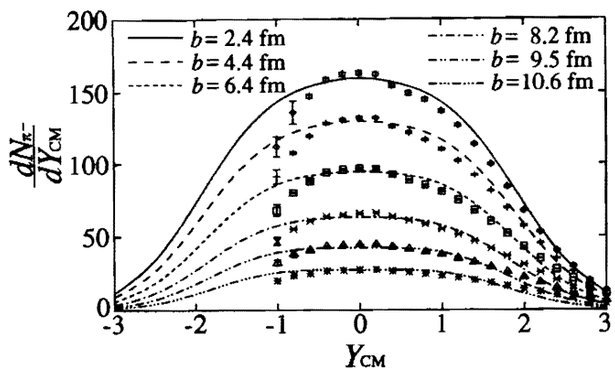

transverse mass distribution

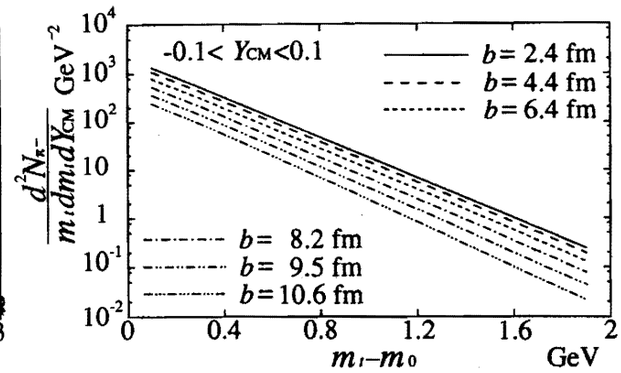

Data from G.E.Cooper, Ph.D thesis, UC Berkeley, April 2000.

Simple scaling for initial condition in non-central collisions

Differential elliptic flow at SPS

v_2 as functions of Y

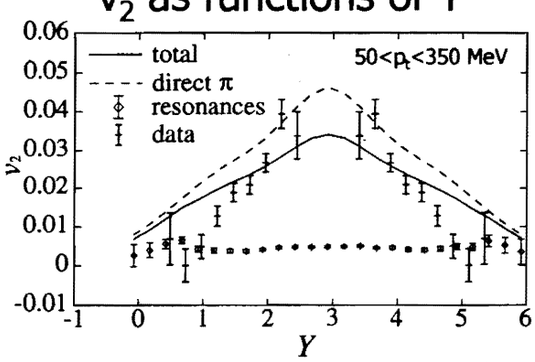

v_2 as functions of p_t

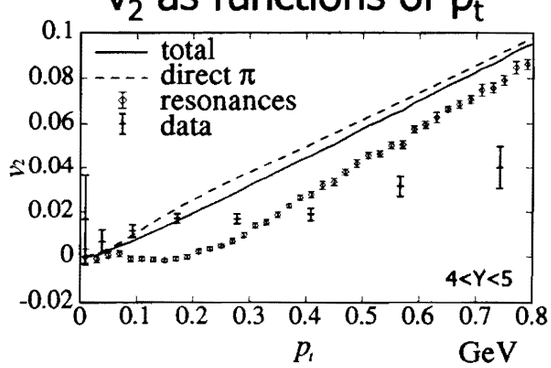

Exp. data:6.5<b<8.0 fm
Results:b=7.2 fm

Data from
http://na49info.cern.ch/na49/Archives/Images/Publications/Phys.Rev.Lett.80:4136-4140,1998

Total v_2 is reduced by **24%** at midrapidity owing to resonance decays.

Total v_2 is reduced by **20%** at p_t=0.25 GeV owing to resonance decays.

Centrality dependence of elliptic flow at SPS

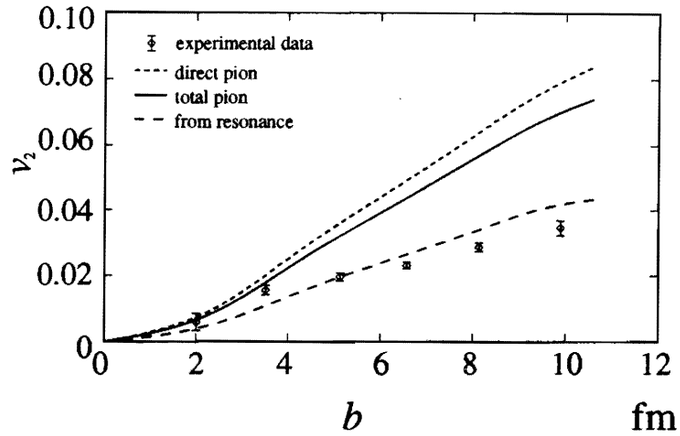

- Range
  $3<Y<6$
  $0.05<p_t<2$ GeV
- Reasonable agreement with exp. data below b~4 fm
- v_2 for total pion is reduced by 11 % owing to resonace decays.

Data from
A.M.Poskanzer et al., Nucl.Phys.**A661**(1999)341c.

Initial parameters at RHIC energy (Au+Au 65+65 A GeV)

INPUT

- Initial time: t_i = 1.0 fm
- Initial energy density: E_0 = 15 GeV/fm^3
- Initial baryon density: n_{B0} = 0.135 fm^{-3}
- Freeze-out energy density: E_f = 132.2 MeV/fm^3
- Impact parameter: b = 2.5 fm
- Initial longitudinal flow depends on x-coodinate.

OUTPUT

- $dN_{ch}/d\eta|_{\eta=0}$ = 620
- pbar/p$|_{\eta=0}$ = 0.57
- $\langle T_f \rangle$= 139 MeV
- $\langle \mu_f \rangle$= 77-99 MeV

EXPERIMENT

- $dN_{ch}/d\eta|_{|\eta|<1}$ = 555±35(syst) (PHOBOS, 6% central)
- $dN_{ch}/d\eta|_{\eta=0}$ = 622±41(syst) (PHENIX, 5% central)
- pbar/p=0.65 (STAR)

p_t dependence of elliptic flow at RHIC

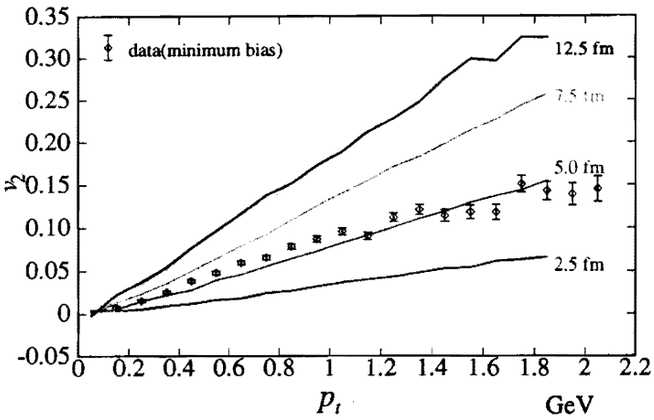

Data from
K.H.Ackermann et al., PRL**86**(2001)402.

- Our results are $v_2(p_t)$ for charged <u>pions</u>, not charged particles.
- $-0.5<Y<0.5$
- Impact parameters in our numerical simulations are 2.5, 5.0, 7.5, 10.0, 12.5 fm.
- Experimental data
  → minimum bias

v_2 rises linearly.

Centrality dependence of elliptic flow at RHIC

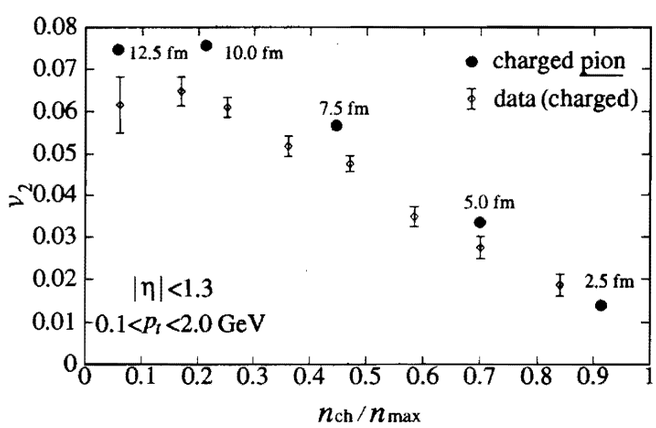

Data from
K.H.Ackermann et al., PRL**86**(2001)402.

- Our results are v_2 for charged <u>pions</u>, not charged particles.
- Impact parameters in our numerical simulations are 2.5, 5.0, 7.5, 10.0, 12.5 fm.

Similar behavior to exp. data

Summary

- (3+1)-dimensional hydrodynamic simulations
- Effect of resonance decays on observed elliptic flow

[redacted]

- **SPS**
  - Central collisions → `Full' thermalization
  - Semi central collisions → `Partial' thermalization
- **RHIC**
  - Central + semi central → `Full' thermalization

Three particles Bose-Einstein correlation in terms of Coulomb wave function

M. Biyajima[1], T. Mizoguchi[2]
[1]Department of Physics, Faculty of Science, Shinshu University, Matsumoto 390-8621, Japan
[2]Toba National College of Maritime Technology, Toba 517-8501, Japan

Abstract

The recent data for Bose-Einstein Correlations (BEC) of three-charged particles obtained by NA44 Collaboration have been analysed using theoretical formula with Coulomb wave functions. It has been recently proposed by Alt et al. It turns out that there are discrepancies between these data and the respective theoretical values. To resolve this problem we seek a possibly modified theoretical formulation of this problem by introducing the degree of coherence for the exchange effect due to the BEC between two-identical bosons. As a result we obtain a modified formulation for the BEC of three-charged particles showing good agreement with the data. Moreover, we investigate physical connection between our modified formulation and the core-halo model proposed by Csörgő et al. Our study indicates that the interaction region estimated by the BEC of three-charged particles in the S + Pb collisions at 200 GeV/c per nucleon is equal to about 1.5 fm$\sim$1.8 fm.

keywords: Bose-Einstein Correlation, three-charged particles, Coulomb wave functions, high energy heavy-ion collisions

Three particles Bose-Einstein correlation in terms of Coulomb wave function

M. Biyajima[1], T. Mizoguchi[2]

[1]Department of Physics, Faculty of Science, Shinshu University, Matsumoto 390-8621, Japan

[2]Toba National College of Maritime Technology, Toba 517-8501, Japan

Outline

§ 1 Introduction

§ 2 Analysis of data ($3\pi^+$) by original formula by Alt, Csörgő, Lörstad and Schmidt-Sorensen

§ 3 Diagram decomposition of their formula and introduction of degree of coherence λ

§ 4 Core-halo model and laser-optical approach in core-part

§ 5 Concluding remarks

Possible formulations for three-charged particles correlations in terms of Coulomb wave functions, in Phys. Lett. B (in press).

§ 1 Introduction

Study on HBT effect (Bose-Einstein correlation (BEC)) is necessary, to detect the QGP in experiments at RHIC & LHC.

Original HBT effect $\cdots$ photon

Hadronic HBT effect $\cdots$ pion, Kaon, proton

1990 : Importance of Higher-order BEC (3rd, 4th, 5th, ...).

1994-5 : To describe the charged BEC, Coulomb wave function is necessary. Formula for two-charged pion correlation function by Coulomb wave function was proposed.

Moreover, from data on $\pi^+\pi^-$ or $K\pi$ combinations, we can estimate R's, because of Coulomb wave functions.

1999 : Formula for three-charged pion correlation by Coulomb wave function was proposed by Alt, Csörgő, Lörstad and Schmidt-Sorensen. We can apply this one to analyse data. However, we had no concrete information from their original one (See 5th transparency).

$\Longrightarrow$ This fact suggests us that we need to look for possibly modified formulas.

Formula for $3\pi^+$ correlation function by Coulomb wave function (Alt et al.)

$$
\begin{aligned}
N^{(3+)}_{Coul} \cong \frac{1}{6}\int & d^3\mathbf{x}_1\rho(\mathbf{x}_1)d^3\mathbf{x}_2\rho(\mathbf{x}_2)d^3\mathbf{x}_3\rho(\mathbf{x}_3) \\
& \cdot\Big|\psi^C_{\mathbf{k}_1\mathbf{k}_2}(\mathbf{x}_1,\ \mathbf{x}_2)\psi^C_{\mathbf{k}_2\mathbf{k}_3}(\mathbf{x}_2,\ \mathbf{x}_3)\psi^C_{\mathbf{k}_3\mathbf{k}_1}(\mathbf{x}_3,\ \mathbf{x}_1) \\
& +\psi^C_{\mathbf{k}_1\mathbf{k}_2}(\mathbf{x}_1,\ \mathbf{x}_3)\psi^C_{\mathbf{k}_2\mathbf{k}_3}(\mathbf{x}_3,\ \mathbf{x}_2)\psi^C_{\mathbf{k}_3\mathbf{k}_1}(\mathbf{x}_2,\ \mathbf{x}_1) \\
& +\psi^C_{\mathbf{k}_1\mathbf{k}_2}(\mathbf{x}_2,\ \mathbf{x}_1)\psi^C_{\mathbf{k}_2\mathbf{k}_3}(\mathbf{x}_1,\ \mathbf{x}_3)\psi^C_{\mathbf{k}_3\mathbf{k}_1}(\mathbf{x}_3,\ \mathbf{x}_2) \\
& +\psi^C_{\mathbf{k}_1\mathbf{k}_2}(\mathbf{x}_2,\ \mathbf{x}_3)\psi^C_{\mathbf{k}_2\mathbf{k}_3}(\mathbf{x}_3,\ \mathbf{x}_1)\psi^C_{\mathbf{k}_3\mathbf{k}_1}(\mathbf{x}_1,\ \mathbf{x}_2) \\
& +\psi^C_{\mathbf{k}_1\mathbf{k}_2}(\mathbf{x}_3,\ \mathbf{x}_1)\psi^C_{\mathbf{k}_2\mathbf{k}_3}(\mathbf{x}_1,\ \mathbf{x}_2)\psi^C_{\mathbf{k}_3\mathbf{k}_1}(\mathbf{x}_2,\ \mathbf{x}_3) \\
& +\psi^C_{\mathbf{k}_1\mathbf{k}_2}(\mathbf{x}_3,\ \mathbf{x}_2)\psi^C_{\mathbf{k}_2\mathbf{k}_3}(\mathbf{x}_2,\ \mathbf{x}_1)\psi^C_{\mathbf{k}_3\mathbf{k}_1}(\mathbf{x}_1,\ \mathbf{x}_3)\Big|^2 \qquad (1)
\end{aligned}
$$

where

$$\psi^C_{\mathbf{k}_i\mathbf{k}_j}(\mathbf{x}_i,\ \mathbf{x}_j) = \Gamma(1+i\eta_{ij})e^{\pi\eta_{ij}/2}e^{i\mathbf{k}_{ij}\cdot\mathbf{r}_{ij}}F[-i\eta_{ij},\ 1;\ i(k_{ij}r_{ij}-\mathbf{k}_{ij}\cdot\mathbf{r}_{ij})],$$

$\mathbf{r}_{ij} = (\mathbf{x}_i - \mathbf{x}_j), \quad \mathbf{k}_{ij} = (\mathbf{k}_i - \mathbf{k}_j)/2,$

$r_{ij} = |\mathbf{r}_{ij}|, \quad k_{ij} = |\mathbf{k}_{ij}|, \quad \eta_{ij} = m\alpha/k_{ij}$

$F[a,\ b;\ x]$: confluent hypergeometric function

$\Gamma(x)$: Gamma function

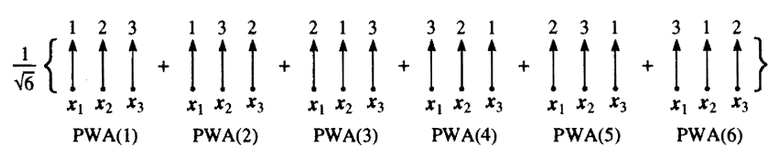

This approximation for $3\pi^+$ collisions is guaranteed by

S. P. Merkurev, Theor. Math. Phys. **32** (1978) 680.

M. Brauner, J. S. Briggs and H. J. Klar, J. Phys. B **22** (1989) 2265.

Notations

$$\frac{N^{(2+\text{ or }2-)}}{N^{BG}} = \frac{P(\mathbf{k}_1,\ \mathbf{k}_2)}{P(\mathbf{k}_1)P(\mathbf{k}_2)}$$

$$\frac{N^{(3+\text{ or }3-)}}{N^{BG}} = \frac{P(\mathbf{k}_1,\ \mathbf{k}_2,\ \mathbf{k}_3)}{P(\mathbf{k}_1)P(\mathbf{k}_2)P(\mathbf{k}_3)}$$

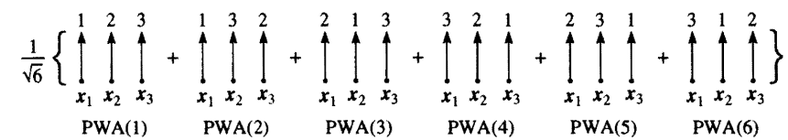

$$
\begin{aligned}
N^{(3+)}_{plane} \cong \frac{1}{6}\int & d^3\mathbf{x}_1\rho(\mathbf{x}_1)d^3\mathbf{x}_2\rho(\mathbf{x}_2)d^3\mathbf{x}_3\rho(\mathbf{x}_3) \\
& \cdot\Big|e^{i(\mathbf{k}_1\cdot\mathbf{x}_1+\mathbf{k}_2\cdot\mathbf{x}_2+\mathbf{k}_3\cdot\mathbf{x}_3)} + e^{i(\mathbf{k}_1\cdot\mathbf{x}_2+\mathbf{k}_2\cdot\mathbf{x}_1+\mathbf{k}_3\cdot\mathbf{x}_3)} \\
& +e^{i(\mathbf{k}_1\cdot\mathbf{x}_2+\mathbf{k}_2\cdot\mathbf{x}_3+\mathbf{k}_3\cdot\mathbf{x}_1)} + e^{i(\mathbf{k}_1\cdot\mathbf{x}_1+\mathbf{k}_2\cdot\mathbf{x}_3+\mathbf{k}_3\cdot\mathbf{x}_2)} \\
& +e^{i(\mathbf{k}_1\cdot\mathbf{x}_3+\mathbf{k}_2\cdot\mathbf{x}_1+\mathbf{k}_3\cdot\mathbf{x}_2)} + e^{i(\mathbf{k}_1\cdot\mathbf{x}_3+\mathbf{k}_2\cdot\mathbf{x}_2+\mathbf{k}_3\cdot\mathbf{x}_1)}\Big|^2
\end{aligned}
$$

$$\rho(\mathbf{x}) = \frac{1}{(2\pi R^2)^{3/2}}\exp\left[-\frac{\mathbf{x}^2}{2R^2}\right]$$

Data corrected by Gamow factor are usually analysed by $N^{(3+)}_{plane}$,

$$G(k_{ij}) = -\frac{e^{2\pi\eta_{ij}}-1}{e^{-2\pi\eta_{ij}}-1}, \quad \eta_{ij} = m\alpha/k_{ij}\ .$$

Notice: Gamow correction $\neq$ Coulomb correction

§ 2 Analysis of data ($3\pi^+$) by original formula by Alt, Csörgő, Lörstad and Schmidt-Sorensen

$$Q_3^2 = (\mathbf{k}_1 - \mathbf{k}_2)^2 + (\mathbf{k}_2 - \mathbf{k}_3)^2 + (\mathbf{k}_3 - \mathbf{k}_1)^2$$

Figure 1: Analysis of $3\pi^+$ BEC in S + Pb collision. (a) and (b) are results of Eqs. (1) and (2), respectively.

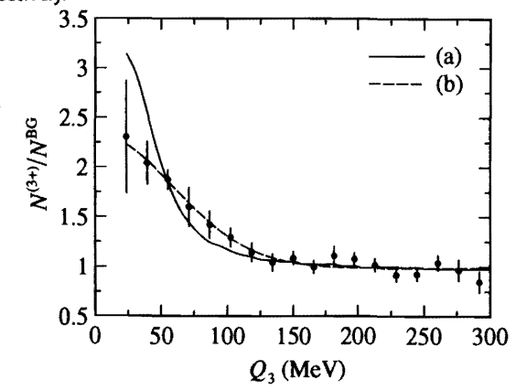

Table 1: Estimated values for the data by Eqs. (1) and (2) using CERN-MINUIT program.

Formulas	C	R [fm]	λ_3	χ^2/N_{dof}
Eq. (1)	0.941±0.026	2.47±0.14	—	17.6/16
Eq. (2)	0.986±0.028	2.36±0.26	1.37±0.19	7.8/15

$$\frac{N^{(3+\text{ or }3-)}}{N^{BG}} = C\left(1 + \lambda_3 e^{-R^2 Q_3^2}\right) \tag{2}$$

Formula by Alt et al. with CERN-MINUIT shows big discrepancies among data and theoretical values !!

Reasons ? $\Longrightarrow$ partially coherence, long-lived resonances, contaminations, temperature, flow effect, ...

§ 3 Diagram decomposition of their formula and introduction of degree of coherence λ

$$\begin{aligned}
A(1) &= \psi^C_{\mathbf{k}_1\mathbf{k}_2}(\mathbf{x}_1,\ \mathbf{x}_2)\psi^C_{\mathbf{k}_2\mathbf{k}_3}(\mathbf{x}_2,\ \mathbf{x}_3)\psi^C_{\mathbf{k}_3\mathbf{k}_1}(\mathbf{x}_3,\ \mathbf{x}_1) \\
&\xrightarrow{\text{PW}} e^{i\mathbf{k}_{12}\cdot\mathbf{r}_{12}}e^{i\mathbf{k}_{23}\cdot\mathbf{r}_{23}}e^{i\mathbf{k}_{31}\cdot\mathbf{r}_{31}} = e^{(3/2)i(\mathbf{k}_1\cdot\mathbf{x}_1+\mathbf{k}_2\cdot\mathbf{x}_2+\mathbf{k}_3\cdot\mathbf{x}_3)}\ , \\
A(2) &= \psi^C_{\mathbf{k}_1\mathbf{k}_2}(\mathbf{x}_1,\ \mathbf{x}_3)\psi^C_{\mathbf{k}_2\mathbf{k}_3}(\mathbf{x}_3,\ \mathbf{x}_2)\psi^C_{\mathbf{k}_3\mathbf{k}_1}(\mathbf{x}_2,\ \mathbf{x}_1) \\
&\xrightarrow{\text{PW}} e^{i\mathbf{k}_{12}\cdot\mathbf{r}_{13}}e^{i\mathbf{k}_{23}\cdot\mathbf{r}_{32}}e^{i\mathbf{k}_{31}\cdot\mathbf{r}_{21}} = e^{(3/2)i(\mathbf{k}_1\cdot\mathbf{x}_1+\mathbf{k}_2\cdot\mathbf{x}_3+\mathbf{k}_3\cdot\mathbf{x}_2)}\ , \\
A(3) &= \psi^C_{\mathbf{k}_1\mathbf{k}_2}(\mathbf{x}_2,\ \mathbf{x}_1)\psi^C_{\mathbf{k}_2\mathbf{k}_3}(\mathbf{x}_1,\ \mathbf{x}_3)\psi^C_{\mathbf{k}_3\mathbf{k}_1}(\mathbf{x}_3,\ \mathbf{x}_2) \\
&\xrightarrow{\text{PW}} e^{i\mathbf{k}_{12}\cdot\mathbf{r}_{21}}e^{i\mathbf{k}_{23}\cdot\mathbf{r}_{13}}e^{i\mathbf{k}_{31}\cdot\mathbf{r}_{32}} = e^{(3/2)i(\mathbf{k}_1\cdot\mathbf{x}_2+\mathbf{k}_2\cdot\mathbf{x}_1+\mathbf{k}_3\cdot\mathbf{x}_3)}\ , \\
A(4) &= \psi^C_{\mathbf{k}_1\mathbf{k}_2}(\mathbf{x}_2,\ \mathbf{x}_3)\psi^C_{\mathbf{k}_2\mathbf{k}_3}(\mathbf{x}_3,\ \mathbf{x}_1)\psi^C_{\mathbf{k}_3\mathbf{k}_1}(\mathbf{x}_1,\ \mathbf{x}_2) \\
&\xrightarrow{\text{PW}} e^{i\mathbf{k}_{12}\cdot\mathbf{r}_{23}}e^{i\mathbf{k}_{23}\cdot\mathbf{r}_{31}}e^{i\mathbf{k}_{31}\cdot\mathbf{r}_{12}} = e^{(3/2)i(\mathbf{k}_1\cdot\mathbf{x}_2+\mathbf{k}_2\cdot\mathbf{x}_3+\mathbf{k}_3\cdot\mathbf{x}_1)}\ , \\
A(5) &= \psi^C_{\mathbf{k}_1\mathbf{k}_2}(\mathbf{x}_3,\ \mathbf{x}_1)\psi^C_{\mathbf{k}_2\mathbf{k}_3}(\mathbf{x}_1,\ \mathbf{x}_2)\psi^C_{\mathbf{k}_3\mathbf{k}_1}(\mathbf{x}_2,\ \mathbf{x}_3) \\
&\xrightarrow{\text{PW}} e^{i\mathbf{k}_{12}\cdot\mathbf{r}_{31}}e^{i\mathbf{k}_{23}\cdot\mathbf{r}_{12}}e^{i\mathbf{k}_{31}\cdot\mathbf{r}_{23}} = e^{(3/2)i(\mathbf{k}_1\cdot\mathbf{x}_3+\mathbf{k}_2\cdot\mathbf{x}_1+\mathbf{k}_3\cdot\mathbf{x}_2)}\ , \\
A(6) &= \psi^C_{\mathbf{k}_1\mathbf{k}_2}(\mathbf{x}_3,\ \mathbf{x}_2)\psi^C_{\mathbf{k}_2\mathbf{k}_3}(\mathbf{x}_2,\ \mathbf{x}_1)\psi^C_{\mathbf{k}_3\mathbf{k}_1}(\mathbf{x}_1,\ \mathbf{x}_3) \\
&\xrightarrow{\text{PW}} e^{i\mathbf{k}_{12}\cdot\mathbf{r}_{32}}e^{i\mathbf{k}_{23}\cdot\mathbf{r}_{21}}e^{i\mathbf{k}_{31}\cdot\mathbf{r}_{13}} = e^{(3/2)i(\mathbf{k}_1\cdot\mathbf{x}_3+\mathbf{k}_2\cdot\mathbf{x}_2+\mathbf{k}_3\cdot\mathbf{x}_1)}\ .
\end{aligned}$$

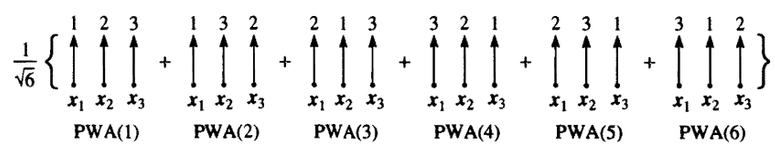

Introducing the degree of coherence $\lambda^{1/2}$ for mark $\times$, we obtain

$$\frac{N^{(3+\text{ or }3-)}}{N^{BG}} \cong C \int d^3\mathbf{x}_1\rho(\mathbf{x}_1)d^3\mathbf{x}_2\rho(\mathbf{x}_2)d^3\mathbf{x}_3\rho(\mathbf{x}_3)[F_1 + \lambda F_2 + \lambda^{3/2}F_3] \quad (3)$$

Our results

Figure 3: Reanalyses of $3\pi^+$ BEC in S + Pb collision.

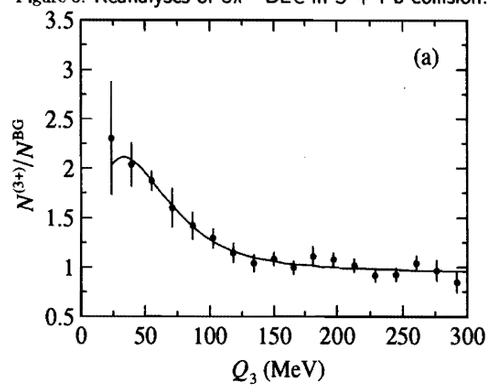

Table 2: Reanalyses of $3\pi^+$ BEC in S + Pb collision by Eqs. (3) and (4).

Formula	C	R [fm]	λ	χ^2/N_{dof}
Eq. (3)	0.917±0.032	1.53±0.20	0.55±0.07	6.7/15
Eq. (4)	0.984±0.029	2.60±0.28	0.33±0.04	7.7/15

$$\text{Eq. (3)} \xrightarrow{\eta_{ij}\to 0} C\left(1 + 3\lambda e^{-\frac{3}{4}R^2Q_3^2} + 2\lambda^{3/2}e^{-\frac{9}{8}R^2Q_3^2}\right) \quad (4)$$

Figure 2: Diagram reflecting three-charged particles Bose-Einstein Correlation (BEC) and Coulombic potential (V_c). $\times$ means the exchange effect of BEC.

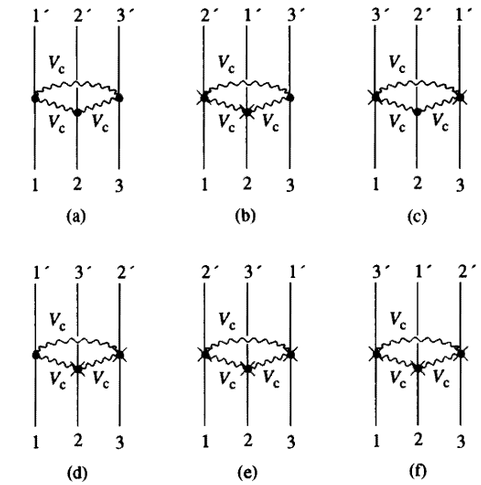

$$F_1 = \frac{1}{6}\sum_{i=1}^{6} A(i)A^*(i) \xrightarrow{\text{PW}} 1 ,$$

$$F_2 = \frac{1}{6}[A(1)A^*(2) + A(1)A^*(3) + A(1)A^*(6) + A(2)A^*(4) + A(2)A^*(5) + A(3)A^*(4) + A(3)A^*(5) + A(4)A^*(6) + A(5)A^*(6) + \text{c. c.}]$$

$\xrightarrow{\text{PW}}$ BEC between two-charged particles

$$F_3 = \frac{1}{6}[A(1)A^*(4) + A(1)A^*(5) + A(2)A^*(3) + A(2)A^*(6) + A(3)A^*(6) + A(4)A^*(5) + \text{c. c.}]$$

$\xrightarrow{\text{PW}}$ BEC among three-charged particles

§ 4 Core-halo model and laser-optical approach in core-part

Figure 4: Physical picture of core-halo model.

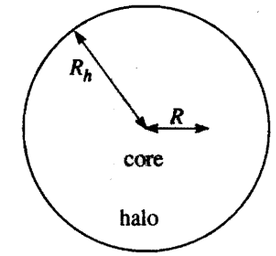

$$\rho(x_i) = \rho_c(x_i) + \rho_{halo}(x_i)\ , \quad f_c = \langle n_c\rangle/\langle n_{tot}\rangle$$
$$\langle n_c\rangle = \langle n_{cho}\rangle + \langle n_{co}\rangle\ , \quad p = \langle n_{cho}\rangle/\langle n_c\rangle$$

$$\begin{aligned}\frac{N^{(3+\text{ or }3-)}}{N^{BG}} \cong\ & C\Big[\int d^3\mathbf{x}_1\rho_c(\mathbf{x}_1)d^3\mathbf{x}_2\rho_c(\mathbf{x}_2)d^3\mathbf{x}_3\rho_c(\mathbf{x}_3)\\ & \cdot(F_1 + f_c^2p^2F_2 + f_c^3p^3F_3)\\ & + \int d^3\mathbf{x}_1\rho_c(\mathbf{x}_1)\cdot\delta^3(\mathbf{x}_1)d^3\mathbf{x}_2\rho_c(\mathbf{x}_2)d^3\mathbf{x}_3\rho_c(\mathbf{x}_3)\\ & \cdot\left(2f_c^2p(1-p)F_2 + 3f_c^3p^2(1-p)F_3\right)\Big] \qquad (5)\end{aligned}$$

$$\begin{aligned}\frac{N^{(2+\text{ or }2-)}}{N^{BG}} \cong\ & C\Big[\int d^3\mathbf{x}_1\rho(\mathbf{x}_1)d^3\mathbf{x}_2\rho(\mathbf{x}_2)(G_1 + f_c^2p^2G_2)\\ & + \int d^3\mathbf{x}_1\rho(\mathbf{x}_1)d^3\mathbf{x}_2\rho(\mathbf{x}_2)\cdot\delta^3(\mathbf{x}_2)2f_c^2p(1-p)G_2\Big] \qquad (6)\end{aligned}$$

where

$$G_1 = \frac{1}{2}\left(\left|\psi^C_{\mathbf{k}_1\mathbf{k}_2}(\mathbf{x}_1,\ \mathbf{x}_2)\right|^2 + \left|\psi^C_{\mathbf{k}_1\mathbf{k}_2}(\mathbf{x}_2,\ \mathbf{x}_1)\right|^2\right)$$
$$G_2 = \mathrm{Re}\left(\psi^{C*}_{\mathbf{k}_1\mathbf{k}_2}(\mathbf{x}_1,\ \mathbf{x}_2)\cdot\psi^C_{\mathbf{k}_1\mathbf{k}_2}(\mathbf{x}_2,\ \mathbf{x}_1)\right)$$

Effective degree of coherence:

$$\lambda_3^* = f_c^2(p^2 + 2p(1-p)) + f_c^3(p^3 + 3p^2(1-p))$$
$$\lambda_2^* = f_c^2(p^2 + 2p(1-p))$$

Table 3: Typical results from analyses of data of NA44 Collaboration by Eqs. (5)~(6).

3π BEC			
p	1.0	0.8	0.6
f_c	0.743±0.050	0.779±0.055	0.856±0.061
λ_3^*	0.964	1.007	1.022
R (fm)	1.53±0.21	1.72±0.25	1.87±0.27
χ^2/N_{dof}	6.7/15	6.6/15	6.6/15
$3\pi \to 2\pi$ BEC			
p	1.0	0.8	0.6
f_c	0.633±0.028	0.647±0.029	0.688±0.032
λ_2^*	0.400	0.402	0.398
R (fm)	4.69±0.45	5.34±0.54	5.85±0.59
χ^2/N_{dof}	14.6/17	14.9/17	14.9/17

Data on 2π are taken from ensemble of 3π.

§ 5 Concluding remarks

- Original formula by Alt et al.

  $\Longrightarrow$ No concrete information on R.

- Modified formula with degree of coherence λ

  phenomelogical formula (# of parameters: λ, R)

- Modified formula with core-halo model can be applied to analyses of data.

Figure 5: Sets of f_c and p estimated in analyses of BEC of two-charged and three-charged pions using the CERN-MINUIT program. Widths of f_c's stand for error bar of $\pm 2\sigma$.

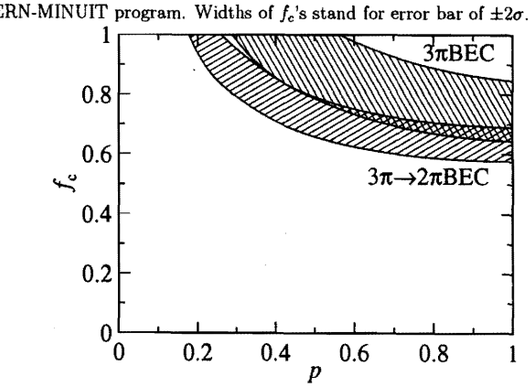

ⓐ Common region for $p(=\langle n_{cho}\rangle/\langle n_c\rangle)$ and $f_c(=\langle n_c\rangle/\langle n_{tot}\rangle)$ exists.

ⓑ More concrete physical picture(# of parameters: f_c, p, R, $R_{halo} \to \infty$)

ⓒ $\lambda = f_c^2$ holds between two modified formulas, providing $p = 1$.

- However there are discrepancies $R\,(2\pi^+) \sim 5$ fm and $R\,(3\pi^+) \sim 1.8$ fm in analyses of data by NA44 Coll.

  $\Longrightarrow$ Numerator $d\sigma/dQ_3$ $(3\pi^+)$ and denominator $d\sigma/dQ_3$ (BG) are necessary.

Electron Measurement in PHENIX

Yasuyuki Akiba for the PHENIX Collaboration

High Energy Accelerator Research Organization (KEK)

One of the unique capabilities of PHENIX among RHIC experiments is the ability to identify and to measure electrons and electron pairs at central rapidity. During the year 2000 RUN, PHENIX has recorded a few million Au+Au collisions at sqrt(s) = 130 A GeV. Electrons from the collisions are clearly identified in pt range from a few hundred MeV/c to 4 GeV/c. The electron channel is sensitive to many interesting processes such as open charm semi-leptonic decays, thermal radiation, and di-lepton decay of vector mesons, while background electron sources include Dalitz decays and photon conversions in the detector. We also measured inclusive spectrum of photon from its conversion to e+ e- pair. The results from the electron measurement in PHENIX will be presented.

PHENIX

Electron Measurement in PHENIX

Y. Akiba (KEK)
for the PHENIX Collaboration

PHENIX The PHENIX Collaboration

PHENIX

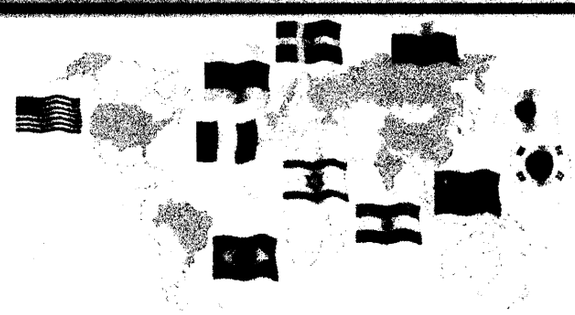

University of São Paulo, São Paulo, Brazil
Academia Sinica, Taipei 11529, China
China Institute of Atomic Energy (CIAE), Beijing, P. R. China
Laboratoire de Physique Corpusculaire (LPC), Universite de Clermont-Ferrand, 63170 Aubiere, Clermont-Ferrand, France
Dapnia, CEA Saclay, Bat. 703, F-91191, Gif-sur-Yvette, France
IPN-Orsay, Universite Paris Sud, CNRS-IN2P3, BP1, F-91406, Orsay, France
LPNHE-Palaiseau, Ecole Polytechnique, CNRS-IN2P3, Route de Saclay, F-91128, Palaiseau, France
SUBATECH, Ecole des Mines at Nantes, F-44307 Nantes, France
University of Muenster, Muenster, Germany
Banaras Hindu University, Banaras, India
Bhabha Atomic Research Centre (BARC), Bombay, India
Weizmann Institute, Rehovot, Israel
Center for Nuclear Study (CNS-Tokyo), University of Tokyo, Tanashi, Tokyo 188, Japan
Hiroshima University, Higashi-Hiroshima 739, Japan
KEK, Institute for High Energy Physics, Tsukuba, Japan
Kyoto University, Kyoto, Japan
Nagasaki Institute of Applied Science, Nagasaki-shi, Nagasaki, Japan
RIKEN, Institute for Physical and Chemical Research, Hirosawa, Wako, Japan
University of Tokyo, Bunkyo-ku, Tokyo 113, Japan
Tokyo Institute of Technology, Ohokayama, Meguro, Tokyo, Japan
University of Tsukuba, Tsukuba, Japan
Waseda University, Tokyo, Japan
Cyclotron Application Laboratory, KAERI, Seoul, South Korea
Kangnung National University, Kangnung 210-702, South Korea
Korea University, Seoul, 136-701, Korea
Myong Ji University, Yongin City 449-728, Korea
System Electronics Laboratory, Seoul National University, Seoul, South Korea
Yonsei University, Seoul 120-749, KOREA
Institute of High Energy Physics (IHEP-Protvino or Serpukhov), Protovino, Russia
Joint Institute for Nuclear Research (JINR-Dubna), Dubna, Russia
Kurchatov Institute, Moscow, Russia
PNPI: St. Petersburg Nuclear Physics Institute, Gatchina, Leningrad, Russia
Lund University, Lund, Sweden
Abilene Christian University, Abilene, Texas, USA
Brookhaven National Laboratory (BNL), Upton, NY 11973
University of California - Riverside (UCR), Riverside, CA 92521, USA
Columbia University, Nevis Laboratories, Irvington, NY 10533, USA
Florida State University (FSU), Tallahassee, FL 32306, USA
Georgia State University (GSU), Atlanta, GA, 30303, USA
Iowa State University (ISU) and Ames Laboratory, Ames, IA 50011, USA
LANL: Los Alamos National Laboratory, Los Alamos, NM 87545, USA
LLNL: Lawrence Livermore National Laboratory, Livermore, CA 94550, USA
University of New Mexico, Albuquerque, New Mexico, USA
New Mexico State University, Las Cruces, New Mexico, USA
Department of Chemistry, State University of New York at Stony Brook (USB), Stony Brook, NY 11794, USA
Department of Physics and Astronomy, State University of New York at Stony Brook (USB), Stony Brook, NY 11794-, USA
Oak Ridge National Laboratory (ORNL), Oak Ridge, TN 37831, USA
University of Tennessee (UT), Knoxville, TN 37996, USA
Vanderbilt University, Nashville, TN 37235, USA

PHENIX

Motivation

- High pt single electron (p_t > 1 GeV/c)
  - heavy quark decay (c→eX, b→eX)
- Photon (by conversion to e+e- pair)
  - Clean photon identification at low pt
  - Thermal radiation
- Electron pair
  - J/Psi suppression
  - continuum from heavy quark decay
  - medium effect on vector mesons
  - Thermal radiation

PHENIX

High pt electron (prediction)

- At ISR, single electron signal is observed at $e/\pi \sim 2\times10^{-4}$.
- At RHIC energy , the signal (from c-qark decay) is expected as $e/\pi \sim 3\text{-}4\times10^{-4}$ in p+p
- The e/π ratio can be as high as 10^{-3} in Au+Au collision, if high pt pions are suppressed (as reported in this conference)

Plot shown in QM95 pre-symposium

"single electron" spectrum in Rhic Au+Au central collisions

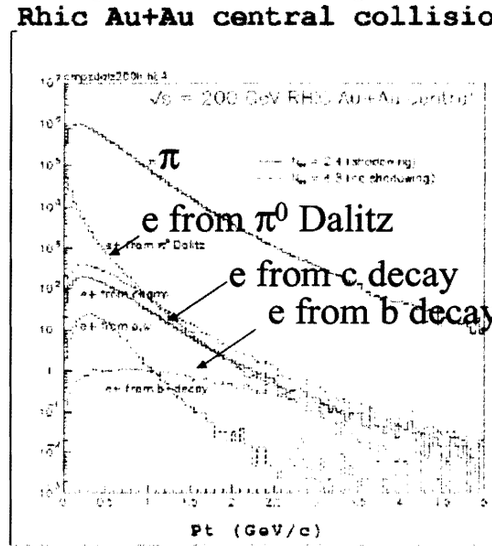

Detectors Included

- Detectors for single electron analysis
  - BBC
    - Trigger
    - vertex position
    - T0 (TOF start)
  - DC and PC1 (W)
    - tracking
  - RICH(W)
    - electron ID
  - PBSC(W):
    - electron ID
    - Energy measurement
    - TOF (pion ID)

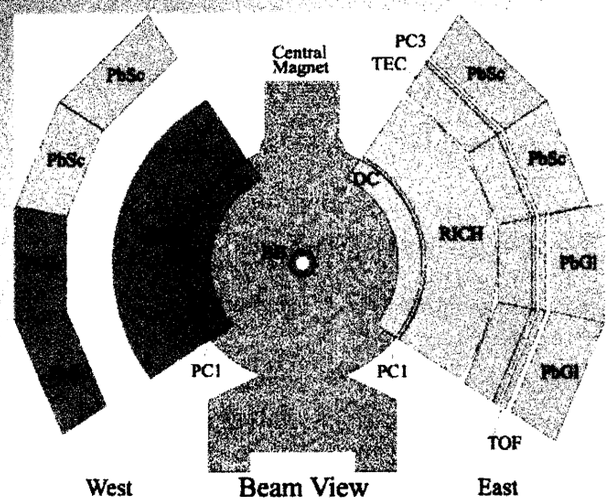

High Pt electron in PHENIX

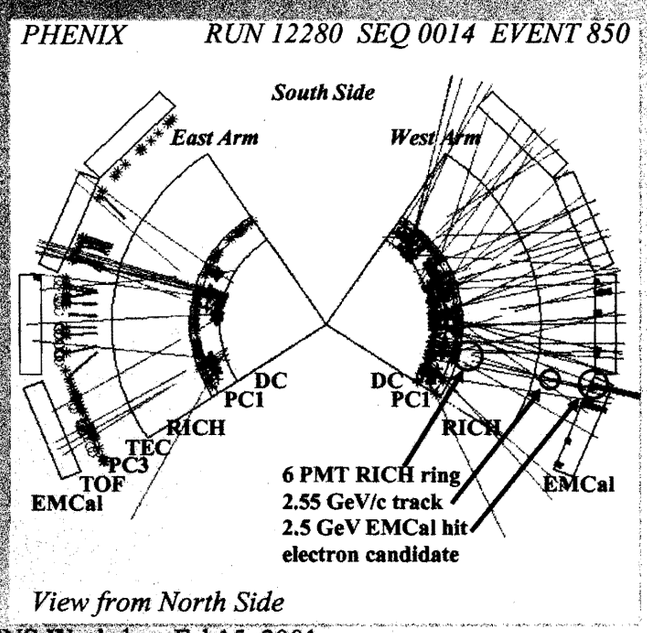

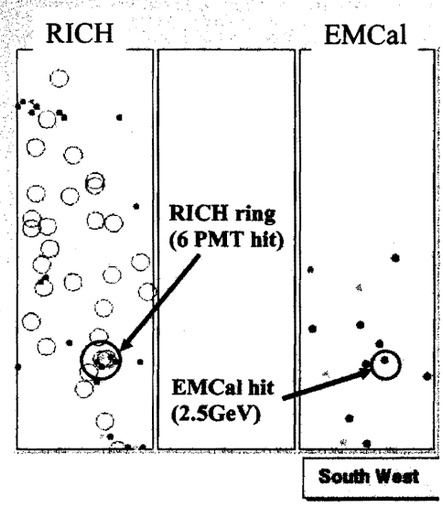

PHENIX

Electron Identification

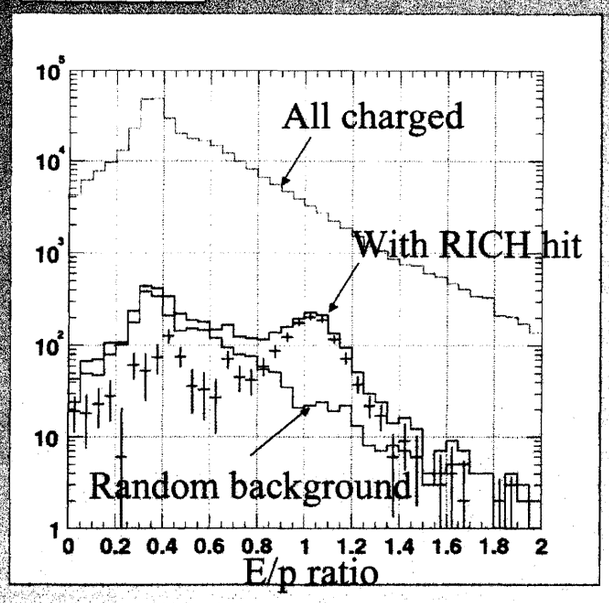

- Electrons are identified by RICH and EMCAL
- A clear peak in energy/momentum (E/p) ratio is seen at 1.0 after RICH hit is required
- EMCAL E/p cut cleans up the rest of the background.
- Random background is also subtracted.

PHENIX

Electron Spectra

- The electron spectrum is measured up to 4 GeV/c, and it is compared with $\pi^{\pm}$ and h^{-} spectra in the same acceptance.
- The $\pi^{\pm}$ spectra are consistent with π^{0}.
- The electron spectrum includes "trivial" background from π^{0} Dalitz decay and photon conversion. The amount of the background can be calculated from the pion spectrum.
- Studies are on-going to look for "excess" electron over the trivial background.

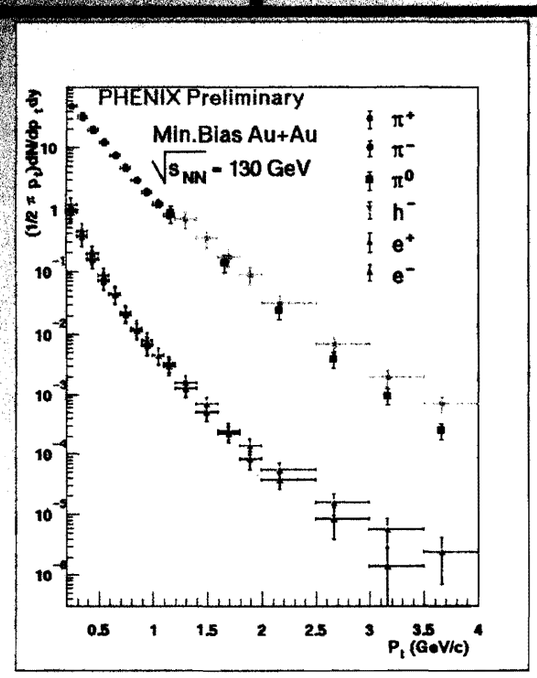

Measurement of photon conversion

- Dalitz decays and photon conversions are observed as very low mass (Mee~0) e+e- pair.
- A clean signal of conversion photon is seen in PHENIX in Au+Au collisions.
  - Conversion pair produced at large radius acquires apparent "mass" due to reconstruction program. (No new particle, at least for now)

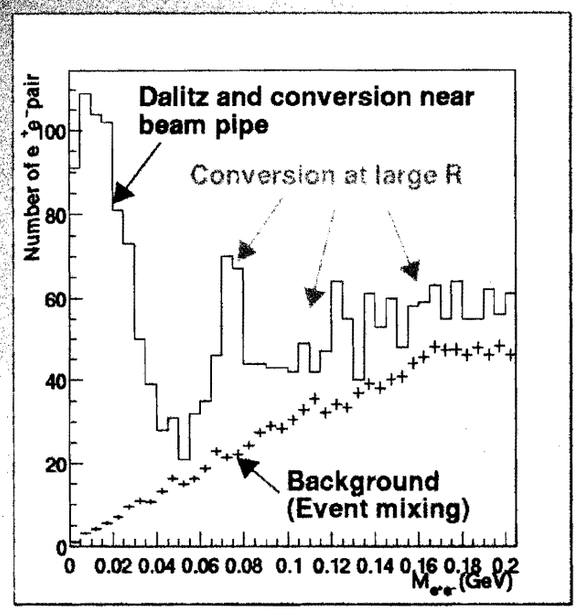

Separation of Dalitz and conversion

- Dalitz pair (from event vertex R=0) and conversion pair (outside of beam pipe) can be distinguished by its angular orientation.
- Very clean conversion pair signal, with little background is obtained.
- The conversion sample is used to measure photon cross section.

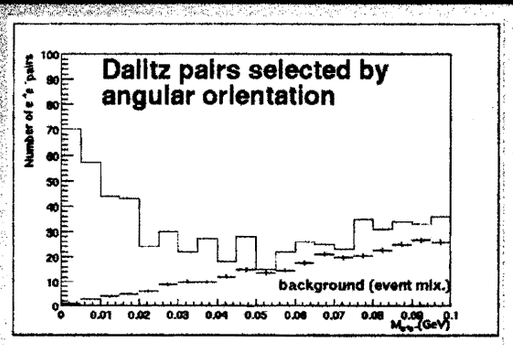

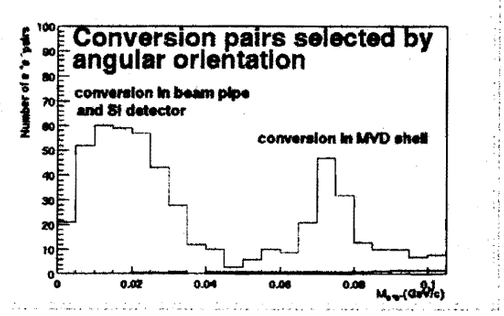

Inclusive Photon spectrum

- Inclusive photon spectrum is obtained from the conversion pair.
- "Photon" spectrum is also obtained from zero field data by EMCAL-RICH coincidence.
- Work is in progress to establish the absolute cross section and to compare the photon yield with that of pion.

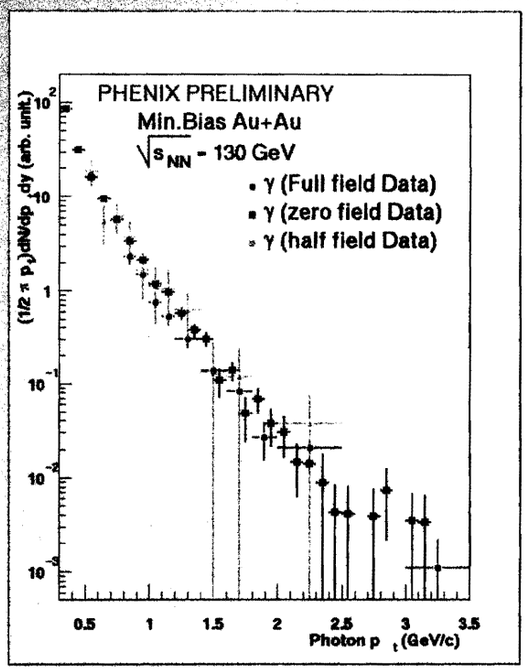

PHENIX as pair spectrometer

- Higher mass e+e- pairs are accessible by using two arms of PHENIX.
- At present, electron ID in the East Arm is limited to RICH. Soon PBGL will be used
- The RUN-00 data (a few M events) is not sufficient for pair physics

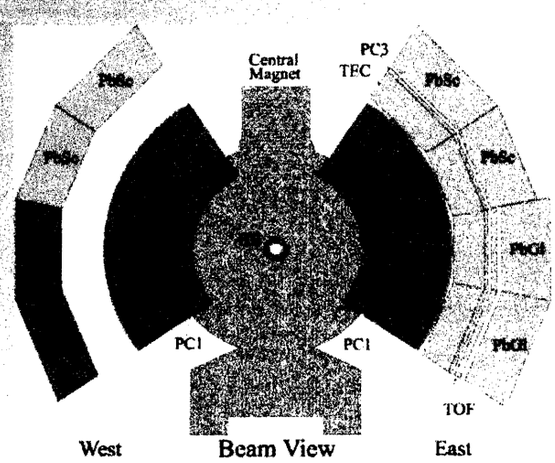

Coming Attraction

- Di-electron mass distribution is measure up to 3 GeV in RUN-00 data
- Most of the pairs are combinatorial background.
- In Run01, we will accumulate a few thousands times of this statistics to measure J/Ψ and light vector mesons with full two arm system.

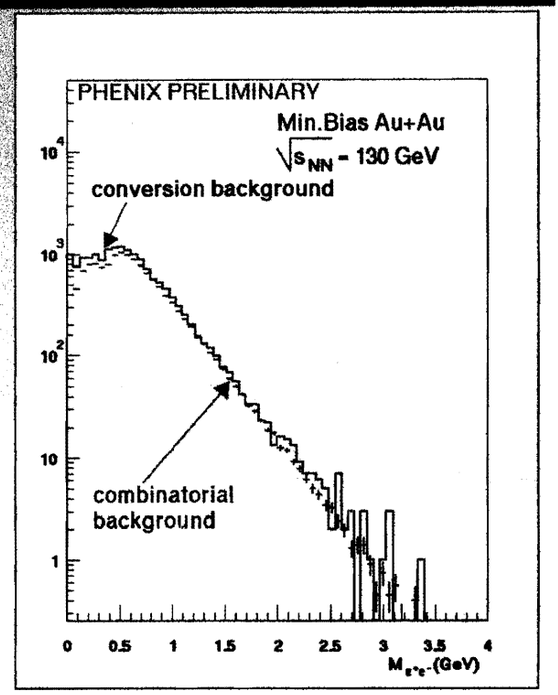

Summary

- PHENIX measured
  - Inclusive electrons
  - Conversion photons
  - Electron pairs

  in Au+Au collisions at sqrt(s_{NN})=130 GeV
- Work is in progress to search for "excess" electrons from heavy quark decays
- Much more data will come in RUN01 with full Two Arm system.

Observation of rho/omega meson modification in nuclear matter

M. Naruki
for KEK-PS E325 collaboration

J. Chiba[a], H. En'yo, H. Funahashi, H. Hamagaki[b], M. Ieiri[a], M. Ishino, M. Kitaguchi, S. Mihara*, T. Miyashita, T. Murakami, R. Muto, M. Nomachi[c], K. Ozawa, F. Sakuma, O. Sasaki[a], H.D. Satoh, M. Sekimoto[a], T. Tabaru, K. Tanaka[a], S. Yadama, S. Yokkaichi, Y. Yoshimura
Kyoto University , *a* KEK , *b* CNS, Univ.of Tokyo , *c* RCNP,
∗ present address, ICEPP, Univ. of Tokyo

Modification of hadron mass and decay width in nuclear medium is one of the most interesting problems facing hadron physics today. We observe decay of ϕ meson from the nuclear targets to inspect hadron properties modification at normal nuclear density. The Experiment is performed to detect $\phi \to e^+e^-$ and $\phi \to K^+K^-$ decay modes simultaneously. We measure the invariant mass spectrum of lepton pairs and branching ratios of two decay modes, sensitive to mass shift of ϕ mesons.

Analysis of recent 1998-1999 data shows that the mass spectrum of e^+e^- pairs originate in Cu target is significantly different from that in case of C or CH2 targets in near ω mass region. The enhancement is seen for the heavier copper target suggesting mass modification effect in nuclear matter. Moreover, the peak is seen in the ϕ mass region. In 2000, we have newly installed the forward lead glass calorimeter and the vertex chamber to improve the particle tracking and identification for the further study of such vector meson modification on omega and phi mesons. The detail of the experimental procedure will be presented with the data we have aquired so far.

Observation of ρ / ω meson modification in nuclear matter

Megumi Naruki

for the KEK-PS E325 collaboration

H. En'yo, H. Funahashi, M. Kitaguchi, M.Ishino, H. Kanda, S. Mihara, T. Miyashita, T. Murakami, R. Muto, K. Ozawa, F. Sakuma, H. D. Sato, T. Tabaru, S. Yamada, S. Yokkaichi, Y. Yoshimura, J. Chiba, M. Ieiri, M. Nomachi, O. Sasaki, M. Sekimoto, K. H. Tanaka, H. Hamagaki

Kyoto Univ., KEK, CNS, Univ. of Tokyo

Contents :

- Physics motivation
- Experimental setup & detectors
- $\rho / \omega \rightarrow e^+e^-$ results
- $\phi \rightarrow K^+K^-$ results
- Summary

Physics

effective quark mass in the QCD vacuum

$m_u \cong m_d \cong 300$MeV, $m_s \cong 500$MeV

→ In HOT/DENSE matter

↓

quark mass could be modified

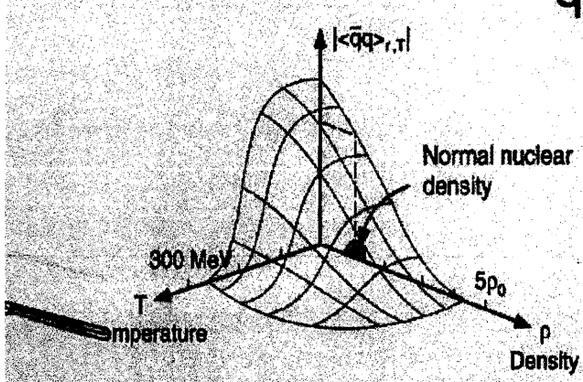

$\langle\bar{q}q\rangle$ quark condensate : order parameter

- to indicate how much the symmetry broken
- but not an observable

➡ Mass of Vector Meson, ρ ω φ

$M_V = 2 \times M_q$ + small interaction term

Vector Meson

Mass of vector mesons, ρ, ω, ϕ

$M_V = 2M_q$ + small interaction term

ϕ has narrow width ($\Gamma = 4.4$ MeV)

→ sensitive to the mass shape modification

small Q value ($Q_{KK} = 35$ MeV)

→ sensitive to the branching ratio

$\Gamma_{\phi \to K^+K^-} / \Gamma_{\phi \to e^+e^-}$

ρ / ω mass modification will be relatively large

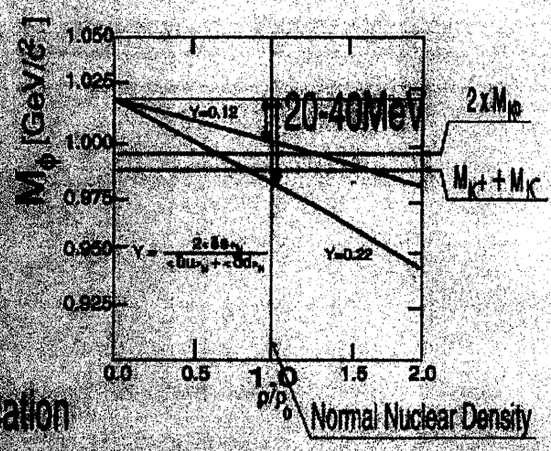

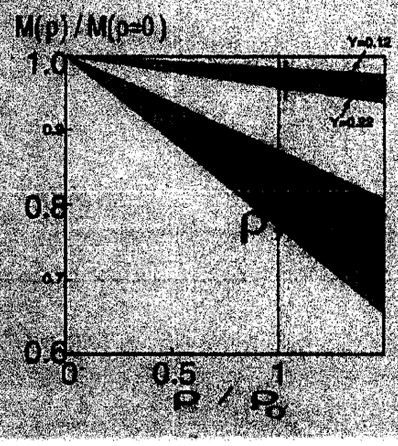

KEK-PS E325 measures ϕ decay inside a nucleus

Also possible to detect ρ, ω decays

- in 12GeV p+A→ ϕ, ρ, ω + X
- we measure
  - invariant mass spectra of e^+e^- and K^+K^-
  - branching ratio $\Gamma_{\phi \to K^+K^-} / \Gamma_{\phi \to e^+e^-}$
- focus on slowly moving ϕ, ρ, ω: $P_{lab} \sim 1$GeV/c
- primary proton beam (10^9/spill)
  - on thin targets (0.2% interaction length)
  - to suppress γ conversions

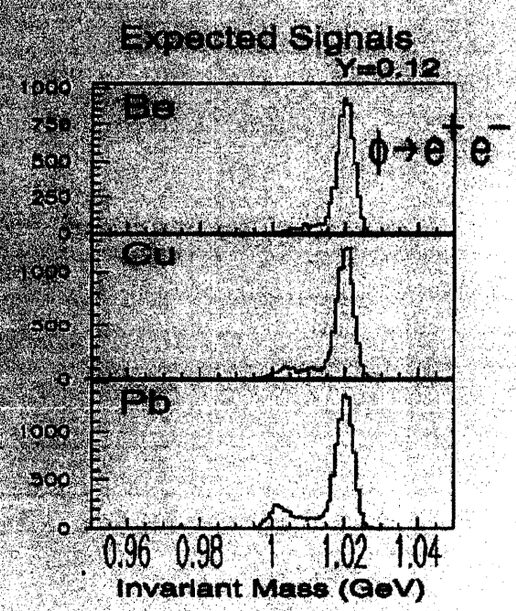

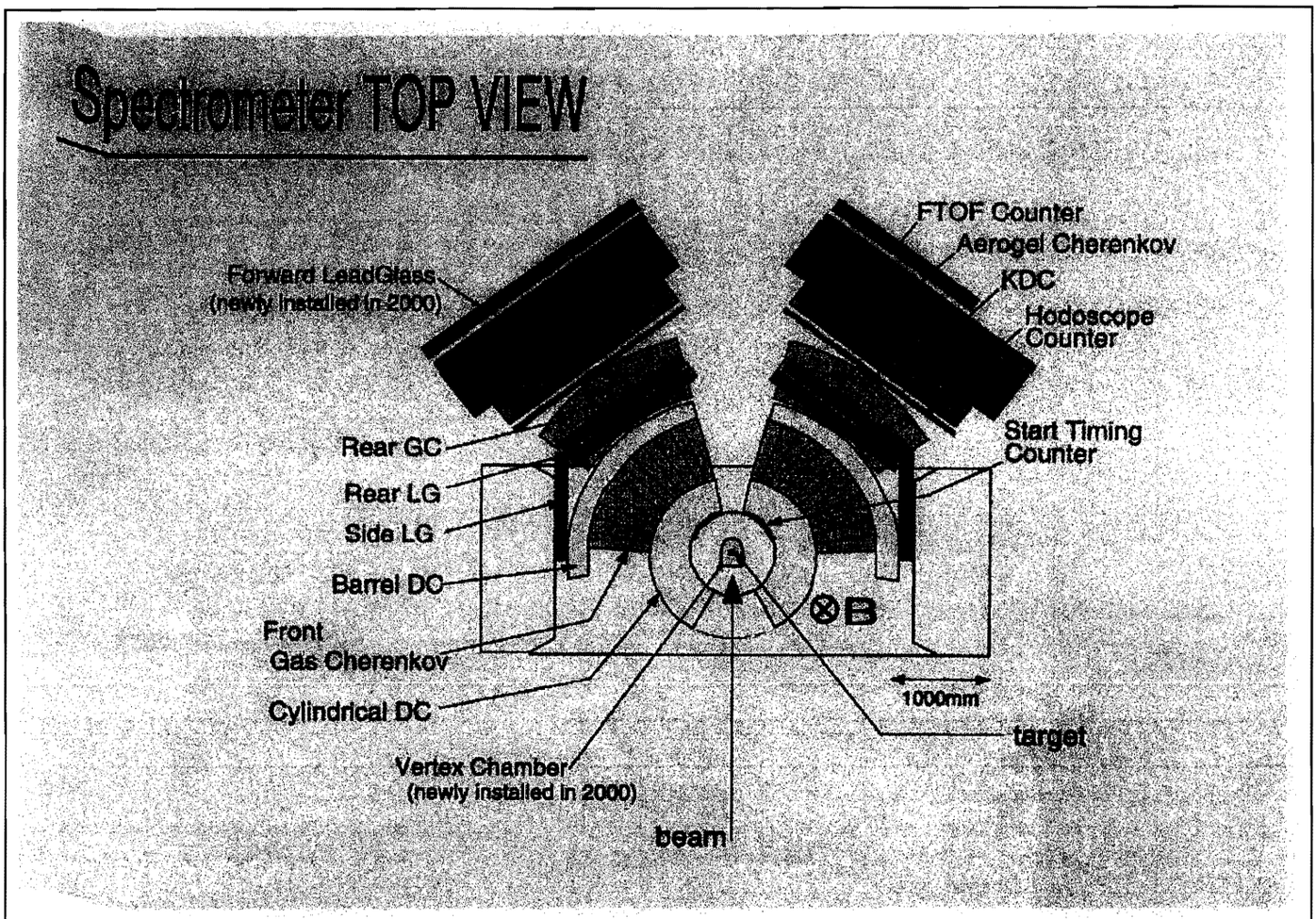
Spectrometer TOP VIEW
FTOF Counter
Aerogel Cherenkov
KDC
Hodoscope Counter
Forward LeadGlass (newly installed in 2000)
Rear GC
Rear LG
Side LG
Barrel DC
Front Gas Cherenkov
Cylindrical DC
Vertex Chamber (newly installed in 2000)
beam
Start Timing Counter
B
1000mm
target

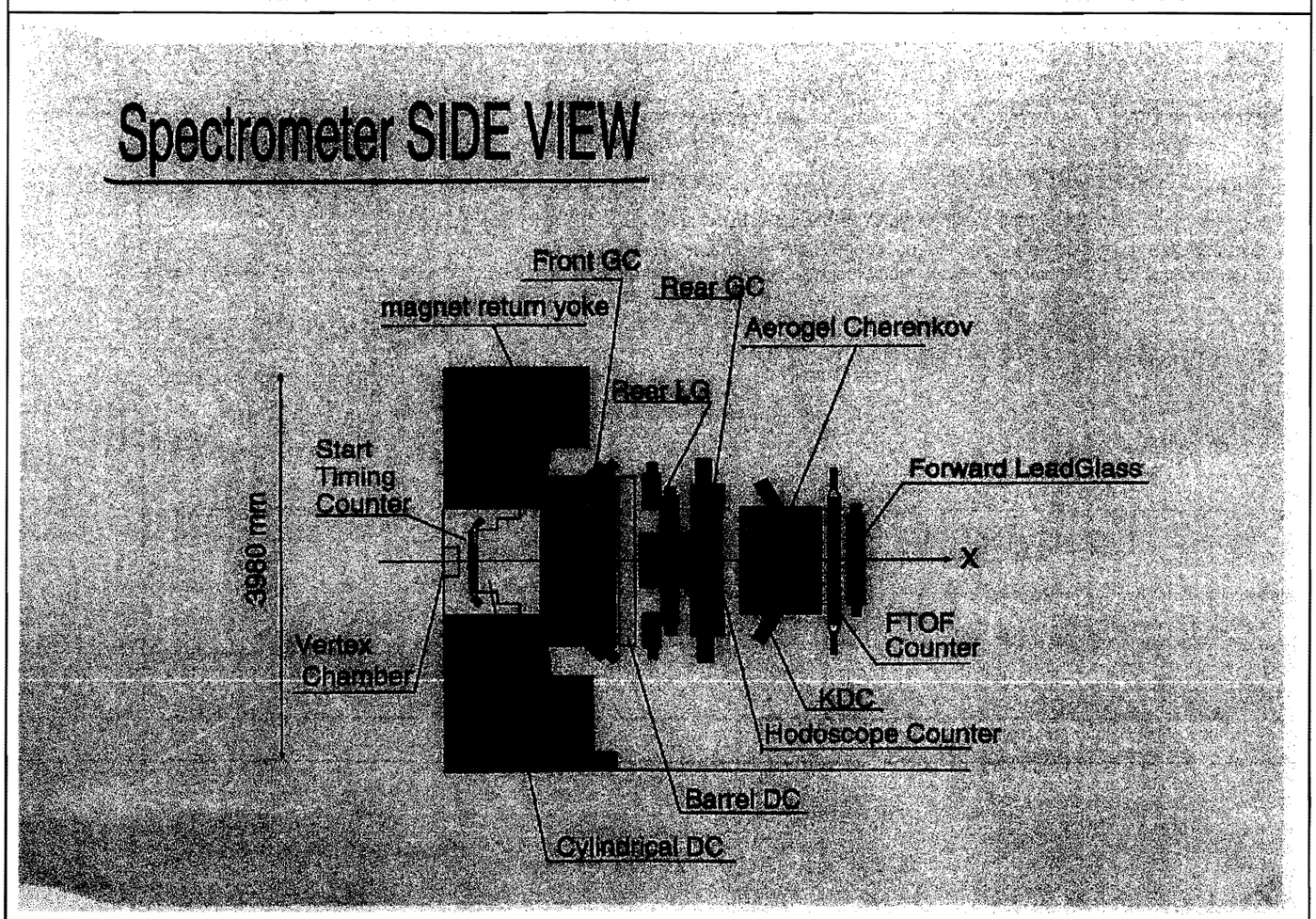
Spectrometer SIDE VIEW
Front GC
Rear GC
magnet return yoke
Aerogel Cherenkov
Rear LG
Start Timing Counter
Forward LeadGlass
3980 mm
X
FTOF Counter
Vertex Chamber
KDC
Hodoscope Counter
Barrel DC
Cylindrical DC

Target

- We used three kind of targets,
  - Cu / C / CH_2
  - total interaction length ~ 0.2%
  - total radiation length ~ 0.5%

- Vertex position
  - three targets were clearly separated.

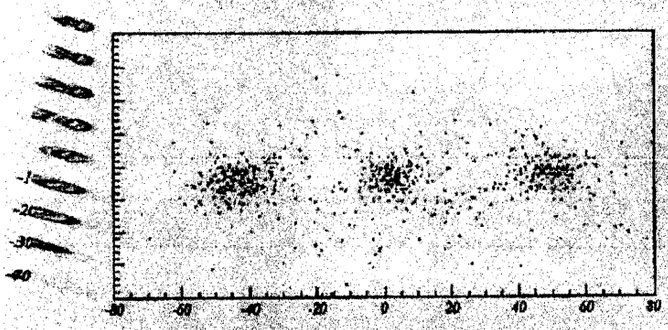

Vertex distribution in X-Y plane

targets in vertex chamber

Aerogel Cherenkov Counter

- separate kaons from pions
  - refractive index : 1.034
  - p : 0.53GeV/c ~ 1.88GeV/c
  - typically ~ 5 p.e.

efficiency for π

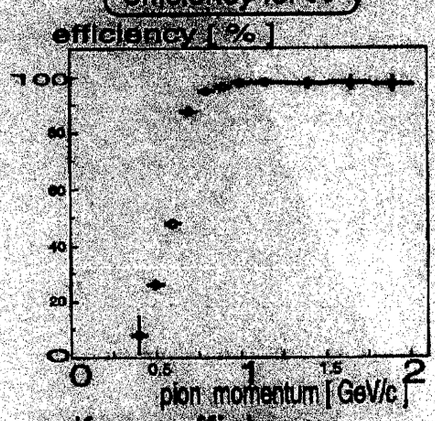

uniform efficiency
for π with p ≥ 1.0 GeV/c

light collection scheme

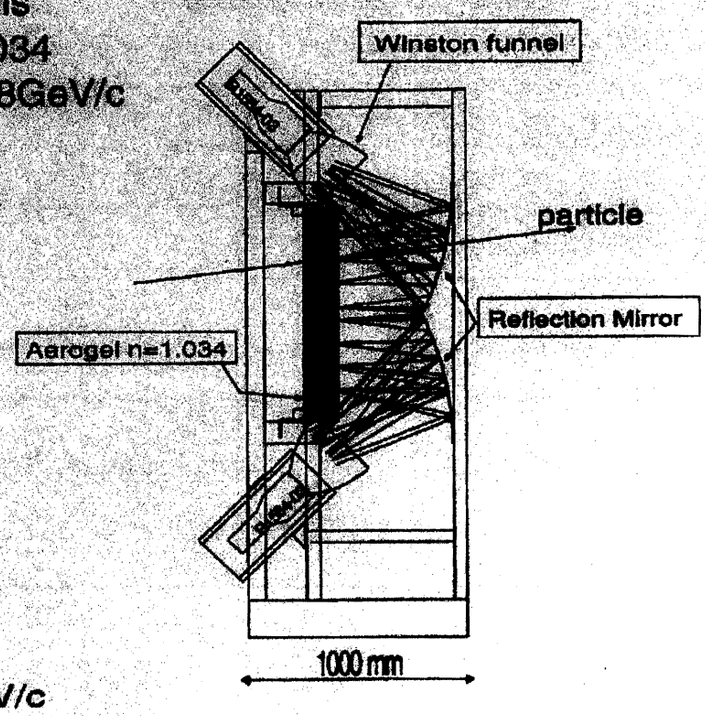

Kaon ID

- Kaon identification was performed by
  - the TOF technique using scintillation counters
  - helped by the pion veto with the AGCs.
    - timing resolution : 360 psec.

Squared Mass Distribution

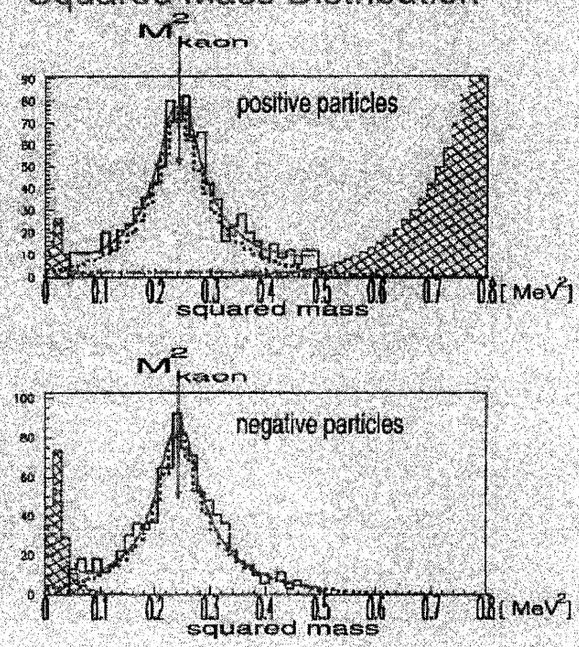

- We concluded that the background due to the miss identification was 10% in the final K^+K^- pairs.

- hatched histograms represents the expected contaminations

E-ID Counters

- Gas Cherenkov counters(FGC/RGC)
  - gas : iso-butane
  - index : 1.00127
- Lead Glass Calorimeter(RLG/SLG)
  - radiation length : 1.7 cm
  - resolution : 15% /$\sqrt{E}$
- New Forward LG Calorimeter(FLG)
  - has been installed in2000
  - improve efficiency of E-ID

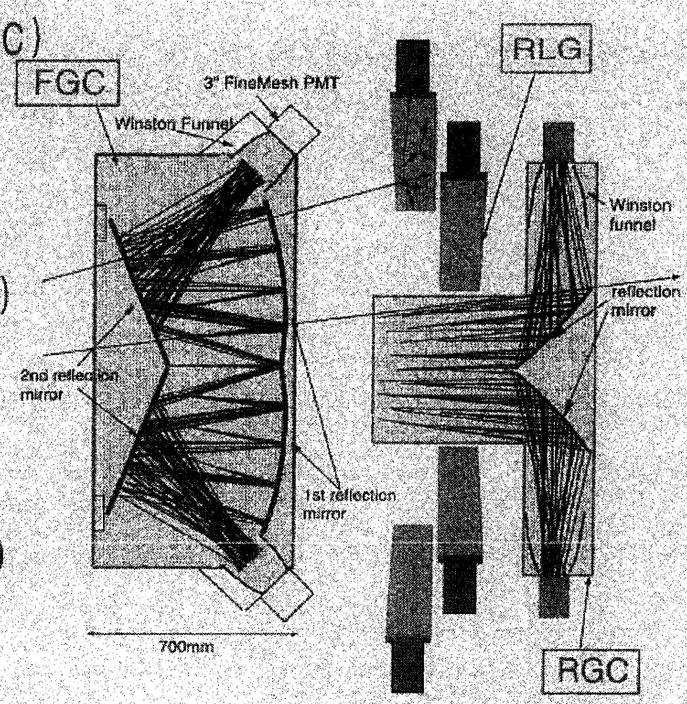

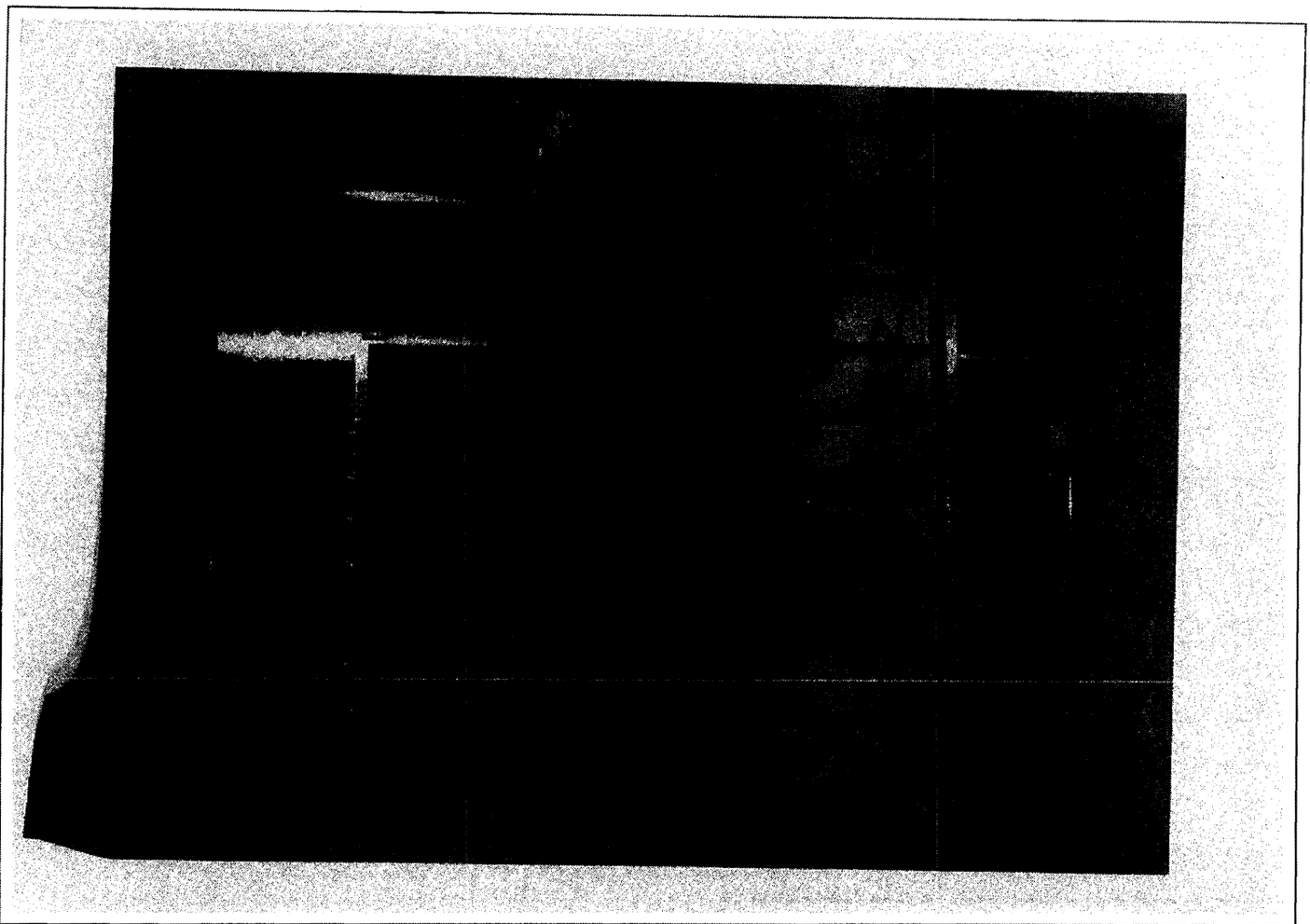

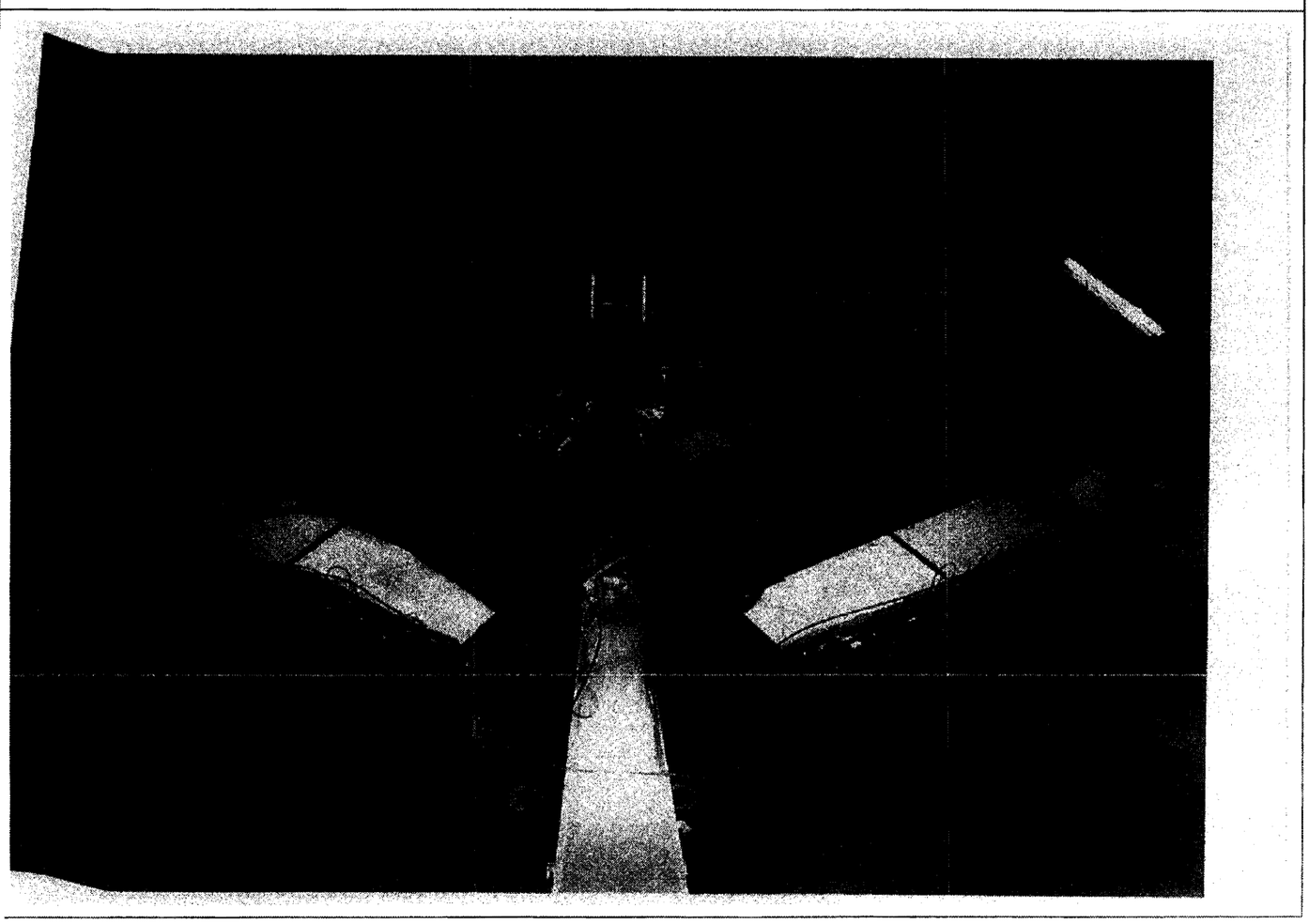

E-ID Performance

- e/π separation in the momentum range of 0.4 GeV/c ~ 2.5 GeV/c

	e efficiency	π contamination (with FGC)
Forward GC	55%	
Rear GC	86%	3.9×10^4
Lead Glass	85%	6.7×10^4

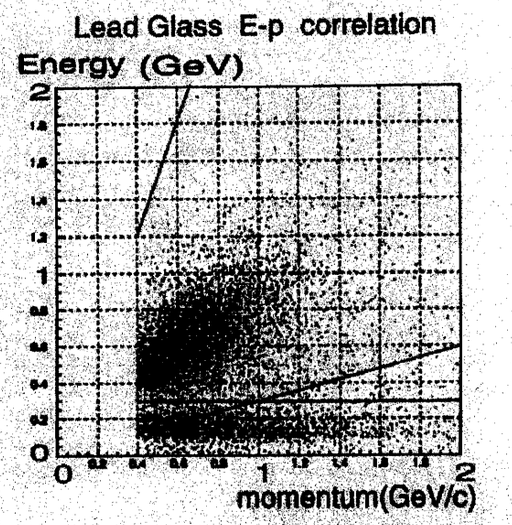

region identified as electrons

- Background due to the miss identification was estimated to be 13% in the final e^+e^- sample.

Mass resolution and energy scale

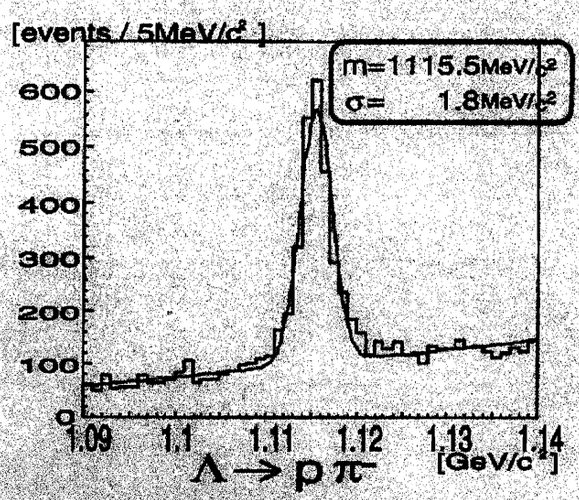

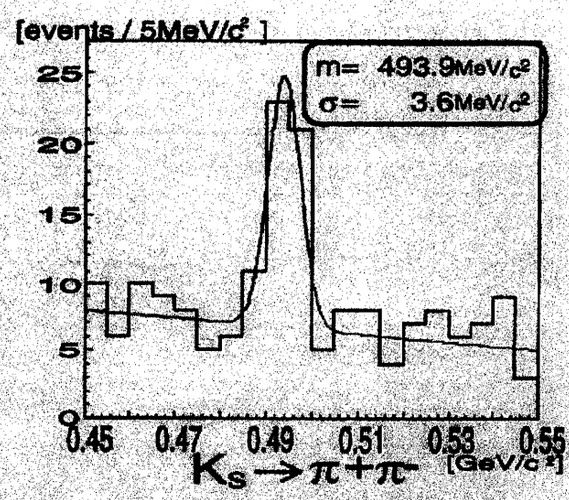

ΔM(measured)= 1.8MeV/c^2
ΔM(M.C.calc.) = 1.9MeV/c^2

Consistent

ΔM(measured)= 3.6MeV/c^2
ΔM(M.C.calc.) = 3.5MeV/c^2

$\omega \to e^+e^-$ ΔM (M.C.calc.) = 9.6MeV/c^2
$\phi \to K^+K^-$ ΔM (M.C.calc.) = 2.4MeV/c^2

The energy scale uncertainty was estimated to be less than 1%.

History and Status

			Total Event	Target
1997	Jun	First Physics Run with K^+K^- trigger	K:100M	Pb/C/CH2
1998	March	Completion of Spectrometer		
1998	May	Production Run with e^+e^- and K^+K^- parallel trigger	K:20M/e:100M	Cu/C/CH2
1999	July	Production Run	K:75M/e:64M	Cu/Gd/C/CH2
2000	June	Run with newly installed Vertex Chamber	K:31M/e:28M	Cu/C/CH2
2000	Dec.	Run with newly installed Forward Lead Glass Calorimeter	K:64M/e:57M	Cu/C
2001		The data taking will be continued		

Invariant mass distribution of electron pair

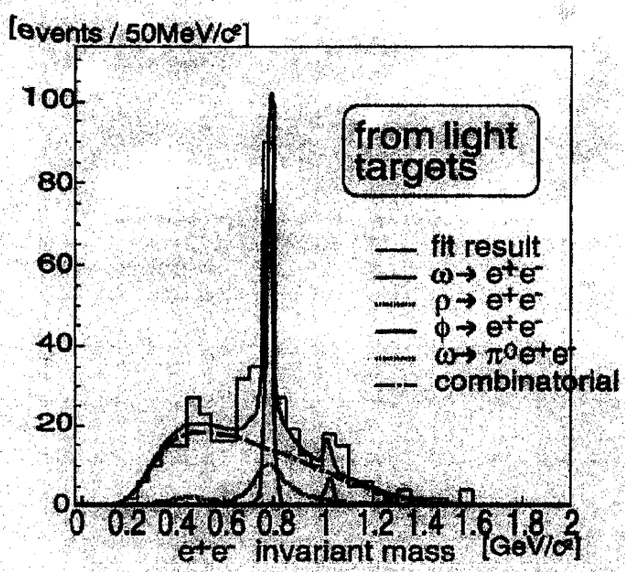

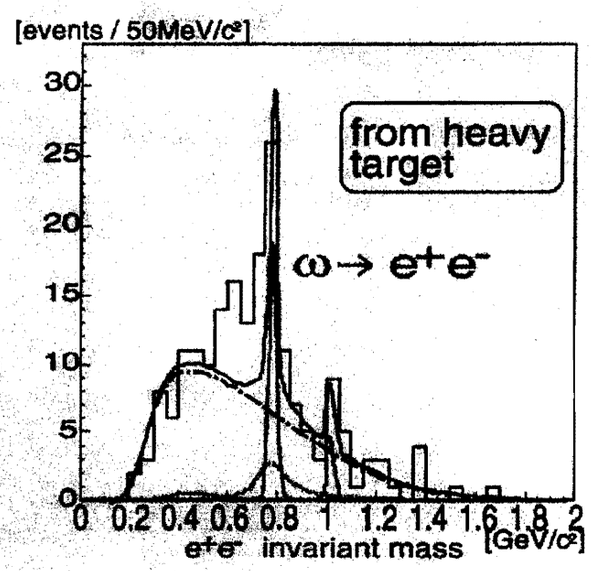

N_ϕ	= 7.4 ± 5.8	5.2 ± 2.7
N_{excess}	= 19.6 ± 11.7	29.5 ± 8.7
N_ω	= 75.5 ± 9.0	20.0 ± 4.8
N_{excess}/N_ω	= 0.26 ± 0.16	1.48 ± 0.56

Fit on the e^+e^- spectra

- Fitting Function

  Resonance ⟶ Breit-Wigner convoluted with mass resolution

  Background ⟶ combinatorial background was obtained by theevent mixing.

- Free Parameters
  - N ($\omega \rightarrow e^+e^-$)
  - N ($\phi \rightarrow e^+e^-$)
  - N ($\eta \rightarrow e^+e^- \gamma$)
  - N (combinatorial)

Invariant Mass Distrubution of K^+K^- ('99)

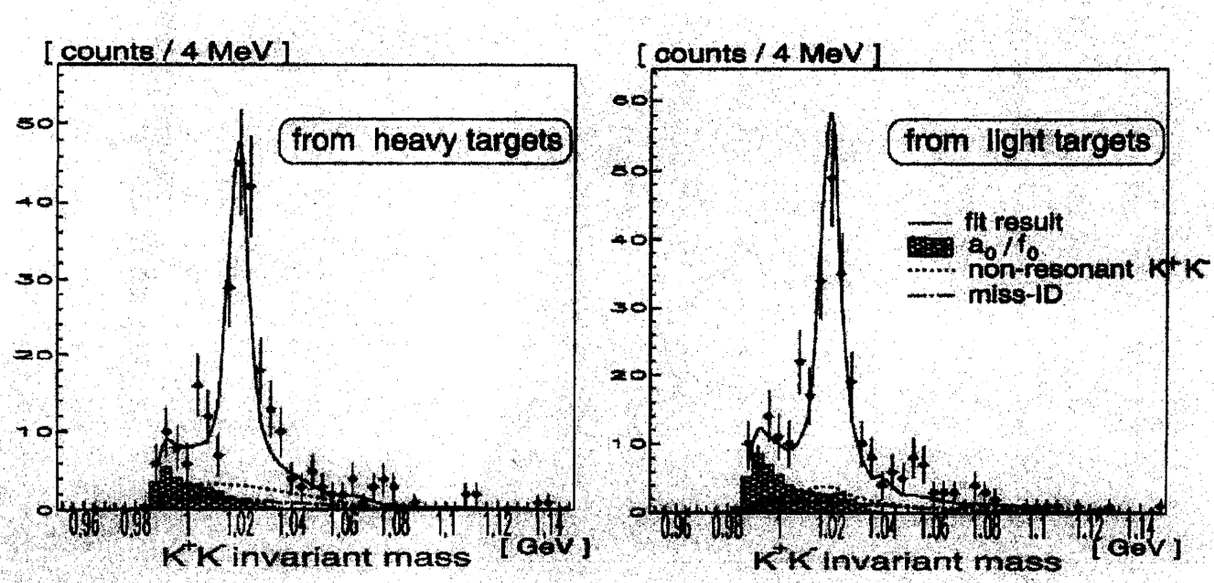

clear resonanse peak corresponding to the $\phi \rightarrow K^+K^-$ decays was observed.
histograms were well reproduced by $\phi \rightarrow K^+K^-$, $a_0/f_0 \rightarrow K^+K^-$ and non-resonant K^+K^- .

Fit on the K^+K^- spectrum

- fitting function
  - resonance of ϕ – Breit-Wigner convoluted with the mass resolution

- Background
  - $a_0/f_0 \rightarrow K^+K^-$
  - non-resonant K^+K^-
  - particle miss identification — amplitude and shape were estimated by the analysis of the data.

for the shape below the ϕ peak, the attempt to reproduce the invariant mass spectrum with these sources was not successful.

- free parameters

  $N(a_0/f_0 \rightarrow K^+K^-)$ / N_ϕ

Mass number dependence of the ϕ production

- In the $\phi \rightarrow K^+K^-$ channel
  - ➔From the data, $\alpha = 1.01 \pm 0.09$.
  - ➔From Monte Carlo (JAM), $\alpha = 1.08 \pm 0.01$.

  $\sigma(A) = A^\alpha \cdot \sigma(1)$

- Kinematical distribution.

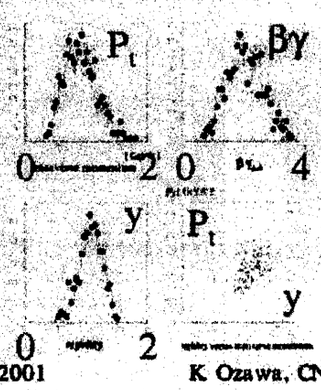

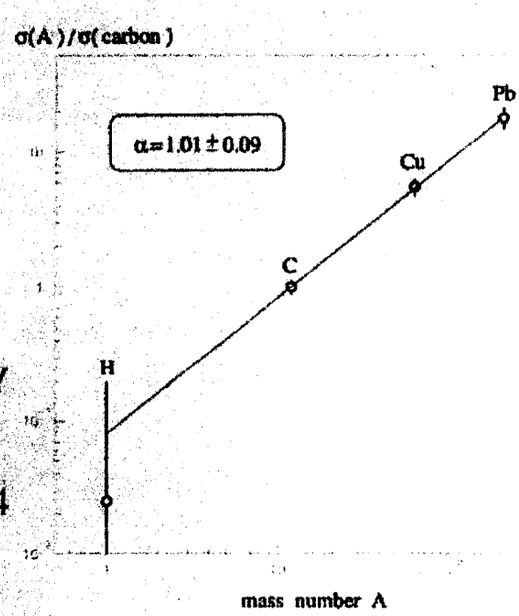

Mass Number Dependence of $\sigma_{\omega,\phi \to e^+e^-}$ '99

$\alpha = 0.63 \pm 0.07$ for ω

$\alpha = 1.03 \pm 0.15$ for ϕ

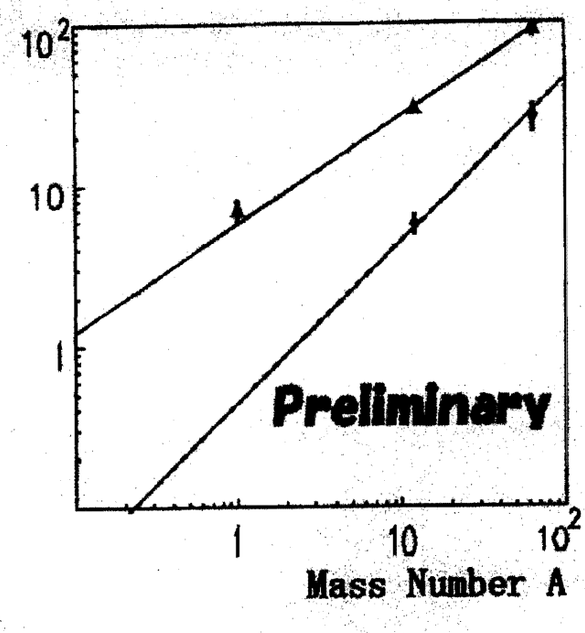

Summary

- The KEK-PS E325 measures the invariant mass distributions of e^+e^- and K^+K^- channels to observe signature of vector meson modification at normal nuclear density in 12GeV p + A interactions.
- Particle identification and the mass resolution are achived to meet the physics demands.
- The analysis of '99 $\phi \to K^+K^-$ data shows no significant signal for meson modification in the invariant mass spectrum of this channel within the current statistics.
- In the '98 e^+e^- data, we have observed an excess over the known hadoronic sources below the ω peak. Natural interpretation of the excess is the ρ / ω meson modification in nuclear matter.
- The analysis of '99 e^+e^- data and 2000 data are now in progress.
- In 2001, the data taking will be continued.
  Statistics will be $\gtrsim 5$ times at the end of this year.

Hadronic constraints for vector mesons in medium

Su Houng Lee

Yonsei University

To identify the existence of quark gluon plasma in heavy ion collision through the measurements of proposed signatures, it is necessary to explore all possible explanation of the proposed signature through hadronic scenarios. In this talk, we will look at the signatures related to the vector mesons observed through the dilepton spectrum. First, in relation to the J/psi suppression phenonomena in hadronic model, we will discuss the J/psi+ pi or J/psi+ rho total inelastic cross sections. Current estimates vary by an order of magnitute. We discuss the uncertainties within each model and discuss new developements within the effective hadronic model approaches. Second, in relation to mass shifts of light vector mesons, we discuss how the QCD sum rule constraints can be used to test the validity of hadronic models to explain the enhancement of low mass dilepton observed in heavy ion collisisons at CERN.

Tokyo 2001

Hadronic constraints for vector mesons in medium

Su Houng Lee, Yonsei Univ.

1. J/ψ suppression

   (a) Motivation;
   is $\sigma_{abs} = 1$ mb compatible with hadronic models

   (b) Meson Exchange Model
   Y Oh, T. Song, SHL; nucl th/0010064, PRC in press

2. Light vector meson
   B. Friman, H.Kim, SHL: NPA 653(99)91

3. Summary

J/ψ suppression

- Signature of QGP in RHIC
  O. Miyamura et.al. (86), Matsui, Satz (86)

- NA50 Collab. Phys. Lett. B 477, 28 (2000)

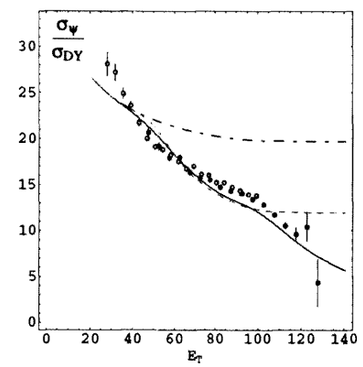

suppression by QGP

example: Blaizot et.al. (PRL 85(00)4012)

suppression when $\epsilon > \epsilon_c$

Models for J/ψ Absorption by Light Hadrons

most important processes relevant for RHIC

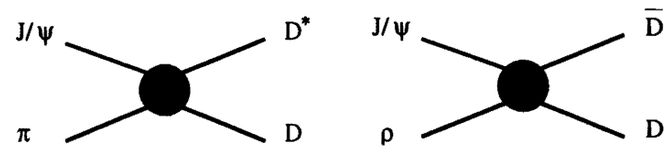

at threshold

method	σ_{abs} near threshold
pQCD in $m_c \to \infty$ limit Kharzeev et al., PLB 334, 155 (1994)	$\simeq O(\mu b)$
quark exchange model Martins et al., PRC 51, 2723 (1995) Wong et al., PRC 62, 045201 (2000)	$\simeq$ 1 mb
meson exchange model Martinvan & Müller, PRC 58, 2994 (1998) Haglin, PRC 61, 031902 (2000) Lin & Ko, PRC 62, 034903 (2000) Oh, Song & Lee, PRC 63, (2001)	$\simeq$ 0.3 mb $\simeq 3 \sim 7$ mb $\simeq 2 \sim 5$mb

•Without QGP

Capella et.al. (PRL 85(00)2080, PRC59(99)395)

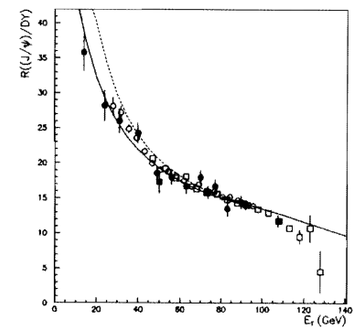

Here, $\sigma_{abs} = 4.5$mb and $\sigma_{co} = 1$mb

- Known from transport model (C.Ko PLB 396(97)39) that $\sigma_{co} > 1$mb can explain J/ψ suppression seen at CERN.

Is 1 mb compatible with estimates from hadronic models?

2. quark exchange model
$\sigma_{\text{abs}} \simeq 1$ mb for $\pi + J/\psi \to D^*\bar{D}, D\bar{D}^*, D^*\bar{D}^*$

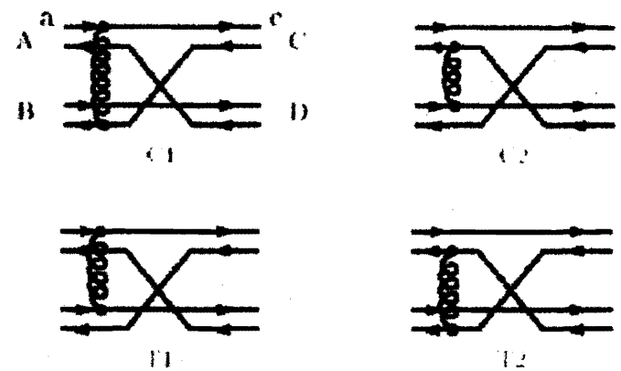

5

1. pQCD in the heavy charm quark mass limit with dipole approximation (Kharzeev et.al.)
$\sigma_{\text{abs}} \simeq O(\mu\text{b})$

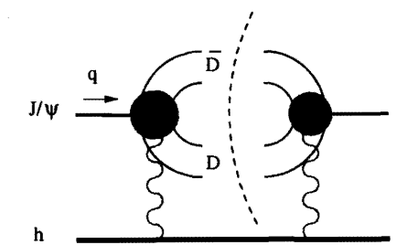

$$i\int dx e^{iqx}\langle h|TJ_{J/\psi}(x)J_{J/\psi}(0)|h\rangle \propto \sum_n^\infty d_n\langle h|O_n|h\rangle\left(\frac{q\cdot h}{\epsilon_0}\right)^n$$

with $\epsilon_0 = 2m_D - m_{J/\psi}$, $q^2 = m^2_{J/\psi}$

But

(a) neglect confinement (coulomb bound state) in calculating d_n

(b) higher twist ? $\langle h|O|h\rangle\frac{1}{m_c^2}$

(c) OPE at separation scale $m_c, \epsilon_0 = 0.8$GeV ?

(d) fit to $\sigma_{\gamma N\to c\bar{c}}$ is not a check because $\epsilon_0 = 3.8$GeV

4

Models for J/ψ Absorption by Light Hadrons

$\sigma_{\text{abs}} > 1$ mb seems compatible with hadronic calculations.

refine the calculation and use this as a guide line for RHIC

3. meson exchange model using effective Lagrangian
   $\sigma_{\text{abs}} \simeq 0.3$ mb (Martinyan et.al.), $3 \sim 7$ mb (Halgin, Ko..), $2 \sim 5$ mb(Oh, Song, Lee),

   example: $\sigma_{\pi+J/\psi\to\bar{D}+D^*} = 1$ mb with $\Lambda = 1$ GeV

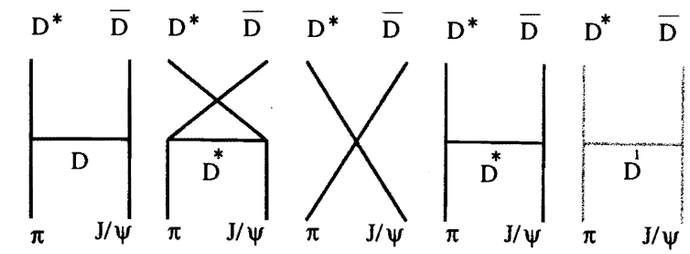

Martinyan.. Haglin, Lin and Ko Oh, Song, Lee

1 10 3 10 ?

relative strength

uncertainty comes from

1. form factor $\Lambda = 1 \sim 2$ GeV
2. four point coupling ($0 \sim$ value at SU(4) limit) (effect of D_1 meson).

1. pQCD in the heavy charm quark mass limit with dipole approximation (Kharzeev et.al.)
$\sigma_{\text{abs}} \simeq O(\mu\text{b})$

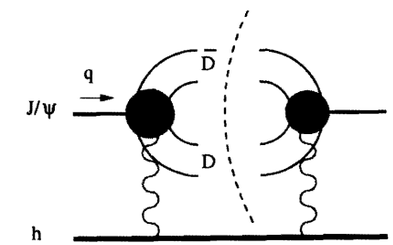

$$i\int dx e^{iqx}\langle h|TJ_{J/\psi}(x)J_{J/\psi}(0)|h\rangle \propto \sum_n^{\infty} d_n\langle h|O_n|h\rangle \left(\frac{q\cdot h}{\epsilon_0}\right)^n$$

with $\epsilon_0 = 2m_D - m_{J/\psi}$, $q^2 = m^2_{J/\psi}$

But

(a) neglect confinement (coulomb bound state) in calculating d_n

(b) higher twist ? $\langle h|O|h\rangle\frac{1}{m_c^2}$

(c) OPE at separation scale $m_c, \epsilon_0 = 0.8$GeV ?

(d) fit to $\sigma_{\gamma N\to c\bar{c}}$ is not a check because $\epsilon_0 = 3.8$GeV

2. quark exchange model
$\sigma_{\text{abs}} \simeq 1$ mb for $\pi + J/\psi \to D^*\bar{D}, D\bar{D}^*, D^*\bar{D}^*$

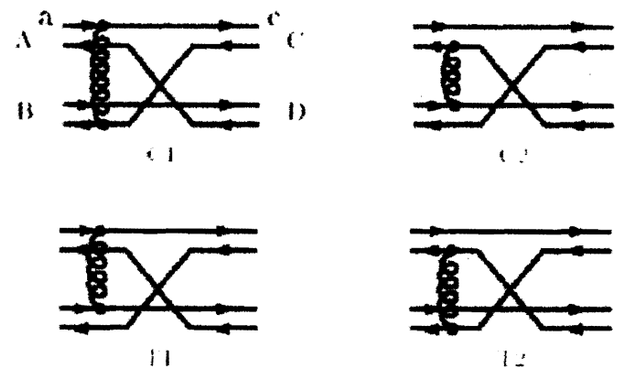

Light vector meson

- Signature of partial chiral symmetry restoration in HIC

Order parameter $\langle \bar{q}q \rangle$

$$\langle V_\mu(x) V_\nu(0) \rangle - \langle A_\mu(x) A_\nu(0) \rangle$$

- CERES Collab. Nucl. Phys. A 661, 23c (1999)

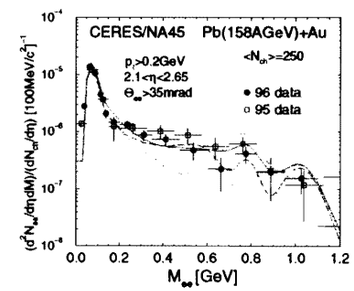

Red: Li,Ko,Brown PRL 75(95)4007
purple: Rapp, Chanfray,Wambach NPA617(97)472

- Explanation of Data

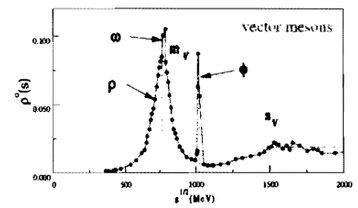

× phase space

- Spectral density in medium

1. mass shift (Brown-Rho, Hatsuda & Lee)
2. conventional many body effects
   (a) $\pi - \pi - \rho$ (b) N-Δ $- \rho$

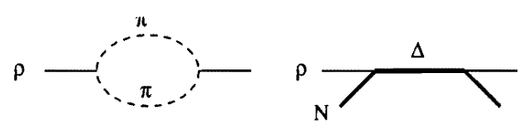

- Consistent use of Form factor satisfies QCD OPE constraints Friman, Kim, Lee NPA653(99)91

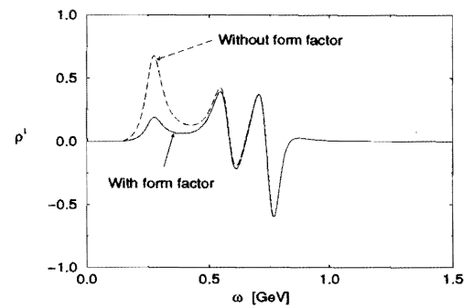

1. necessary to refit the CERES data?
2. Models used in Manybody approaches have to be re-tested (example: p-A reaction, constant phase space)

- N-Δ $-$ ρ couplings

	$I(J^P)$	Γ_{Total}(GeV)	l_ρ	$f_{RN\rho}$	S_Σ
N(940)	$\frac{1}{2}(\frac{1}{2}^+)$	0	1	7.7	4
N(1520)	$\frac{1}{2}(\frac{3}{2}^-)$	120	0	7	8/3
N(1650)	$\frac{1}{2}(\frac{1}{2}^-)$	150	0	0.9	4
N(1680)	$\frac{1}{2}(\frac{5}{2}^+)$	130	1	6.3	6/5
N(1720)	$\frac{1}{2}(\frac{3}{2}^+)$	150	1	7.8	8/3
Δ(1232)	$\frac{3}{2}(\frac{3}{2}^+)$	120	1	15.3	16/9
Δ(1620)	$\frac{3}{2}(\frac{1}{2}^-)$	150	0	2.5	8/3
Δ(1700)	$\frac{3}{2}(\frac{3}{2}^-)$	300	0	5.0	16/9
Δ(1905)	$\frac{3}{2}(\frac{5}{2}^+)$	350	1	12.2	4/5

$$\Sigma = \mathrm{q}^2 \left(\frac{f_{RN\rho}}{m_\rho}\right)^2 [F(\mathrm{q})]^2 \frac{E_R(\mathrm{q}) - m_N}{\omega^2 - (E_R(\mathrm{q}) - m_N)^2}$$

For Δ(1232) used $f_{N\Delta\rho}$ from Bonn potential

$$f_{N\Delta\rho} = 15.3, \quad \text{with} \quad F(\mathrm{q}) = \left(\frac{\Lambda^2}{\Lambda^2 + \mathrm{q}^2}\right)^1$$

but in Bonn potential,

$$f_{N\Delta\rho} = 15.3, \quad \text{with} \quad F(\mathrm{q}) = \left(\frac{\Lambda^2 - m_\rho^2}{\Lambda^2 + \mathrm{q}^2}\right)^2$$

almost a factor of 4 smaller

Summary

1. Models for J/ψ Absorption by Light Hadrons

   (a) $\sigma_{\text{abs}} > 1$ mb seems compatible with hadronic calculations.

   (b) refine the calculation and use this as a guide line for RHIC

2. Light vector meson

   (a) Models used in Manybody approaches have to be re-tested

   (b) h-A reaction to produce vector meson in medium would be very useful (constant phase space)

12

J/ψ in pA and AA

H. FUJII (University of Tokyo, Komaba)

I will present a brief review on the production of J/ψ in pA and AA collisions.

In 1996 the results from NA50 collaboration at CERN–SPS showed a dramatic drop in the 'J/ψ/DY' ratio from the 'base-line', which has been attracting much interest and arousing many discussions in the community.

First I'd like to talk about what is the baseline. Historically the J/ψ suppression in the O–U collisions was discovered by NA38 (1989) shortly after the proposal by Matsui and Satz in 1986 as one of the QGP signatures. However, the following experiments of S–U as well as p–A revealed two facts: (i) the observed suppression in A–B is explained with the same 'absorption' cross section ($\sigma_{\psi N} \sim 6$ mb) in p–A, and (ii) in the p–A events the J/ψ and the ψ' show the same suppression. People then granted that the observed suppression is the 'normal', nuclear effect, because we don't expect QGP in p–A.

Theoretically these two facts are understood with the 'pre-resonance' state in the hadro-production of the quarkonium; The $c\bar{c}$ pair created in a hard parton scattering needs a 'formation time', typically $1/(m_{D\bar{D}} - m_{\psi})$ ~fm, to become a physical resonance. Within this duration there is no difference between the J/ψ and the ψ'. Furthermore the NRQCD calculations suggests the 'dominance' of the color-octet $c\bar{c}$ state in the quarkonium production in the Tevatron $p\bar{p}$ experiments, which may explain the large cross section ~6 mb of the nuclear 'absorption'.

For the heavier system such as Pb–Pb, the quarkonium state will be formed inside the hadronic matter where a bunch of produced mesons exist. Unfortunately we don't have the right value of the J/ψ-meson cross section. There are several theoretical estimates based on the quark exchange model, the meson exchange model, the short distance QCD and so on, but they differ by several orders of magnitude! The comover suppression scenarios have been considered extensively, taking into account the uncertainty (e.g.) in the cross section with the comovers. However, they seem incapable of explaining the 'threshold'-like structure of the anomalous J/ψ suppression observed in NA50 collaboration, and the QGP formation remains a likely scenario to interprete the data.

Recently the NRQCD calculation is subjected to trial at Tevatron, and the NRQCD prediction for the quarkonium polarization produced at high-$p_{\perp}$ in the $p\bar{p}$ collision is inconsistent with the data! The crisis for the color octet production scenario? In QM2001 conference, Qiu and Sterman suggested that the polarization could be understood in a more consistent QCD calculation. Within their framework of the quarkonium production, nuclear suppression effects appear differently from those in the NRQCD and may explain the anomalous J/ψ suppression without QGP! I'd like to mention about their work if possible.

Therefore, it seems fair to say that more systematic experimental study for the J/ψ is needed using BNL–RHIC and CERN–SPS as well as the theoretical efforts to understand the data before drawing any final conclusion, although the NA50 data undoubtedly suggests something new.

J/ψ in pA and AA

H.FUJII (U of Tokyo, Komaba

1. Basic idea
2. Time scale
3. p-A~S-U
4. Pb-Pb
5. Some discussions
6. Outlook

Quarkonium melting in QGP

Debye Screening (Matsui+Satz PLB178('86))

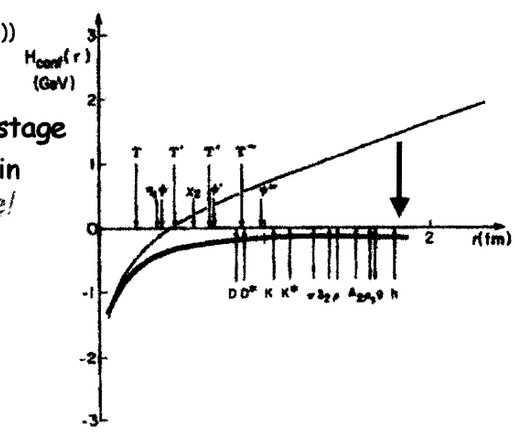

- Q's produced only in the early stage
- Screened Potential btwn quarks in dense medium → *no bound state!*

- At hadronization, too far apart
- Note
  - Assuming static, infinite medium
  - Collective effects

Satz

	Ψ (1S)	Ψ(2S)	χ(1P)
μ_D[GeV]	0.68	0.35	0.35
T/T_C	1.2	1	1

Screening vs Collisionaldissociation

Two reasons for expecting the suppression in QGP

1. Color screening...quarkonium melts in QGP
   - Collective effect, I just explained
2. Gluon Dissociation ... only hard thermal qluon in QGP breaks Q'm
   - Incoherent effect
   - At T~.2GeV,
     - Gluons in hadron is soft: $\langle k \rangle_{conf}$~.6T~.1GeV
     - Gluons in QGP is hard: $\langle k \rangle_{deconf}$~3T~.6GeV~BE of ψ

- Analogy: 'mean field' and 'collision term' in the Boltzmann eq.
- In QCD, either of two effects dominates, or both?

Questions asked in '86 paper

- Can ψ escape before the plasma formation?→Maybe not
- Debye length, quarkonium radius in medium → LQCD
- Non-plasma suppression? → observed
- Can the ψ suppression in the plasma survive the transition?→I hope so
- Can the ψ be observed? → observed

How to look at NA50 data? Let's go thru pp, pA, AB

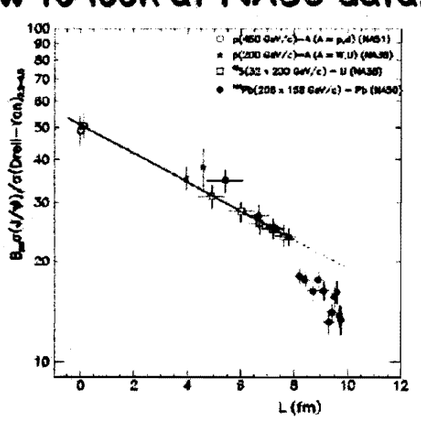

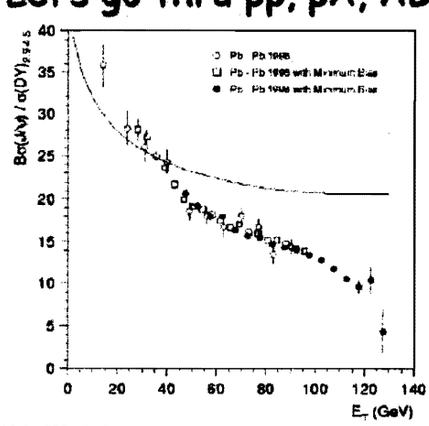

Scales of Quarkonium and HIC

- cc pair produced~1/2mc~0.1fm/c
- Bound state formation ~1fm/c

- At SPS, 2R~14fm,2R/γ~1.4fm
- At RHIC, 2R~14fm,2R/γ~0.14fm

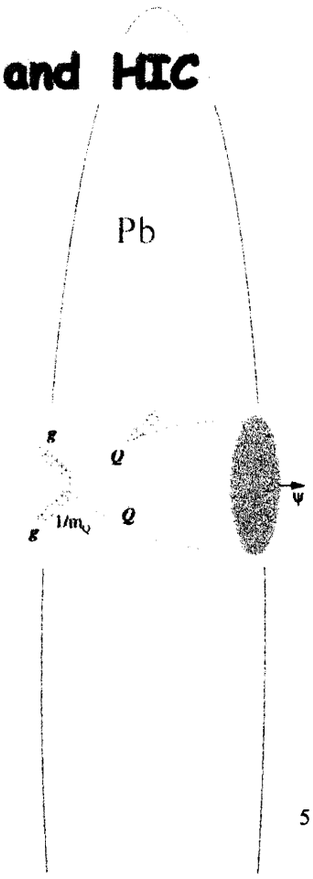

p-A ~ S-U; nuclear absorption

ψ suppression observed by NA38 in 1987!

Surprises up to S-U Cf. Kharzeev et al. ZPC74(97)307

1. The same σ_{abs}~6.5mb explains P-A and A-B (L-scaling or Glauber model)
2. The ψ'/ψ equally suppressed

Naïve expectation was

1. $\sigma_{tot}^{\psi N}$~3.5mb [photo-production]
2. σ(ψ'N)/σ(ψN)~4 [size of onia]

Interpretation:

No QGP: This is 'normal'

Pre-meson, dominantly octet, state propagates in nuclear medium

Needs justification...

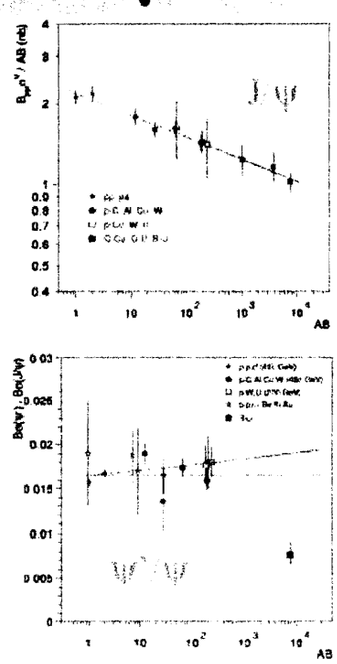

PLB466,408

Quarkonium production in NRQCD

Motivation for Color Singlet Model

- Pair Creation — Relativistic effect: fast
- Bound state formation — Internal motion: slow

⇒ factorization assumption:

$$d\sigma(ab \to \psi X) = \sum_{ij} \int dx_i dx_j G_{i/a}(x_i) G_{j/b}(x_j) d\hat{\sigma}(ij \to [c\bar{c}]_1 X) \cdot R_\psi^2(0)$$

Fails to explain the s_{tot} and p_T dep at Tevatron

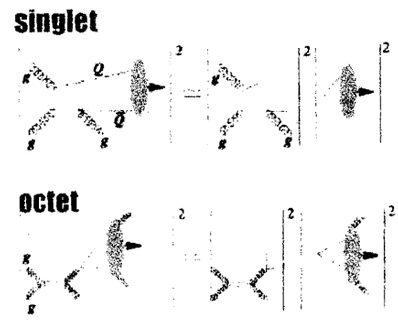

Theory developments: Octet Model

- Parton fragmentation at high p_T
- Importance of Color-octet component

$$|\psi> = |(Q\bar{Q})_1> + O(v)|(Q\bar{Q})_8 g> + \ldots$$

- Caveat; octet elements not small

Beneke+Kramer,PRD55

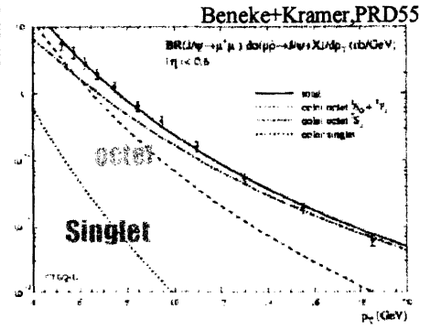

Pre-meson to physical meson

- ψ'/ψ ratio drops at S-U
- Interpretation
  - Pre-meson is evolving to physical one
  - 'σ_{abs}' changes in the evolution

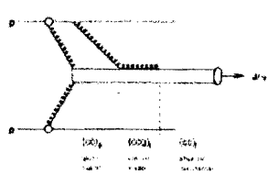

- A supportive trend observed at FNAL-α E866; 800GeV/c p-A, Be, Fe, W
  - Fast x_F>0.6; same suppression
  - Slow x_F~0; stronger for ψ'
    - Physical resonance in nuclear medium

FNAL E866, PRL84,3256

$$\sigma_A = \sigma_N \times A^\alpha$$

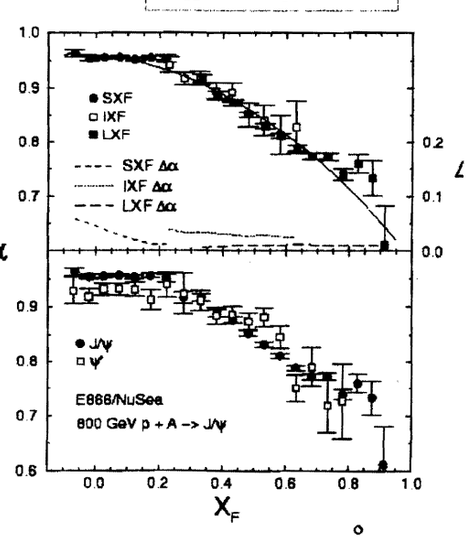

Pb-Pb collisions

Surprises

- Sudden drop of ψ at 8fm in L-scaling
- The ψ well below the 'normal' absorption
  ←→ No threshold for ψ' ?

Tempting interpretation: QGP formaion

BE(ψ')~50MeV, BE(χ)~200MeV, BE(ψ)~650MeV

Other scenarios possible?

NB.
•In the finer bins, the ψ/DY ratio behaves smoother
•Drop around largest Et may be fluctuations (Ding et al. QM01)

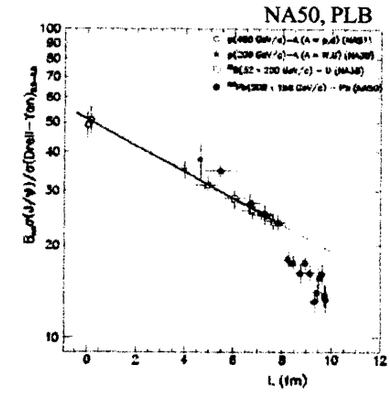

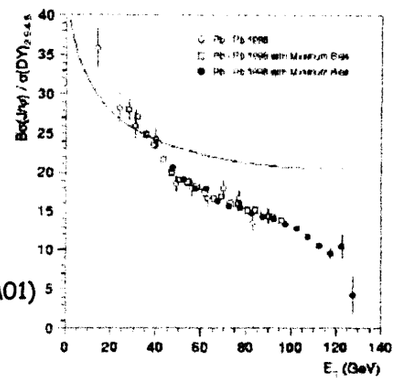

Comovers? $_{\pi,K,N,...}$

- There are a lot of comovers
- Model assumptions
  - Constant x-sec.
    E.g. $\sigma^{\psi N}_{abs}$~4.8, σ^{co}_{abs}~0.7mb
  - Number of comover ∝ Np
- Incapable of describing the structure of ψ suppression

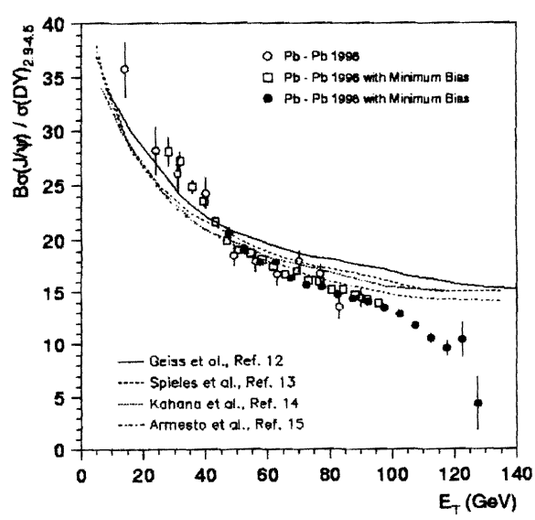

ψ-*h* absorption cross sections

Also S.-H. Lee's talk

$\psi\pi$, $\rho \rightarrow D^{bar}D$; Largely unknown...

1. Quark exch model
   - Uncertain confining potential
2. Constant (comover param)
3. Meson exch model
   - Range $1/m_D$~0.1fm
   - formfactor
4. Short distance QCD
   - Small ... soft gluons in *h*
   - Maybe not heavy enough

and so on.

Braun-Munzinger+Redlich, QM99

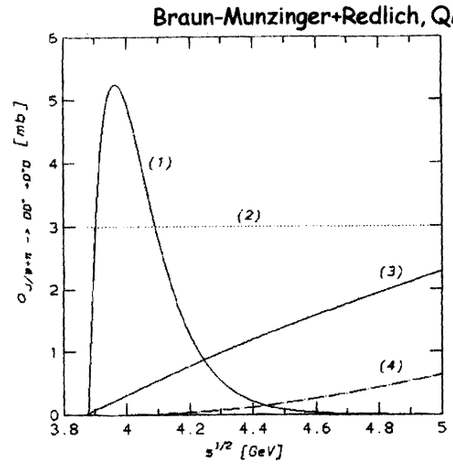

Relevant relative kinetic E ~ 0.3 GeV

Any consistent view for ψ and ψ'?

- ψ' ...hadronic absorption or melting? Lourenco, NA38 QM01
- At first glance, very similar to the ψ case in Pb-Pb
- Naive comovers cannot explain the ψ and ψ' at the same time (Vogt)

NA38
PLB 466 (1999) 408

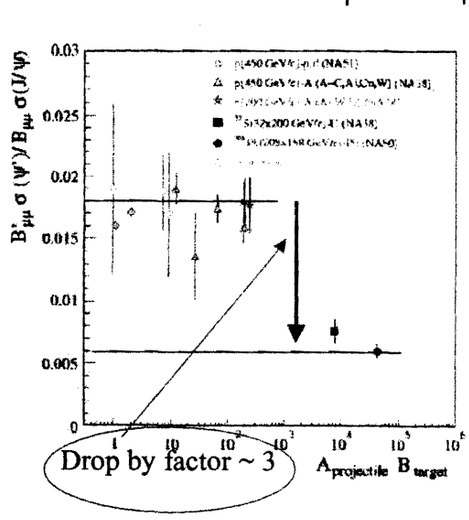

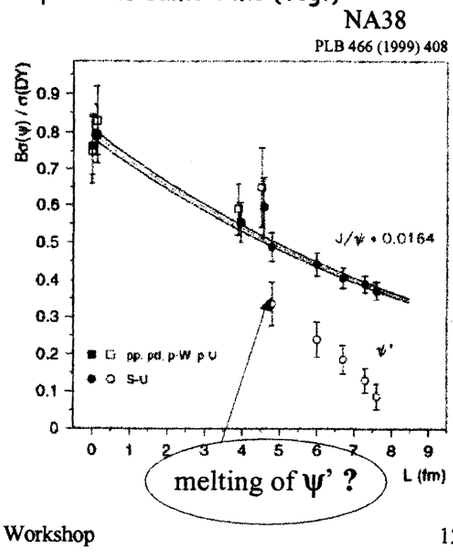

Pt broadening

Any other qualitative change in ψ observable?

Not quite

p_T broadening is observed and understood as

- multiple scattering of initial parton - random walk
- Final state interactions w/comovers may possible

QGP scenario

- high pt ψs escape from QGP; increase?
- QGP reduces ψs from hot zone; decrease?

NA50

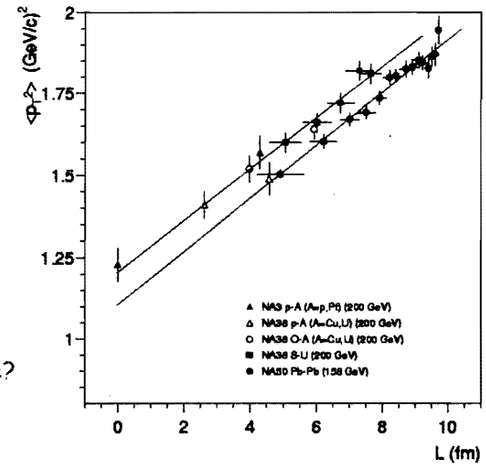

Personal interests

- What we saw might be the L-scaling breaking for ψ at Pb-Pb, the similar was observed for ψ' at S-U before; Cf. analysis x_F-dep. by E866
- Description with σ_{abs}~6.5mb, 'x-sec of octet state', constant seems crude; it may well change in resonance formation -> Qiu,QM01

->> Consistent description of ψ and ψ' (10,30% of ψ come from ψ' and χ)

- Quarkonium formed with medium effects, both screening and collisional dissociation

->>More quantum description for $Q^{bar}Q$ → Q'm in QCD medium possible?

New scenario for the suppression

For details, Qiu et al.@QM01

Color octet model fails in pol of ψ at high p_t

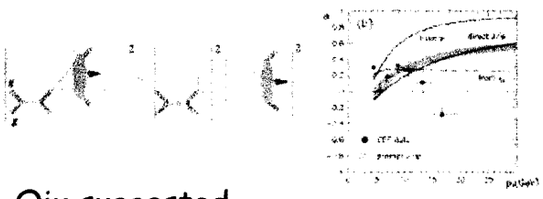

Qiu suggested...

More consistent QCD calc.:

- Parton fragmentation changes the polarization
- Probability of $c^{bar}c$ to γ depends on change of m_{cc} by radiation as well as w.f. of ψ

- Modeling the ψ suppression
  - $m_{cc} \rightarrow m_{cc}+\varepsilon^2 L$; interaction of cc w/matter
  - Params; ε, form of prob., cc creation
  - Capable of explaining p-A, AA, they claim

New estimate for the nuclear suppression

- J/ψ production as a function of effective medium length:

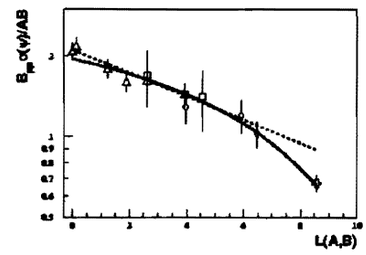

- Ratio of J/ψ over Drell-Yan as a function of E_T:

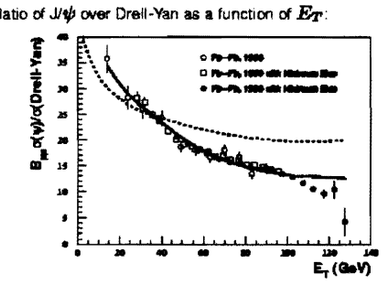

Outlook

- RHIC will be different;
  - Thin nuclei $2R/\gamma \sim 0.1$fm.....L-scaling of multiple collisions? (Matsui)
  - Pre-meson in the co-mover gas/QGP
    - 'n_{co} propto N_p' could break
    - How to describe the pre-meson in QGP?
  - Above which γ the difference obvious?
    - That's one of our interests (Matsui)
- Data show up soon!
- Keep your mind open...
  - ψ enhancement?

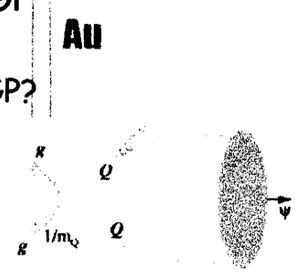

Quark matter in neutron stars

T. Tatsumi

Department of Physics, Kyoto University, Kyoto 606-8502

I would like to give a review about quark matter in neutron stars, based on our recent works[(1),(2)]. Quark matter may be the final form of matter in the high density limit. As an alternative it may be the ground state of finite density QCD. Since there is no clear indication, at present, about the critical density of the deconfinement transition at finite baryon density, we can take it rather wide region. For long years many people believe that quark matter is a weakly interacting system by exchanging gluons due to the asymptotic freedom of QCD and it may be a simple system different from the ordinary condensed matter. Recently, some interesting ideas have been actively discussed about the *structure* of quark matter: color superconductivity and the mixed phase of quark-hadron matter may be typical examples.

I will forcus on two current topics in my talk; one is ferromagnetism of quark matter[(1)] and the other is the mixed phase of quark-hadron matter[(2)]. In the recent paper I proposed a possibilty of ferromagnetism of quark matter by a simple consideration and found that one gluon exchange interaction always favors the spin alignment and the critical density of ferromagnetism should be order of nuclear density, below which saturated ferromagnetism is realized. I also suggested that the superstrong magnetic field observed in magnetars may be understood from the microscopic point of view if we consider magnetars as quark stars. I will present the basic idea and some new concepts inherent in quark ferromagnetism.

There is a controversy about the existence of mixed phase of quark-hadron matter and this issue should be related to a basic theorem in statistical physics. Original statement is very clear: if there is a first order phase transition with more than one conserved quantities, we must apply the Gibbs conditions to get the equilibrium equation of state. In the case of quark-hadron phase transition, if it is of the first order, charge conservation and baryon number conservation must be ratained during the phase transition. Then it has been discussed that the mixed phase composed of quark-hadron matter may appear well *below* the critical density of the phase transition and develop over a wide density region. For example you can imagine an appearance of quark droplets immersed in nuclear matter. So this issue is a problem of the structured phase in other sense. I will discuss this issue by showing how creation of droplets is difficult if we take into account the Debye screening effect.

References:

(1) T. Tatsumi, Phys. Lett. **B 489**, (2000) 280.

(2) T. Tatsumi, D.N. Voskresensky and M. Yasuhira, to be submitted.

Quark matter is a rather simple system where quarks weakly interact with each other by gluon exchange? ⟶ Maybe no.

Condensed matter physics of QCD: (Similarities & Differences)

- Color superconductivity
- Quark ferromagnetism
- Structured quark matter – Quark-Hadron mixed phase
  Debye screening
- ...

15 Feb. 2001 (T.T.)

Quark matter in neutron stars

T. Tatsumi

Department of Physics, Kyoto University, Kyoto 606-8502

Introduction

"Neutron stars = Astrophysical laboratory for nuclear physics"

Observations – from radio to gamma ray or neutrino:

- Radio (X ray) Pulsars
- Gamma-ray Bursters
- Supernovae
- ...

Quark stars as the third branch of compact stars subsequent to neutron stars or Strange star conjecture
⟶ How are they produced and how are they observed?

Critical density for deconfinement transition:

- above 8 times of the nuclear density (standard view?) $\gtrsim 8\rho_0$
- around the nuclear density (quark matter is the ground state of finite density QCD (Witten)) $\sim \rho_{bag} \simeq 1.5\rho_0$

1st order p.t.

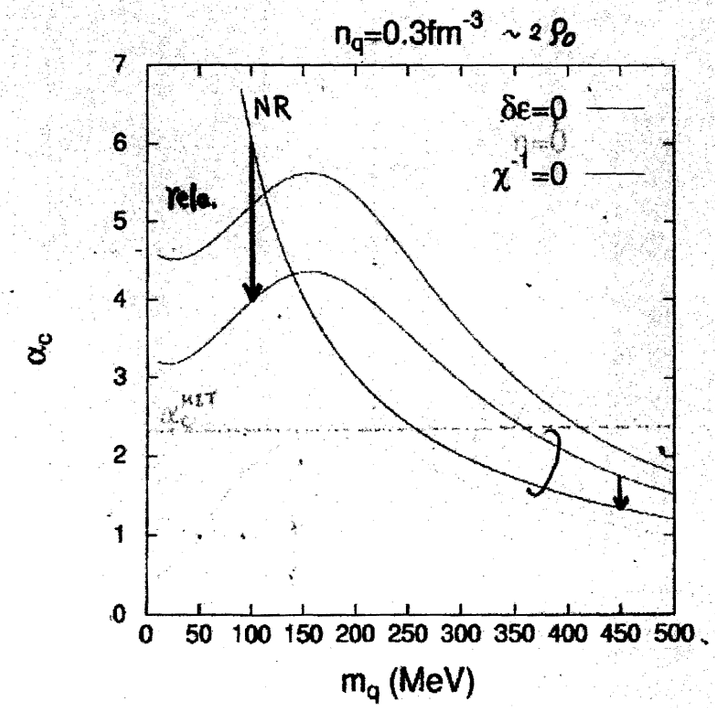

I. Ferromagnetism (FM) of quark matter

Origin of strong magnetic field in neutron stars ($B_s \sim 10^{12-13}$G)

⟶ Discovery of magnetars with superstrong magnetic field.
Two pulsars in SGR (Soft-Gamma-ray Repeaters)- magnetar candidates

◇ SGR 1806-20 (Kouvelitou et al., 1998)

◇ SGR 1900+14 (Hurley et al., 1999)

⟶ $B_s \sim 10^{14-15}$G from the $P-\dot{P}$ curve etc.

∘ Presentation of an idea, ferromagnetism (FM) of quark liquid, by a *perturbative approach* (P.L. B489 (2000)280.).

i) Fock exchange int. *always* favors spin alignment.

ii) There is a different mechanism in the rela. region.

rela. FM

$$E_{ex}/V \sim -\frac{\alpha_c k_F^4}{2\pi^3}\left[(1+p)^{4/3}+(1-p)^{4/3}\right] \quad \text{(NR)},$$
$$\sim +\frac{\alpha_c}{8\pi^3}k_F^4\left[(1+p)^{4/3}+(1-p)^{4/3}+2(1-p^2)^{2/3}\right] \quad \text{(ER)},$$

with $p \equiv N_+/N_-$ (polarization parameter).

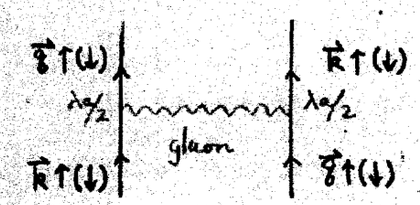

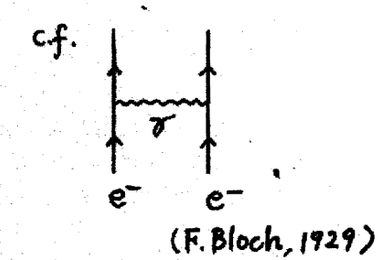

⟶ **Nonperturbative approach beyond the perturbation**

II. Self-consistent apporaoch

Perturbative sol.≡ H.F. sol. in the **non-rela.** theories. $\psi_{\vec{p}} = \chi_s e^{i\vec{p}\cdot\vec{x}}$
⟵ Decoupling of spin and motion.

Total energy E with OGE:

$$E = \sum_{\zeta} \int \frac{d^3k}{(2\pi)^3} \bar{u}(k,\zeta)(\mathbf{k}\,\gamma + m_q)u(k,\zeta)$$
$$- \frac{g^2}{2} \mathrm{tr}(\lambda_s/2\lambda_a/2) \sum_{\zeta,\zeta'} \int \frac{d^3k}{(2\pi)^3} \int \frac{d^3q}{(2\pi)^3} \bar{u}(k,\zeta)\gamma_\mu u(q,\zeta')\bar{u}(q,\zeta')\gamma_\nu u(k,\zeta) \underline{D^{\mu\nu}(k-q)}.$$

$$\frac{g^{\mu\nu}}{(k-q)^2}$$

Chiral invariance:

The Fock exchange interaction is chiral inv. under the transformation:

$$u(q) \longrightarrow \exp(i\gamma_5\theta)u(q).$$

Fierz trans.:

$$\bar{u}(k,\zeta)\gamma_\mu u(q,\zeta')\bar{u}(q,\zeta')\gamma^\mu u(k,\zeta)$$
$$= (1\bullet 1 - \gamma^5 \bullet \gamma^5) - 1/2(\gamma_\mu \bullet \gamma^\mu - \gamma^5\gamma_\mu \bullet \gamma^5\gamma^\mu), \quad \text{(NJL type)}$$

where $\Gamma \bullet \Gamma \equiv \bar{u}(k,\zeta)\Gamma u(k,\zeta)\bar{u}(q,\zeta')\Gamma u(q,\zeta')$.

Hartree-Fock (HF) eq.:

$$(\not{p} - m_q)u(p,\zeta) + \left[U_s(p,\zeta) + U_{ps}(p,\zeta)\gamma^5 + \not{U}_v(p,\zeta) + \gamma_5\not{U}_a(p,\zeta)\right] u(p,\zeta) = 0.$$

$\longrightarrow$ non-local mean fields

$$\underline{(\not{p}^* - m^* + \gamma_5\not{U}_a)u(p,\zeta) = 0,}$$

where $p^* = p + U_v$ and $\underline{m^* = m - U_s}$, assuming that $U_{ps} = 0$. Note that our theory is almost *chiral symmetric, if* $m \ll |U_s|$

$U_s < 0$

IV. Strange quark stars as magnetars

Let's consider a possibility of the strange quark matter, which would be a ground state of matter with low quark density, $n_q \sim n_0 - 3n_0(n_0 = 0.16\mathrm{fm}^{-3})$ (Chin and Kerman, Witten, Farhi and Jaffe).

If a ferromagnetic quark liquid exists stably or metastably, it has some implications on the properties of **strange quark stars and strange quark nuggets**. They should be magnetized in a macroscopic scale.

For strange quark stars:
The dipolar magnetic field at the surface,

$$B_{max} = \frac{8\pi}{3}\left(\frac{r_q}{R}\right)^3 \mu_q n_q,$$

amounts to order of $O($[redacted]$)$G for $n_q = O(0.1)\mathrm{fm}^{-3}$ **enough for magnetars**.

Neutron stars vs Quark stars

A mechanism of SGR has been proposed in the context of strange quark stars. (e.g., K.S. Cheng and Z.G. Dai, P.R.L. 80(1998) 18.)

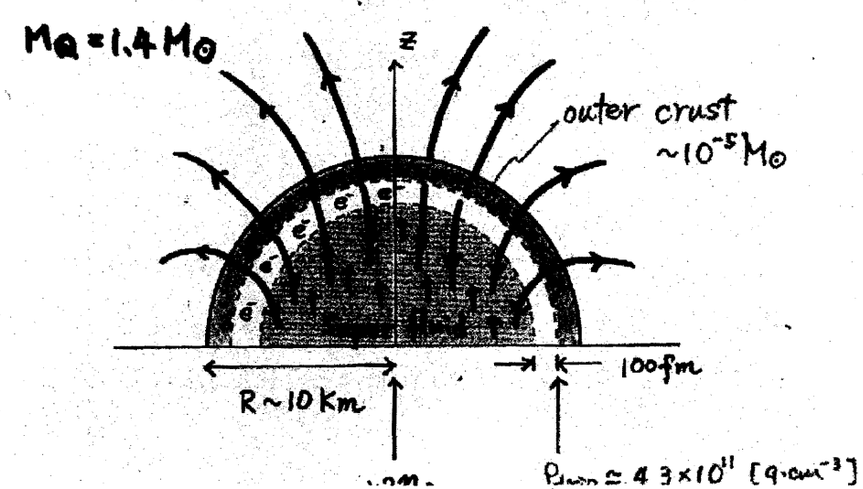

FM solutions:

Single-particle energy

The quark propagator is given by

$$S(p) = \frac{1}{\not{p}^* - m^* + \gamma_5 \not{U}_a^*} \equiv \frac{N}{D}.$$

When $U_a^0 = 0$, the positive energy solutions ($D = 0$) are given by

$$E_p^{\pm} = -U_v^0 + \sqrt{E_p^{*2} + |\mathbf{U}_a|^2 \pm 2\sqrt{(\mathbf{p}^* \cdot \mathbf{U}_a)^2 + m^{*2}|\mathbf{U}_a|^2}},$$

with $E_p^* = (m^{*2} + |\mathbf{p}^*|^2)^{1/2}$.

$$\to -U_v^0 + m^* + \frac{p^{*2}}{2m} \pm |\mathbf{U}_a| \text{ (NR)}$$

- Splitting of the energy for spin-up and -down states
- Anisotropy in dispersion relation $\longrightarrow$ deformation of Fermi sea

$\vec{p}^* \vec{U}_a$ ($\vec{U}_a // \hat{z}$)

rot. symm. breaking

sketch

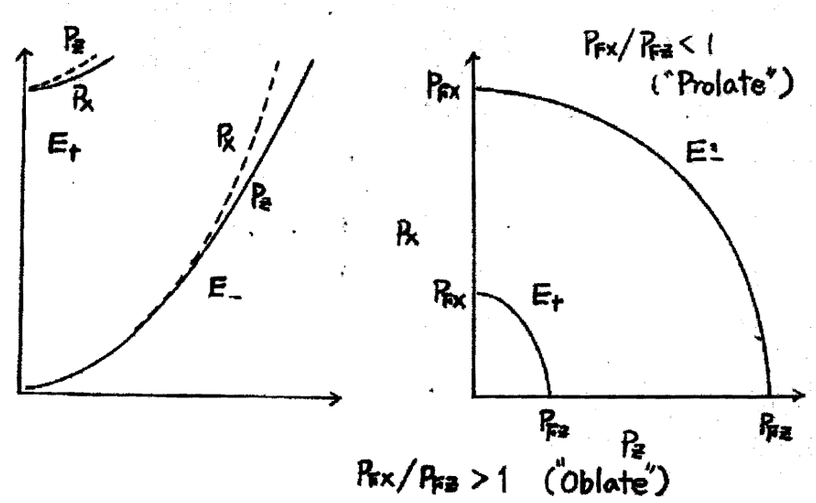

Axial-vector mean field:

$$U_a^\mu(p,\zeta) = \frac{2g^2}{3}\sum_{\zeta'}\int \frac{d^3q}{(2\pi)^3}\bar{u}(q,\zeta')\gamma_5\gamma^\mu u(q,\zeta')D(p-q).$$

$$U_a^i \propto \Sigma^i = \gamma_0\gamma_5\gamma^i \ (\textit{Spin vector}).$$

"Spin polarization $\Longleftrightarrow$ AWC (Axial-vector wave cond.)"

(K. Takahashi and T.T., P.R. C63(2000) 015205.)

Similarity to pion condensation (p-wave BEC)

- Ferromagnetic structure (Spatially uniform) (Bloch)
- Anti-ferromagnetic structure $\longrightarrow$ Spin-density wave (Overhauser)

c.f. M. Kutschera, W. Broniowski, A. Kotlorz, N.P. A516(1990) 566; P. L. B271(1990)159. (Quark-meson coupling model)

Duality

FM	$\Longleftrightarrow$	BEC (p-wave) π, ^{3}He, n
M($\mathbf{U}_a$)	$\Longleftrightarrow$	$\mathbf{A} \propto \nabla\phi$ ($\vec{k}_c$)
Spin wave	$\Longleftrightarrow$	Goldstone boson

Fierz trans. (local limit)

Useful

Second order p.t.

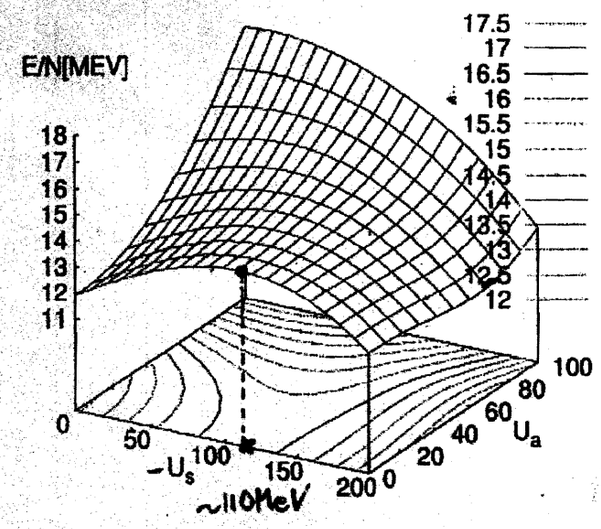

$n = 0.5 fm^{-3}$

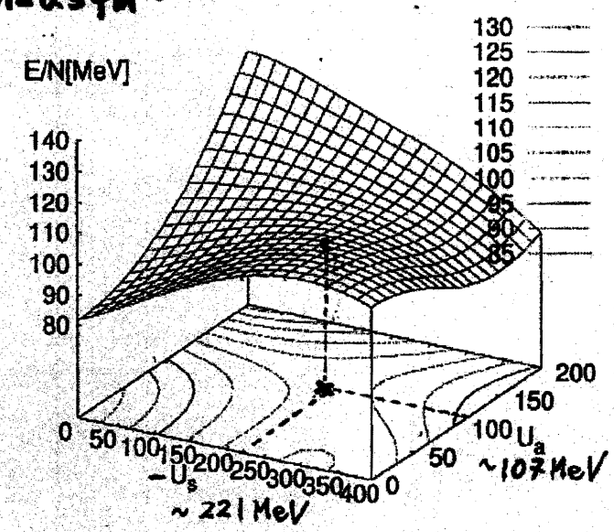

III. Rela. Stoner model

(S. Ushida and T.T.)

If the propagator $D(p-q)$ is replaced by the constant $-1/\Lambda^2$, each mean field becomes local one.

$\longrightarrow$ Eff. coupling strength $= g^2/\Lambda^2$ or α_c/Λ^2[MeV^{-2}]

meaning of Λ:

- Screening mass of gluons$\longrightarrow m_D \sim g\mu$
- NJL approx.$\longrightarrow \Lambda =$const.
- Density dep. of $\Lambda \longrightarrow E_{full}(p=0) = E_{Stoner}(p=0)$
- ...

Then we can easily see that $U_a^0 = U_v^i = U_{ps} = 0$ are self-consistent solutions, and other mean fields are constant. We can put $U_v^0 \equiv U_v$ in this case.

The total energy density is given by

$$\epsilon = 3\int \frac{d^3q}{(2\pi)^3}\left[E_q^-\theta_- + E_q^+\theta_+\right] - \frac{9}{8g^2}U_s^2\Lambda^2 + \frac{9}{4g^2}U_v^2\Lambda^2 + \frac{9}{4g^2}U_a^2\Lambda^2,$$

with $\theta_\pm = \theta(E_F - E_q^\pm)$.

c.f. T. Maruyama & T.T., NP (2001)
(nuclear matter)

Structured Mixed phase of Quark and Hardron matter

Problem of first order phase transitions with *more than one chemical potential*.(N.K. Glendenning, P.R. D46(1992) 1274.)

- Deconfinement phase transition
- BEC of kaons and pions c.f. liquid-gas p.t.

⟶Is mixed phase possible?

Structured mixed phases in neutron stars:

droplets ⟶ *rods* ⟶ *slabs* ⟶ ...

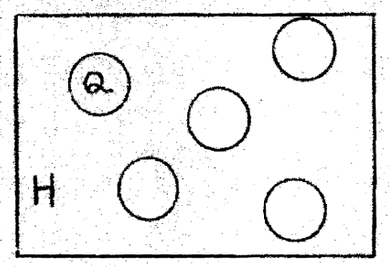

Finite size effects:

- Surface tensition, Curverture effect, ...
- Coulomb energy (breaking of local charge n.)

(M. Christiansen et al., P.R. C62(2000) 025804, T. Norsen and S. Reddy, nucl-th/0010075.)

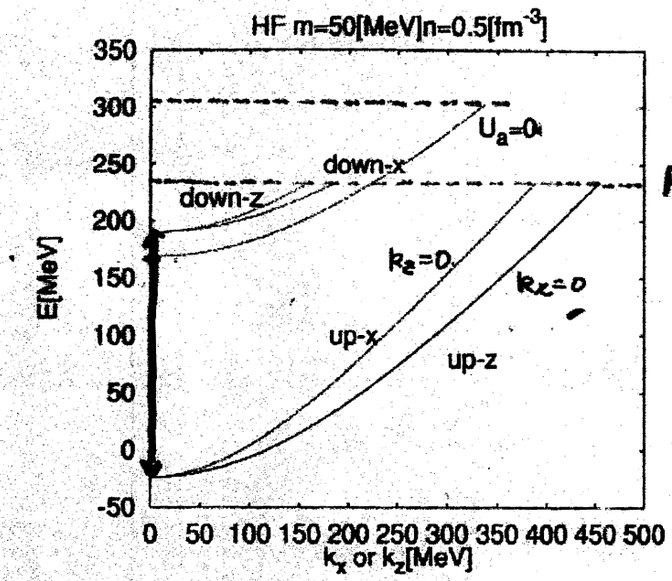

Single-particle energy $E_\pm(\vec{k})$

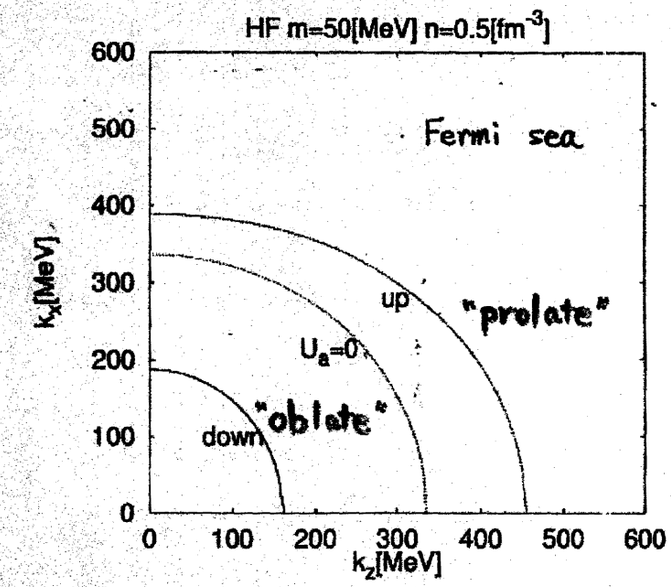

Consider the electric potential V explicitly.

Energy $E = \int d^3x\epsilon$:

$$\epsilon_Q = \epsilon_Q^{bag} + \epsilon_e + \epsilon_V + \epsilon_{Q,V} + \epsilon_{S,Q}$$

$$\epsilon_H = \underset{vol.}{\epsilon_B} + \epsilon_e + \epsilon_V + \epsilon_{B,V} + \epsilon_{S,H}$$

where

$$\epsilon_e + \epsilon_V = \frac{(3\pi^2\rho_e)^{4/3}}{4\pi^2} - \frac{(\nabla V)^2}{8\pi\alpha} + \rho_e V$$

$$\epsilon_{Q,V} = -V\rho_q^Q,$$

TF eqs.:

$$\frac{\delta\Omega}{\delta\rho_i(\mathbf{r})} = 0,$$

where

$$\Omega = E - \mu_q Q - \mu_B B \equiv -PV_W,$$

Note that *TF eqs. automatically ensures the Gibbs conditions.*

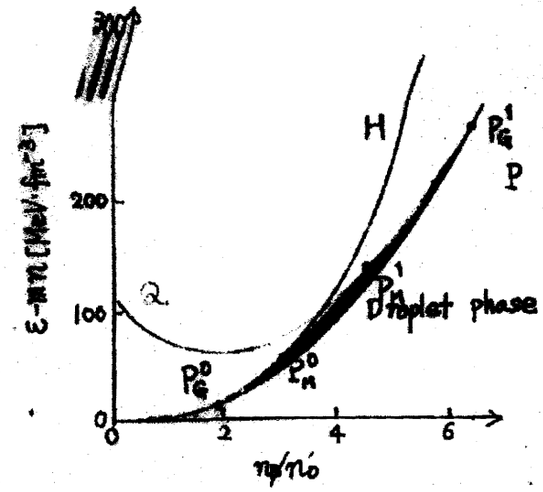

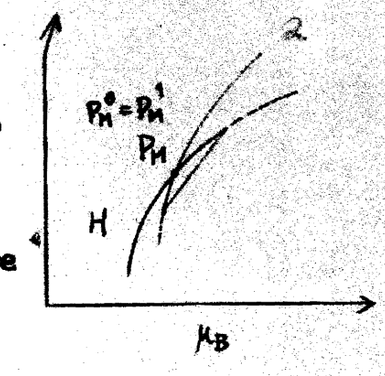

$P^H = P^Q$

$\mu_B^H = \mu_B^Q$

(Maxwell construction)

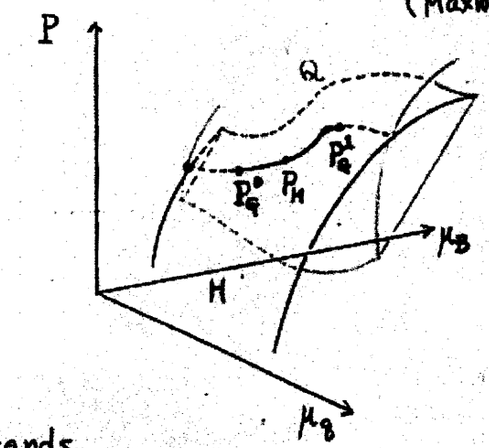

Gibbs conds.

$P^H = P^Q$

$\mu_B^H = \mu_B^Q$

$\mu_q^H = \mu_q^Q$

Global charge neutrality

Consider the electric potential V explicitly.

Energy $E = \int d^3x\epsilon$:

$$\epsilon_Q = \epsilon_Q^{bag} + \epsilon_e + \epsilon_V + \epsilon_{Q,V} + \epsilon_{S,Q}$$

$$\epsilon_H = \epsilon_B + \epsilon_e + \epsilon_V + \epsilon_{B,V} + \epsilon_{S,H}$$

vol.

where

$$\epsilon_e + \epsilon_V = \frac{(3\pi^2\rho_e)^{4/3}}{4\pi^2} - \frac{(\nabla V)^2}{8\pi\alpha} + \rho_e V$$

$$\epsilon_{Q,V} = -V\rho_q^Q,$$

TF eqs.:

$$\frac{\delta\Omega}{\delta\rho_i(\mathbf{r})} = 0,$$

where

$$\Omega = E - \mu_q Q - \mu_B B \equiv -PV_W,$$

Note that *TF eqs. automatically ensures the Gibbs conditions.*

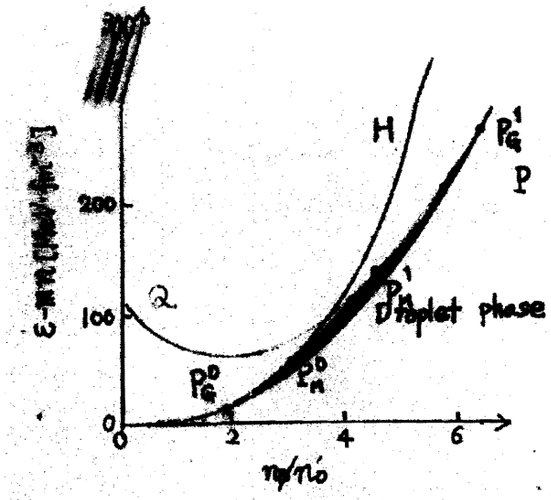

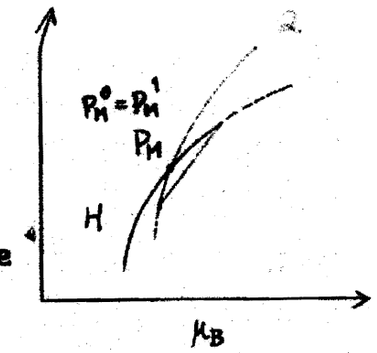

$P^H = P^Q$

$\mu_B^H = \mu_B^Q$

(Maxwell construction)

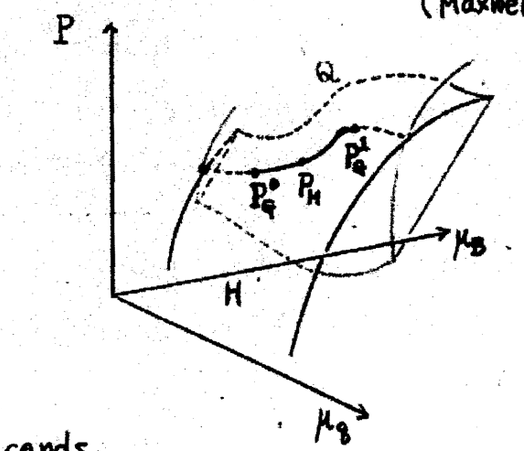

Gibbs conds.

$P^H = P^Q$

$\mu_B^H = \mu_B^Q$

$\mu_q^H = \mu_q^Q$

Global charge neutrality

Finite size effects for Q-H mixed phase

(D.N. Voskresensky, M. Yasuhira and T.T.)

Thomas-Fermi (local density) approx.:
fuctionals w.r.t. $\rho_i(\mathbf{r})$, i=u,d,s,e,p,n.
Wigner-Seitz shell: total volume $V_W = 4\pi/3 \cdot R_W^3$.

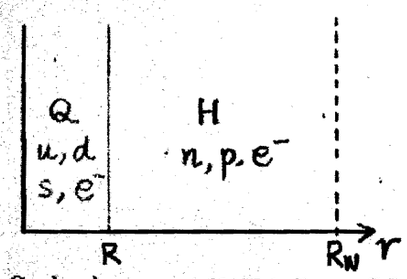

$f = \left(\frac{R}{R_W}\right)^3$

Pure Coulomb case: (H. Heiselberg, C.J. Pethick and E.F. Staubo, P.R.L.70 (1993)1355.)

$$E/V_W = f\epsilon_Q^{bag} + (1-f)\epsilon_B + (E_S + E_C)/V_W,$$

E_S (Surface tensition):

$$E_S/V_W = \sigma 4\pi R^2/V_W = f \times \sigma 4\pi \frac{1}{R},$$

E_C (Coulomb energy):

$$E_C/V_W = \frac{3}{5}\frac{Z^2e^2}{RV_W} = f \times \frac{16\pi^2}{15}(\rho_q^Q - \rho_q^H)^2 R^2.$$

Hence,

$$\frac{\delta(E/V_W)}{\delta R} = 0|_{f:fixed} = 0 \implies \underline{E_S = 2E_C.}$$

However, note that $E/V_W(R = R_D)$ is *not necessarily* lower than E^H/V_W.

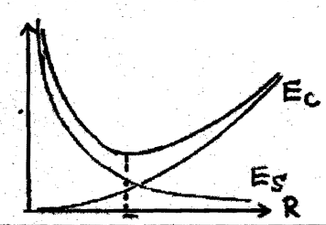

Maxwell eq.:

$$\underline{\Delta V + \kappa_D^2 V = const.,}$$

within the linear response theory.

Debye screening lengths:

$$1/\lambda_D^2 = 4\pi\alpha \sum_i Q_i^2 \frac{\partial \rho_i}{\partial \mu_i} (\equiv \kappa_D^2)$$

Order of estimate;

$$\lambda_D^e \geq O(13\text{fm}), \quad \lambda_D^p \geq O(10\text{fm}), \quad \lambda_D^q \simeq O(5\text{fm}).$$

$$\lambda_D^q \ll \lambda_D^e, \lambda_D^p$$

Boundary conds.:

$$V(0) \leq \infty, V'(R_W) = 0$$

Solution:

$$V = \frac{C_1}{r}\text{sh}(\kappa^Q r) + const., \quad r < R,$$

$$V = \frac{C_2}{r}\exp(-\kappa^H r) + \frac{C_3}{r}\exp(\kappa^H r) + const., \quad r > R$$

Profile:

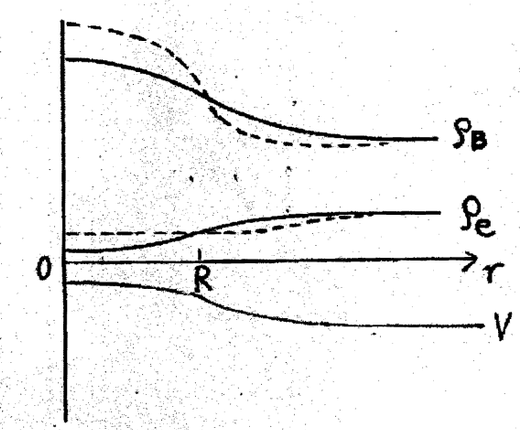

III. Summary and Concluding remarks

- Quark ferromagnetism
  - i) Similarity to pion cond. We call it "duality".
  - ii) Breaking of rotational and chiral symmetry and low-energy excitations in FM. $\longrightarrow$
    Can spin wave be considered as "pions"??
- Some applications
  - i) Modeling magnetars
  - ii) Magnetized quark nuggets in RHIC
  - iii) Origin of the primordial magnetic field after QCD transition in the early universe
- Theoretical interests
  - i) Coexistence problem with color superconductivity
  - ii) Dispersion relation of spin wave

- Finite size effects in H-Q phase transition
  - i) Debye screening effect is essential for Q-H mixed phase
  - ii) Appearance and stability of droplets is very difficult
    $\longrightarrow$ Maxwell construction is OK?
  - iii) There should not be the mixed phase in neutron stars
- Study other systems, e.g. kaon condensation
  $\longrightarrow$ Can finite size effects save the anomalous situation in the chiral model?
- Thermal and neutrino transport processes are much affected, if the mixed phase exists.

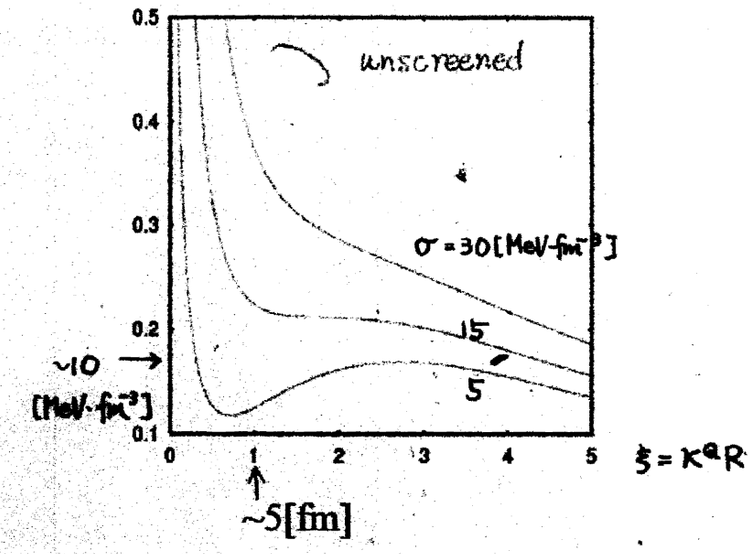

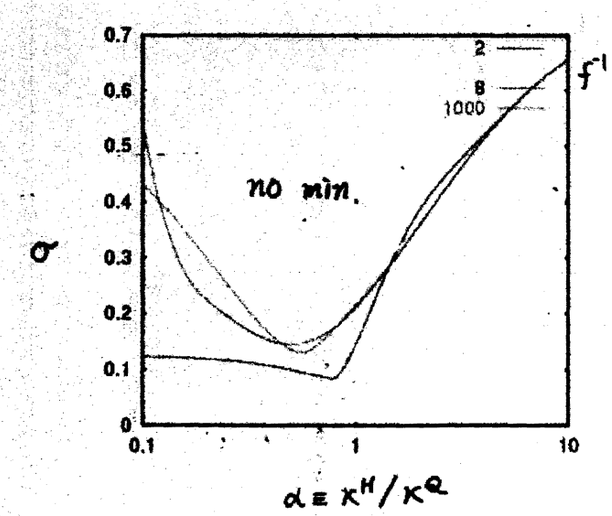

Direct Photons in Pb+Pb Collisions

Terry C. Awes, Oak Ridge National Laboratory
for the *WA98 Collaboration*

The observation of a new phase of strongly interacting matter, the quark-gluon plasma (QGP), is one of the most important goals of current nuclear physics research. An extensive experimental program to search for and investigate the QGP is nearing completion at the AGS at BNL and at the SPS at CERN, with more recent efforts just getting underway at RHIC and in the planning stages at the LHC. Several observations from the program at CERN, such as suppression of the J/ψ resonance, and enhancement of strangeness, hint at interesting new behavior of the matter produced in these collisions.

While many of the observations imply a hot and dense initial phase with strong rescattering, consistent with the assumption that a quark-gluon plasma was formed, a direct signature of the plasma and its properties is missing. Thermal radiation of photons (both real and virtual) was one of the earliest proposed signatures of QGP formation. Unlike hadrons, photons are likely to escape from the hot and dense system immediately after production, without further interaction. Thus, photons carry information about their emission sources from throughout the entire collision history, especially from the initial hot and dense phase. In contrast, hadronic observables provide information about the late stages in the evolution of the system.

Recently, Aurenche et al. have shown that the photon production rates in a QGP are considerably greater than those calculated in earlier lowest order estimates. Following this result, Srivastava has shown that at sufficiently high temperatures the photon yield from quark matter may significantly exceed the contribution from the hadronic phase which might then provide a direct probe of the quark matter phase.

Excess photons (real and virtual) have been observed in 158 A Pb+Pb collisions at the CERN SPS. These measurements are presented and the results are discussed in terms of pQCD and in terms of thermal models which might allow to extract information about the initial temperature and the critical temperature.

Direct Photons in Pb+Pb Collisions

- Motivation
- Direct Photons
  - Analysis Details
  - Systematic Errors
  - Results
- Comparison to pA and Theory
- Dileptons
- Conclusions

Evolution of Relativistic Heavy-ion Collision

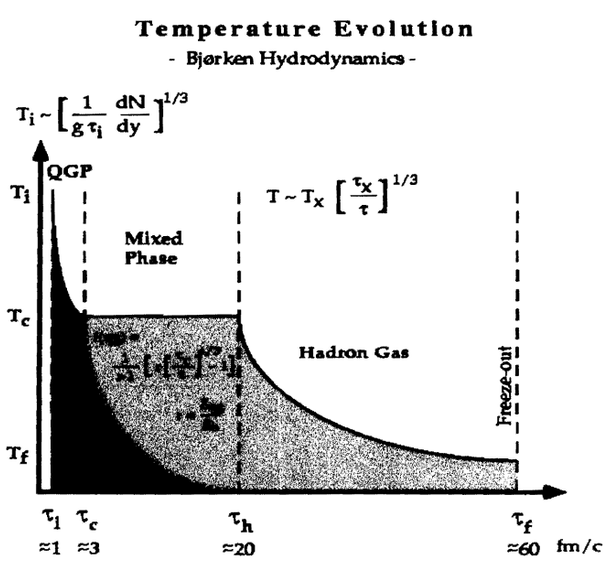

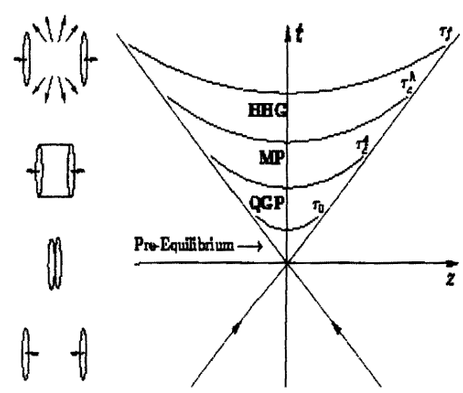

Total single photon production
QGP + Mixed + Hadronic Gas

Searching for QGP Phase Transition with γ's

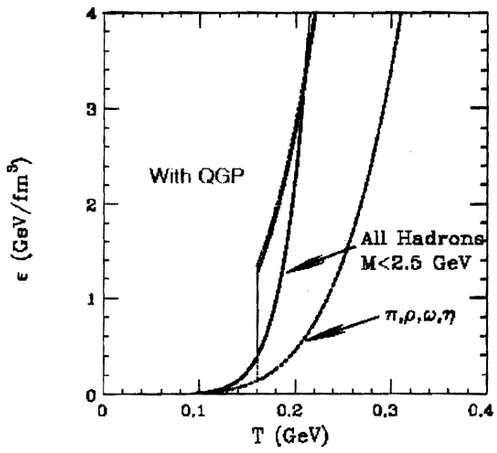

•Cleymans,Redlich, and Srivastava et al., PRC 55 (1997) 1431.

"Classic" method: study heat capacity as a function of temperature to deduce change in degrees of freedom.

» Heat from calorimetry (Transverse Energy)

» Temperature from spectrum of radiation (Photons)

Or, if emission rates are very different, γ yield might directly indicate quark matter.

Quark Matter vs Hadronic Matter Emission Rates

"HM shines as brightly as QM"

»Photons good thermometer

Kapusta et al., PRD 44 (1991) 2774.

But, Aurenche et al. have shown that "new" NLO processes dominate the γ rate in QM.

PRD 58 (1998) 085003.

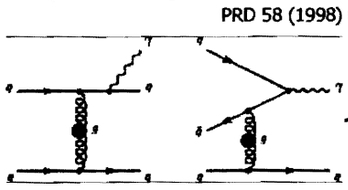

Bremsstrahlung Annihilation with rescattering

F.D.Steffen, PhD thesis, Giessen, nucl-th/9909035

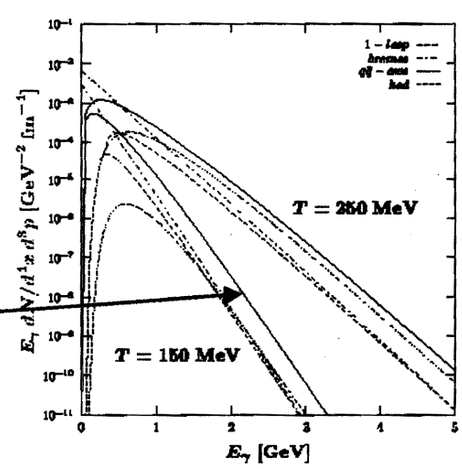

The WA98 Experiment

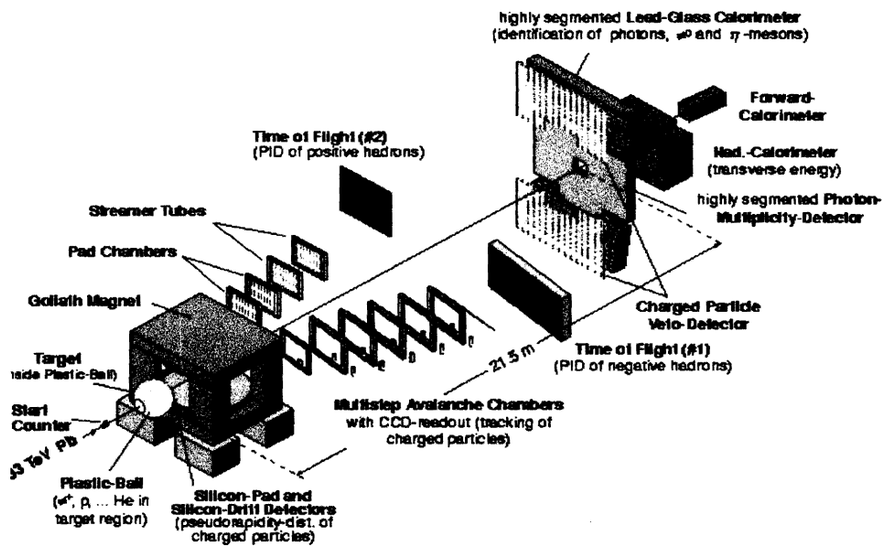

WA98 Acceptance

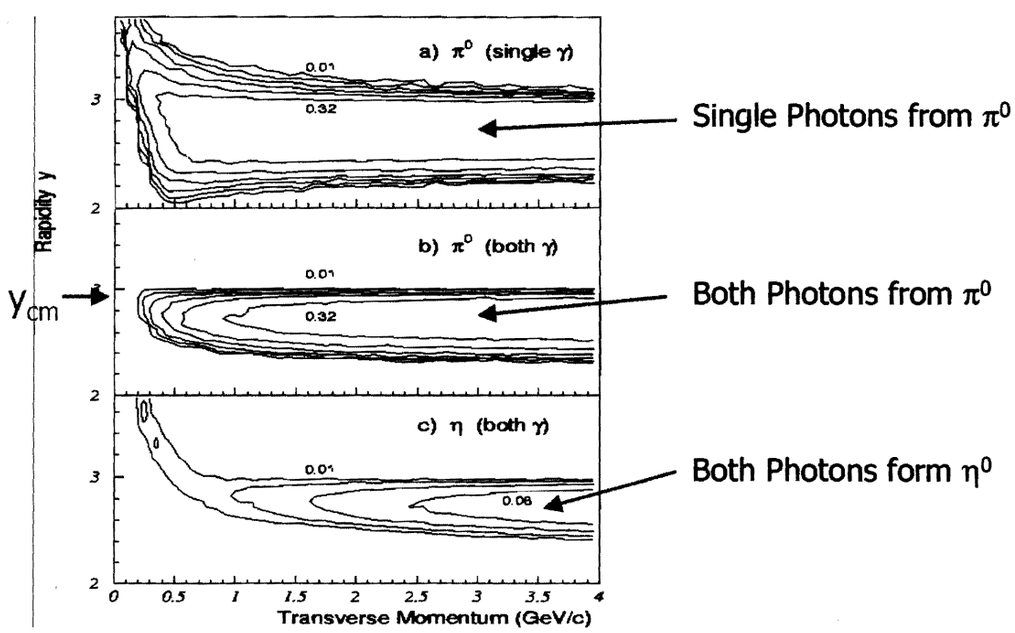

Effect of Shower Overlap on Efficiency

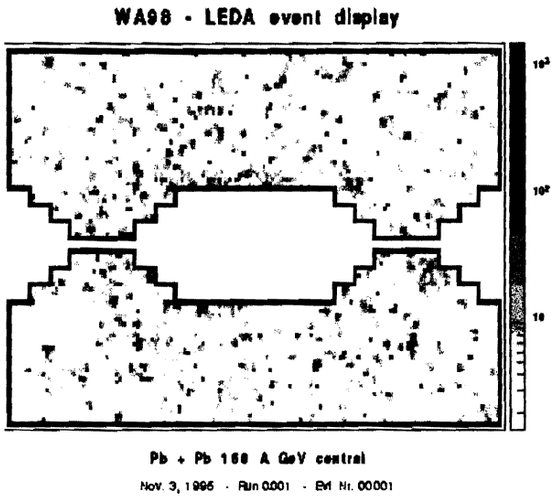

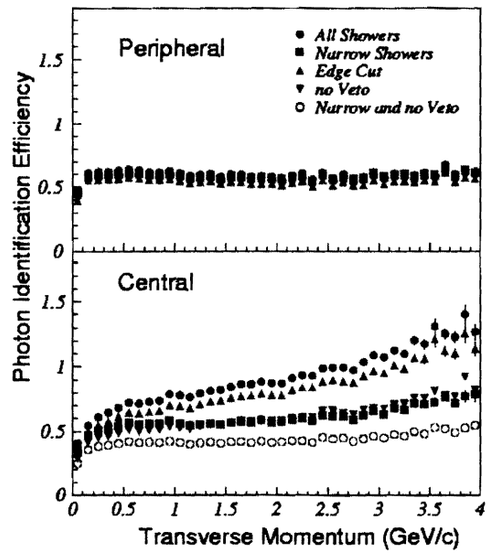

Direct Photon Analysis Overview

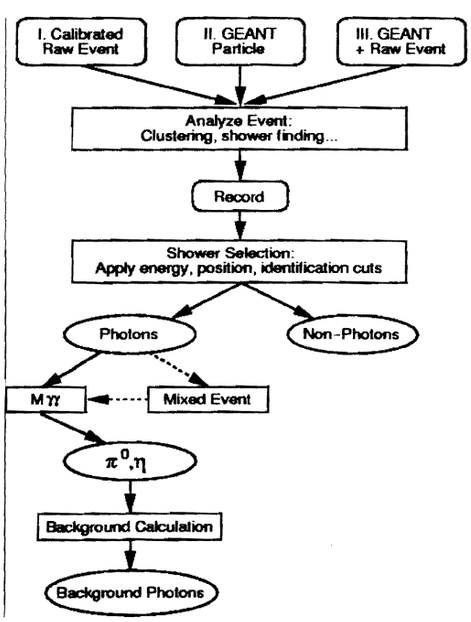

- Statistical Basis: Compare measured γ spectrum to calculated decay γ spectrum.
- Decay γ's calculated from measured π^0's and η^0's
- Use GEANT "test" particles to determine efficiency (overlap effects)
- Vary γ identification criteria to investigate systematical errors.

Event Selection

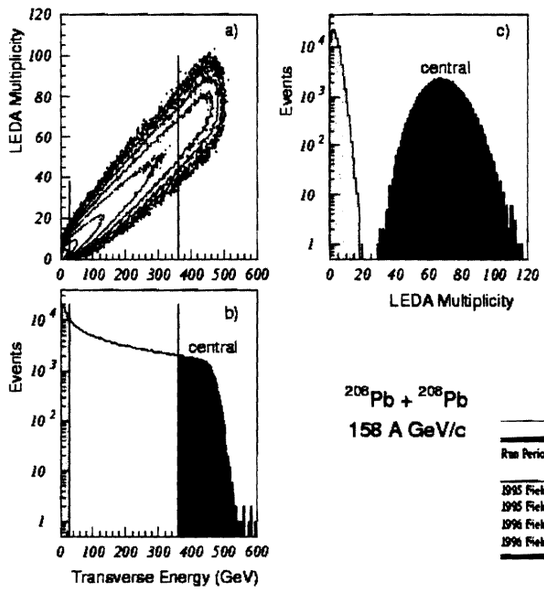

- 10% most central = QGP search sample.
- 20% most peripheral = Reference sample - pQCD prompt photons.

$^{208}Pb + ^{208}Pb$
158 A GeV/c

TABLE I. Summary of the event selection.

Run Period	^{208}Pb Target Thickness (mg/cm^2)	Minimum Bias $\sigma_{minbias}$ (mb)	Peripheral Collisions N_{events}	Central Collisions N_{events}
1995 Field On	495.	6192. (56.)	3694928	2879652
1995 Field Off	495.	5971. (30.)	159291	213170
1996 Field On	239.	6451. (53.)	1203407	2937565
1996 Field Off	239.	6202. (58.)	222917	650571

Charged-Hadron Background

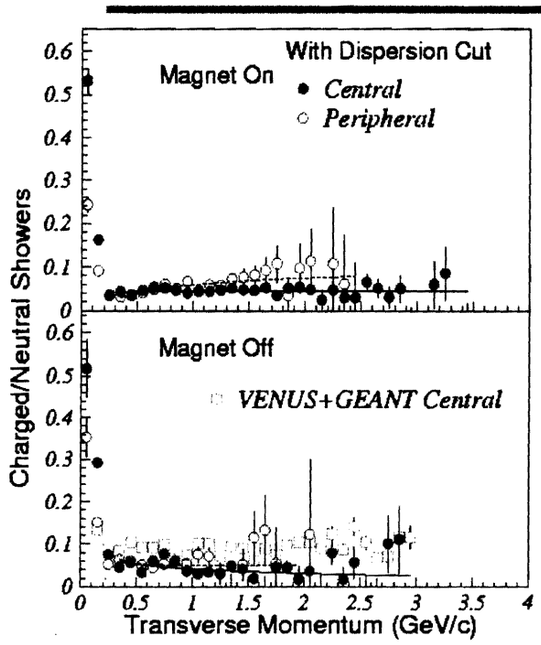

Case:
Narrow Showers = γ Candidates

- Use Charged-Particle Veto to tag charged showers.
- Correct for γ conversions, CPV efficiency, random association.

5% charged-hadron contamination.

Charged-Hadron Background

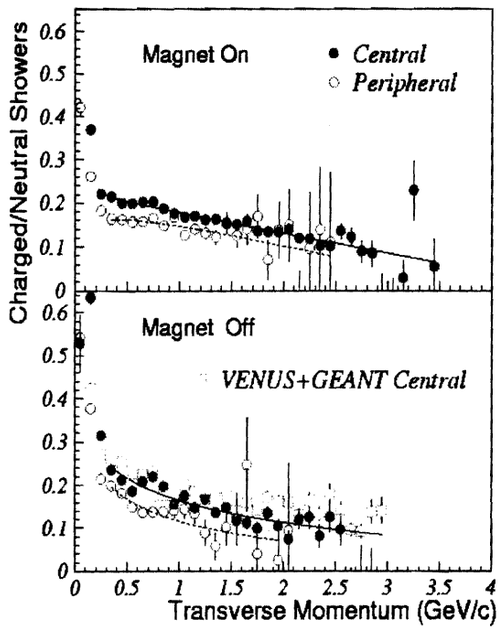

Case:
All Showers = γ Candidates

- Use Charged-Particle Veto to tag charged showers.
- Correct for γ conversions, CPV efficiency, random association.

10-20% charged-hadron contamination.

Neutron + Anti-neutron Background

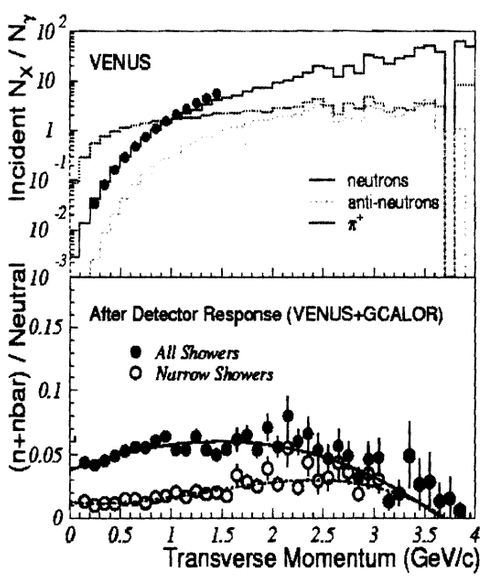

- Calculated correction - Assumes VENUS+GEANT (Check $(n/\gamma)_{VENUS}$ vs. p_{NA49}/γ_{WA98})
- Incident flux is large!
- Large reduction due to detector response (small energy deposit)
- Further reduction by γ-like shower requirement.

1-6% Contamination correction

Final γ p_T Spectra

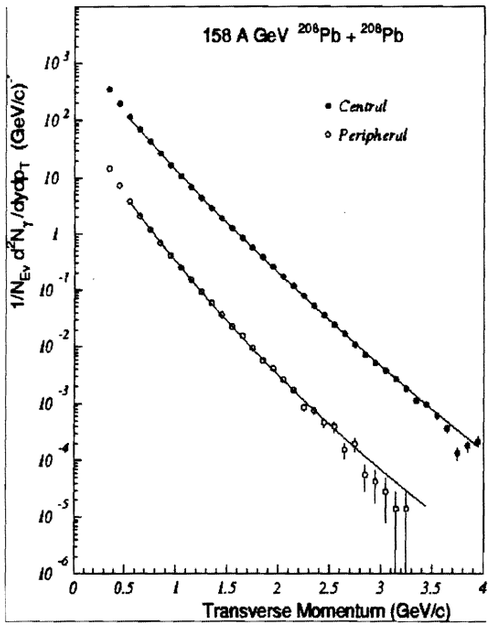

Corrected for charged and neutral background, efficiency, and acceptance.

Fit to power-law form:

$$\left(\frac{p_0}{p_0 + p_T}\right)^n$$

Inverse slope:

$$T = p_0/n + p_T/n$$

$$T_{Central} = 198 + p_T/37 \text{ MeV}$$

$$T_{Peripheral} = 147 + p_T/22 \text{ MeV}$$

Systematical Error on γ Yield

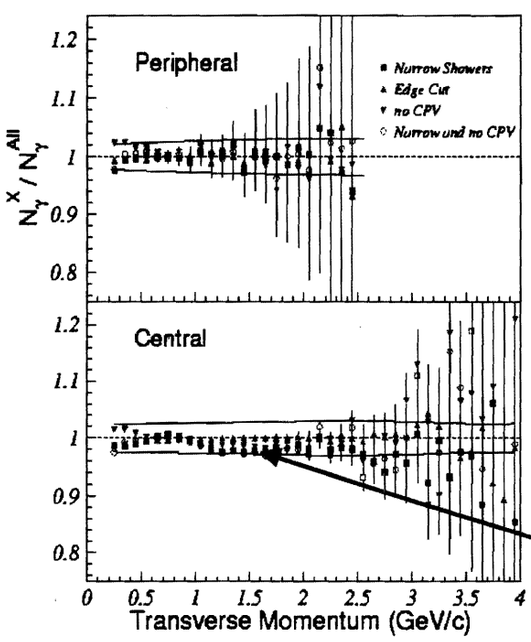

- Check consistency of final result with different γ identification criteria.
- Sensitivity to charged-hadron and neutron backgrounds vary by factors of 2-4.
- Identification efficiency varies by 2-3 for different methods for central case.

Systematical error on γ yield ~3%

Decay Background γ Sources

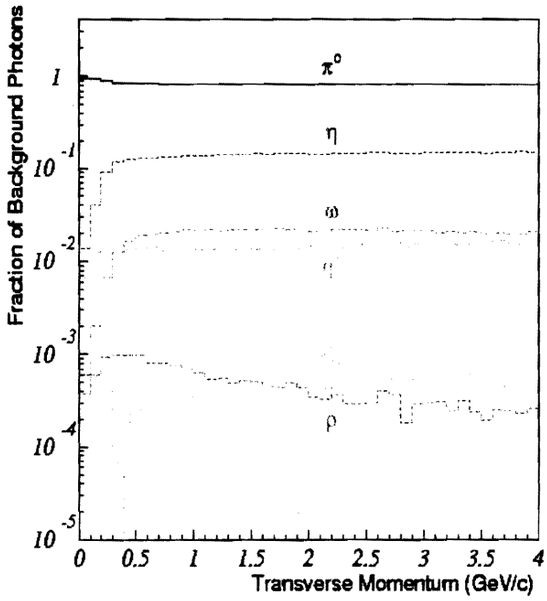

- Direct γ's extracted from difference between measured γ's and calculated decay γ's.
- ~97% decay γ's from measured π^0 and η^0.
- Assume m_T-scaling for η^0 and others.

TABLE I. Dominant radiative decays which contribute to the inclusive photon background.

State	Mass	R_{X/π^0} (p_{T} → ∞)	$\sigma(X)/\sigma(\pi^0)$	Decay Branch	Branching Ratio
π^0	134.98			$\gamma\gamma$	98.798%
				$e^+e^-\gamma$	1.198%
η	547.3	0.55 (0.43%)	0.08	$\gamma\gamma$	39.21%
				$\pi^0\pi^-\gamma$	4.77%
				$e^+e^-\gamma$	$4.9\cdot10^{-3}$
				$\pi^0\gamma\gamma$	$7.1\cdot10^{-4}$
				$\pi^0e^+e^-\gamma$	$3.1\cdot10^{-4}$
ρ^0	770.0	1.0	0.05	$\pi^0\pi^-\gamma$	$9.9\cdot10^{-1}$
				$\pi^0\gamma$	$7.9\cdot10^{-4}$
ω	781.9	1.0	0.05	$\pi^0\gamma$	8.5%
				$\eta\gamma$	$6.5\cdot10^{-4}$
η'	957.8	1.0	0.02	$\rho\gamma$	30.2%
				$\omega\gamma$	3.01%
				$\gamma\gamma$	2.11%
K_S^0	497.7	0.4	0.07	($\pi^0\pi^0$)	(31.39%)
Σ^0	1192.6	1.0	0.007	$\Lambda\gamma$	100.%

Extraction of π^0 Yield

Combinatorial γγ Background Problem: Use mixed γγ events to determine shape of background.

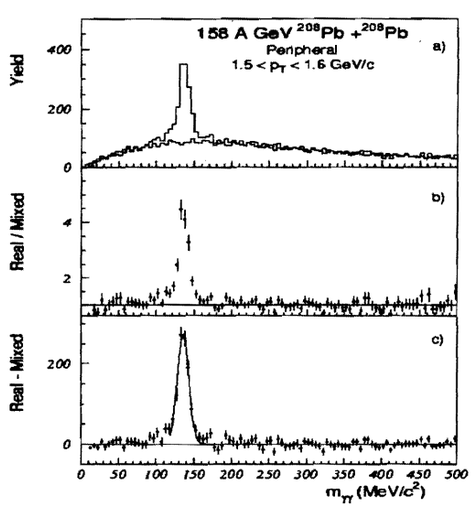

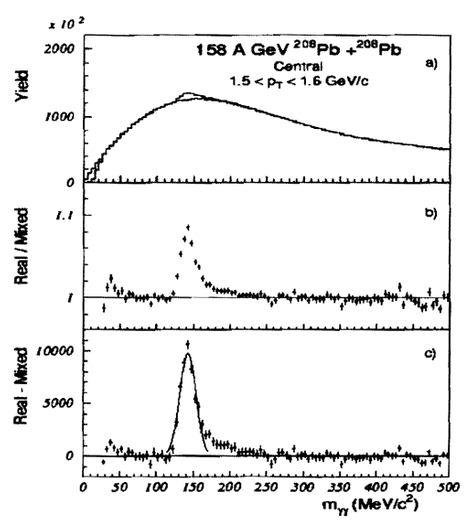

Shower Overlap Effects Again: π^0

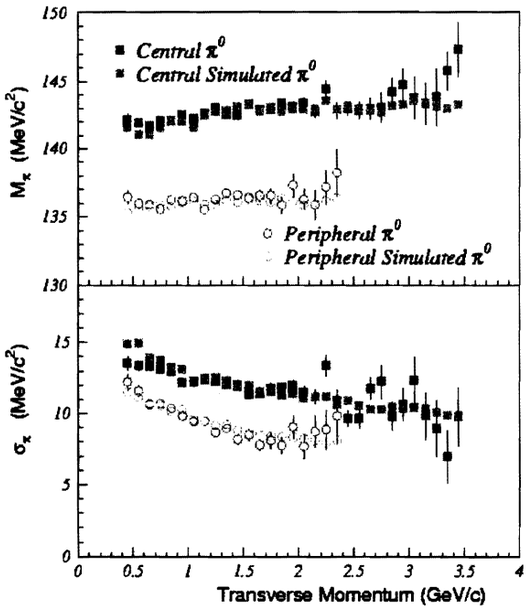

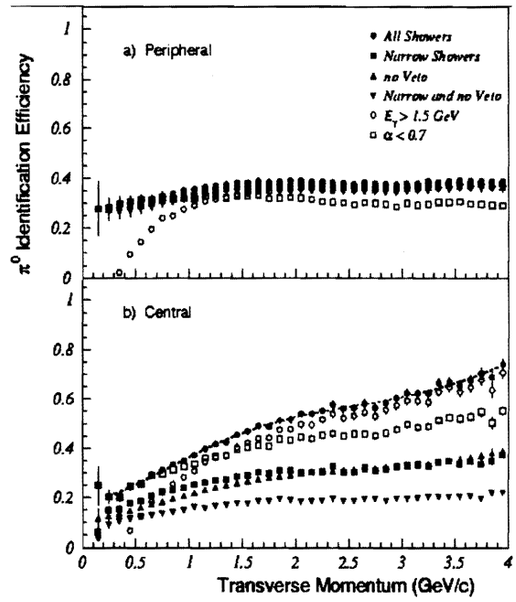

Final π^0 p_T Spectra

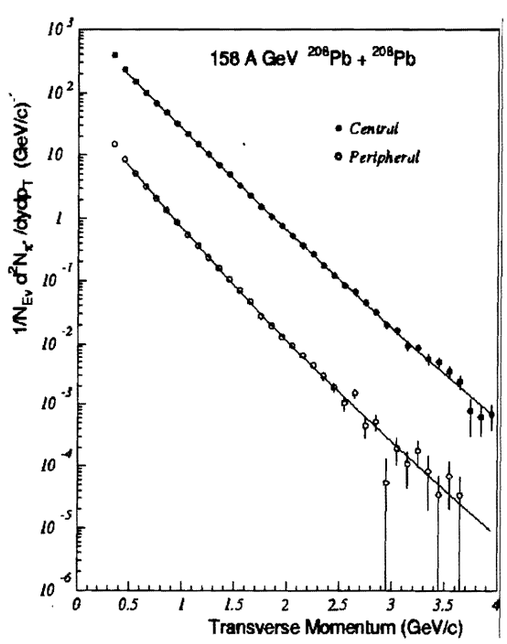

Corrected for efficiency, and acceptance.

Fit to power-law form:

$$\left(\frac{p_0}{p_0 + p_T}\right)^n$$

Inverse slope:

$T = p_0/n + p_T/n$

$T_{Central} = .250 + p_T/80$ GeV

$T_{Peripheral} = .216 + p_T/45$ GeV

Systematical Error on π^0 Yield

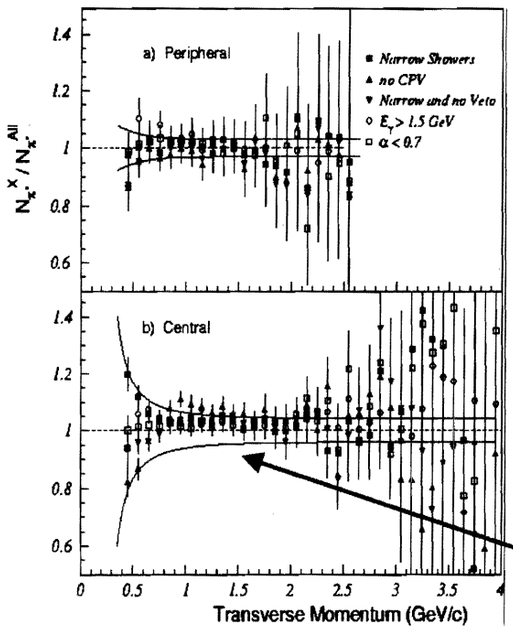

- Check consistency of final result with different γ identification criteria.
- Combinatorial background varies by factor of ~2
- Identification efficiency varies by 2-3 for different methods for central case.

Systematic error on π^0 yield ~3-6%

Extraction of η^0 Yield

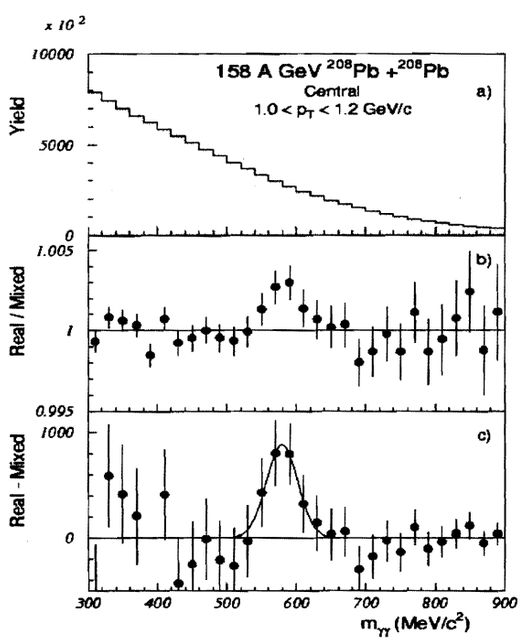

- HUGE $\gamma\gamma$ combinatorial background.
- At limit of statistics for central, no signal for peripheral.
- Goal: check m_T-scaling assumption for central.

m_T-scaling and η^0/π^0 Ratio

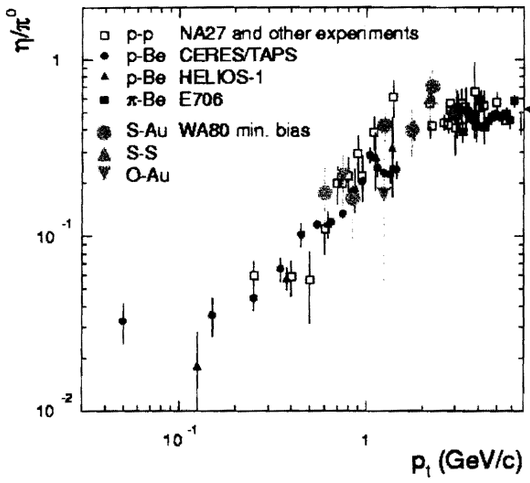

Compilation:

$\eta^0/\pi^0(p_T \rightarrow \infty) = 0.55 \pm 0.02$

WA98 mT-scaling of η^0/π^0 :

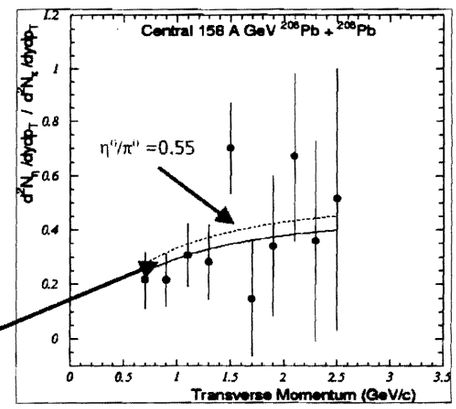

WA98 Central:

$\eta^0/\pi^0(p_T \rightarrow \infty) = 0.49 \pm 0.08 \pm 0.1$

Direct γ search: Peripheral Pb+Pb

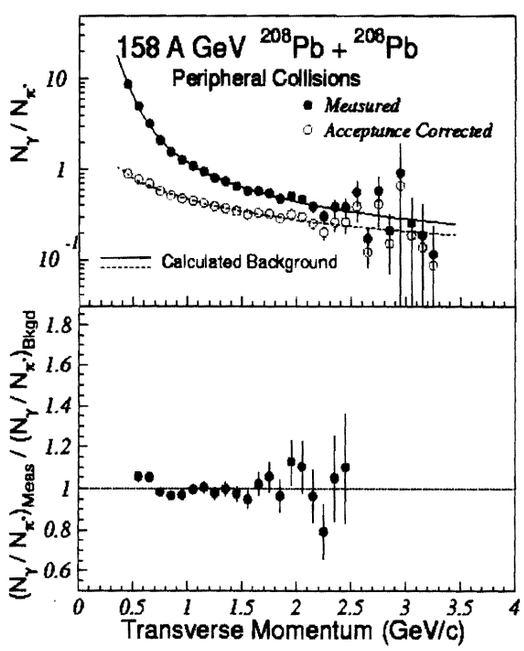

- First, consider γ/π^0 ratio and compare to calculated decay background γ/π^0 ratio.
  (many errors cancel)
- N_γ and N_π measured at each p_T for "all showers" condition
  (largest corrections - errors)

No significant γ excess within statistical errors (low p_T though)

Direct γ search: Central Pb+Pb

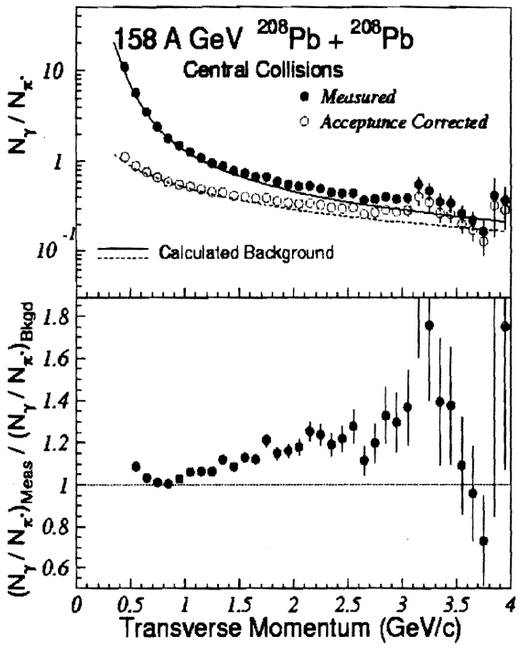

- First, consider γ/π^0 ratio and compare to calculated decay background γ/π^0 ratio.
  (many errors cancel)
- N_γ and N_π measured at each p_T for "all showers" condition
  (largest corrections - errors)

Clear γ excess beyond statistical errors - must consider systematic errors.

Comparison of γ Excess to Errors

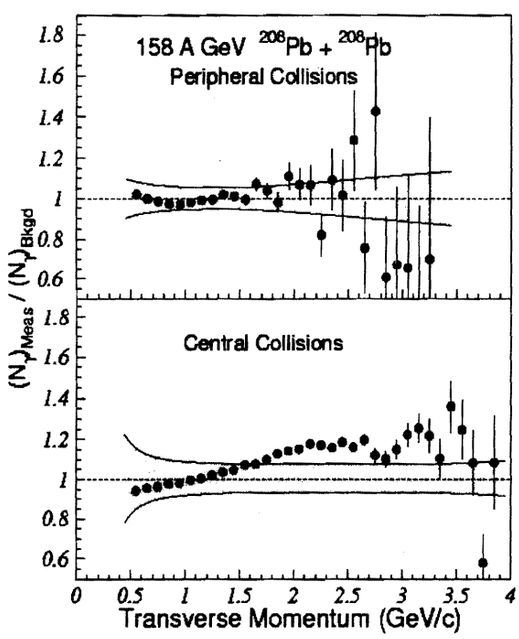

- Compare measured γ yield to calculated background γ.
- Total errors include those of $(\gamma/\pi^0)_{Meas}$ $(\gamma/\pi^0)_{Bkgd}$ and the π^0 fit uncertainty.

Significant excess γ beyond $\sigma_{stat} + \sigma_{syst}$ for central collisions at high p_T.

Direct γ Systematical Error Summary

TABLE I. Various sources of systematical error in the WA98 Pb direct photon analysis.

Source of Error	Peripheral Collisions (20% σ_{min}) $p_{T\gamma}$ at 1.0 GeV/c	Peripheral Collisions (20% σ_{min}) $p_{T\gamma}$ at 2.5 GeV/c	Central Collisions (10% σ_{min}) $p_{T\gamma}$ at 1.0 GeV/c	Central Collisions (10% σ_{min}) $p_{T\gamma}$ at 2.5 GeV/c
Charged Particle background[+]	1.7	2.2	1.3	1.3
γ conversion correction[+]	0.5	0.5	0.5	0.5
Neutrons[+]	0.6	1.0	0.9	1.9
γ reconstruction efficiency[+]	2.0	2.0	2.0	2.0
a) γ yield measurement	2.7	3.2	2.6	3.1
γ conversion correction[*]	0.5	0.5	0.5	0.5
π^0 yield extraction[*]	0.3	<0.1	5.1	1.0
π^0 reconstruction efficiency[*]	3.0	3.0	4.0	4.0
a) π^0 yield measurement	3.1	3.0	6.5	4.2
a) Non-target background	1.5	<0.1	<0.1	<0.1
a) Energy scale calibration	0.9	1.7	0.8	1.7
b) Detector acceptance	0.5	0.5	0.5	0.5
b) η/π ratio, $m_{T\eta}$-scaling	2.9	3.2	+3.4 (-4.8)	+3.7 (-5.2)
b) Other radiative decays	1.0	1.0	1.0	1.0
c) π^0 fit	1.6	6.8	2.9	0.4
Total: (quadratic sum)	5.7	8.9	+8.3 (-9.1)	+6.7 (-7.6)

[+] Included in γ yield measurement error. [*] Included in π^0 yield measurement error.

Central Pb+Pb Direct γ p_T Spectrum

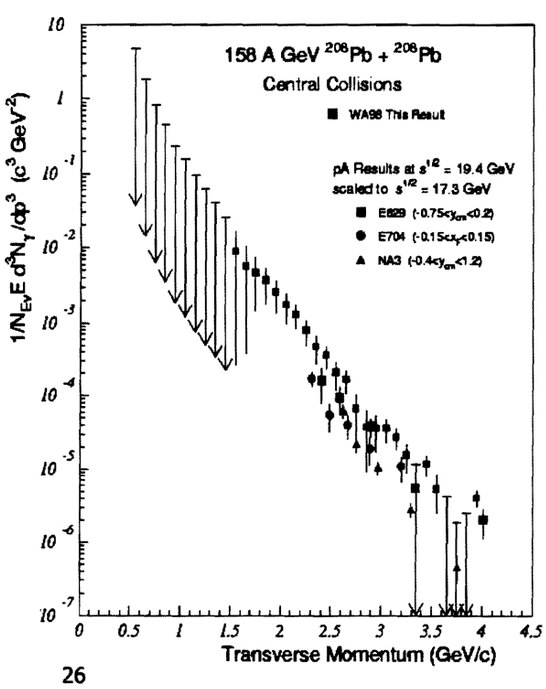

- Compare to proton-induced prompt γ results:
  - » Assume hard process - scale with the number of binary collisions (=660 for central).
  - » Assume invariant yield has form $f(x_T)/s^2$ where $x_T=2p_T/s^{1/2}$ for $s^{1/2}$-scaling.
- Factor ~2 variation in p-induced results.

Similar γ spectral shape for Pb case, but factor ~2-3 enhanced yield.

WA98 nucl-ex/0006007, PRL 85 (2000) 3595.

Direct γ: Comparison to pQCD Calculation

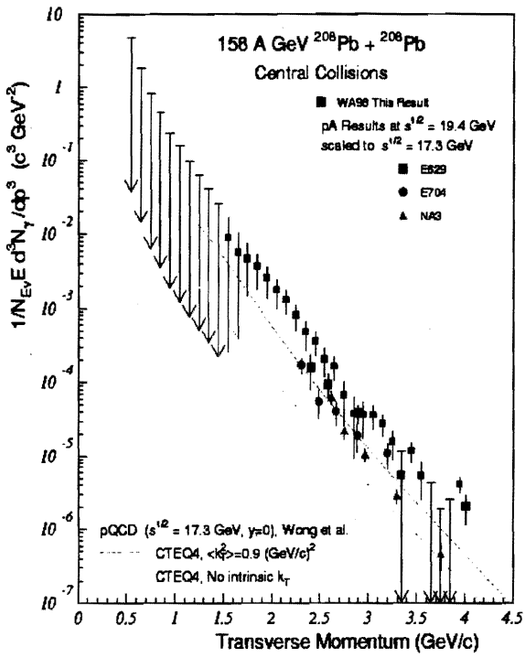

- NLO pQCD calculations factor of 2-5 below $s^{1/2}$ =19.4 GeV p-induced prompt γ results.
- But p-induced can be reproduced by effective NLO (K-factor introduced) if intrinsic k_T is included.
- Same calculation at $s^{1/2}$=17.3 GeV reproduces p-induced result scaled to $s^{1/2}$ =17.3 GeV

  Similar γ spectrum shape for Pb case, but factor ~2-3 enhanced yield.

Direct γ: Comparison to Model Calculations

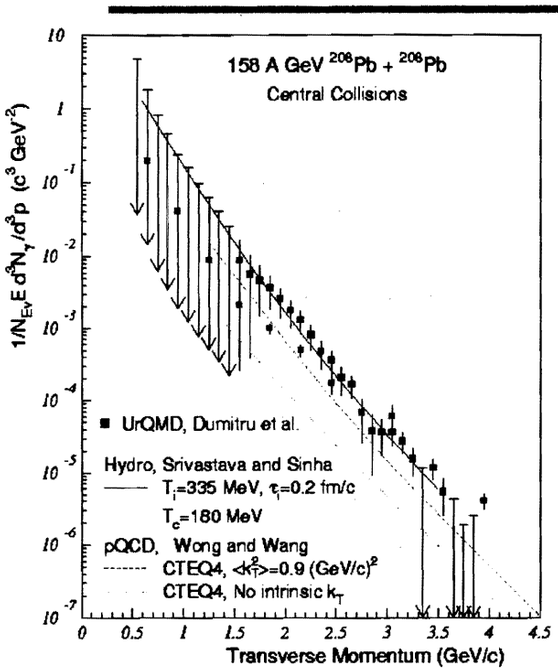

- Good agreement with Hydro calculation including QGP.
  - » Annihilation with rescattering process in QM dominates at high p_T
  - » High Temperature: T_i = 335 MeV (from $\tau_i T_i$ = 1/3 = 0.2fm/c)
  - » Short formation time equivalent to inclusion of prompt and preequilibrium contributions?
- URQMD predicts large preequilibrium component at high pT

WA98 nucl-ex/0006007

Hydro Prediction for hadron spectra

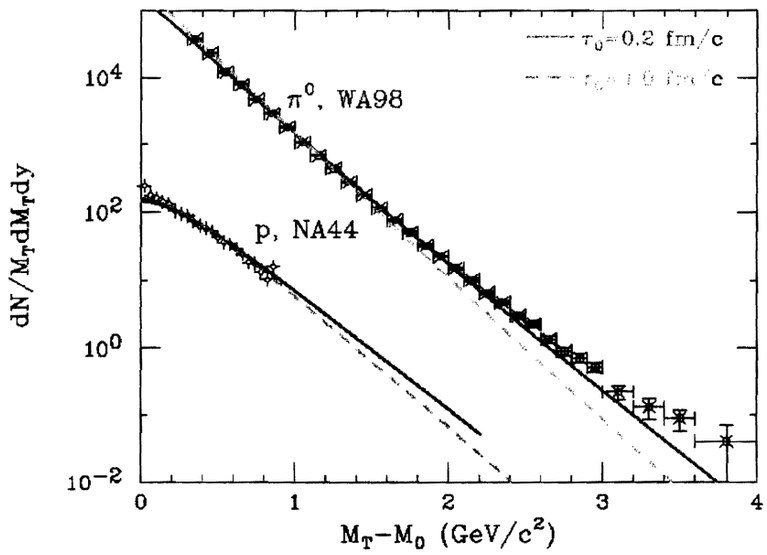

NA50 Intermediate Mass $\mu^+\mu^-$ Excess

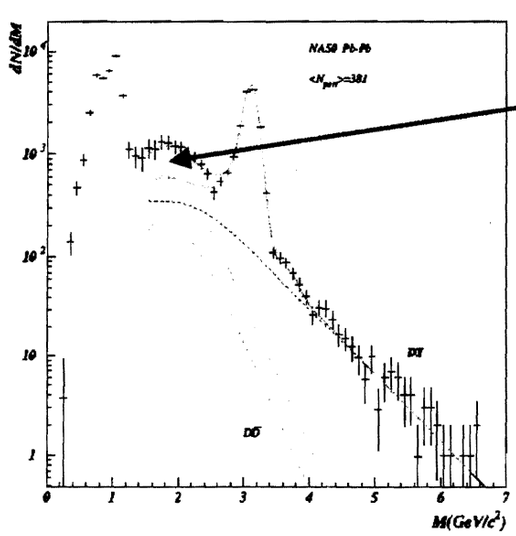

NA50 observes excess $\mu^+\mu^-$ pairs in intermediate mass region between ϕ and J/ψ

Has same shape as open charm contribution.

Could it have a thermal origin?

Thermal Intermediate Mass $\mu^+\mu^-$ Excess?

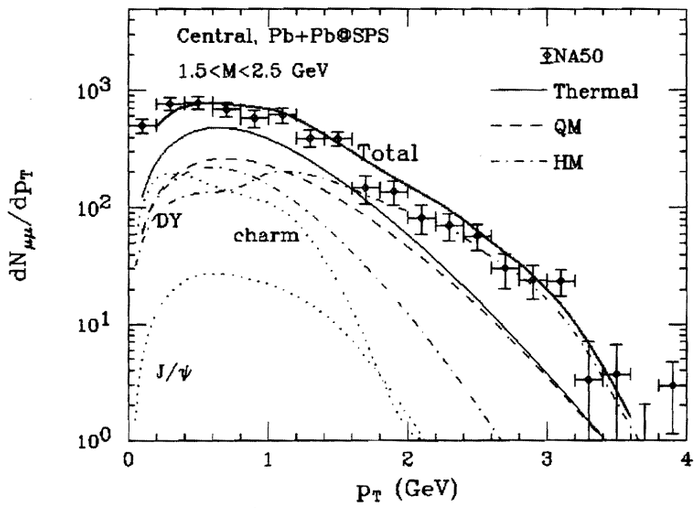

Same hydrodynamic model calculation can explain excess $\mu^+\mu^-$ pairs in intermediate mass region and γ excess.

Srivastava and Gale

Centrality dependence of the NA50 $\mu^+\mu^-$ enhancement

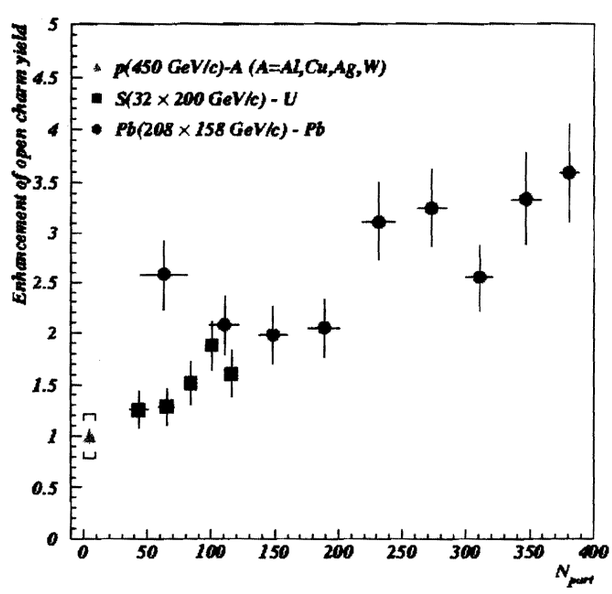

Summary

- Significant direct photon excess observed in Central Pb+Pb collisions for $p_T \geq 1.5$ GeV/c.
- Excess is ~2-3 times greater than the prompt photon production expected from scaled p-induced measurements, or from pQCD calculations.
- In a hydrodynamical model the observed excess can be explained as result of thermal radiation from the quark matter at an initial temperature $T_i = 335$ MeV with T_c=180 MeV, implied by a short thermalization time $\tau_0 = 0.2$ fm/c.
- The NA50 intermediate mass $\mu^+\mu^-$ excess has also been suggested to have a thermal origin, but dominantly from hadronic matter with much lower $T_i = 192$ MeV.
- Important to investigate consistency of the interpretations and additional k_T or pre-equilibrium contributions.

Look forward to early γ, π^0 results from PHENIX!

Photon and Dilepton Emission Rates from Ultra-Relativistic Heavy Ion Collisions

Jan-e Alam
Physics Department, University of Tokyo, Tokyo 113-0033, Japan

Abstract

The production of (both real and virtual) photons from matter created in nuclear collisions at CERN SPS energies will be discussed for the following two scenarios:

(i) Nucleus + Nucleus →Hadronic Phase,
and
(ii) Nucleus +Nucleus →QGP→Mixed Phase→Hadronic Phase,

by taking into account the in-medium effects on the hadronic properties. It is observed that the photon spectra measured by the WA98 collaboration is well reproduced by (i), if a substantial reduction of hadronic masses is considered in the thermal bath. The data is also well described by (ii), it is rather difficult to distinguish between (i) and (ii) at present. The initial temperature of the thermal bath is found to be $\sim$ 200 MeV. The enhancement of dilepton yield in Pb + Au collisions at low invariant mass region measured by CERES collaboration can also be described with a similar value of initial temperature.

Collaborators:

T. Hatsuda, T. K. Nayak, S. Sarkar and B. Sinha

CNS WORKSHOP
TOKYO, Feb. 14-16, '01

Photon and Dilepton Emission Rates from Ultra-Relativistic Heavy Ion Collisions

Jan-e Alam
(Physics Department, University of Tokyo)

- **Introduction**
- **Emission of Electromagnetic Probes**
- **Medium Effects**
- **Space Time Evolution**
- **Results and Discussions**

•Sources:
- Annals of Physics, **286** (2000) 159-248;
- Physical Review C, **63** (2001) 021901(R);
- nucl-th/0011032

• **Prompt Photons**

$$E\frac{d\sigma}{d^3p}(A+B \to \gamma + ...) = \int \frac{dx_a}{x_a}\frac{dx_b}{x_b} F_{a/A}(x_a) F_{b/B}(x_b)\, E\frac{d\hat{\sigma}}{d^3p}$$

$$E\frac{dN}{d^3p} = T_{AA}\, E\frac{d\sigma_{pp}}{d^3p}$$

* T_{AA} = Average Number Nucleon- Nucleon Collisions/ σ_{in}

(WA98 Collaboration, Phys. Rev. Lett. 85 (2000) 3595)

* For intrinsic k_T of partons: $f(k_T) = \exp[-k_T^2/\langle k_T^2\rangle]/\pi\langle k_T^2\rangle$; $\langle k_T^2\rangle = 0.9$ GeV^2

(Ferbel & Molzon 1984; Owens 1987; Wong & Wang 1998.)

Scaling:

Dimensionality - GeV^{-4} ⇒ supplied by Mandelstam variables (quark mass =0 and strong and EM couplings are dimensionless.)

In general the invariant cross section can be expressed as a function of $\underline{s}$ (or $\underline{p_T}$), $\underline{\theta}$ and $\underline{x_T}(= 2p_T/\sqrt{s})$

If two of the dimensionless variables held constant then the dimensionality arguments leads to:

$$E\frac{d\sigma_{pp}}{d^3p} = \frac{F(x_T,\theta)}{s^2}$$

This scaling can be spoiled by the momentum dependence of α_s and from the scaling violation of structure functions

* Hard QCD photons ⇒ normalize the scaled p-p data (E704).

• Ultra-Relativistic Heavy Ion Collisions:

• (i) A + A→ Hadronic Matter

• (ii) A + A→ [Hadronic Matter]*

• (iii) A + A→ QGP→ Mix. Phase ↔ Hadronic Matter*

- Electromagnetic γ, l^+l^-
  - * large mean free path
  - * negligible final state interactions
  - * emitted at all stages.

• Sources of real PHOTONS:

- Decay photons $\pi^0 \to \gamma\gamma$, $\eta \to \gamma\gamma$
- <u>Prompt photons</u> $(A + B \to \gamma + X)$
- Thermal Photons
  - * <u>from quark matter</u>
  - * <u>from hadronic matter</u>

• Sources of DILEPTONS (virtual photons):

- <u>Dalitz</u> (e.g. $\pi^0 \to \gamma e^+e^-$).
- Drell-Yan $(A + B \to l^+l^- + X)$; D meson decays
- Thermal Dileptons
  - * <u>from quark matter</u>
  - * <u>from hadronic matter</u>

• **From QGP** (QCD Compton, Annihilation, Bremsstrahlung & $q\bar{q}$ annihilation with scattering):

(Kapusta et al, 1991; Baier et al 1992; Aurenche et al 1998.)

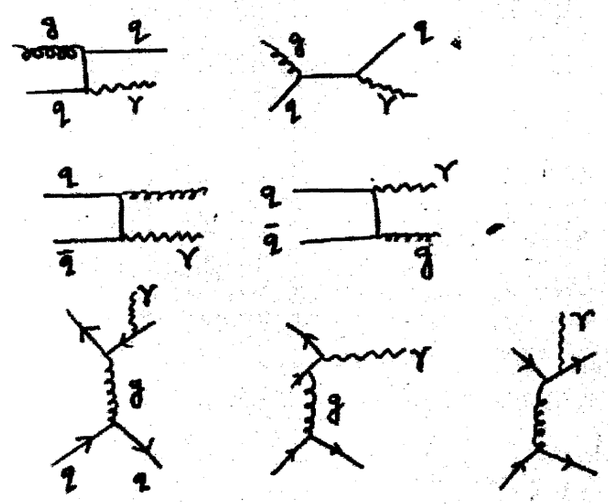

$$E\frac{dR}{d^3p} = \frac{5}{9}\frac{\alpha\alpha_s}{2\pi^2}\exp(-E/T)\left[\ln\left(\frac{2.912\,E}{g^2T}\right) + 16\frac{(J_T - J_L)}{\pi^3}\{\ln 2 + \frac{E}{3T}\}\right]$$

where $J_T \simeq 4.45$, $J_L \simeq -4.26$ and

$$\alpha_s = \frac{6\pi}{(33-2n_f)\ln(\kappa T/T_c)} \quad ; \kappa = 8$$ (Karsch, 1988)

$\alpha_s(T = 200MeV) \sim 0.3 \Rightarrow g^2 \sim 4$

$\underline{g << 1 \Rightarrow \alpha_s << 0.08}$

Thermal Dilepton/Photon Emission Rates:

(McLerran & Toimela 1985; Gale & Kapusta 1991.)

$$\frac{dR}{d^4q} = -\frac{\alpha}{12\pi^3}q^2\left(1+2m^2/q^2\right)\sqrt{1-4m^2/q^2}\,(\rho_T+\rho_L)\,f_{BE}(q_0)$$

$$\rho_{T,L} \equiv -\frac{1}{\pi}\frac{Im\Pi^R_{T,L}}{(q^2+Re\Pi^R_{T,L})^2+(Im\Pi^R_{T,L})^2}$$

Plasma resonances ⇒ Signal of deconfinement.

(Weldon, 1991.)

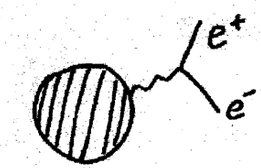

Medium Effects

- **Quantum Hadrodynamics(QHD)**

The effective mass of ρ/ω can be parametrized as:

$$m_\rho^* = m_\rho\left[1 - 0.127\left(\frac{T(\mathrm{GeV})}{0.16}\right)^{5.24}\right]$$

$$m_\omega^* = m_\omega\left[1 - 0.044\left(\frac{T(\mathrm{GeV})}{0.16}\right)^{7.09}\right]$$

(Sarkar et al, 1999)

- **Universal Scaling Hypothesis**

$$\frac{m_V^*}{m_V} = \frac{f_V^*}{f_V} = \frac{\omega_0^*}{\omega_0} = \left(1 - 0.2\frac{n_B}{n_0}\right)\left(1 - \frac{T^2}{T_c^2}\right)^\lambda,$$

$\lambda = 1/6(\underline{1/2})$ Brown – Rho($\underline{\text{Nambu}}$) Scaling

(Brown & Rho, 1996)

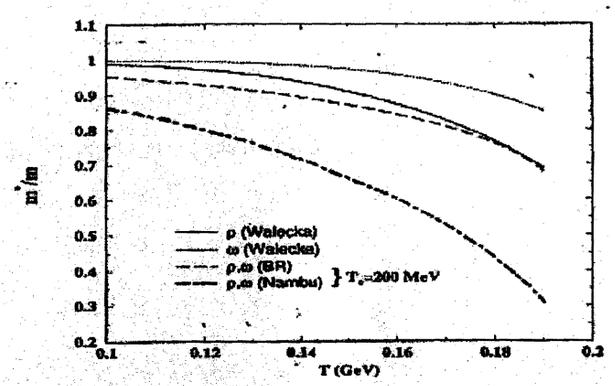

Thermal photons from hot hadronic matter

Essential components are π, ρ, η, ω, a_1

$$\mathcal{L} = -\underline{g_{\rho\pi\pi}}\vec{\rho}^\mu \cdot (\vec{\pi} \times \partial_\mu\vec{\pi}) - eJ^\mu A_\mu + \frac{e}{2}F^{\mu\nu}(\vec{\rho}_\mu \times \vec{\rho}_\nu)_3,$$

where

$$J^\mu = (\vec{\rho}_\nu \times \vec{B}^{\nu\mu})_3 + (\vec{\pi} \times (\partial^\mu\vec{\pi} + g_{\mu\pi\pi}\vec{\pi} \times \vec{\rho}^\mu))_3$$

To $O(e^2 g_{\rho\pi\pi}^2)$ imaginary part leads to rates for

$$\left.\begin{array}{l}\pi\pi \to \rho\gamma \\ \pi\rho \to \pi\gamma \\ \underline{\rho \to \pi\pi\gamma}\end{array}\right\}$$

For example:

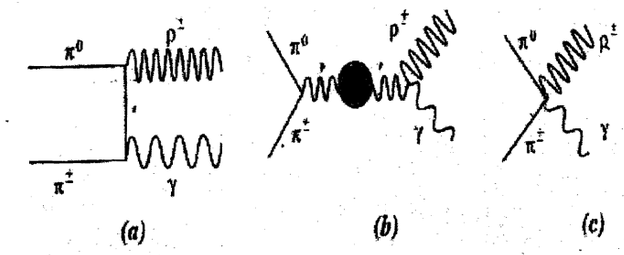

We also include $\mathcal{L} = \frac{g_{\rho\rho\eta}}{m_\eta}\epsilon_{\mu\nu\alpha\beta}\partial^\mu\rho^\nu\partial^\alpha\rho^\beta\eta + \frac{g_{\omega\rho\pi}}{m_\pi}\epsilon_{\mu\nu\alpha\beta}\partial^\mu\omega^\nu\partial^\alpha\rho^\beta\pi + \frac{e m_\rho^2}{g_\rho}A_\mu\rho^\mu$

$$\left.\begin{array}{l}\pi\eta \to \pi\gamma \\ \pi\pi \to \eta\gamma \\ \underline{\omega \to \pi\gamma}\end{array}\right\}$$

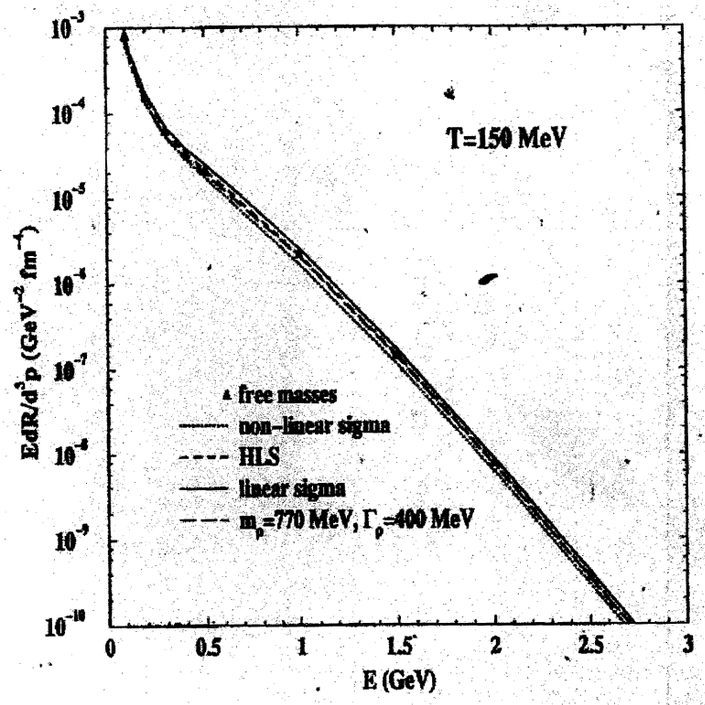

The change in the photon spectra due to the finite temperature effects on the hadronic masses in the Gauged Linear & Non-Linear Sigma Model and Hidden Local Symmetry approach at T= 150 MeV.

Thermal photon

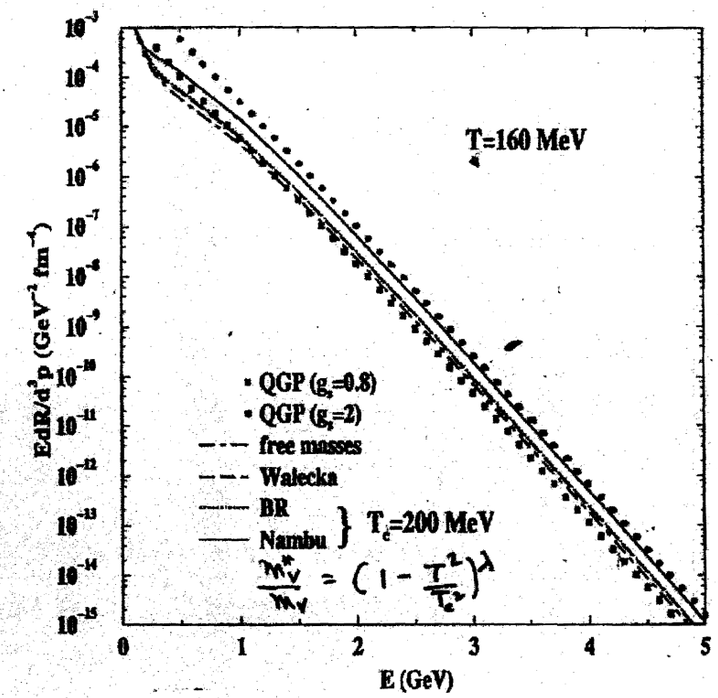

Thermal photon spectra at $T = 160$ MeV. Solid dots (square) indicates photon emission rate from QGP with both one loop and two loops contributions for $g = 2(0.8)$. Dotdash line represents photon spectrum from hot hadronic gas without medium effects. The result with the in-medium effects within the scope of the Walecka model calculations is shown by long dashed line. Dotted (solid) line indicates photon spectrum with BR (Nambu) scaling mass variation scenario.

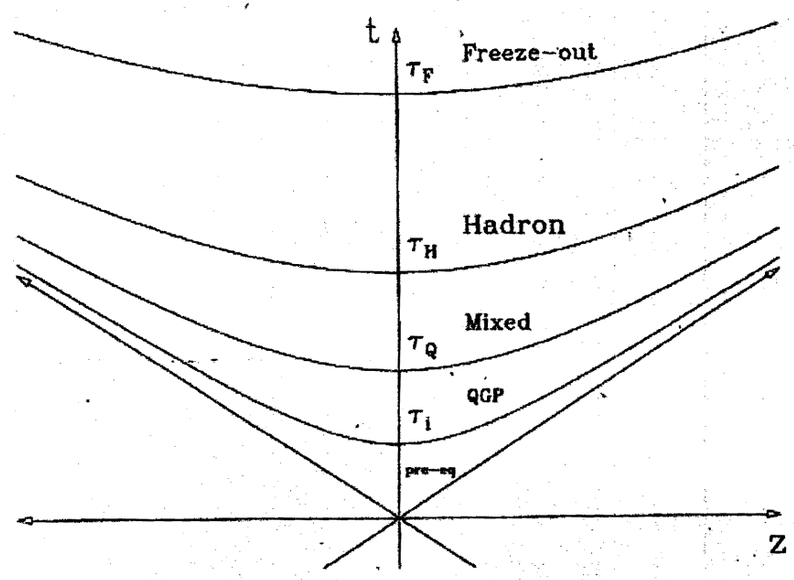

EOS and Space Time Evolution

- QGP:

$$\epsilon_{QGP} = 3\frac{\pi^2}{90} g_{QGP} T^4 + B;$$
$$P_{QGP} = \frac{\pi^2}{90} g_{QGP} T^4 - B$$
$$s_{QGP} = 4\frac{\pi^2}{90} g_{QGP} T^3$$

- Mixed Phase:

$$s_{mix} = f_Q(\tau) s_Q^c + f_H(\tau) s_H^c$$

(Bjorken's hydrodynamics)

where

$$f_Q(\tau) = \frac{1}{r-1}\left(r\frac{\tau_Q}{\tau} - 1\right)$$

$r = g_Q/g_H$

$\tau_H = r\,\tau_Q$

- Hadronic Matter (π, ρ, ω, η, a_1 and N)

$$\epsilon_H = \sum_i g_i \int \frac{d^3p}{(2\pi)^3} E_i\, f(E_i, T)$$
$$P_H = \sum_i g_i \int \frac{d^3p}{(2\pi)^3} \frac{p^2}{3\,E_i} f(E_i, T)$$

$$s_H = \frac{\epsilon_H + P_H}{T} \equiv 4a_{\rm eff}(T)\,T^3 = 4\frac{\pi^2}{90} g_{\rm eff}(m^*(T), T) T^3$$

Sound Velocity, $c_s^{-2} = \dfrac{T}{s_H}\dfrac{ds_H}{dT} = \left[\dfrac{T}{g_{\rm eff}}\dfrac{dg_{\rm eff}}{dT} + 3\right]$

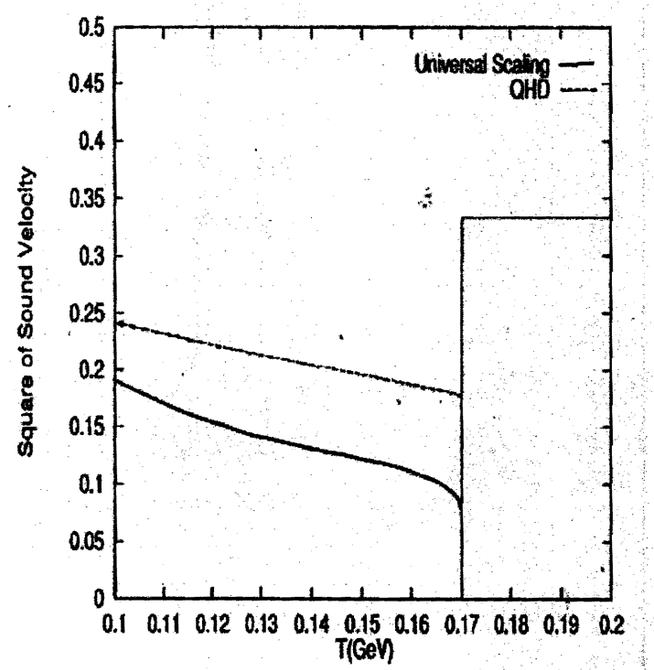

$$T \sim \frac{1}{\tau^{c_s^2}}$$

$c_s < c_s^{ideal}$ $\Rightarrow$ Slow Cooling.

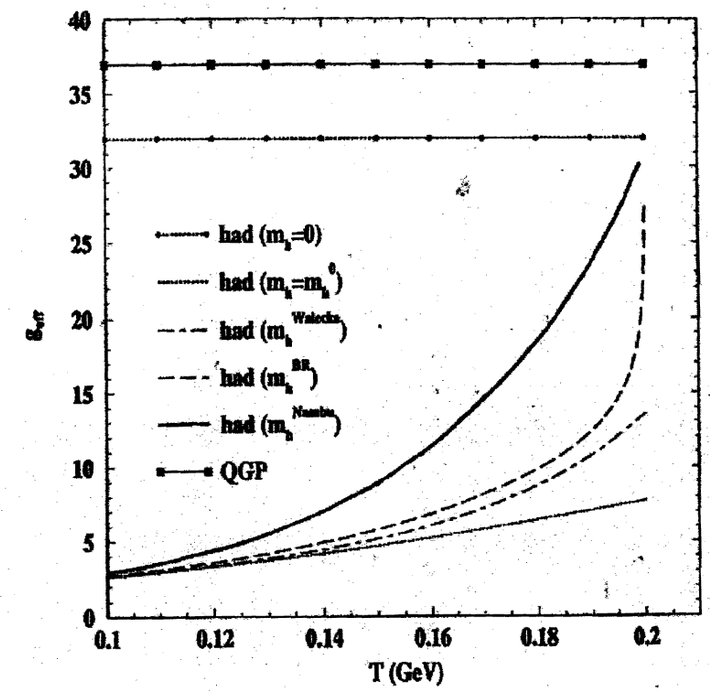

Variation of effective degeneracy, g_{eff} as a function of temperature. g_{eff} has a strong temperature dependence in a mass variation scenario.

Initial Conditions (3+1)D Hydrodynamics:

$$\frac{dS}{\pi R_A^2 \tau_i dy} \propto \frac{dN}{\pi R_A^2 \tau_i dy} = \left(\frac{45\zeta(3)}{2\pi^4}\right) 4 a_{\rm eff} T_i^3$$

If the fluid fields vary appreciably over a length scale of mean free path then the effects of viscosity will be important.

(Viscous effects ⇒ lower T_i, J. Phys. G 23 (1997) 469).

$$\frac{dN}{dy} = \frac{45\zeta(3)}{2\pi^4} \pi R_A^2 4 a_{\rm eff} T_i^3 \tau_i$$

$$\frac{\pi^2}{90} \times g_{eff}.$$

$$\tau_i = 1 \text{ fm/c}$$

$$\epsilon(\tau_i, r) = \frac{\epsilon_0}{\exp(r - R_A)/\delta + 1}$$

(von Gersdorff et al, 1986.)

$$v_r(\tau_i, r) = v_0 \frac{\alpha + 2}{2} \left(\frac{r}{R_A}\right)^{\alpha}$$

(Heinz et al, 1992; Braun-Munzinger et al 1996)

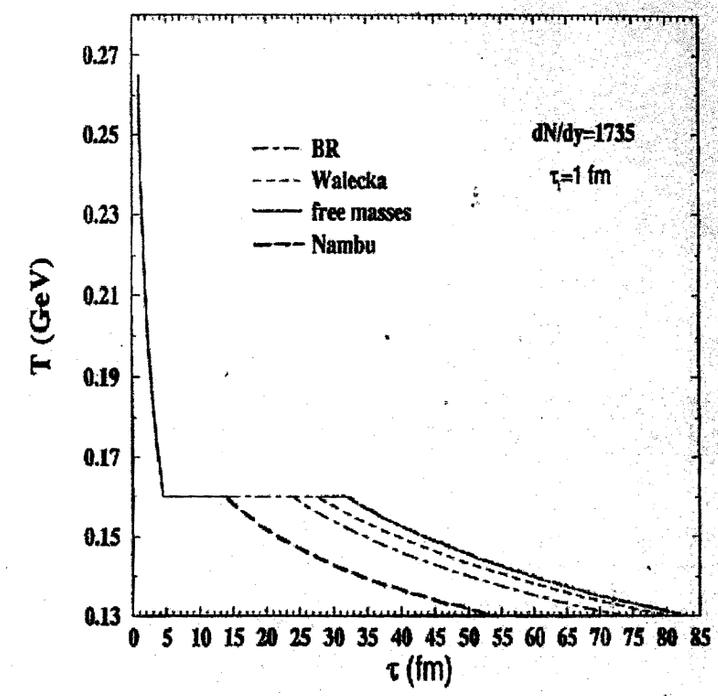

Life time of the mixed phase $\tau_H - \tau_Q = (g_Q/g_H - 1)\tau_Q$

Photons from S + Au collisions at CERN SPS energies

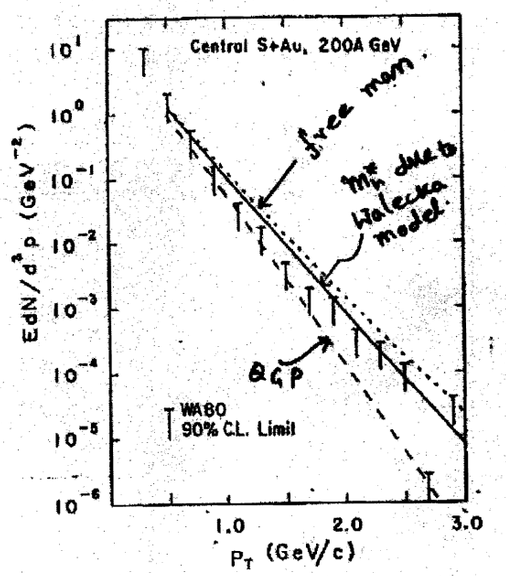

Physical Review C 1999

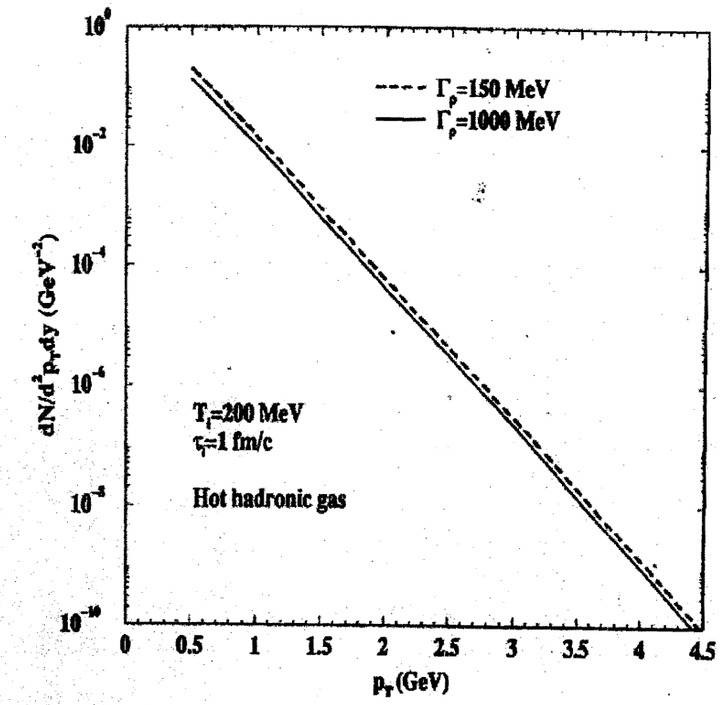

Thermal photon spectra for $T_i = 200$ MeV and $\tau_i = 1$ fm/c. Solid (dashed) line indicates photon yield with large broadening of the ρ spectral function (vacuum spectral function).

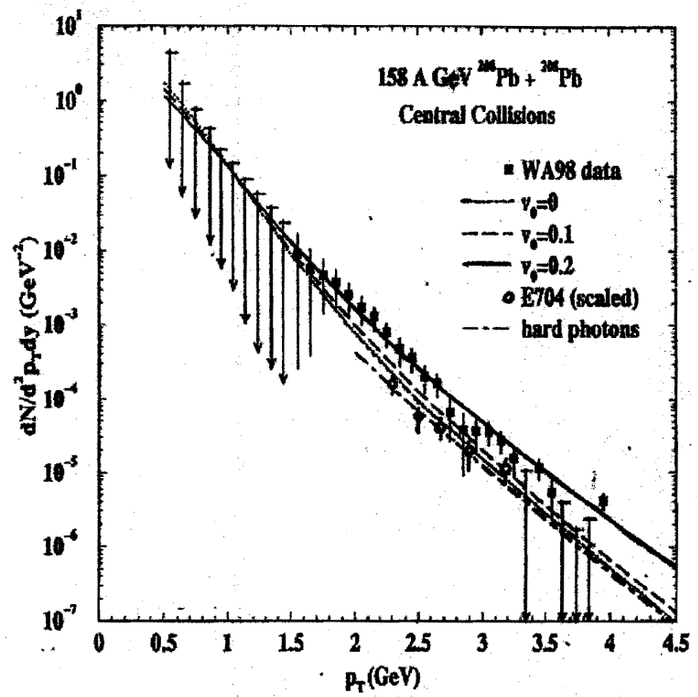

Total photon yield in Pb + Pb collisions at 158 A GeV at CERN-SPS. The theoretical calculations contain hard QCD and thermal photons. The system is formed in the QGP phase with initial temperature $T_i = 196$ MeV.

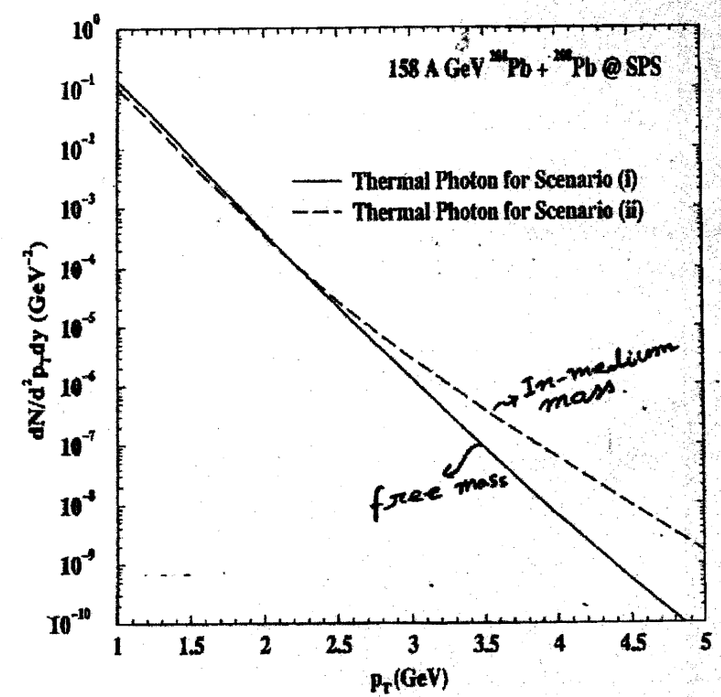

Transverse momentum distribution of thermal photons with and without medium effects.

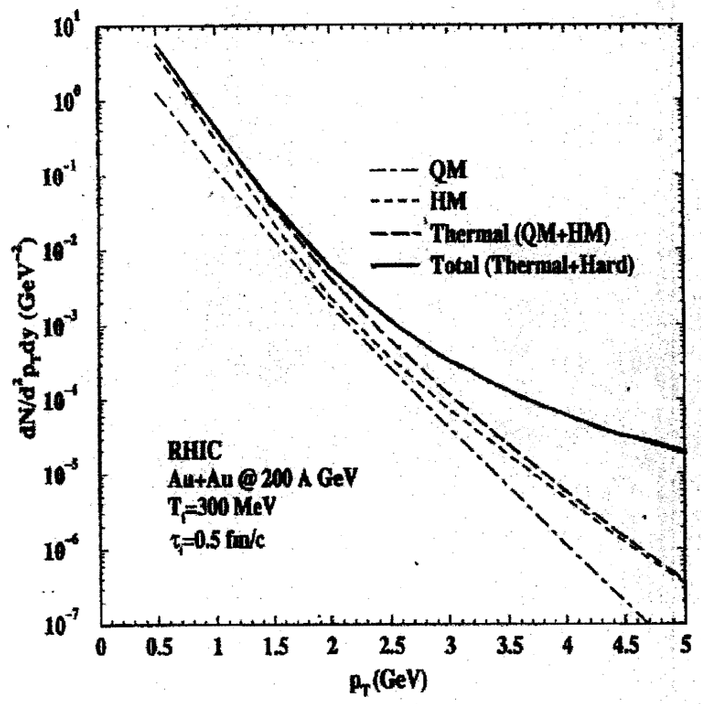

Photon spectra at RHIC for Au + Au collisions.

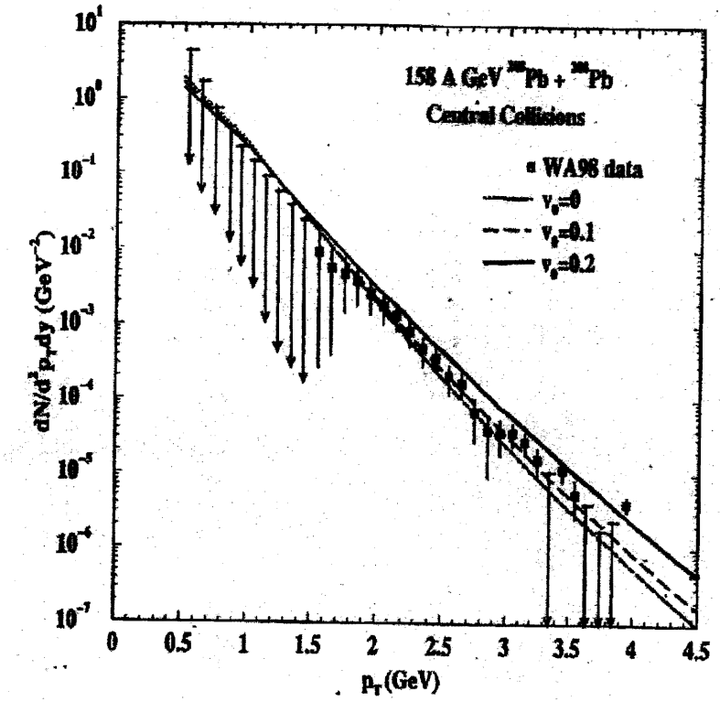

Total photon yield in Pb + Pb collisions at 158 A GeV at CERN SPS. The theoretical calculations contain hard QCD and thermal photons. The system is formed in the hadronic phase with the hadronic masses approaching zero at initial temperature $T_i = 205$ MeV.

	QGP	vacuum mass	QHD	Scaling T_c= 170 MeV	Scaling T_c= 200 MeV
$\frac{dN_{ch}}{d\eta}$	T_i (MeV)	T_i (MeV)	T_i (MeV)	T_i (MeV)	T_i (MeV)
150	161	209	199	168	181
210	171	219	206	171	187
270	179	227	212	179	192
350	187	235	217	187	196

$T_f = 120$ MeV

- **Thermal Dilepton Emission Rates**

$$\frac{dR}{d^4q} = \frac{\alpha}{12\pi^4 q^2} \mathrm{Im} W^R_{\mu\mu} f_{BE}(q_0)$$

- **QGP** $q\bar{q} \to e^+e^-$

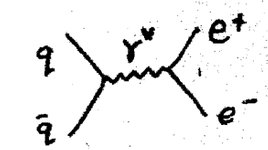

$$\frac{dR}{dM^2\, p_T\, dp_T\, dy} = \frac{5}{9}\frac{\alpha^2}{4\pi^3} e^{-M_T \cosh y/T}$$

- **Hadronic matter** $\pi^+\pi^- \to e^+e^-$

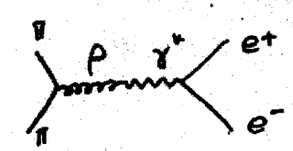

$$\frac{dR}{dM^2\, p_T\, dp_T\, dy} = \frac{\alpha^2}{\pi}\frac{m_\rho^{*4}}{M^2 g^2_{\rho\pi\pi}} f_{BE} \left[\frac{1}{\pi}\frac{\mathrm{Im}\Pi^{\rho R}}{(M^2 - m_\rho^{*2}) + [\mathrm{Im}\Pi^{\rho R}]^2}\right]$$

- $V \to e^+e^-$

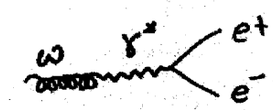

$$\frac{dR}{dM^2\, p_T\, dp_T\, dy} = \frac{(2J+1)}{4\pi} M \Gamma^{\mathrm{vac}}_{V\to e^+e^-} f_{BE} \left[\frac{1}{\pi}\frac{\mathrm{Im}\Pi^{\rho R}}{(M^2 - m_\rho^{*2}) + [\mathrm{Im}\Pi^{\rho R}]^2}\right]$$

$\omega\pi \leftrightarrow \pi\pi$, $\omega\pi \to 3\pi$, $\omega\pi \to \rho$

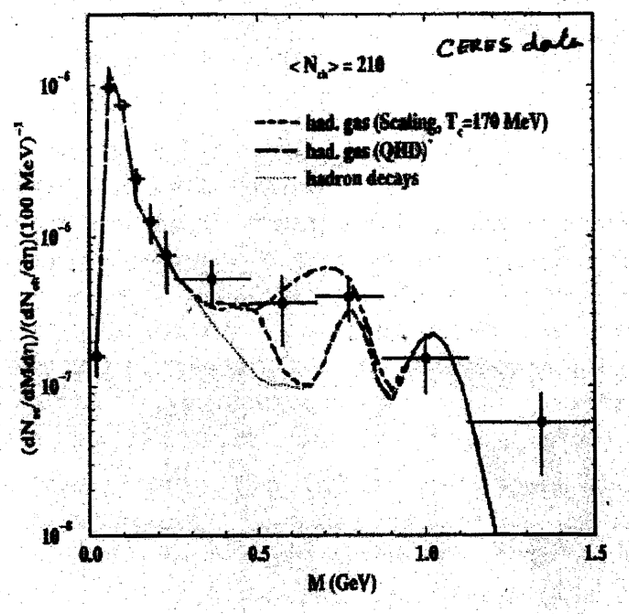

Dilepton spectra for $\langle N_{ch} \rangle$=210. The dashed line (dash-dotted) indicates e^+e^- pair yield when the system is formed in the hadronic phase and hadronic masses vary according to universal scaling (QHD).

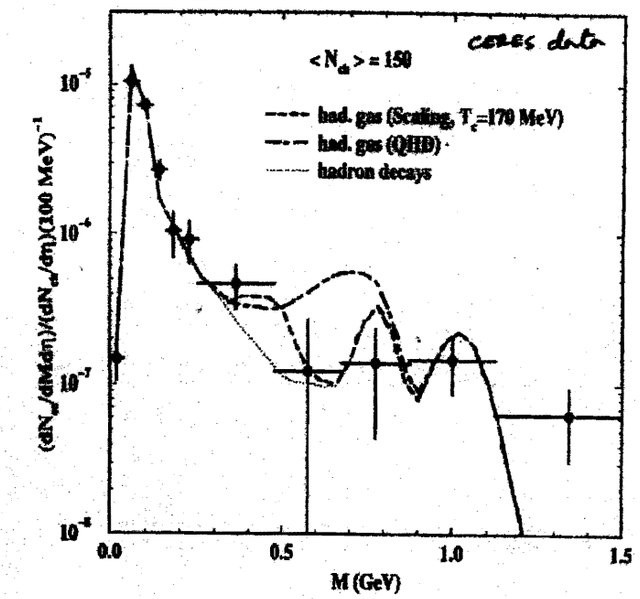

Dilepton spectra for $\langle N_{ch} \rangle$=150. The dashed line (dash-dotted) indicates e^+e^- pair yield when the system is formed in the hadronic phase and hadronic masses vary according to universal scaling (QHD). Note that these also include the yield from hadronic decays at freeze-out (dotted line).

G. Agakichiev et al, 1998.
B. Lenkeit, Doctoral Thesis, 1998
(CERES)

Discussions:

- The number of $\pi - \pi$ collisions in the region $M \sim m_\rho^*$ is given by

$$N_{\pi\pi} = 2 \times 3 \times \frac{\Gamma_\rho^*}{B_\rho} \frac{dN}{dM d\eta}|_{M=m_\rho^*}$$ (Kajantie et al 1986)

Thermal equilibrium may not be realized in the case of $dN_{ch}/d\eta = 150$ and 210 since the number of collisions per particle in the system, $\sim N_{\pi\pi}/(1.5 dN_{ch}/d\eta) < 1$. This quantity is $\sim 2-3$ for $dN_{ch}/d\eta = 270$ and 350.

- The condition $\tau^\pi_{scatt} < \tau_{exp}$ is satisfied throughout the evolution process, indicating that the use of hydrodynamics is reasonable for space-time description.

- For $dN_{ch}/d\eta = 150$ and 210, dileptons seem to originate from a hadronic source with initial temperature ~ 170 MeV. For the higher values (270 and 350), however, the data can be described by both QGP and hadronic initial states.

- We conclude that in order to reproduce the CERES dilepton data or WA98 photon data either a substantial reduction in vector meson masses or the formation of QGP in the initial stage with $T_i \sim 200$ MeV is necessary. A simple hadronic model is inadequate to reproduce the data.

- Although the dilepton data can be described by a large broadening of ρ, the p_T distribution of photon is almost unaffected by such phenomenon.

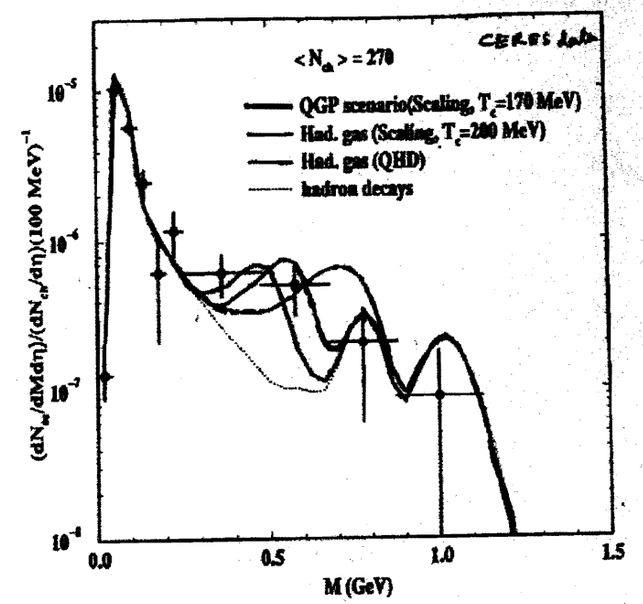

Dilepton spectra for $\langle N_{ch} \rangle$=270 for different initial states and mass variation scenarios. Solid line indicates dilepton yield when QGP is formed. (Here QGP scenario indicates sum of yields from QGP phase+QGP part of the mixed phase +hadronic part of the mixed phase +hadronic phase) The dashed line (dash-dotted) indicates e^+e^- pair yield when the system is formed in the hadronic phase and vector meson masses vary according to universal scaling (QHD).

Re-Hardening of Hadron Transverse Mass Spectra in Relativistic Heavy-Ion Collisions

A. Ohnishi[a], N. Otuka[ab], P.K. Sahu[a], M. Isse[a], and Y. Nara[c]

a Division of Physics, Graduate School of Science, Hokkaido University, Sapporo 060-0810, Japan

b Advanced Science Research Center, Japan Atomic Energy Research Institute, Tokai, Ibaraki 319-11, Japan

c Physics Department, Brookhaven National Laboratory, Upton, N.Y. 11973, U.S.A.

Transverse mass spectra of hadrons are important as a measure of pressure generated during heavy-ion collisions. Expecially, the inverse slope parameter of transverse mass spectra is known to be a linear function of particle mass, $T'(M) = T_0 + M\,\beta^2/2$, where T_0 and β are interpreted as the temperature and collective radial flow velocity at freeze-out. This collective radial flow exhibits a maximum at around AGS energies, and decreases at SPS. In other words, the *softening* of matter is observed at AGS-SPS energies. The softening phenomena might signal QGP formation, but it can be mimicked also by hadronic (resonance and string) DOFs [1,2]. In a hadronic scenario, a large part of energy is exhaused to populate abundant heavy resonances or hadron strings at high energy densities, then the translational kinetic energy cannot grow linearly as a function of the energy density.

Then it would be very interesting if a *re-hardening* of hadron spectra is observed above SPS energies. Since there is no narrow structure of hadrons in the higher mass region than 2 GeV, it is very hard to explain re-hardened spectra of hadrons at higher energy densities in a hadronic scenario. Actually, recent analysis of RHIC data by PHENIX collaboration suggests this behavior, as shown by H. Ohnishi et al. at the previous JPS meeting in Niigata [3].

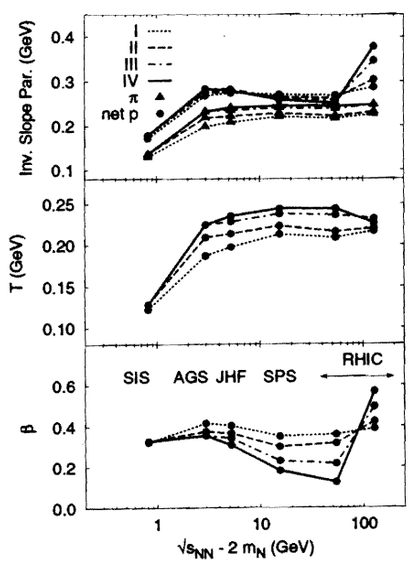

In this presentation, we analyze the hadron spectra in heavy-ion collisions at relativistic energies from 2 A GeV to 65+65 A GeV by using a jet-implemented hadron-string cascade model, JAM [4]. We show that the data at AGS and SPS are well described, and that the above expected re-hardening really emerges in the calculated results in JAM, as shown in the right figure.

[1] S.K.Sahu et al., Nucl. Phys. **A672** (2000), 376.
[2] N. Otuka, Theis, Hokkaido Univ., March 2001: N. Otuka et al., in preparation.
[3] H. Ohnishi for PHENIX collaboration, JPS meeting in Niigata Univ., Sep. 2000.
[4] Y. Nara et al., Phys. Rev. **C61**(2000), 024901.

⋆ QGP Signals

⋆ Anomalous J/ψ supression
○ : Deconf. phase → No Bound State (Matsui & Satz)
△ : $\sigma(J/\psi\text{-}h)$ = constant (?) ($h = N, \pi, \rho, N^*$, strings, ...)

⋆ Strangeness Enhancement
○ : QGP → Fast Chem. Equilibrium
△ : Rope formation (Sorge),
× : multi-π → Strange particles (C. Greiner)

⋆ Low-E Dilepton Enh.
△ : Partial χ-rest. rather than Deconf.
(Hatsuda & Lee)

⋆ Softening of particle spectra
○ : Decrease of Directed Flow (SIS-AGS)
× : It can be explained in Hadron-String Scenario
(Hadronic DOF + Mean Field, Sahu et al.; Otuka Thesis)

• Possible Explanation

1. QGP is formed at SPS energy Pb+Pb Collisions.
2. Hot and Dense (Heavy-)Resonance-String Gas (Approximate Hagedorn Gas) is formed.
   ⋆ $J/\psi + N^* \to D\bar{D}$
   ⋆ string + string → Rope → $Y\bar{Y}$
   ⋆ Large Mass Energy ↔ Smaller Pressure

Key Logic: Hadron Gas becomes Softer and Softer at High Energy Density. (Hagedorn, 1965)

Re-Hardening of Hadron Transverse Mass Spectra in Relativistic Heavy-Ion Collisions

Akira Ohnishi[a]
in collaboration with
N. Otuka[ab], P.K. Sahu[a], M. Isse[a], Y. Nara[c]
a. Hokkaido U., *b.* JAERI, *c.* BNL

1. Introduction
2. Pion and Proton Spectra at RHIC energies
3. Re-Hardening
4. Summary

Abstract

We analyze the spectra of pions and protons in heavy-ion collisions at relativistic energies from 2 A GeV to 65+65 A GeV by using a jet-implemented hadron-string cascade model, JAM. In this energy region, hadron transverse mass spectra first show softening until SPS energies, and re-hardening may emerge at RHIC energies. Since hadronic matter is expected to show only softening at higher energy densities, this re-hardening of spectra can be a good signature of the quark-gluon plasma formation.

Collective Flow

P.K.Sahu et al., NPA672(2000)376

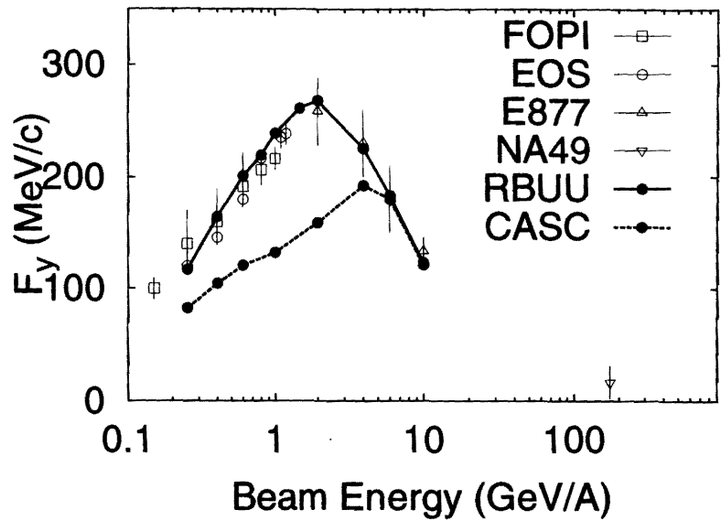

Why does it become soft ?

Hadronic DOFs + Reduction of MF

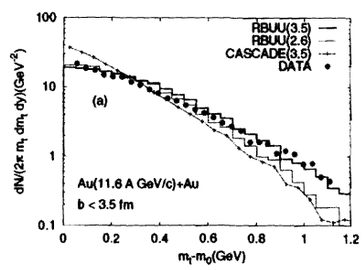

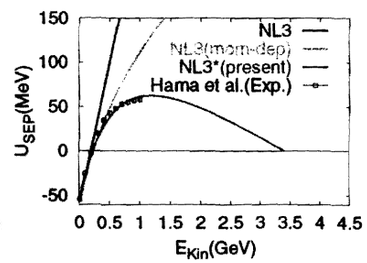

Y.Nara et al., PTP Suppl. 129(1997)33, N.Otuka, Thesis; to be submitted.

⋆ Softening at SIS-AGS-SPS

Chujo, Thesis.

Temperature

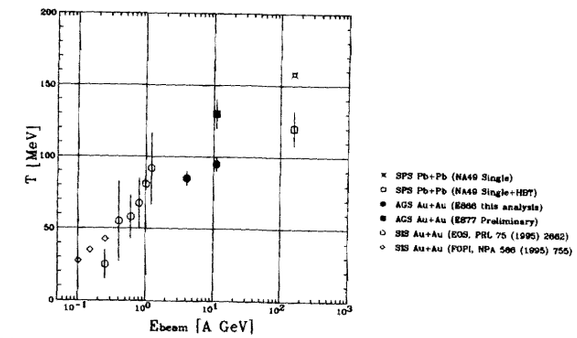

Radial Flow

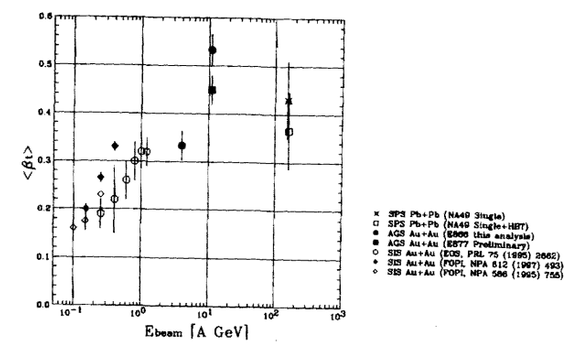

Thermal Evolution of Matter (JAM and HANDEL)

Temperature during HIC

$$T \simeq P/\rho \quad \text{(Ideal Gas EOS)}$$

ρ= Total Hadron Number Density

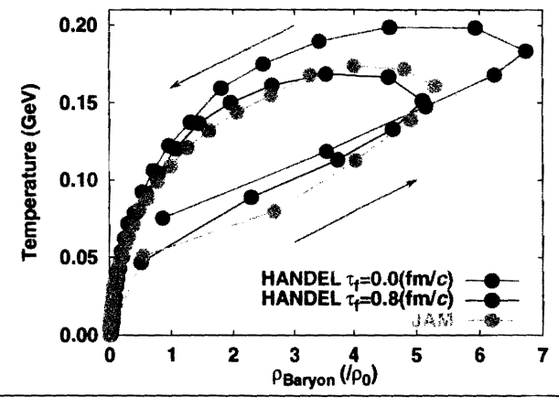

Why Multi Pion Production Reduces P (and thus T)?
→ "Blob" may play a role of Massive (Continuum) DOF.

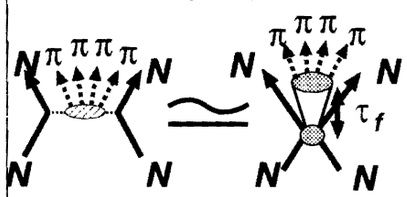

"Blob"

$$\Gamma \simeq \frac{\hbar}{\tau_f}$$

⋆ Thermal Properties of Hadronic Cascade

☞ Small DOF models may give Too Stiff Spectra
... Why do ARC and ART Explain Data ?

Answer: Multiparticle Prod. with finite Formation Time Generates Effective Large DOFs.

ARC: Y.Pang et al. PRL68('92)2743,
ART: B.A.Li & C.M.Ko, PRC52('95)2037; PRC57('98)2065.

M_t Spectra with Multi. Prod. (HANDEL)

Au(11.6 A GeV/c)+Au → p,π^+,π^-

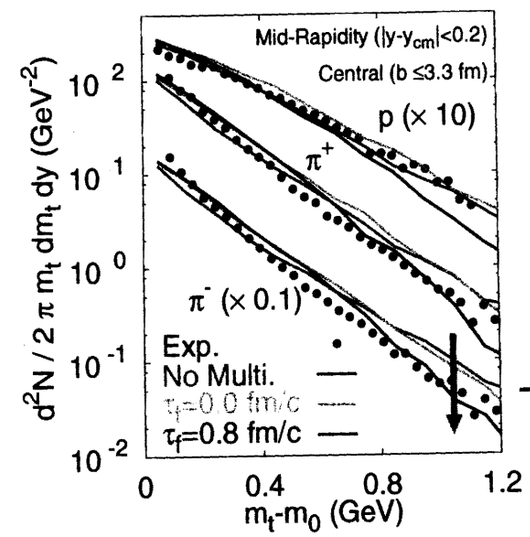

Larger τ_f

→ *Larger DOF ?*

JACEE results

(Y.Takahashi et al., NPA461(1987)263c)

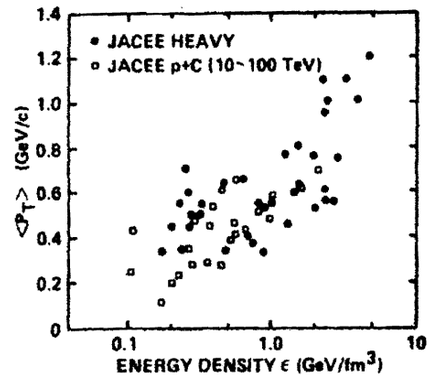

Hydro + UrQMD results

(Bass et al., PRC61(2000)064909)

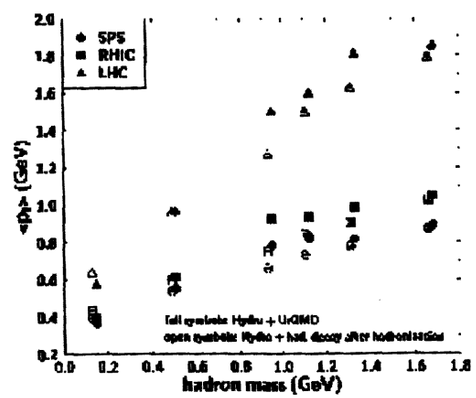

☞ How about Re-Hardening ?

- Preliminary RHIC data
  - ⋆ Pion Slope Parameter = 291 MeV (Phenix)
  - ⋆ Proton Slope Parameter ≃ (400-500) MeV (H.Ohnishi for Phenix @ JPS)

… Very Hard Spectra compared to those at SPS
Very Hard to explain in Hadronic Scenario

- Earlier Suggestions of Hardening
  - ⋆ JACEE observation ($< P_t >$ grows quickly)
  - ⋆ Hydro + UrQMD ($< P_t >$ grows quickly)
  - ⋆ Nu Xu @ QM2001 (β(RHIC) > β(SPS))

… In this work,

⋆ We study proton and pion M_t spectrum in SIS-AGS-JHF-SPS-RHIC energy region systematically, by using a jet-implemented hadron-string cascade (JAM),

⋆ and demonstrate that the "Re-Hardening" is actually expeced in the calculation.

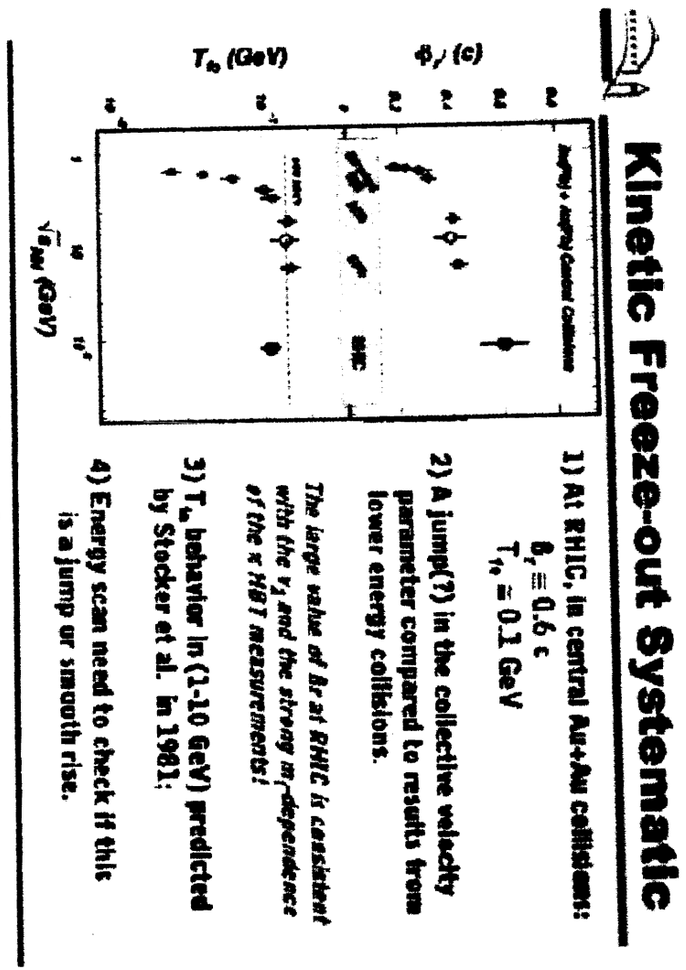

Nu Xu, Presentation at QM2001.

JAM (Jet Aa Microscopic transport model)

Y. Nara et al., PRC61('00), 024901.

⋆ DOF: h(B, B*, M, M* (m $\leq$ 2 GeV)) + s(Strings)
+ Partons (at higher energies)

⋆ σ: Hadronic ($hh \leftrightarrow hh$, $hh \leftrightarrow h$)
+ Soft ($hh \leftrightarrow s$, $hh \rightarrow hs$, $hh \rightarrow ss$, $s \rightarrow hhh$... [1]
$ch \leftrightarrow ch$, $ch \rightarrow cs$ (c= (qq), q, $\bar{q}$) [2])

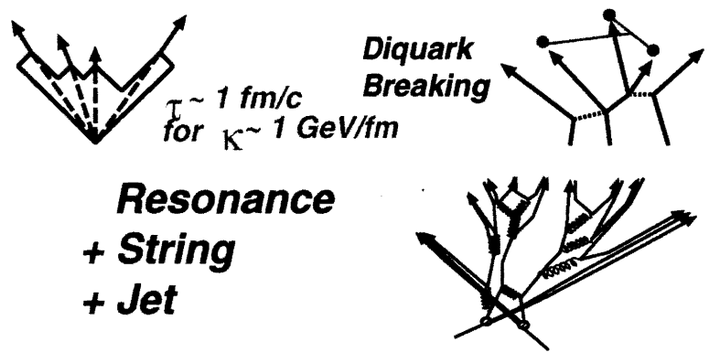

+ Hard (Jet Production, at higher energies) [3]

⋆ No Mean Field (in progress), No Medium Modification

[1] "DPM + Lund" (~ HIJING) + Phase Space
[2] Consituent Rescattering (~ RQMD), c= (qq), q, $\bar{q}$
[3] Jetset (Pythia)

Version: JAM1.009.27 (April 2000 Version)

⋆ M_t Spectra: Measure of Generated Pressure

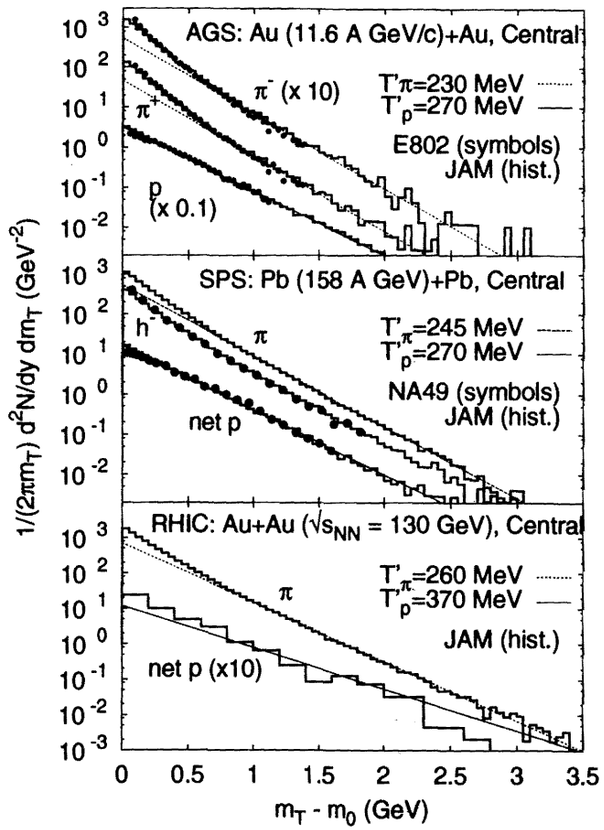

Nicely Reproduced, except for
Low Energy Protons (No Mean Field)

⋆ Rapidity Distributions: Hadron Yields

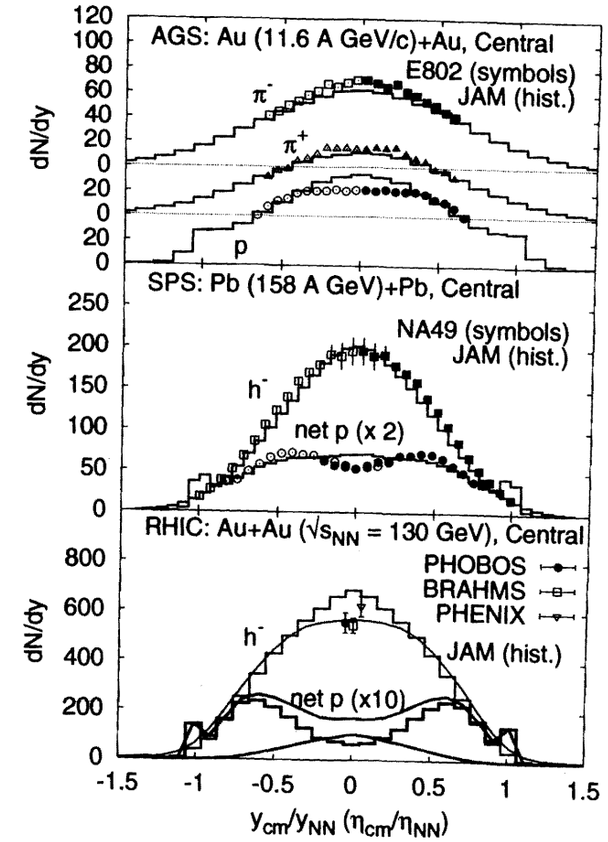

⋆ Globally Good, except for
Systematically Larger Stopping Power of Protons.

⋆ Summary and Conclusion

- Re-Hardening of Hadron Spectra

  is very hard to explain in Hadronic Scenario since more and more hadronic heavy DOFs are activated, (Otuka, Thesis)

  then it can be a good signature of BULK QGP formation.

- RHIC preliminary results and JAM cal.

  show re-hardening between SPS and RHIC energies.

⋆ JAM results systematically reproduces AGS-SPS-RHIC energy heavy-ion collisions.

- ∘ $dN/d\eta$(charged) $\simeq 570$
- ∘ $\bar{p}/p \simeq 0.63$
- ∘ Slopes: a little softer than data

⋆ Local Maximum of β may appear at around JHF-NSP energies. It can be a consequence of "the highest baryon density".

⋆ Decomposition to T and β

$$\frac{d^2N}{M_t dM_t dY d\phi} \propto \exp(-M_t/T'), \quad T'(M) = T + \frac{1}{2} M \beta^2$$

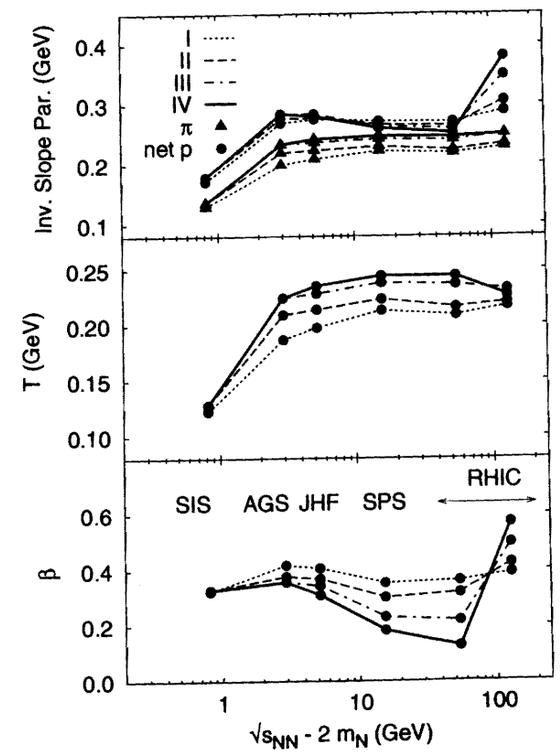

Re-Hardening emerges between SPS and RHIC energies

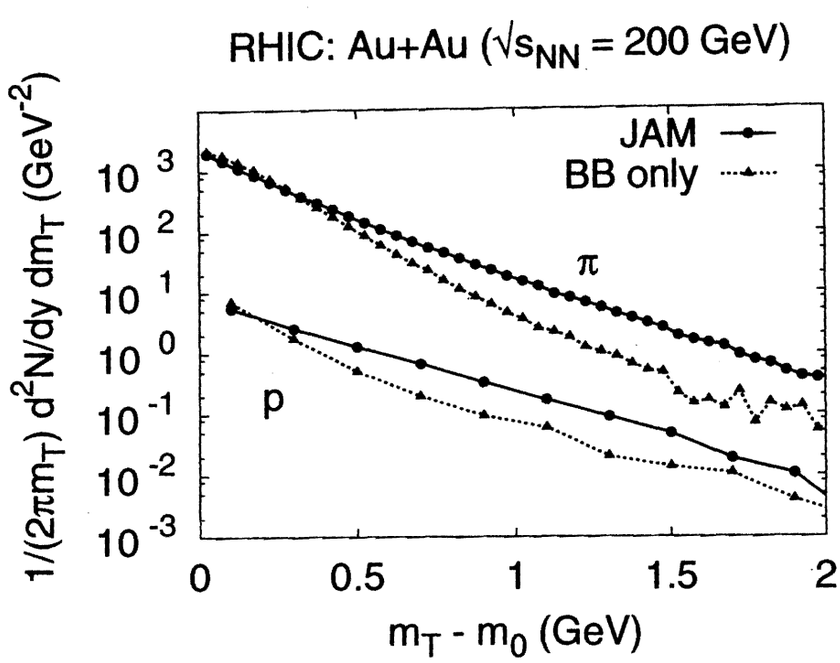
RHIC: Au+Au ($\sqrt{s_{NN}}$ = 200 GeV)
JAM
BB only
π
p
$1/(2\pi m_T)\, d^2N/dy\, dm_T$ (GeV^{-2})
10^3
10^2
10^1
10^0
10^{-1}
10^{-2}
10^{-3}
0
0.5
1
1.5
2
$m_T - m_0$ (GeV)

Quark-gluon Plasma and Lattice QCD at Finite Temperature and Density

Chiho NONAKA

Department of Physics, Hiroshima University, Higashi-Hiroshima 739-8526, Japan

abstract

The study of the quark-gluon plasma (QGP) is one of the hottest topics in the high energy nuclear physics and many analyses have been done from both experimental and theoretical side to understand the QGP phenomena. QGP is a new state which is predicted by QCD under the extreme temperature and density conditions. Lattice QCD provides us powerful tools to understand the nature of QGP from the first principles. Here, we present the recent development in lattice QCD from the point of view of the investigation of QGP phenomena.

Recently, thermal freeze-out and chemical freeze-out analyses are discussed based on statistical mechanics in the heavy ion collisions. These results show that the concept of temperature and the chemical potential have some meanings. Lattice QCD can describe the statistical mechanics in equilibrium state. Therefore data of lattice QCD contribute the explanation of the data of experiment (CERN SPS and BNL RHIC).

First, we introduce the formulation of the lattice QCD at finite temperature and density briefly. The phase transition structure is one of the interesting subjects. In lattice QCD the confinement/de-confinement phase transition is evaluated by behavior of the expectation value of the Polyakov line.

We focus on the specific topics of the recent development in lattice QCD, which is directly related to QGP phenomena. There are several technical advances in lattice QCD in addition to improvement of computer performance. The several improved actions have been proposed to remove finite size artifact and to obtain the solutions near to the continuum limit. By using anisotropic lattice, some physical quantities such as glue-ball mass which was difficult to measure can be measured with relatively high accuracy.

At finite temperature, many calculations have been done and various physical quantities are measured. Concerning critical temperature and the equation of state, the most of results which are obtained by using several kinds of action are consistent. The hadron spectra is the one of the interesting topics. Recently the J/ψ suppression and possibility of the mass shift of ρ are reported in the ultra-relativistic nuclear collisions. We discuss relevant lattice calculations. The transport coefficients are also discussed.

On the other hand, at finite density the progress of the study is slow. There exist difficulties of the evaluation of the fermion determinant in SU(3) QCD calculations, i.e., the complex action problems. Though many trial calculations in SU(3) QCD such as Glasgow algorithm, the conclusive work has not been presented. Now, the new approach to SU(3) QCD is presented. From QCD-like theories such as SU(2) QCD, models with quarks in the adjoint representation, and QCD at finite isospin density we obtain the some information of SU(3) QCD. Here, we report the recent work of SU(2) lattice QCD at finite density.

Quark-gluon Plasma and Lattice QCD at Finite Temperature and Density

Chiho NONAKA

Hiroshima University

February 15, 2001, CNS workshop

Contents

- Introduction
- Formulation of lattice QCD
  - Finite temperature
  - Finite density
- Recent developments of lattice QCD
- Lattice QCD at finite temperature and density
  Recent Results
- Summary

Introduction

- Thermal Freeze-out and Chemical Freeze-out

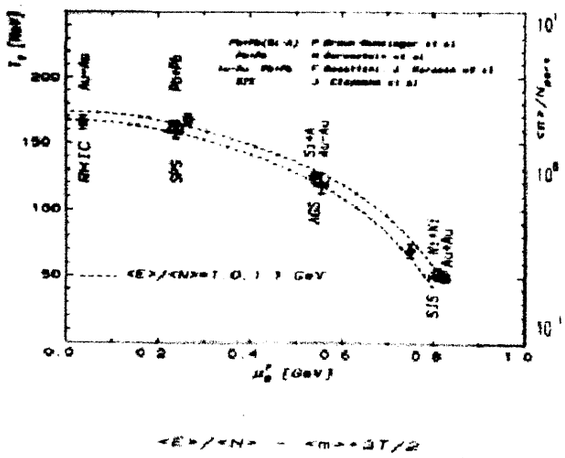

By Redlich, QM2001

Temperature
and
Chemical potential

Lattice QCD
⬇
Statistical mechanics

Formulation of LQCD (1)

- finite temperature
  - Matsubara formalism for finite temperature

$$Z = \mathrm{Tr}\ e^{-\beta H} = \int [d\phi]\, e^{-S[\phi]}$$

$$S[\phi] = \int_0^{\beta} dx_4 \int d^3x L$$

$$T = \frac{1}{N_t a}$$

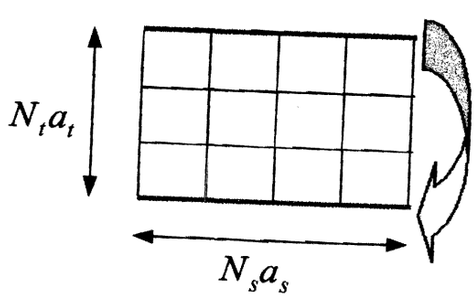

a : lattice spacing

boson : periodic
fermion : anti-periodic

Formulation of LQCD (2)

- Finite density
  - Introduction of chemical potential

    Wilson fermion

$$Z = \mathrm{Tr}\, e^{-\beta(H-\mu N)} = \int DUD\bar{\ }D \quad e^{-(S_G+S_F)}$$

$$S_F = \bar{\ }W$$

$$W = 1-\kappa \sum_{\mu=1}^{4} \left\{(1-\gamma_\mu)U_\mu(x)\delta_{x',x+\hat{\mu}} + (1+\gamma_\mu)U_\mu^\dagger(x)\delta_{x',x-\hat{\mu}}\right\}$$

κ: hopping parameter $\Longleftrightarrow$ quark mass

$$P_4 \Rightarrow P_4 - i\mu$$

$$W = 1-\kappa \sum_{i=1}^{3} \left\{(1-\gamma_i)U_i(x)\delta_{x',x+\hat{i}} + (1+\gamma_i)U_i^\dagger(x)\delta_{x',x-\hat{i}}\right\}$$

$$-\kappa \left\{e^{\mu a}(1-\gamma_4)U_4(x)\delta_{x',x+\hat{4}} + e^{-\mu a}(1+\gamma_4)U_4^\dagger(x')\delta_{x',x-\hat{4}}\right\}$$

C.NONAKA, Hiroshima Univ.

Formulation of LQCD (3)

- phase transition
  - Confinement /Deconfinement

    Polyakov line (order parameter)

$$\langle L \rangle \equiv \left\langle \frac{1}{N_s^3} \sum L(x) \right\rangle \sim e^{-\Delta F_q \beta}$$

ΔF_q: free energy of the static charge

$\langle L \rangle \neq 0$ deconfined (ΔF_q finite)

$\langle L \rangle = 0$ confined (ΔF_q infinite)

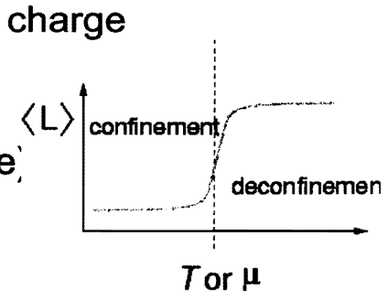

C NONAKA, Hiroshima Univ.

Recent Developments of LQCD(1)

- improved actions

Reduce discretization effect $(a \neq 0)$ on coarse lattice

$S_{\text{gauge}} = -\beta\{c_0 \sum \mathrm{Tr}$ $+ c_1 \sum \mathrm{Tr}$ $+ c_2 \sum \mathrm{Tr}$ 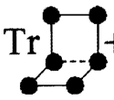 $+ c_3 \sum \mathrm{Tr}$ 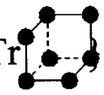

$$c_0 + 8c_1 + 16c_2 + 8c_3 = 1$$

- Renormalization group improvement
  Iwasaki, perfect action etc.
- Symanzik improvement
  Mean-field improvement (tadpole improvement) etc.

C.NONAKA, Hiroshima Univ.

Recent Developments of LQCD(2)

- anisotropic lattice (Karsch, Burgers, Nakamura, Klassen, Engels et.al.)
  - High accuracy measurement
    anisotropy

$$= \frac{a_s}{a_t} > 1$$

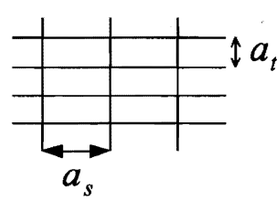

» pole mass analyses at finite temperature
temperature ↗ N_t ↘
» glueball mass (Morningstar et.al.PRD56('97)4043)

- problems
  » a_s is large
  » Complicated analysis with anisotropy

C.NONAKA, Hiroshima Univ.

LQCD
at finite temperature and density

- Finite temperature
  - Many analyses
    - » Critical temperature, EoS, Hadron spectrum Transport coefficients, etc.
- Finite density
  - Complex action problem in SU(3) QCD
  - Response to chemical potential at $\mu = 0$
  - QCD-like theory
    - » SU(2) QCD
    - » Models with quarks in the adjoint representation
    - » QCD at finite isospin density

C.NONAKA, Hiroshima Univ.

LQCD at Finite Temperature (1)

- Critical temperature

action	Ref.	Nf	Nt	Tc[MeV]
plaquette	[1,2]	0	∞	268
Symanzik	[1]	0	∞	269
RG	[3]	0	∞	276
RG+clover	[4]	2	4	171(4)
Symanzik+p4	[5]	2	4	173(8)
Symanzik+p4	[5]	3	4	154(8)

[1] Beinlich et.al.
[2] Edwards et.al
[3] CP-PACS
[4] CP-PACS
[5] Karsch et.al.

Ejiri hep-lat/0011006

- Order of phase transition

Nf=0 1st order
Nf=2 2nd order
Nf=2+1 on progress

C.NONAKA, Hiroshima Univ.

LQCD at Finite Temperature (2)

- Hadron spectrum

NA 50 J/ψ suppression

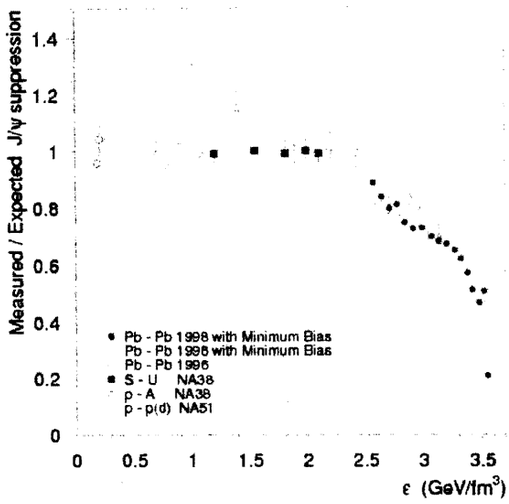

Mass shift of ρ ?

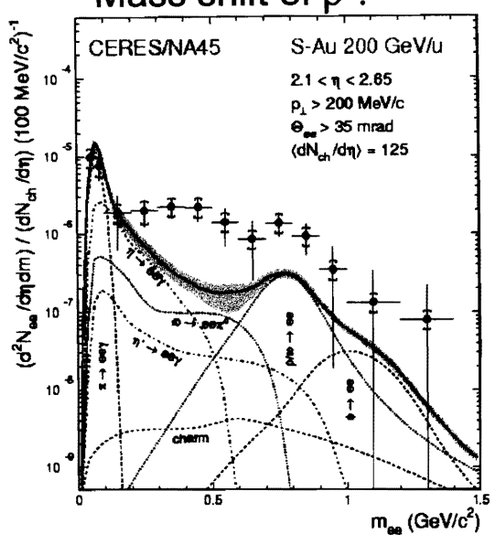

C.NONAKA, Hiroshima Univ.

LQCD at Finite Temperature (3)

- Maximum Entropy Method Analysis

Y.Nakahara, M.Asakawa, and T.Hatsuda

PRD60(1999)091305, hep-lat/0011040

Spectral Function ***T=0***

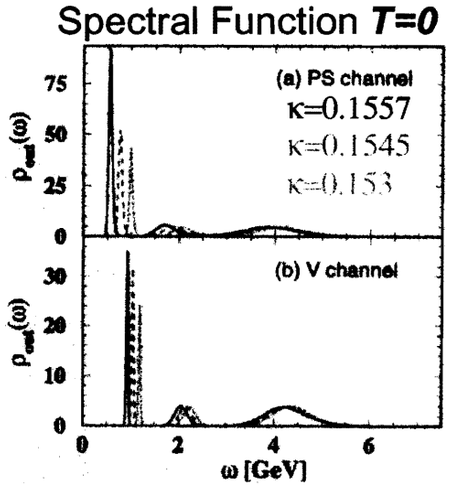

➡ Finite Temperature

C.NONAKA, Hiroshima Univ.

LQCD at Finite Temperature (4)

- Chamonia near the deconfining transition

T.Umeda, R.Katayama, O.Miyamura, and H.Matsufuru, hep-lat/0011085

Wave function

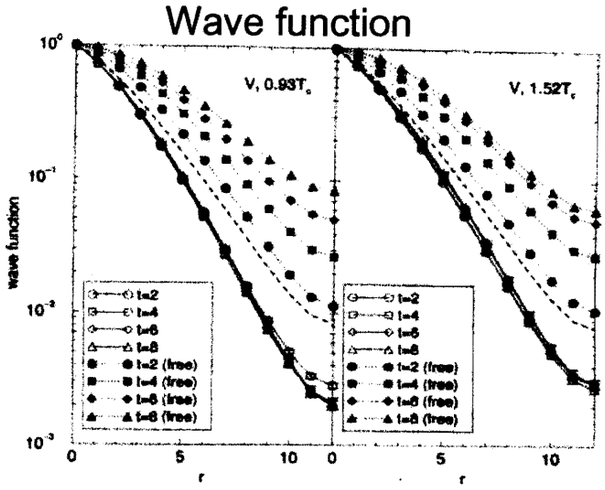

Gentle slope ⟷ Spread

•Strong spatial correlation

$J/$ may not easily be melted until 1.5 T_c

C.NONAKA, Hiroshima Univ.

LQCD at Finite Temperature (5)

- Heavy quark potential close to Tc

F.Karsch, E.Laermann, and A.Peikert, hep-lat/0012023

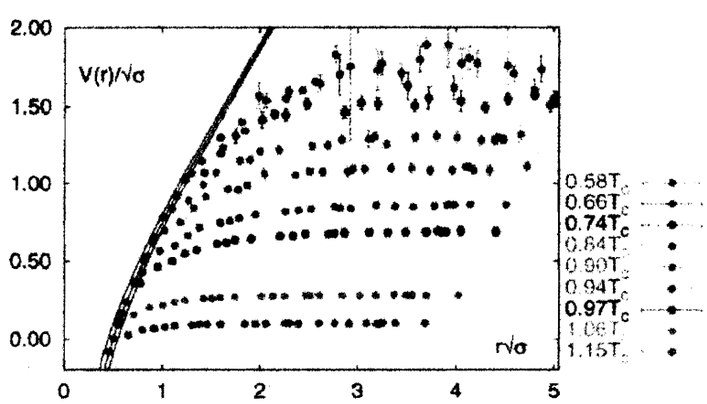

$N_f = 3$

$\frac{m_{PS}}{m_V} \sim 0.7$

C NONAKA, Hiroshima Univ.

LQCD at Finite Temperature (6)

- Transport Coefficients

S.Sakai, A.Nakamura, and T.Saito, NPA(1998)515c

– space-time evolution of hot and dense matter

Relativistic Hydrodynamical Model

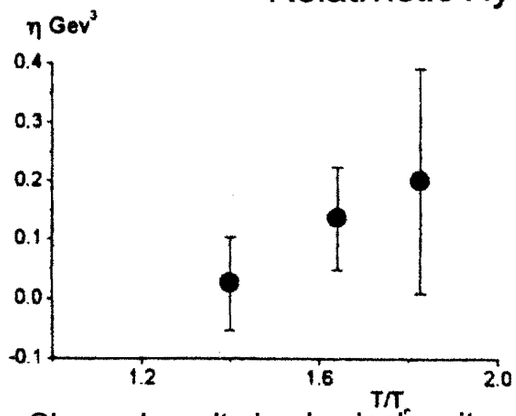

Shear viscosity in physical unit

$16^3 \times 8$

Iwasaki 's improved action quench

C.NONAKA, Hiroshima Univ.

LQCD at Finite Density (1)

- Hadron mass response to chemical potential

S.Choe, Y.Liu, and O.Miyamura (QCDTARO collaboration)

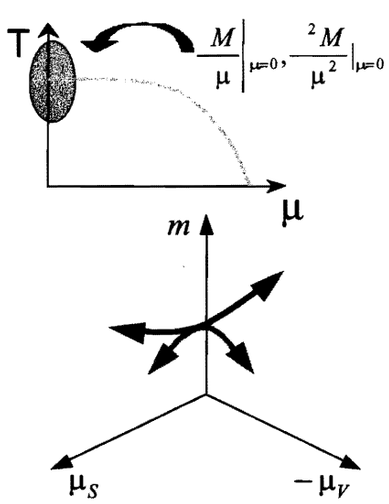

Staggered fermion (Nf=2) $16 \times 8^2 \times 4$

Screening mass

Ps	T = 0.97Tc	T = 1.1Tc
Response to μ_S ($\mu_S = \mu_u + \mu_d$)		
Mass	0.295~0.427	0.75
2nd	small (0.18~0.35)	large (5.39~4.31)
Response to μ_V ($\mu_V = \mu_u - \mu_d$)		
1st	very weak	very weak
2nd	large (negative) (-13.1~-8.56)	weak (-1.32~-1.54)

C.NONAKA, Hiroshima Univ.

LQCD at Finite Density (2)

	β=5.26 (0.97 Tc)		
	$ma = 0.0125$	$ma = 0.017$	$ma = 0.025$
$\vec{M}$	0.295(0.001)	0.352(0.001)	0.427(0.001)
2nd response	0.18(0.52)	0.27(0.35)	0.35(0.29)
	β=5.34 (1.1 Tc)		
$\vec{M}$	0.751(0.001)	0.747(0.001)	0.756(0.002)
2nd response	5.39(0.10)	5.82(0.16)	4.31(0.10)

P_S to μ_S
($\mu_S = \mu_u + \mu_d$)

	β=5.26 (0.97 Tc)		
	$ma = 0.0125$	$ma = 0.017$	$ma = 0.025$
1st response	0.006(0.057)	0.023(0.036)	0.005(0.021)
2nd response	-13.1(0.60)	-10.28(0.47)	-8.56(0.32)
	β=5.34 (1.1 Tc)		
1st response	0.0007(0.0071)	-0.0008(0.0065)	0.0022(0.0023)
2nd response	-1.32(0.32)	-1.48(0.32)	-1.54(0.41)

P_S to μ_V
($\mu_V = \mu_u - \mu_d$)

C.NONAKA, Hiroshima Univ.

LQCD at Finite Density (3)

- SU(2) Lattice QCD

  S.Muroya, A.Nakamura, and C.N, hep-lat/0010073

  – Wilson fermion (Wilson action, Iwasaki action)

  – Link by link update $4^4, 4^3 \times 8$

Number density

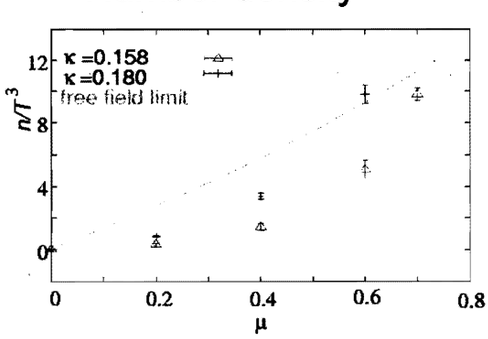

Expectation value of Polyakov line

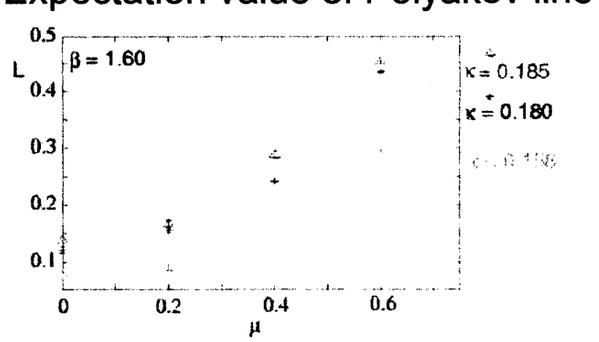

C.NONAKA, Hiroshima Univ.

Eigen value of W

S.Muroya et.al hep-lat/0010073

- Shell and bean structure (β=1.6. $\kappa = 0.180$)

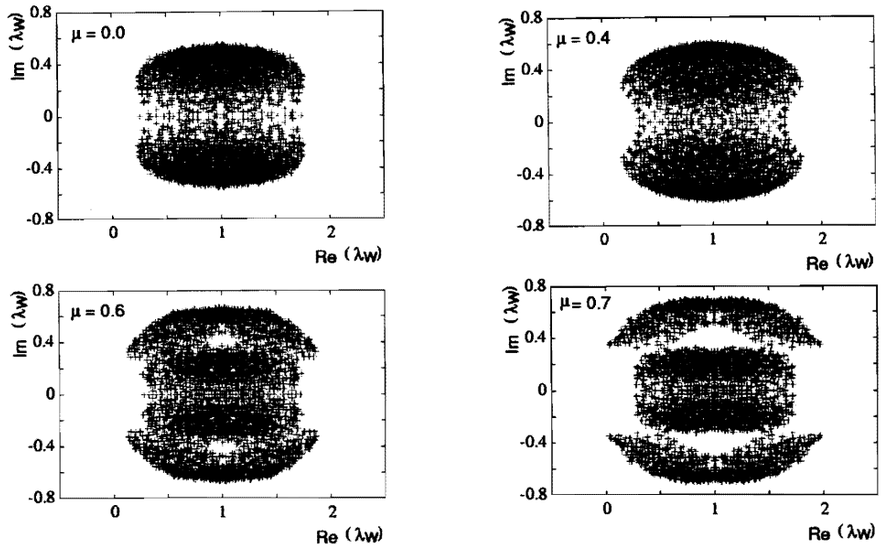

C.NONAKA, Hiroshima Univ.

SU(2) LQCD

S.Muroya et.al hep-lat/0010073

- Mass of π, ρ at chiral limit

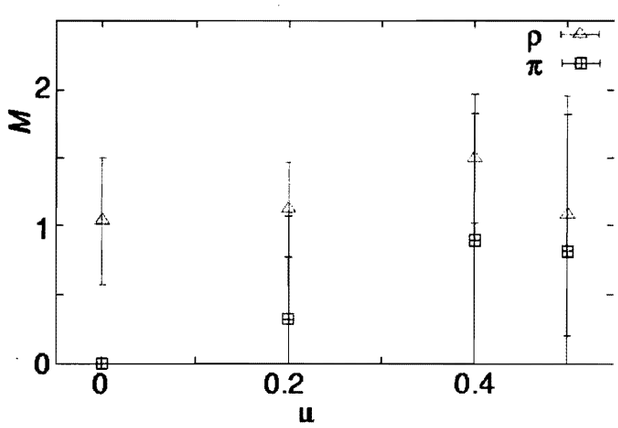

$\mu > 0.4$ $\pi \rightarrow$ massive

Chiral symmetry restoration

C.NONAKA, Hiroshima Univ.

Summary

- Lattice QCD

  Powerful Tools to understand QGP physics
- Recent developments of lattice QCD
  - High accuracy measurement
    improved actions, anisotropic lattice
    computer performance
- Lattice QCD at finite temperature
  - Many analyses
- Lattice QCD at finite density
  - Response to chemical potential, QCD-like theory

C.NONAKA, Hiroshima Univ.

CNS Workshop (first circular)

Title: Physics of QCD many-body systems
-- What we learn from the RHIC Year-1 --

Place: Lecture Room 1220, the 4th Science Building
Hongo campus, the University of Tokyo
Date: February 14(Thu), 15(Fri), 2001

Properties of nuclear matter under extreme conditions of high temperature and high density, and of hadrons in the nuclear matter, have been drawing strong interest of both nuclear and particle physicists. Experimental studies with high-energy heavy-ion collisions have been a strong driving force in the progress of this field. With the startup of the RHIC operation in the summer of 2000, further progress is expected in understanding properties of hadrons and QCD many-body systems.

The main focus of this workshop is on the hot results from the RHIC Year-1, with enough time slots for discussions. Related topics are alos covered; experimental results from KEK, GSI and CERN-SPS, and recent theoretical processes on neutron star, color super-conductivity etc.

Those who want to have further information, are recommended to visit the home-page listed below.

* Home page: http://phenix.cns.s.u-tokyo.ac.jp/cns-ws/index.html
* Due date: December 10th (Sun)
* Email: ws_secretary@cns.s.u-tokyo.ac.jp

Organizers:

H. Hamagaki (CNS/Tokyo)	hamagaki@cns.s.u-tokyo.ac.jp
T. Hatsuda (U. Tokyo)	hatsuda@phys.s.u-tokyo.ac.jp
H. En'yo (Kyoto U.)	enyo@nh.scphys.kyoto-u.ac.jp
M. Asakawa (Nagoya U.)	yuki@nuc-th.phys.nagoya-u.ac.jp
S. Sawada (KEK)	shinya.sawada@kek.jp
K. Ozawa (CNS/Tokyo)	ozawa@cns.s.u-tokyo.ac.jp
J. Nakano (CNS/Tokyo)	jnakano@cns.s.u-tokyo.ac.jp
T. Sakaguchi (CNS/Tokyo)	takao@cns.s.u-tokyo.ac.jp

CNS Workshop Program

Physics of QCD many-body systems

-- What we learn from the RHIC Year-1 --

2/14 (WED)

9:00 - *Registration*

9:30 - 10:15 (40+5 min.)

RHIC: the year in review — D. Morrison (BNL)

10:15 - 11:00 (40+5 min.)

Measurements of Global Variables at PHENIX — K. Homma (Hiroshima Univ.)

11:00 - 11:30 (25+5 min.)

First results from the STAR experiment at RHIC — A. Ogawa (Penn State Univ.)

11:30 - 12:00 (25+5 min.)

First results from the STAR experiment at RHIC - soft hadron physics - — M. Kaneta (LBNL)

========== Lunch ==========

13:30 - 14:00 (25 + 5 min.)

π^0 Production in Au+Au Collisions at $s^{1/2}$ = 130 GeV — K. Oyama (Univ. of Tokyo)

14:00 - 14:30 (25 + 5 min.)

Charged Hadron pt Spectra — T. Chujo (BNL)

14:30 - 15:00(25 + 5 min.)

Particle ratios in PHENIX at RHIC — H. Ohnishi (BNL)

========== Coffee Break ==========

15:30 - 16:00 (25 + 5 min.)

CERN SPS hadron measurement

- Flow measurement with a puzzle, and interpretation of low mt enhancement of pion spectrum.

S. Sato (Univ. of Tsukuba)

16:00 - 16:35(30 + 5 min.)

Hydrodynamical analysis of elliptic flow at SPS and RHIC

T. Hirano (Waseda Univ.)

16:35 - 16:55 (15 + 5 min.)

Three particles Bose-Einstein correlation in terms of Coulomb wave function

M. Biyajima(Shinshu Univ.)

18:00 - *Reception*

2/15 (THU)

9:15 - 9:45 (25 + 5 min.)
Electron Measurement in PHENIX — Y. Akiba (KEK)

9:45 - 10:15 (25 + 5 min.)
Observation of ρ/ω meson modification in nuclear matter
M. Naruki (Kyoto Univ.)

10:15 - 10:50 (30 + 5 min.)
Hadronic constraints for vector mesons in medium. — Su Houng Lee (Yonsei)

10:50 - 11:25 (30 + 5 min.)
J/Ψ in pA and AA — H. Fujii (Univ. of Tokyo)

11:25 - 12:00 (30 + 5 min.)
Quark matter in neutron stars — T. Tatsumi (Kyoto Univ.)

========== Lunch ==========

13:30 - 14:05 (30 + 5 min.)
Direct Photons in Pb+Pb Collisions — T. Awes (ORNL)

14:05 - 14:40 (30 + 5 min.)
Photon and Dilepton Emission Rates from Ultra-Relativistic Heavy Ion Collisions
Jan-e Alam (Univ. of Tokyo)

14:40 - 15:15 (30 + 5 min.)
Re-Hardening of Hadron Transverse Mass Spectra in Relativistic Heavy-Ion ollisions.
A. Ohnishi (Hokkaido Univ.)

15:15 - 15:50 (30 + 5 min.)
Quark-gluon Plasma and Lattice QCD at Finite Temperature and Density
C. Nonaka (Hiroshima Univ.)

Participant	List			
Akiba	Yasuyuki	秋葉	康之	KEK
Alam	Jane			University of Tokyo
Awes	Terry			ORNL
Bentz	Wolfgang			Dept. of Physics, School of Science, Tokai Univ.
Biyajima	Minoru	美谷島	實	信州大学理学部
Chujo	Tatsuya	中条	達也	Brookhaven National Laboratory
Danmura	Ayako	団村	絢子	筑波大学物理学系(三明研)
Esumi	Shinichi	江角	晋一	筑波大学物理学系(三明研)
Fujii	Hirotugu	藤井	宏次	東京大学大学院総合文化研究科相関基礎科学系
Fukushima	Kenji	福嶋	健二	東京大学大学院理学系研究科
Hayashigaki	Arata	林垣	新	東京大学大学院理学系研究科(初田研)
Hirano	Tetsufumi	平野	哲文	早稲田大学理工学部
Homma	Kensuke	本間	謙輔	広島大学大学院理学研究科物理科学専攻
Ishihara	Aya	石原	安野	The University of Texas at Austin
Ikeda	Takashi	池田	貴	東京大学大学院理学系研究科(初田研)
Kajihara	Fukutaro	梶原	福太郎	早稲田大学理工学部
Kajimoto	Kohei	梶本	こうへい	早稲田大学 大場・中里研究室
Kaneta	Masashi	金田	雅司	Lawrence Berkeley National Laboratory
Kim	Hungchong			Institute of Physics and Applied Physics, Yonsei Univ.
Kiyomichi	Akio	清道	明男	Inst. of Physics, University of Tsukuba
Lee	Su Houng			Institute of Physics and Applied Physics, Yonsei Univ.
Lange	Soren			FRANKFURT Univ.
Maedan	Shinji	前段	真治	Tokyo National College of Technology
Masui	Hiroshi	増井	宙	筑波大学物理学系(三明研)
Mineo	Hirobumi	峯尾	博文	東京大学大学院理学系研究科(初田研)
Miyama	Masanori	深山	正紀	Department of Physics, Tokyo Metropolitan University
Mizoguchi	Takuya	溝口	卓哉	鳥羽高専
Morrison	Dave			BNL
Morita	Kenji	森田	健司	早稲田大学理工学部(大場研)
Muroya	Shin	室谷	心	Tokuyama Women's College
Muto	Ryotaro	武藤	亮太郎	京都大学 理学部
Naruki	Megumi	成木	恵	京都大学理学部
Nonaka	Chiho	野中	千穂	広島大学大学院理学研究科物理科学専攻
Ogawa	Akio	小川	暁生	Penn State Univ / BNL
Ohnishi	Akira	大西	明	北海道大学理学部物理学教室
Ohnishi	Hiroaki	大西	宏明	Brookhaven National Laboratory
Ohnishi	Kazuaki	大西	一聡	東京大学大学院総合文化研究科
Oyama	Ken	大山	健	東京大学原子核科学研究センター
Saito	Naohito	斎藤	直人	RIKEN/RIKEN BNL Research Center
Sakai	Shingo	佐久間	真吾	筑波大学物理学系(三明研)
Sakuma	Fuminori	佐久間	史典	京都大学 理学部
Sakurai	Katsunori	櫻井	勝則	早稲田大学 大場・中里研究室
Sato	Susumu	佐藤	進	Inst. of Physics, University of Tsukuba
Shovkovy	Igor			School of Physics and Astronomy, University of Minnesota
Sumi	Yoshio	鷲見	義雄	Department of Clinical Radiology, Hiroshima International University
Suzuki	Naomichi	鈴木	尚道	松商学園短期大学
Tatsumi	Toshitaka	巽	敏隆	京都大学 理学部
Torii	Hisayuki	鳥井	久行	Kyoto Univ./RIKEN
tsuda	keiichi	津田	佳一	早稲田大学 大場・中里研究室
Yabu	Hiroyuki	藪	博之	東京都立大学理学部
Yokkaichi	Satoshi	四日市	悟	RIKEN
Yokokawa	Kazuo	横川	一夫	東京大学大学院理学系研究科(初田研)
Yoshida	Shigefumi	吉田	茂史	早稲田大学理工学部 物理・応用物理学科 大場・中里研究室
Zaic	William			Columbia University

世話人				
Hamagaki	Hideki	浜垣	秀樹	
Hatsuda	Tetsuo	初田	哲男	
En'yo	Hideto	延與	秀人	
Asakawa	Masayuki	浅川	正之	
Sawada	Shin'ya	澤田	真也	
OZAWA	Kyoichiro	小沢	恭一郎	
Nakano	Joe	中野	譲	
Sakaguchi	Takao	坂口	貴男	
CNS学生				
Matsumoto	Takashi	松元	貴志	
Kametani	Soichiro	亀谷	聡一郎	
Tamai	Munetaka	玉井	宗孝	
Kato	Koichi	加藤	公一	